



University
of Glasgow

<https://theses.gla.ac.uk/>

Theses Digitisation:

<https://www.gla.ac.uk/myglasgow/research/enlighten/theses/digitisation/>

This is a digitised version of the original print thesis.

Copyright and moral rights for this work are retained by the author

A copy can be downloaded for personal non-commercial research or study,
without prior permission or charge

This work cannot be reproduced or quoted extensively from without first
obtaining permission in writing from the author

The content must not be changed in any way or sold commercially in any
format or medium without the formal permission of the author

When referring to this work, full bibliographic details including the author,
title, awarding institution and date of the thesis must be given

Enlighten: Theses

<https://theses.gla.ac.uk/>
research-enlighten@glasgow.ac.uk

**BENDING AND TORSION OF
THIN-WALLED OPEN SECTION BEAMS**

by

Martin M. Black, B.Sc., M.Sc.

Summary of

**Thesis presented for the Degree of
Doctor of Philosophy of the University
of Glasgow.**

November, 1965.

ProQuest Number: 10647905

All rights reserved

INFORMATION TO ALL USERS

The quality of this reproduction is dependent upon the quality of the copy submitted.

In the unlikely event that the author did not send a complete manuscript and there are missing pages, these will be noted. Also, if material had to be removed, a note will indicate the deletion.



ProQuest 10647905

Published by ProQuest LLC (2017). Copyright of the Dissertation is held by the Author.

All rights reserved.

This work is protected against unauthorized copying under Title 17, United States Code
Microform Edition © ProQuest LLC.

ProQuest LLC.
789 East Eisenhower Parkway
P.O. Box 1346
Ann Arbor, MI 48106 – 1346

The subject matter of this thesis concerns the flexural-torsional behaviour of thin-walled beams under conditions of small and large displacements. The relevant aspects are examined both theoretically and experimentally and consideration is also given to the nonlinear unstable behaviour of such beams.

The published literature covering theoretical and experimental work is reviewed in Chapter I with special reference to beams of open section such as channels and angles. The review has been orientated to survey in particular, the analytical concepts introduced by previous investigators which are relevant to a solution for the problem of large elastic deformations of thin-walled open sections.

In the theoretical analysis presented in Chapter II, the governing differential equations based on small displacement approximations, are first considered. Solutions of these equations for selected cases are obtained in closed form. It is further shown that by neglecting the St. Venant torsional rigidity term, the solutions can be appreciably simplified. The limitations implicit in this approximation are

discussed.

The general problem considering finite displacements is then examined and the corresponding nonlinear governing differential equations established. In developing these equations, additional effects such as initial axial stress, axial displacement and longitudinal stress due to the 'shortening effect' are included. Solutions of these equations using the Galerkin approach are presented. The results obtained give torque/angle of twist equilibrium paths under both stable and unstable conditions and are shown to be applicable to the determination of critical bending moment values causing flexural-torsional instability. The approximations used in obtaining the solutions are indicated and their limitations discussed.

The experimental programme, apparatus and techniques are described in Chapter III. In this, the various experimental test rigs, including a controlled angle of twist loading arrangement used to examine both stable and unstable behaviour, and the arrangement for tests to failure, are described.

The experimental results obtained and their comparison with corresponding theoretical values are

presented in Chapter IV. In this it is shown that, in general, good agreement is obtained between theoretically predicted and experimentally determined values in respect of both deformations and stresses.

The application of the experimentally substantiated small displacement theory to practical structural design is presented in Chapter V. In this, specific cases of practical significance are analysed and discussed.

The principal findings of the investigation are summarised in Chapter VI and the thesis concludes with a Bibliography, Author Index and Appendices. The latter give full details of the theoretical solutions, the material and section properties of the specimens tested and also includes a suggested safe load table for thin-walled channel sections.

BENDING AND TORSION OF
THIN-WALLED OPEN SECTION BEAMS

by

Martin M. Black, B.Sc., M.Sc.

Thesis presented for the Degree of
Doctor of Philosophy of the University
of Glasgow.

November, 1965.

I N D E X

Page No.

ABSTRACT	v	
PRINCIPAL NOTATION	viii	
CHAPTER I	REVIEW OF PUBLISHED LITERATURE	1
CHAPTER II	THEORETICAL ANALYSIS	47
CHAPTER III	EXPERIMENTAL INVESTIGATIONS	89
CHAPTER IV	COMPARISON OF THEORETICAL AND EXPERIMENTAL RESULTS	109
CHAPTER V	PRACTICAL DESIGN APPLICATIONS	132
CHAPTER VI	SUMMARY AND CONCLUSIONS	144
CHAPTER VII	BIBLIOGRAPHY AND AUTHOR INDEX	151
CHAPTER VIII	APPENDICES	161
	ACKNOWLEDGEMENTS	150
	FIGURES	246

C O N T E N T S

	Page No.
ABSTRACT	v
PRINCIPAL NOTATION	viii
CHAPTER I - REVIEW OF PUBLISHED LITERATURE	
Introduction	2
I.1 Bending of Thin-Walled Open Section Beams	4
I.2 Torsion of Thin-Walled Open Section Beams	9
I.3 Combined Bending and Torsion of Thin-Walled Open Section Beams	19
I.4 Lateral and Torsional Buckling of Thin-Walled Open Section Beams	34
I.5 Critical Summary	42
CHAPTER II - THEORETICAL ANALYSIS	
II.1 Linear Small Displacement Flexural- Torsional Behaviour of Thin-Walled Open Section Beams	48
II.2 Nonlinear Large Displacement Flexural- Torsional Behaviour of Thin-Walled Open Section Beams	66
II.3 Particular Solutions of the Generalised Differential Equations of Bending Moment and Torque Equilibrium	72
II.4 Flexural-Torsional Instability of Thin-Walled Open Section Beams	85

CHAPTER III - EXPERIMENTAL INVESTIGATIONS

III.1	Stable Behaviour - Linear Torque/ Angle of Twist Equilibrium Paths - Small Displacements	91
III.2	Stable Behaviour - Nonlinear Torque/ Angle of Twist Equilibrium Paths - Large Displacements	95
III.3	Stable and Unstable Behaviour - Nonlinear Torque/Angle of Twist Equilibrium Paths - Large Displacements	98
III.4	Flexural-Torsional Failure of Thin- Walled Open Section Beams due to Applied Bending Moment	107

CHAPTER IV - COMPARISON OF THEORETICAL AND
EXPERIMENTAL RESULTS

IV.1	Stable Behaviour - Linear Torque/Angle of Twist Equilibrium Paths - Small Displacements	110
IV.2	Stable Behaviour - Nonlinear Torque/ Angle of Twist Equilibrium Paths - Large Displacements	114
IV.3	Stable and Unstable Behaviour - Nonlinear Torque/Angle of Twist Equilibrium Paths - Large Displacements	118
IV.4	Flexural-Torsional Failure of Thin- Walled Open Section Beams due to Applied Bending Moment	127

CHAPTER V - PRACTICAL DESIGN APPLICATIONS 132

CHAPTER VI - SUMMARY AND CONCLUSIONS 144

CHAPTER VII - BIBLIOGRAPHY AND AUTHOR INDEX

VII.1	Bibliography	152
VII.2	Author Index	159

CHAPTER VIII - APPENDICES

VIII.1	Theoretical Solutions	162
VIII.2	Effect of Neglecting Bending Moment Components $M_3 \frac{d\bar{u}}{dz}$, $M_3 \frac{d\bar{v}}{dz}$	173
VIII.3	Experimental Measurement of Material and Section Properties of Brass and Steel Angle Sections	177
VIII.4	Details of Test Specimens	180
VIII.5	Graphical Presentation of the Comparison of Theoretical and Experimental Results	184
VIII.6	Suggested Safe Load Table for Thin-Walled Channel Sections	242

ACKNOWLEDGEMENTS	150
------------------	-----

FIGURES	246
---------	-----

ABSTRACT

The subject matter of this thesis concerns the flexural-torsional behaviour of thin-walled beams under conditions of small and large displacements. The relevant aspects are examined both theoretically and experimentally and consideration is also given to the nonlinear unstable behaviour of such beams.

The published literature covering theoretical and experimental work is reviewed in Chapter I with special reference to beams of open section such as channels and angles. The review has been orientated to survey in particular, the analytical concepts introduced by previous investigators which are relevant to a solution for the problem of large elastic deformations of thin-walled open sections.

In the theoretical analysis presented in Chapter II, the governing differential equations based on small displacement approximations, are first considered. Solutions of these equations for selected cases are obtained in closed form. It is further shown that by neglecting the St. Venant torsional rigidity term, the solutions can be appreciably simplified. The limitations implicit in this approximation are

discussed.

The general problem considering finite displacements is then examined and the corresponding nonlinear governing differential equations established. In developing these equations, additional effects such as initial axial stress, axial displacement and longitudinal stress due to the 'shortening effect' are included. Solutions of these equations using the Galerkin approach are presented. The results obtained give torque/angle of twist equilibrium paths under both stable and unstable conditions and are shown to be applicable to the determination of critical bending moment values causing flexural-torsional instability. The approximations used in obtaining the solutions are indicated and their limitations discussed.

The experimental programme, apparatus and techniques are described in Chapter III. In this, the various experimental test rigs, including a controlled angle of twist loading arrangement used to examine both stable and unstable behaviour, and the arrangement for tests to failure, are described.

The experimental results obtained and their comparison with corresponding theoretical values are

presented in Chapter IV. In this it is shown that, in general, good agreement is obtained between theoretically predicted and experimentally determined values in respect of both deformations and stresses.

The application of the experimentally substantiated small displacement theory to practical structural design is presented in Chapter V. In this, specific cases of practical significance are analysed and discussed.

The principal findings of the investigation are summarised in Chapter VI and the thesis concludes with a Bibliography, Author Index and Appendices. The latter give full details of the theoretical solutions, the material and section properties of the specimens tested and also includes a suggested safe load table for thin-walled channel sections.

PRINCIPAL NOTATION

E	Young's modulus
G	Rigidity modulus
c	Shear centre
g	Centroid
x, y, z	Co-ordinate axes
x', y', z'	Displaced co-ordinate axes
u, v	Deflections relative to displaced axes
\bar{u}, \bar{v}	Deflections relative to undisplaced axes
β	Angle of twist
A	Cross-sectional area
t	Wall thickness
I_x, I_y	Principal second moments of area
I_c	Polar second moment of area
K_x, K_y	Third moments of area
K_c	Fourth moment of area
C	Torsion constant
Γ	Torsion-bending constant
ω	Vlasov's sectorial co-ordinate
$M_{x(x')}, M_{y(y')},$ $M_{z(z')}$	Moment vectors

T	Torque
B	Vlasov's bi-moment
L	Beam span
λL	Beam parameter where

$$\lambda = \sqrt{\frac{GC}{EI}}$$

Further definitive details of the above and of any additional symbols used are given where necessary in the text.

CHAPTER I

REVIEW OF PUBLISHED LITERATURE

Introduction

The necessity for high strength to weight ratios in aircraft structures has given rise to the production and use of a wide range of thin-walled open sections. Similar sections, produced by cold forming hot rolled steel strip, have also been developed for use in lightweight building structures. In both cases the sections have been used as main and secondary structural components.

The behaviour of these sections, under various load actions, has been the subject of much theoretical and experimental investigation. In these investigations, the basic concepts of bending, uniform torsion and non-uniform torsion of thin-walled open sections, have been presented. These concepts have been used in the development of the theoretical analyses of instability and buckling of thin-walled beams and columns.

In this chapter the published results of these investigations are briefly reviewed. For simplicity of presentation, this review is considered under four main headings culminating in a critical summary, that is:

1. Bending of thin-walled open section beams.
2. Torsion of thin-walled open section beams.
3. Combined bending and torsion of thin-walled open section beams.
4. Lateral and torsional buckling of thin-walled open section beams.

To illustrate fully the development of the theoretical analyses, the results of investigations into the corresponding behaviour of conventional hot rolled sections are also considered. It should be noted that the work included in this review has been selected as that representative of the main development of the analytical thought and corresponding experimental work in this particular field.

I.1 Bending of Thin-Walled Open Section Beams

The stable flexural behaviour of open form beam sections was first investigated by BACH (1909)¹. In his tests, Bach used a conventional hot rolled steel channel section. The channel, with its web vertical, was tested as a simply supported beam carrying vertical loads as shown in Fig. I.1. The two important results of his tests were:

- (i) that the strains produced by the loads acting in the plane of the centroid were different to those produced by loading in the web plane.
- (ii) in neither case did the measured strains agree with those calculated from simple bending theory.

Bach explained these discrepancies as being due to the unsymmetrical nature of the channel beam. MAILLART (1921)² examined Bach's results in more detail and noted that the discrepancy between measured and theoretical values of strain decreased as the plane of loading moved from the centroid to the web. He

considered that if the loading plane was further displaced from the centroid to a position behind the web the discrepancy between theoretical and experimental strains would vanish. He referred to this third characteristic point as the 'shear centre' and developed an approximate solution for determining its position on the horizontal axis of symmetry of the channel.

Maillart also developed expressions for the longitudinal strain caused by the twisting of the channel when the loads do not act in the plane of the shear centre. Using these expressions he calculated values of strain for Bach's channel tests which agreed substantially with the measured values.

The flexural behaviour of channel beams was further investigated by SEELY, PUTNAM and SCHWALBE (1930)³. In their work the position of the shear centre was obtained experimentally and the results compared with theoretical values obtained from an alternative expression to that developed by Maillart. Satisfactory agreement between experimental and theoretical values was obtained.

They also presented a method for computing major

longitudinal stresses normal to a transverse section of a beam which is subjected to bending and torsion or to torsion only. This analysis was limited by the fact that the beam had to be restrained in such a way that one cross-section remained fixed without distortion. This situation obtains at the central section of a symmetrically loaded, simply supported beam or at the fixed end of a cantilever beam. Results of this analysis were compared with experimentally measured strains and corresponding stresses on a channel section cantilever beam and some measure of agreement was obtained.

The flexural behaviour of thin-walled open sections has also been examined in detail by TIMOSHENKO (1945)⁴. In his work he considered first the bending of a prismatical bar of arbitrary cross-section by pure moment actions and established expressions for the longitudinal stresses which are produced. This analysis was then extended to the bending of such bars by transverse force action. At this stage he introduced the 'shear centre' concept and derived expressions for locating the shear centre position of some particular cross-sections.

The analysis was then developed further and

general expressions for the shear centre co-ordinates of any arbitrary thin-walled open section were obtained. Fig. I.2 shows the cross-section of a thin-walled beam where g is the centroid and gx and gy are the principal centroidal axes. The wall thickness at any point is t and the second moments of area of the cross-section about gx and gy are I_x and I_y respectively. The shear centre is the point c whose co-ordinates are x_c and y_c with reference to the principal axes gx and gy respectively. The expressions derived by Timoshenko for the co-ordinates x_c and y_c are

$$x_c = \frac{1}{I_x} \int_0^m \omega_s y t ds \quad \text{and} \quad y_c = -\frac{1}{I_y} \int_0^m \omega_s x t ds \quad \text{I.1.1}$$

where x and y are the co-ordinates of any point on the centre line of the section wall, s is the distance measured along the centre line, m is the total length of the wall centre line and

$$\omega_s = \int_0^s r ds \quad \text{I.1.2}$$

where r is the perpendicular distance from the centroid to a tangent at a point on the wall.

In developing these expressions for the shear

centre co-ordinates, Timoshenko showed that his analysis of the bending of prismatic bars by transverse loads could be used for thin-walled open section beams as long as the transverse loads were applied through the shear centre axis. If the loads did not act through this axis the problem became more complex due to the torsional deformations which would obtain. In this situation the stresses could not be calculated from simple bending theory.

Results similar to those of Timoshenko had also been presented by VLASOV (1940)⁵ who investigated, in some detail, the behaviour of thin-walled beams under various load actions. He also developed expressions for the co-ordinates of the shear centre of various cross-sections and noted the deformations produced by loads not passing through the shear centre axis.

Both Timoshenko and Vlasov extended their analyses to the problems of torsion, combined bending and torsion and buckling of thin-walled open sections. The results of their investigations into these aspects of thin-walled beam behaviour are outlined in later sections of this review.

I.2 Torsion of Thin-Walled Open Section Beams

The original theory of torsion of prismatic bars was presented by COULOMB (1784)⁶. In his analysis, he assumed that plane sections perpendicular to the axis of the bar remained plane after twisting. This assumption was valid for uniform bars of circular cross-section only. In torsion of bars of non-circular cross-section, longitudinal strains were developed which caused distortion of plane sections after twisting. This distortion has been referred to as warping.

The general solution for the problem of torsion of non-circular section bars was derived by ST. VENANT (1855)⁷. In his analysis, St. Venant recognised the presence of warping and assumed that it was the same for all cross-sections. This assumption is applicable only if the bar is twisted by couples applied at the ends, in planes perpendicular to the axis of the bar, and if the ends are free to warp. This condition is referred to as 'uniform torsion'.

The fundamental equation of torsion, derived by St. Venant can be written as

$$\frac{\partial^2 \phi}{\partial x^2} + \frac{\partial^2 \phi}{\partial y^2} = -2$$

I.2.1

where ϕ is a stress function that, as well as satisfying equation I.2.1, has to be a constant around the cross-section boundary.

The solution of equation I.2.1 gave rise to the following relationship between the torque T and the angle of twist β .

$$T = GC \frac{d\beta}{dz} \quad \text{I.2.2}$$

where C , the torsion constant, was given by the expression

$$C = 2 \iint \phi \, dx \, dy \quad \text{I.2.3}$$

St. Venant showed how to solve these equations by what is known as the semi-inverse method; that is, he started by considering an expression for the stress function that satisfied equation I.2.1 and then examined the cross-section that his expression implied. In this way he obtained the value of C for several of the simpler geometrical shapes.

PRANDTL (1903)⁸ showed that the solution of the torsion problem could be obtained by considering the equation of equilibrium of a membrane under transverse pressure. This equation was of the form

$$\frac{\partial^2 w}{\partial x^2} + \frac{\partial^2 w}{\partial y^2} = -\frac{p}{s} \quad \text{I.2.4}$$

where w is the membrane deflection, s is the membrane tension per unit length and p is the intensity of transverse pressure.

Recognising the similarity between equations I.2.1 and I.2.4, Prandtl showed that by using a soap film all the information of stress distribution in torsion could be obtained experimentally.

This method of analysis of the torsion problem, usually referred to as the 'membrane analogy', was used by GRIFFITH and TAYLOR (1917)⁹ to determine the torsional rigidities of bars of various complex forms of cross-section. TIMOSHENKO¹⁰ has illustrated an analytical solution, based on the membrane analogy, for torsion of a thin rectangular cross-section of length b and thickness t . The value of the torsion constant was found to be

$$C = \frac{1}{3} b t^3 \quad \text{I.2.5}$$

In the case of a thin-walled open section of constant thickness t a value of C of sufficient accuracy was given by the expression

$$C = \frac{1}{3} m t^3 \quad \text{I.2.6}$$

where m is the developed length of the middle line of the cross-section.

The St. Venant solution of the torsion problem applied only to cases with no warping restraint and where the cross-sections all warped in the same manner and by the same amount. This condition implied that the torque was applied by means of shearing stresses distributed over the ends of the bar in the same way as at any intermediate cross-section. If the distribution of stresses at the ends did not comply with this condition, local disturbances in the stresses resulted. In this situation, the St. Venant solution was only valid in regions at some distance from the ends of the bar. This form of behaviour where warping varies is usually referred to as 'non-uniform torsion'. The variation in the warping has been shown to arise if any cross-section of the bar is restrained from longitudinal deformation or if the applied torque varies along the bar.

TIMOSHENKO (1905)¹¹ investigated the problem of torsion of an I-section with a built-in end. He found that to compute accurate values of the angle of twist, bending stresses in the flanges had to be considered as well as the St. Venant torsional shear stresses. The

differential equation of torque equilibrium for the I-section was shown by Timoshenko to be

$$T = GC \frac{d\beta}{dz} - \frac{Dh^2}{2} \frac{d^3\beta}{dz^3} \quad \text{I.2.7}$$

The first term on the right hand side of equation I.2.7 is due to the St. Venant torsional shear stresses and the second arises from the flange bending stresses. In this latter term D denotes the flexural rigidity of one flange in its own plane and h is the distance between the centroids of the flanges. For the general case of a thin-walled open section, equation I.2.7 can be presented in the following form

$$T = GC \frac{d\beta}{dz} - EI \frac{d^3\beta}{dz^3} \quad \text{I.2.8}$$

where I is the torsion bending constant for the beam cross-section.

The results obtained by Timoshenko were also found by WEBER (1926)¹² who examined the twisting of channel sections and by VLASOV (1940)⁵ in his analysis of torsion of thin-walled open sections. REISSNER (1955)¹³, using variational methods, has also derived an equation of the same form as equation I.2.8. GOODIER and BARTON (1944)¹⁴ extended Timoshenko's

analysis by considering distortion of the beam cross-section in its own plane. The differential equation of torque equilibrium which they derived can be written as

$$T = A \frac{d\beta}{dz} - B \frac{d^3\beta}{dz^3} + C \frac{d^5\beta}{dz^5} \quad \text{I.2.9}$$

where A , B and C are constants depending on the material and section properties of the beam.

In the investigations described so far, the solutions obtained for the torsion problem were restricted to small angles of twist. For the analysis of large torsional deformations, the effect of higher order terms, due to longitudinal stresses, should be considered. The first indication of this condition was given by YOUNG (1807)¹⁵ in his comments on the twisting of circular shafts. He pointed out that whilst the main resistance to applied torque was provided by shearing stresses in the cross-sectional planes, a small additional resistance, proportional to the cube of the angle of twist, obtained due to a system of longitudinal stresses.

This system of longitudinal stresses has been considered by WEBER (1921)¹⁶ in his analysis of the

'shortening effect' of torsion. This effect is explained by considering the behaviour of a generator, originally parallel to the axis of the bar which, after twisting, becomes a helix. The distance between the ends of this helix, measured parallel to the axis of the bar, is less than the original length of the fibre, by an amount proportional to the pitch angle of the helix. This, in its turn, varies directly with the distance of the fibre from the axis of twist of the bar. If no external longitudinal forces are applied to the end sections of the bar, the outer fibres will be in tension compared with those nearer the axis of twist which are compressed. This condition results in an overall shortening of the bar.

For a given applied torque, the angle of twist calculated on the basis of shear stresses alone would be greater than that determined by considering both shear and longitudinal stresses since part of the torque is used to maintain the longitudinal stress system. The effect of the longitudinal stresses is more pronounced at large angles of twist and gives rise to a nonlinear torque/angle of twist relationship.

Weber, in his analysis of this phenomenon, derived a differential equation of torque equilibrium

for the torsion of a bar having a thickness t and breadth b . This equation can be written as

$$T = \frac{1}{3} b t^3 G \frac{d\beta}{dz} + \frac{1}{360} b^5 t E \left(\frac{d\beta}{dz} \right)^3 \quad \text{I.2.10}$$

The first term on the right hand side of equation I.2.10 is the usual St. Venant expression and the second term is the torque due to the shortening effect. This analysis is valid for free ended torsion only, that is, there are no external longitudinal force actions at the ends of the bar.

Weber's work was extended by CULLIMORE (1949)¹⁷ who analysed the shortening effect in the torsion of thin-walled open sections. His theoretical analysis was substantiated by results he obtained from torsion tests on aluminium alloy I-sections and zeds. Cullimore also presented a tentative theory which indicated a connection between the shortening stresses and the position of the axis of twist in an open section subjected to pure torsion.

GREGORY (1961)¹⁸ also investigated the problem of the shortening effect in torsion of thin-walled open sections. His analysis showed that the appropriate differential equation of torque equilibrium could be

derived by considering an arbitrary reference axis for twist. The final form of the equation which he presented can be applied to any cross-sectional shape and included the warping term corresponding to non-uniform torsion behaviour. His equation can be written as

$$T = GC \frac{d\beta}{dz} + \frac{1}{2} E \left(\frac{d\beta}{dz} \right)^3 \left(K_c - \frac{I_c^2}{A} - \frac{K_y^2}{I_y} - \frac{K_x^2}{I_x} \right) - E \Gamma \frac{d^3\beta}{dz^3} \quad \text{I.2.11}$$

The second term on the right hand side of equation I.2.11 is the torque due to the shortening effect. Gregory indicated that equation I.2.11 was in general not easily solved. He suggested that in many cases it appeared reasonable to neglect initially the term involving $\left(\frac{d\beta}{dz} \right)^3$, solve the resulting equation in the normal way and then treat the shortening effect as a superimposed perturbation.

In his theoretical analysis, Gregory also presented a general solution for the problem of torsion of thin-walled open sections subjected to initial axial force or bending moment. The effect of tension on the torsional rigidity of strips was first observed by WILBERFORCE and CAMPBELL (1913)¹⁹ and a simple theory.

for the increase in torsional rigidity of a bar subjected to initial axial tension was presented by BUCKLEY (1914)²⁰. A similar theory was also developed by WAGNER (1936)²¹ in his investigations into the torsional buckling of compressed aircraft stiffeners. He showed that, if a thin-walled open section is subjected to initial axial compressive stress, the torsional rigidity of the member is reduced.

This effect of initial axial stress on the torsional rigidity of thin-walled open sections was later analysed by GOODIER (1950)²². He extended the St. Venant solution for torsion and showed that, in the presence of axial stress, the torque equilibrium equation I.2.2 was modified to the following form

$$T = (GC + \sigma I_c) \frac{d\beta}{dz} \quad \text{I.2.12}$$

where the initial axial stress σ , is positive if tensile and negative when compressive. That is, the torsional rigidity increases if an axial tensile stress is present and decreases if the stress is compressive. Goodier also considered the problem of initial axial stress due to bending actions. This aspect of his work will be described in the next section of this review.

I.3 Combined Bending and Torsion of Thin-Walled Open Section Beams

VLASOV (1940)⁵, in his investigations into the behaviour of thin-walled beams, considered the problem of combined bending and torsion of thin-walled open sections. The general theory which he presented was based on considering a thin-walled section as a spatial system of the cylindrical or prismatic shell form with rigid section contour. In his analysis of the beam deformations in the presence of restrained warping, he did not employ the usual hypothesis of plane sections remaining plane. Instead he assumed that the projection of the shape of the cross-section on a plane perpendicular to the longitudinal axis remained unchanged after twisting and that there were no shear strains in the middle surface of the cross-section. These assumptions constituted the basis of a new law of distribution of longitudinal stresses in the cross-section which he referred to as the 'law of sectorial areas'.

The differential equations defining the problem of combined bending, torsion and axial force which he presented are

$$\begin{aligned}
 EA \frac{d^2 w}{dz^2} + q_z &= 0 \\
 EI_x \frac{d^4 v}{dz^4} - q_y &= 0 \\
 EI_y \frac{d^4 u}{dz^4} - q_x &= 0 \\
 EJ_\omega \frac{d^4 \beta}{dz^4} - GJ_d \frac{d^2 \beta}{dz^2} - m &= 0
 \end{aligned}
 \tag{I.3.1}$$

In the last of equations I.3.1, the constant J_ω was defined by Vlasov as the 'sectorial moment of inertia', and corresponds to the torsion-bending constant usually denoted by Γ , and J_d is the torsion constant more commonly defined by the symbol C . The term m denotes the value of an externally applied torsional couple per unit length of the beam.

Vlasov then presented the following four generalised force actions

$$\begin{aligned}
 N &= EA \frac{dw}{dz} \\
 M_x &= -EI_x \frac{d^2 v}{dz^2} \\
 M_y &= EI_y \frac{d^2 u}{dz^2} \\
 B &= -EJ_\omega \frac{d^2 \beta}{dz^2}
 \end{aligned}
 \tag{I.3.2}$$

The last of these force actions B , was new and was

referred to as the 'bi-moment'. The value of B as defined by the last of equations I.3.2 can be obtained by solving the last of equations I.3.1.

The resulting expression for the longitudinal stress σ at any point on the cross-section was shown by Vlasov to be

$$\sigma = \frac{N}{A} - \frac{M_y x}{I_y} + \frac{M_x y}{I_x} + \frac{B \omega}{J_\omega} \quad \text{I.3.3}$$

where ω is defined as the 'sectorial co-ordinate' of the point and can be calculated from the expression

$$\omega = \int^s h ds \quad \text{I.3.4}$$

In this equation h is the perpendicular distance from the shear centre to a tangent at the point and s is the distance to the point measured along the middle line of the section.

Vlasov indicated that the theory of restrained torsion, more commonly referred to as non-uniform torsion, which he had developed, was analogous in its mathematical formulation to the elementary theory of beam flexure. He also pointed out that, for thin-walled open sections, where the ratio of wall-thickness to the characteristic dimension of the cross-section

is of the order of 0.02 or less, the torsional rigidity GJ_d can be set equal to zero without appreciable error.

If this simplification is adopted then the last of equations I.3.1 becomes

$$EJ_w \frac{d^4 \beta}{dz^4} = M \quad \text{I.3.5}$$

and is of the same form as the basic equation for the simple theory of bending.

As a result of these analogies, Vlasov made the following proposition:

'All the analytical methods based on the law of plane sections which are used in the theory of strength of materials and structural engineering for calculating beams and systems in flexure, can be completely generalised and extended to include the theory of restrained torsion of thin-walled beams, or systems consisting of such beams and of ribbed arches.'

As already noted in section I.1 of this review, the theory of bending, torsion and buckling of thin-walled open sections was also presented by TIMOSHENKO (1945)⁴. Vlasov has stated that in defining the fundamental problem of flexural-torsional

behaviour of a thin-walled open section beam, Timoshenko has also started from the idea of examining the beam as a shell. He points out that, apart from a difference of notation, Timoshenko's work is a brief exposition of his own theoretical analysis of the problem.

Both Vlasov and Timoshenko described how transverse loads which did not pass through the shear centre produced not only bending but also torsion of the beam. In analysing this problem they suggested replacing each force which did not pass through the shear centre axis by a parallel force passing through that axis and a couple acting in a plane perpendicular to the axis of the bar. In this way the problem was divided into two parts:

- (i) the investigation of bending by forces distributed along the shear centre axis.
- (ii) the investigation of torsion by couples acting in planes perpendicular to the axis of the bar.

The analysis of the first part of the problem was based

on simple bending theory and for the second part the non-uniform torsion equation was employed. Both authors presented closed solutions for particular small displacement cases and considered both concentrated and uniformly distributed loads. It is to be noted, however, that Timoshenko did not employ the bi-moment concept suggested by Vlasov, nor did he consider the possible simplification of the non-uniform torsion equation, obtained by neglecting the St. Venant torsional rigidity term.

The particular problem of combined bending and torsion of thin-walled channel sections was investigated by WINTER, LANSING and McCALLEY (1949)²³. In their theoretical analysis they presented general equations of equilibrium adapted from the work of Timoshenko. These equations consider the equilibrium of bending moments and torque about the displaced axes x' , y' and z' , as shown in Fig. I.3, and were written as

$$\begin{aligned}
 M_{x'} &= -EI_x \frac{d^2 u}{dz^2} = M_x + \beta M_y - \frac{du}{dz} M_z \\
 M_{y'} &= EI_y \frac{d^2 u}{dz^2} = -\beta M_x + M_y - \frac{dv}{dz} M_z \\
 \frac{d}{dz} (M_{z'}) &= GC \frac{d^2 \beta}{dz^2} - EI' \frac{d^4 \beta}{dz^4} \\
 &= \frac{d^2 u}{dz^2} M_x + \frac{d^2 v}{dz^2} M_y + m_z
 \end{aligned}
 \tag{I.3.6}$$

In these equations, the angle of twist β is considered to be small and the approximations

$\sin \beta = \beta$ and $\cos \beta = 1$ are adopted. The symbol m_z used in the last of equations I.3.6, defines the intensity of a uniformly distributed torque about the shear centre axis.

The authors examined the case where the load plane was parallel to one of the principal planes such as for a channel beam loaded in the plane of the web. Putting $M_x = M$, $M_y = 0$ and neglecting certain terms which they said could be shown to be of higher order, equations I.3.6 were reduced to the following single expression

$$EI \frac{d^4 \beta}{dz^4} - GC \frac{d^2 \beta}{dz^2} - \frac{M^2 \beta}{EI_y} = -m_z \quad \text{I.3.7}$$

The boundary conditions to be satisfied in obtaining an approximate solution to equation I.3.7 were then indicated for the particular case of a channel of length $2l$ and depth $2h$, subjected to a single concentrated load $2P$ applied at mid-span at the top of the web. In such a case $M = P(l-z)$, $m_z = 0$ and if the origin of co-ordinates is located at mid-span, the appropriate boundary conditions are

$$\frac{d\beta}{dz}(0) = \beta(l) = \frac{d^2\beta}{dz^2}(l) = 0 \text{ and } \frac{d^3\beta}{dz^3}(0) = \frac{P[e + h\beta(0)]}{EI}$$

The value shown for $\frac{d^3\beta}{dz^3}(0)$ is found by integrating the first and second parts of the last of equations I.3.6 and noting that, at mid-span, $\frac{d\beta}{dz} = 0$ and, as illustrated by Fig. I.4,

$$M_z' = -P[e + h\beta(0)]$$

At this stage of the investigation the possible simplifications which could be made in the analysis for determining β were considered. It was suggested that since the angles of twist were small, the influence of bending moment about the minor axis could be neglected. Also for thin-walled sections the value of C was small when compared with the other section properties. Thus, by neglecting the second and third terms in the left hand side of equation I.3.7, the following simplified equation was obtained

$$EI \frac{d^4\beta}{dz^4} = -M_z \quad \text{I.3.8}$$

This equation is similar to equation I.3.5 derived by Vlasov.

Winter, Lansing and McCalley extended their investigation to consider the effect of intermediate

bracing of the channel. They showed that the torque actions produced higher values of stress at certain points on the channel cross-section, than would be calculated from simple bending theory. The resistance to the torque actions was shown to arise mainly from the lateral bending of the flanges. This resistance could be increased by providing intermediate bracing between the flanges of the channel. A design approach for determining the strength and spacing of such bracing based on an 'overstress criterion' was presented. It was shown that it was never necessary to provide more than four braces between supports in order to limit the overstress to 10%.

TERRINGTON (1958)²⁴ investigated the bending and torsion of crane girders due to oblique transverse loads which did not pass through the shear centre of the girder. In his analysis, he developed differential equations of stability which, in their contracted form, were similar to equations I.3.6 presented by Winter, Lansing and McCalley.

Terrington's equations were also established by considering equilibrium of bending moments and torque about the displaced axes of the beam and can be written as

$$\begin{aligned}
M_x' &= EI_x \frac{d^2 \psi}{dz^2} = -M_x + M_y \beta + M_z \frac{du}{dz} \\
M_y' &= EI_y \frac{d^2 u}{dz^2} = -M_x \beta - M_y - M_z \frac{dv}{dz} \\
M_z' &= GC \frac{d\beta}{dz} - EI' \frac{d^3 \beta}{dz^3} \\
&= M_x \frac{du}{dz} - M_y \frac{dv}{dz} + M_z
\end{aligned}
\tag{I.3.9}$$

As in previous investigations, the angle of twist was considered to be small and the approximations $\sin \beta = \beta$ and $\cos \beta = 1$ could be used.

Terrington indicated that equations I.3.9 had been solved directly for bisymmetrical and monosymmetrical sections by PETTERSSON (1949)²⁵ and DOHRENWEND (1941)²⁶. The method of solution adopted by these authors was to reduce equations I.3.9 to a single fourth order differential equation which could be solved by the solution of infinite series and the use of Bessel functions. Terrington suggested that this form of solution was too complex for practical design calculations due to the numerous factors which had to be derived. In his analysis of the problem, he presented an approximate method of solution in which he neglected terms of the second order of small

quantities and thus modified equations I.3.9 to the following form

$$\begin{aligned}
 M_x' &= EI_x \frac{d^2 v}{dz^2} = -M_x \\
 M_y' &= EI_y \frac{d^2 u}{dz^2} = -M_x \beta - M_y \\
 M_z' &= GC \frac{d\beta}{dz} - EI' \frac{d^3 \beta}{dz^3} \\
 &= M_x \frac{du}{dz} + M_z
 \end{aligned}
 \tag{I.3.10}$$

In solving these equations for a beam loaded symmetrically about the centre of the span, the angle of twist β was assumed to be parabolic in terms of β_0 , the angle of twist at mid-span.

In the various solutions described so far, for the problem of combined bending and torsion of beams, the effect of the bending stresses on the torsional rigidity of the beam was not considered. This condition was, however, examined by GOODIER (1950)²² as an extension to his analysis of the problem of torsion of a beam subjected to an initial axial stress. He indicated that when such a stress σ is due to a bending moment in a principal plane, it is given by the expression

$$\sigma = \frac{M}{I} (y - y_g) \quad \text{I.3.11}$$

The torque/angle of twist relationship, allowing for this stress, becomes

$$\tau = \left(GC + \frac{KM}{I} \right) \frac{d\beta}{dz} \quad \text{I.3.12}$$

The addition to GC can be positive or negative according to the sign of M and thus the resulting effective torsional rigidity can be increased or decreased.

In Goodier's analysis the axes ox , oy and oz were oriented with oz along the axis of torsional rotations and ox and oy parallel to the principal centroidal axes of the section. The plane of the bending moment M was parallel to the yz plane, I was the appropriate second moment of area and y_g was the co-ordinate of the centroid. The constant K is a geometrical property of the beam section and is given by the expression

$$K = \iint (y - y_g) r^2 dx dy \quad \text{I.3.13}$$

where $r^2 = x^2 + y^2$

Goodier pointed out that this constant vanishes - and with it the effect of bending moment on torsional

rigidity - in the following cases:

- (i) the section has two axes of symmetry
- (ii) the section has point symmetry, for example a zed section
- (iii) the section has one axis of symmetry and the bending moment vector is in the same direction, that is, the axis of symmetry is perpendicular to the plane of bending.

The solution of equation I.3.12 was later discussed by ENGEL and GOODIER (1953)²⁷ when examining the behaviour of a thin-walled equal angle section loaded as shown in Fig. I.5. In their investigation it was shown that before twisting, the bending moment, being in a plane normal to the axis of symmetry, had no effect on the torsional rigidity. However, after twisting, a bending moment component in a plane parallel to the axis of symmetry was produced. This component produced an increase or decrease in the torsional rigidity of the angle according to the direction of twist as illustrated by Fig. I.6. This behaviour was shown in a graph of torque against angle of twist at mid-span for various applied bending

moments and is reproduced in Fig. I.7. The corresponding experimental results obtained from their angle tests are reproduced graphically in Fig. I.8. The authors indicated that although the experimental curves agreed in form with the corresponding theoretical relationships, there were considerable quantitative differences. They suggested that such differences were due, at least in part, to the presence of initial twist in the test specimen. It is to be noted, however, that whilst the theoretical curves are plotted for angles of twist up to 2 radians the experimental values do not exceed 0.2 radian.

Further examination of the theoretical curves showed that it was possible for a point of instability to be reached. Once this point was passed, the curve might descend to intersect the twist axis and then rise again to intersect it once more. This form of curve is shown in Fig. I.9 where the last point of intersection with the twist axis represented a stable deformed equilibrium state under zero applied torque. This condition was in fact obtained experimentally by Engel and Goodier by applying bending moment to the angle and twisting it by hand until it took up the deformed equilibrium position. However, they did not

record experimentally the complete torque/angle of twist equilibrium path for this unstable form of flexural-torsional behaviour.

The effect of bending stresses on torsional rigidity was also discussed by GREGORY (1961)¹⁹. He considered a thin-walled member of arbitrary open cross-section with no axes of symmetry. For such a section both K_x and K_y had values and the torque/angle of twist relationship which he presented was written as

$$T = \left(GC + \frac{K_x M_x}{I_x} + \frac{K_y M_y}{I_y} \right) \frac{d\beta}{dz} \quad \text{I.3.14}$$

The significance of the geometrical constant K for a cross-section in the analysis of lateral and torsional buckling of thin-walled beams is described in the next section of this review.

I.4 Lateral and Torsional Buckling of Thin-Walled Open Section Beams

The problem of lateral buckling of beams was first considered by PRANDTL (1899)²⁸. He investigated the behaviour of a beam of narrow rectangular cross-section subjected to bending moment in the plane of maximum flexural rigidity. As a result of his analysis, the critical value of bending moment, M_c which initiates lateral buckling was given by the following expression

$$M_c = \frac{\pi}{L} \sqrt{EI_y GC} \quad \text{I.4.1}$$

where GC was the St. Venant torsional rigidity and EI_y was the flexural rigidity for lateral bending.

A similar solution for the critical bending moment was obtained independently by MICHELL (1899)²⁹.

In the Prandtl and Michell analyses, first order approximations were taken for direction cosines and curvatures and the solutions were limited to beam sections having small ratios of EI_y and GC to the major flexural rigidity EI_x .

A modified form of equation I.4.1 was later presented by REISSNER (1904)³⁰. In his analysis, he

introduced more exact geometrical considerations by means of the general equations for the bending and twisting of rods. In this way a modified expression for the critical bending moment was obtained which took account of the ratio of the principal second moments of area of the beam cross-section. This expression was written as

$$M_c = \frac{\pi}{L} \sqrt{\frac{EI_y GC}{1 - \frac{I_y}{I_x}}} \quad \text{I.4.2}$$

GOODIER (1951)³¹ examined the Reissner modification and pointed out that as the ratio of the second moments of area I_x and I_y approached unity, the value of critical bending moment increased without limit. This appeared to indicate that lateral buckling ceased to be possible and that some other form of buckling, not represented in the theory, obtained. To explain this condition, he introduced his analysis of the effect of initial bending stress on the torsional rigidity of the beam section. This effect produced the torque/twist relationship described by equation I.3.12, that is

$$T = \left(GC + \frac{KM}{I} \right) \frac{d\beta}{dz} \quad \text{I.4.3}$$

In this equation the addition to GC could be positive or negative according to the sign of M . If this addition was negative and sufficiently large, the

apparent torsional rigidity could be reduced to zero. In this condition the beam could fail by torsional buckling. The value of critical bending moment for this form of buckling would be given by the expression

$$M_c = - \frac{GC I}{K} \quad \text{I.4.4}$$

Goodier pointed out that equation I.4.4 assumes that the axis of rotation of the beam is restrained from transverse displacement. He also indicated that his analysis assumed the condition of free warping. If the warping was restrained, modifications would have to be introduced which allowed for the non-uniform torsion condition.

The problem of lateral and torsional buckling with restrained warping was first discussed by TIMOSHENKO (1905)³² in his examination of the stability of an I-section beam in plane bending. In a later investigation, TIMOSHENKO (1945)⁴ considered the stability of a thin-walled member subjected to bending and compression as illustrated in Fig. I.10. In his analysis, he derived general equations of equilibrium for the buckled form of the member due to the bending and compressive force actions. These equations assumed that the effect of the force P on the bending

stresses could be neglected and that the longitudinal stress at any point was independent of z . The equations are of the following form

$$\begin{aligned}
 EI_y \frac{d^4 u}{dz^4} + P \frac{d^2 u}{dz^2} + (Py_c + M_x) \frac{d^2 \beta}{dz^2} &= 0 \\
 EI_x \frac{d^4 v}{dz^4} + P \frac{d^2 v}{dz^2} - (Px_c - M_y) \frac{d^2 \beta}{dz^2} &= 0 \\
 EI \frac{d^4 \beta}{dz^4} - (GC + M_x \alpha_1 - M_y \alpha_2 - Pr_c^2) \frac{d^2 \beta}{dz^2} \\
 + (Py_c + M_x) \frac{d^2 u}{dz^2} - (Px_c - M_y) \frac{d^2 v}{dz^2} &= 0
 \end{aligned} \tag{I.4.5}$$

where

$$\begin{aligned}
 \alpha_1 &= \frac{\int_A y^3 dA + \int_A x^2 y dA}{I_x} - 2y_c \\
 \alpha_2 &= \frac{\int_A x^3 dA + \int_A x y^2 dA}{I_y} - 2x_c
 \end{aligned}$$

If bending only is present, then the appropriate governing equations can be obtained by putting $P = 0$ in equations I.4.5, thus

$$\begin{aligned}
 EI_y \frac{d^4 u}{dz^4} + M_x \frac{d^2 \beta}{dz^2} &= 0 \\
 EI_x \frac{d^4 v}{dz^4} + M_y \frac{d^2 \beta}{dz^2} &= 0 \\
 EI \frac{d^4 \beta}{dz^4} - (GC + M_x \alpha_1 - M_y \alpha_2) \frac{d^2 \beta}{dz^2} \\
 + M_x \frac{d^2 u}{dz^2} + M_y \frac{d^2 v}{dz^2} &= 0
 \end{aligned} \tag{I.4.6}$$

Timoshenko then considered the particular case of a beam having a flexural rigidity in one principal

plane many times greater than in the other and subjected to pure bending in the plane of greater rigidity. Assuming that the $\psi\beta$ plane is the plane of greater rigidity and that the beam is bent in this plane by couples M_x , the following expression for the critical value of M_x can be obtained, using the first and last of equations I.4.6, thus

$$(M_x)_c = \frac{P_1 \alpha_1}{2} \pm \sqrt{\frac{P_1^2 \alpha_1^2}{4} + P_1 P_3 r_c^2} \quad \text{I.4.7}$$

where

$$P_1 = \frac{\pi^2 E I_y}{L^2}, \quad P_2 = \frac{\pi^2 E I_x}{L^2}, \quad P_3 = \frac{1}{r_c^2} (G C + E I \frac{\pi^2}{L^2})$$

$$r_c^2 = x_c^2 + y_c^2 + \frac{I_x + I_y}{A}$$

Timoshenko indicated that the constant α_1 vanished from equation I.4.7 for a section with

- (i) two axes of symmetry
- (ii) point symmetry as in the case of a zed section
- (iii) one axis of symmetry with the bending couples acting in the plane perpendicular to that axis of symmetry.

Thus, for any of these cases the expression for the critical bending moment became

$$(M_x)_c = \sqrt{P_1 P_2 \gamma_c^2} = \frac{\pi}{L} \sqrt{EI_y \left(E\Gamma \frac{\pi^2}{L^2} + GC \right)} \quad \text{I.4.8}$$

It is to be noted that the conditions which apply to the constant α_1 are comparable with those indicated by GOODIER (1950)²² for the constant K . Both these constants arise from considering the effect of initial axial bending stresses on the torsional behaviour of the beam section. The only difference between them is one of definition. Thus, Goodier's constant K , which does not include the appropriate second moment of area, is defined with the shear centre as the origin of co-ordinates. The constant α_1 derived by Timoshenko, refers to an origin of co-ordinates at the centroid of the section and includes the appropriate second moment of area.

In deriving equations I.4.7 and I.4.8, it was assumed that EI_y was small in comparison with EI_x . Timoshenko indicated that if GC and $E\Gamma$ were also small, then buckling would occur at small values of M_x . If EI_x was of the same order as EI_y lateral buckling would occur at small values of M_x only if GC and $E\Gamma$ were very small.

The results described so far have considered bars bent by couples applied at the ends which produce

longitudinal stresses independent of z . For this form of loading, the coefficients of the terms in equations I.4.5 are constant. If, however, the bar is bent by transverse load, the longitudinal stresses vary with z and a system of linear conditions with variable coefficients is obtained. Timoshenko pointed out that for this situation the calculation of critical values of loads became more involved and had been obtained only for the simple cases of single transverse loads or uniformly distributed loads. Several cases of this kind have been discussed by TIMOSHENKO (1905)¹¹, (1910)³² and (1936)³³, and also by VLASOV (1940)⁵.

The values of critical bending moment calculated from the equations which have been included in this review, have corresponded to the condition of failure by 'general buckling'. This form of buckling involves translation and rotation of the beam cross-sections, but excludes distortion of the cross-section. Failure can also occur due to 'local buckling' of the plate elements forming the beam section when such elements are in compression. In local buckling, the cross-sections are distorted in their own plane. The analysis of this form of buckling has been developed from the results of investigations into the buckling

behaviour of thin plates subjected to end compressive stress and with various edge support conditions.

A review of the more important aspects of the local buckling failure of thin-walled beams has been presented by RICHARDS (1947)³⁴ and CHILVER (1961)³⁵.

I.5 Critical Summary

The review of published work on bending and torsion of thin-walled open sections has shown that much of the theoretical analysis was developed from investigations on the corresponding behaviour of conventional hot-rolled sections. Due to the approximations used in the methods of analysis, the resulting solutions have been limited usually to small displacement problems. This is illustrated in the analysis of stable flexural-torsional behaviour of thin-walled members, presented by TIMOSHENKO and VLASOV, where bending and torsion effects are treated separately. The stresses due to bending moments are calculated from simple bending theory and the angle of twist and warping stresses are obtained from the solution of the non-uniform torsion equation. Additional components of torque and bending moment due to axial displacement were not considered. The omission of these components is valid only if the displacements are small.

VLASOV's proposition, derived from the analogy between the basic equations of the theory of bending and those of his own theory of restrained torsion, makes it possible to use techniques of analysis

developed for the simple theory of bending, for the solution of restrained torsion problems. This approach to the analysis of the flexural-torsional behaviour of beams does not appear to have been fully appreciated by other investigators.

The theoretical analysis of bending and torsion effects in girders, presented by TERRINGTON, is also limited to stable small displacement behaviour. His solution, however, was developed from differential equations of equilibrium which included components of bending moment and torque due to axial displacement. In allowing for these components, small angle approximations are used and in obtaining his final solution, terms of the second order of small quantities are neglected. WINTER, LANSING and McCALLEY used equations of bending moment and torque equilibrium, similar to those of TERRINGTON, in their investigation of the flexural-torsional behaviour of thin-walled channel sections. Their analysis is also limited by small angle approximations.

In all the solutions described so far, the effect of initial axial stress on the torsional rigidity of the member was not considered. This effect was included by TIMOSHENKO and VLASOV in their

general equations of equilibrium for the buckled form of a beam subjected to bending and compression. These equations, which were used in the analysis of the unstable flexural-torsional behaviour range of thin-walled members, also considered components of bending moment and torque due to axial displacement. They did not include, however, the action of externally applied torques.

The detailed investigations of torsional rigidity changes due to initial axial stress, carried out by ENGEL and GOODIER, indicated more clearly the conditions that could lead to torsional buckling of beams. They also appear to have been the first to consider nonlinear torque/angle of twist relationships due to combined bending and torsion effects. Previously, the phenomenon of nonlinearity had been considered only in the 'shortening effect' of torsion discussed by WEBER, CULLIMORE and GREGORY. In their theoretical analysis, ENGEL and GOODIER did not consider either the 'shortening effect' or the effects of axial displacement, although they calculated theoretical values of twist of more than 2 radians. However, in their experimental work they did not measure such high angles of twist and did not obtain

the torque/angle of twist relationship in the unstable range of behaviour.

In the theoretical investigations which have been discussed, no single solution has considered all the specific effects associated with stable and unstable flexural-torsional behaviour. This can be seen in TABLE I.1 which indicates the terms considered in the more significant investigations included in the review.

AUTHOR	TERMS INCLUDED					BEHAVIOUR RANGE
	GC	$E\Gamma$	M , T COMPONENTS	INITIAL AXIAL STRESS	SHORTENING EFFECT	
TIMOSHENKO	*	*				STABLE
VLASOV	*	*				
TERRINGTON	*	*	*			
GOODIER	*	*		*		
WINTER	*	*	*			
GREGORY	*	*		*	*	
TIMOSHENKO	*	*	*	*		UNSTABLE
VLASOV	*	*	*	*		
PRANDTL/ MICHELL	*		*			
REISSNER	*		*			
GOODIER	*			*		

TABLE I.1

All the solutions for flexural-torsional beam behaviour which have been discussed were derived on the basis of small displacement approximations and cannot be applied satisfactorily to the more general large displacement problems.

The theoretical and experimental investigations presented in this thesis were planned both to reassess and to extend the applicability of the current theoretical approaches. In this sense, the theoretical treatment, suggested by VLASOV, is employed for the analysis of small displacement problems. Thereafter, the differential equations of bending moment and torque equilibrium are generalised by including in them all the additional effects which have been indicated in previous investigations.

These equations are then used for the theoretical analysis of large deformations in the nonlinear stable and unstable ranges of flexural-torsional behaviour. Experimental evidence of both stable and unstable flexural-torsional behaviour is presented.

CHAPTER II

THEORETICAL ANALYSIS

The treatment of linear small displacement problems is based on the analogy between the basic equations of the theory of bending and those of the theory of restrained torsion, as observed by VLASOV. To obtain a solution for large nonlinear elastic displacements, the basic differential equations of bending moment and torque equilibrium are generalised to include all the additional effects described in previous investigations. Particular solutions of these equations using a single term Galerkin technique are outlined and nonlinear stable and unstable torque/angle of twist equilibrium paths are predicted. This analysis is then used to derive an expression for the critical bending moment causing flexural-torsional instability.

II.1 Linear Small Displacement Flexural-Torsional Behaviour of Thin-Walled Open Section Beams

The basic differential equations defining the displacements u , v and β at any section z of a beam subjected to combined bending and torsion, can be written as

$$\begin{aligned} EI_x \frac{d^4 v}{dz^4} &= q_y \\ EI_y \frac{d^4 u}{dz^4} &= q_x \\ EI \frac{d^4 \beta}{dz^4} - GC \frac{d^2 \beta}{dz^2} &= m \end{aligned}$$

II.1.1

The first two of equations II.1.1 can be solved using the simple theory of bending and are presented more frequently in terms of bending moment, thus:

$$\begin{aligned} EI_x \frac{d^2 v}{dz^2} &= -M_x \\ EI_y \frac{d^2 u}{dz^2} &= M_y \end{aligned} \quad \text{II.1.2}$$

The last of equations II.1.1 is the non-uniform torsion equation differentiated with respect to z , thus:

$$\frac{d}{dz} \left(EI \frac{d^3 \beta}{dz^3} - GC \frac{d\beta}{dz} + T \right) = 0 \quad \text{II.1.3}$$

which gives

$$EI \frac{d^4 \beta}{dz^4} - GC \frac{d^2 \beta}{dz^2} = m \quad \text{II.1.4}$$

where $m = -\frac{dT}{dz}$ is the intensity of a uniformly distributed torque.

The force action associated with equation II.1.4 is Vlasov's 'bi-moment' B and is defined by the expression

$$B = -EI \frac{d^2 \beta}{dz^2} \quad \text{II.1.5}$$

The longitudinal stresses at any point x , y , z in a beam cross-section produced by the moments M_x and M_y and the bi-moment B are

$$\frac{M_x \cdot y}{I_x} ; \frac{M_y \cdot x}{I_y} ; \frac{B \omega}{r'} \quad \text{II.1.6}$$

In the last of expressions II.1.6, the symbol ω is defined as the 'sectorial co-ordinate' and is found for any point in the beam cross-section, from the expression

$$\omega = \int^s h \cdot ds \quad \text{II.1.7}$$

where h is the perpendicular distance from the shear centre to a tangent at the point and s is the distance from a pole to the point measured along the middle line of the section.

To illustrate the calculation of the sectorial co-ordinate, the case of a channel section as shown in Fig. II.1 is considered. The point A is the shear centre and D, the point where the axis of symmetry intersects the web, is the pole. The value of the sectorial co-ordinate at the point p on the web is given by the product $(e \cdot s)$ and is twice the area swept by a radius vector AM rotating from AD to Ap. The sign of the sectorial co-ordinate at any point is positive if the radius vector rotates clockwise to reach the point.

A diagrammatic representation of the sectorial

co-ordinate at any point in a channel section of depth d and breadth b is shown in Fig. II.2. The values for the points of the web below the AX axis are positive, since the radius vector is rotating clockwise. For the flange, the sectorial co-ordinate decreases as the distance from the web increases. At the point C , which is the same distance from the web as the shear centre A is from the pole D , the sectorial co-ordinate is zero. Thereafter, the value is of opposite sign and increases linearly to a maximum at the free edge of the flange. Thus, the maximum longitudinal stresses due to the bi-moment occur at the web to flange junction and the free edge of the flange.

The value of the bi-moment B is found from the solution of equation II.1.4, which can be transformed in terms of B and expressed as

$$\frac{d^2 B}{dz^2} - \lambda^2 B = -\pi \quad \text{II.1.8}$$

$$\text{where } \lambda = \sqrt{\frac{GC}{EI}} \quad \text{II.1.9}$$

The general solution of equation II.1.8 is of the form

$$B = C_1 \sinh \lambda z + C_2 \cosh \lambda z + B_0 \quad \text{II.1.10}$$

where C_1 and C_2 are constants which can be determined in any particular case, by the loading and

boundary conditions, and B_0 is the particular solution. If a uniformly distributed torque is present then

$$B_0 = \frac{m}{\lambda^2} \quad \text{II.1.11}$$

If the beam is subjected to concentrated torques, the particular solution is zero.

The principal forms of boundary conditions at the ends of a beam are

(i) Fixed end $\beta = 0$, $\frac{d\beta}{dz} = 0$

(ii) Simply supported (angular deformation restrained)

$$\beta = 0 , \frac{d^2\beta}{dz^2} = 0 \quad \text{hence} \quad B = 0$$

(iii) Free end

$$\frac{d^2\beta}{dz^2} = 0 \quad \text{hence} \quad B = 0 , T (\text{torque}) = 0$$

Additional conditions can obtain in symmetrical problems as will be indicated in the following examples of solution of equation II.1.8.

CASE I

A beam subjected to a concentrated torque T at the centre of the span L as shown in Fig. II.3. The end conditions are simply supported with angular deformation restrained. This is a symmetrical problem

and the general solution need only be found for a half span, that is $0 \leq z < \frac{L}{2}$. The boundary conditions

are $(z=0, B=0)$ and $(z=\frac{L}{2}, \frac{dB}{dz}=\frac{T}{2})$ II.1.12

The second condition is obtained from equation II.1.3

noting that at $z=\frac{L}{2}, \frac{d\beta}{dz}=0$

The general solution for B is thus:

$$\begin{matrix} B \\ 0 \leq z < \frac{L}{2} \end{matrix} = C_1 \sinh \lambda z + C_2 \cosh \lambda z \quad \text{II.1.13}$$

$$\begin{matrix} \frac{dB}{dz} \\ 0 \leq z < \frac{L}{2} \end{matrix} = \lambda C_1 \cosh \lambda z + \lambda C_2 \sinh \lambda z \quad \text{II.1.14}$$

Using the boundary conditions II.1.12, the constants are

$$C_1 = \frac{T}{2\lambda \cosh \frac{\lambda L}{2}} \quad \text{and} \quad C_2 = 0 \quad \text{II.1.15}$$

Thus

$$\begin{matrix} B \\ 0 \leq z < \frac{L}{2} \end{matrix} = \frac{T \sinh \lambda z}{2\lambda \cosh \frac{\lambda L}{2}} \quad \text{II.1.16}$$

This general solution for B can now be used to obtain the corresponding solution for the angle of twist β , thus from equation II.1.5

$$\frac{d^2 \beta}{dz^2} = - \frac{B}{EI} \quad \text{II.1.17}$$

and substituting for B from equation II.1.16, then

$$\frac{d^2\beta}{dz^2} = -\frac{1}{EI} \cdot \frac{T \sinh \lambda z}{2\lambda \cosh \frac{\lambda L}{2}} \quad \text{II.1.18}$$

Thus, by integration

$$\frac{d\beta}{dz} = -\frac{1}{EI} \cdot \frac{T \cosh \lambda z}{2\lambda^2 \cosh \frac{\lambda L}{2}} + A_1 \quad \text{II.1.19}$$

$$\beta = -\frac{1}{EI} \cdot \frac{T \sinh \lambda z}{2\lambda^3 \cosh \frac{\lambda L}{2}} + A_1 z + B_1 \quad \text{II.1.20}$$

Using the boundary conditions ($z = 0, \beta = 0$) and ($z = \frac{L}{2}, \frac{d\beta}{dz} = 0$) the values of the integration constants are

$$A_1 = \frac{T}{2EI\lambda^2} \quad \text{and} \quad B_1 = 0$$

Thus

$$\beta = -\frac{1}{EI} \cdot \frac{T \sinh \lambda z}{2\lambda^3 \cosh \frac{\lambda L}{2}} + \frac{T}{2EI\lambda^2} \cdot z \quad \text{II.1.21}$$

$0 \leq z < \frac{L}{2}$

CASE II

A beam subjected to a uniformly distributed torque m per unit length, of span L as shown in Fig. II.4. The end conditions are simply supported with angular deformation restrained. The boundary conditions are

$$(z=0, \beta=0) \quad \text{and} \quad (z=L, \beta=0) \quad \text{II.1.22}$$

The general solution for B is thus

$$B = C_1 \sinh \lambda z + C_2 \cosh \lambda z + \frac{m}{\lambda^2} \quad 0 \leq z < L \quad \text{II.1.23}$$

Using the boundary conditions II.1.22 the constants are

$$C_1 = \frac{m}{\lambda^2} \cdot \frac{\cosh \lambda L - 1}{\sinh \lambda L} \quad \text{and} \quad C_2 = -\frac{m}{\lambda^2} \quad \text{II.1.24}$$

Thus

$$B = \frac{m}{\lambda^2} \left(\frac{\cosh \lambda L - 1}{\sinh \lambda L} \cdot \sinh \lambda z - \cosh \lambda z + 1 \right) \quad 0 \leq z < L \quad \text{II.1.25}$$

As before, this general solution for B can be used to obtain the corresponding general solution for the angle of twist. Thus, substituting for B from equation II.1.25 in equation II.1.17 then

$$\frac{d^2 \beta}{dz^2} = -\frac{m}{E \Gamma \lambda^2} \left(\frac{\cosh \lambda L - 1}{\sinh \lambda L} \cdot \sinh \lambda z - \cosh \lambda z + 1 \right) \quad \text{II.1.26}$$

Thus, by integration

$$\frac{d\beta}{dz} = -\frac{m}{E \Gamma \lambda^2} \left(\frac{\cosh \lambda L - 1}{\sinh \lambda L} \cdot \frac{\cosh \lambda z}{\lambda} - \frac{\sinh \lambda z}{\lambda} + z \right) + A_2 \quad \text{II.1.27}$$

$$\beta = -\frac{m}{E \Gamma \lambda^2} \left(\frac{\cosh \lambda L - 1}{\sinh \lambda L} \cdot \frac{\sinh \lambda z}{\lambda^2} - \frac{\cosh \lambda z}{\lambda^2} + \frac{z^2}{2} \right) + A_2 z + B_2 \quad \text{II.1.28}$$

Using the boundary conditions ($z = 0, \beta = 0$) and ($z = L, \beta = 0$), the values of the integration constants are

$$A_2 = \frac{mL}{2E\Gamma\lambda^2} \quad \text{and} \quad B_2 = -\frac{m}{E\Gamma\lambda^4}$$

Thus

$$\begin{aligned} \beta_{0 \leq z < L} = & -\frac{m}{E\Gamma\lambda^2} \left(\frac{\cosh \lambda L - 1}{\sinh \lambda L} \cdot \frac{\sinh \lambda z}{\lambda^2} - \frac{\cosh \lambda z}{\lambda^2} + \frac{z^2}{2} \right) \\ & + \frac{mL}{2E\Gamma\lambda^2} \cdot z - \frac{m}{E\Gamma\lambda^4} \end{aligned} \quad \text{II.1.29}$$

Similar forms of solution for B and β can be obtained for other cases of loading and end conditions. Such solutions increase in complexity when the beam is subjected to unsymmetrical combinations of concentrated and uniformly distributed torque actions. However, in dealing with thin-walled sections, the analysis usually can be simplified due to the relative magnitudes of the torsional rigidity GC and the warping rigidity $E\Gamma$. Thus, for a thin-walled open section $E\Gamma$ usually is many times larger than GC and consequently, in practice, approximate solutions for B and β can be obtained by neglecting the GC term in equation II.1.4. The resulting equation becomes

$$E\Gamma \frac{d^4 \beta}{dz^4} = m \quad \text{II.1.30}$$

The solution of equation I.1.30 is obtained by the methods used for the solution of the basic equation of the simple theory of bending, that is

$$EI_x \frac{d^4 v}{dz^4} = q_y \quad \text{II.1.31}$$

In developing the solution, singularity functions are used to define the intensity of loading on the beam. Thus, consider the case of a beam of span L subjected to a concentrated torque T at a distance a from one end, as shown in Fig. II.5. The ends of the beam are simply supported with angular deformation restrained.

From the analogous case of a simply supported beam carrying a concentrated load W at a distance a from one end, the values of the reaction torques at the supports will correspond to the support reactions in the plane bending problem, thus

$$T_0 = -\frac{T(L-a)}{L} \quad \text{and} \quad T_L = -\frac{Ta}{L} \quad \text{II.1.32}$$

The intensity of loading m in terms of the applied and reaction torques is given by the expression

$$m = -\frac{T(L-a)}{L} \langle z \rangle_{-1} + T \langle z-a \rangle_{-1} - \frac{Ta}{L} \langle z-L \rangle_{-1} \quad \text{II.1.33}$$

where $\langle z \rangle_{-1}$, $\langle z-a \rangle_{-1}$, and $\langle z-L \rangle_{-1}$ are singularity functions as used in the Macauley analysis for beam deflections.

Thus, from equation II.1.30

$$\begin{aligned} E\Gamma \frac{d^4\beta}{dz^4} &= m \\ &= -\frac{T(L-a)}{L} \langle z \rangle_{-1}^+ + T \langle z-a \rangle_{-1}^- - \frac{Ta}{L} \langle z-L \rangle_{-1}^- \end{aligned} \quad \text{II.1.34}$$

by integration

$$\begin{aligned} E\Gamma \frac{d^3\beta}{dz^3} &= -\frac{T(L-a)}{L} \langle z \rangle^0 + T \langle z-a \rangle^0 - \frac{Ta}{L} \langle z-L \rangle^0 + C_1 \\ E\Gamma \frac{d^2\beta}{dz^2} &= -\frac{T(L-a)}{L} \langle z \rangle' + T \langle z-a \rangle' - \frac{Ta}{L} \langle z-L \rangle' + C_1 z + C_2 \\ E\Gamma \frac{d\beta}{dz} &= -\frac{T(L-a)}{2L} \langle z \rangle^2 + \frac{T}{2} \langle z-a \rangle^2 - \frac{Ta}{2L} \langle z-L \rangle^2 \\ &\quad + \frac{C_1}{2} z^2 + C_2 z + C_3 \\ E\Gamma \beta &= -\frac{T(L-a)}{6L} \langle z \rangle^3 + \frac{T}{6} \langle z-a \rangle^3 - \frac{Ta}{6L} \langle z-L \rangle^3 \\ &\quad + \frac{C_1}{6} z^3 + \frac{C_2}{2} z^2 + C_3 z + C_4 \end{aligned} \quad \text{II.1.35}$$

The terms involving singularity functions vanish when the bracket $\langle \rangle$ is zero or negative. Using the boundary conditions

$$\begin{aligned} (z=0, \beta = \frac{d^2\beta}{dz^2} = 0) \text{ and} \\ (z=L, \beta = \frac{d^2\beta}{dz^2} = 0) \end{aligned} \quad \text{II.1.36}$$

The values of the integration constants are

$$C_1 = C_2 = C_4 = 0 \quad \text{and} \quad C_3 = \frac{TL(L-a)}{6} - \frac{T(L-a)^3}{6L}$$

Thus, the expression for the bi-moment is obtained from the second of equations II.1.35 as

$$B = -EI \frac{d^2 \beta}{dz^2}$$

Thus

$$B = \frac{T(L-a)}{L} \langle z \rangle' - T \langle z-a \rangle' + \frac{Ta}{L} \langle z-L \rangle' \quad \text{II.1.37}$$

and if $(L-a) = b$ then at $z = a$

$$B = \frac{Tab}{L} \quad \text{II.1.38}$$

The expression for the angle of twist is given by the last of equations II.1.35 as

$$\begin{aligned} \beta = \frac{1}{EI} \left[-\frac{T(L-a)}{6L} \langle z \rangle^3 + \frac{T}{6} \langle z-a \rangle^3 - \frac{Ta}{6L} \langle z-L \rangle^3 \right. \\ \left. + \frac{TL(L-a)}{6} \cdot z - \frac{T(L-a)^3}{6L} \cdot z \right] \quad \text{II.1.39} \end{aligned}$$

as before, if $(L-a) = b$ then at $z = a$

$$\beta = \frac{Ta^2 b^2}{3EIL} \quad \text{II.1.40}$$

These values of B and β are analogous to the corresponding plane bending results, thus

$$M = \frac{Wab}{L} \quad \text{and} \quad \nu = \frac{Wa^2 b^2}{3EI_x L} \quad \text{II.1.41}$$

The analogy is also observed in the distribution diagrams of torque and shear, and bi-moment and bending moment as shown in Fig. II.6.

If $a = b = \frac{L}{2}$, as in the closed solution for Case I, then the bi-moment B at $z' = \frac{L}{2}$ becomes

$$\begin{aligned} B &= \frac{T \frac{L}{2} \cdot \frac{L}{2}}{L} \\ &= \frac{TL}{4} \end{aligned} \quad \text{II.1.42}$$

and the corresponding angle of twist at $z = \frac{L}{2}$ is

$$\begin{aligned} \beta &= \frac{T \left(\frac{L}{2}\right)^2 \left(\frac{L}{2}\right)^2}{3EI_L} \\ &= \frac{TL^3}{48EI} \end{aligned} \quad \text{II.1.43}$$

These values are also analogous to the corresponding plane bending results for a central point load, that is

$$M = \frac{WL}{4} \quad \text{and} \quad v = \frac{WL^3}{48EI_x} \quad \text{II.1.44}$$

In the case of a uniformly distributed torque of intensity m /unit length, the solution is obtained as follows

$$EI \frac{d^4 \beta}{dz^4} = m \quad \text{II.1.45}$$

by integration

$$EI \frac{d^3\beta}{dz^3} = mz + C_1$$

$$EI \frac{d^2\beta}{dz^2} = \frac{m}{2} z^2 + C_1 z + C_2$$

$$EI \frac{d\beta}{dz} = \frac{m}{6} z^3 + \frac{C_1}{2} z^2 + C_2 z + C_3$$

$$EI \beta = \frac{m}{24} z^4 + \frac{C_1}{6} z^3 + \frac{C_2}{2} z^2 + C_3 z + C_4$$

II.1.46

As before, the appropriate boundary conditions are

$$(z=0, \beta = \frac{d^2\beta}{dz^2} = 0) \text{ and}$$

$$(z=L, \beta = \frac{d^2\beta}{dz^2} = 0)$$

II.1.47

The values of the integration constants are

$$C_2 = C_4 = 0, \quad C_1 = -\frac{mL}{2} \text{ and } C_3 = \frac{mL^3}{24}$$

Thus, the expression for the bi-moment is obtained from the second of equations II.1.46 as

$$B = -EI \frac{d^2\beta}{dz^2}$$

Thus

$$B = -\frac{m}{2} z^2 + \frac{mL}{2} z$$

II.1.48

and at $z = \frac{L}{2}$, the value of B is

$$\begin{aligned}
 \beta &= -\frac{m}{2} \left(\frac{L}{2} \right) \left(\frac{L}{2} \right) + \frac{mL}{2} \left(\frac{L}{2} \right) \\
 &= \frac{mL^2}{8}
 \end{aligned}
 \tag{II.1.49}$$

The expression for the angle of twist is found from the last of equations II.1.46 as

$$\beta = \frac{1}{EI} \left(\frac{m}{24} z^4 - \frac{mL}{12} z^3 + \frac{mL^3}{24} z \right)
 \tag{II.1.50}$$

again at $z = \frac{L}{2}$

$$\begin{aligned}
 \beta &= \frac{1}{EI} \left[\frac{m}{24} \left(\frac{L}{2} \right)^4 - \frac{mL}{12} \left(\frac{L}{2} \right)^3 + \frac{mL^3}{24} \left(\frac{L}{2} \right) \right] \\
 &= \frac{5 mL^4}{384 EI}
 \end{aligned}
 \tag{II.1.51}$$

Once again these values are analogous to the corresponding plane bending results, that is

$$M = \frac{wL^2}{8} \quad \text{and} \quad v = \frac{5wL^4}{384 EI_x}
 \tag{II.1.52}$$

A summary of the results from these approximate analyses for the problem of restrained torsion compared with the corresponding values for the analogous plane bending problem is given in TABLE II.1.

The analyses which have been presented have illustrated how values of bi-moment and angle of twist can be obtained without difficulty if the St. Venant torsional rigidity is neglected in the solution of the

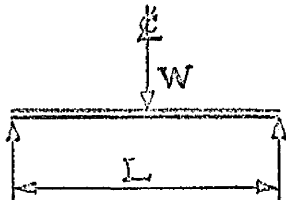
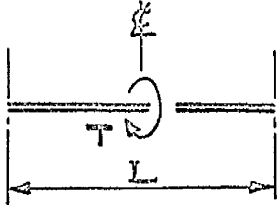
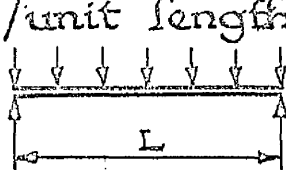
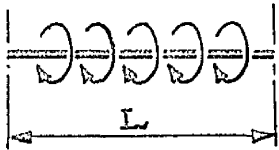
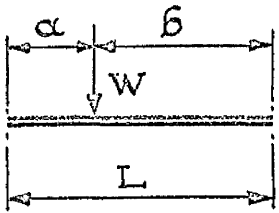
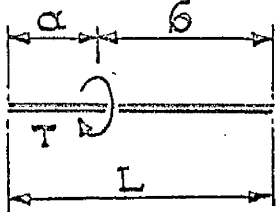
BEAM LOADING	BI - MOMENT B OR BENDING MOMENT M.	ANGLE OF TWIST β OR VERTICAL DEFLECTION y
	$M \text{ at } z = \frac{L}{2}$ $= \frac{WL}{4}$	$y \text{ at } z = \frac{L}{2}$ $= \frac{WL^3}{48EI}$
	$B \text{ at } z = \frac{L}{2}$ $= \frac{TL}{4}$	$\beta \text{ at } z = \frac{L}{2}$ $= \frac{TL^3}{48EI}$
ω /unit length 	$M \text{ at } z = \frac{L}{2}$ $= \frac{\omega L^2}{8}$	$y \text{ at } z = \frac{L}{2}$ $= \frac{5\omega L^4}{384EI}$
m /unit length 	$B \text{ at } z = \frac{L}{2}$ $= \frac{mL^2}{8}$	$\beta \text{ at } z = \frac{L}{2}$ $= \frac{5mL^4}{384EI}$
	$M \text{ at } z = \alpha$ $= \frac{W\alpha\beta}{L}$	$y \text{ at } z = \alpha$ $= \frac{W\alpha^2\beta^2}{3EIL}$
	$B \text{ at } z = \alpha$ $= \frac{T\alpha\beta}{L}$	$\beta \text{ at } z = \alpha$ $= \frac{T\alpha^2\beta^2}{3EFL}$

TABLE II. 1.

non-uniform torsion equation. The magnitude of the errors arising from this approximation can be estimated by comparing the true and approximate values of bi-moment and angle of twist for different values of the beam parameter λL .

Thus, for the case of a concentrated torque at mid-span of a simply supported beam with ends restrained from angular deformation, the true and approximate expressions for bi-moment and angle of twist at mid-span are

$$B_{true} = \frac{T \tanh \frac{\lambda L}{2}}{2\lambda}, \quad B_{approx.} = \frac{TL}{4} \quad \text{II.1.53}$$

$$\beta_{true} = \frac{TL}{4E\Gamma\lambda^2} - \frac{T \tanh \frac{\lambda L}{2}}{2E\Gamma\lambda^3}, \quad \beta_{approx.} = \frac{TL^3}{48E\Gamma} \quad \text{II.1.54}$$

Introducing the symbols f_1 and f_2 for the bi-moment and angle of twist coefficients, defined as

$$f_1 = \frac{B}{TL} \quad \text{and} \quad f_2 = \frac{\beta}{\frac{TL^3}{E\Gamma}} \quad \text{II.1.55}$$

then for the approximate solution

$$f_1 = \frac{\frac{TL}{4}}{TL} = 0.25 \quad \text{and} \quad f_2 = \frac{\frac{TL^3}{48E\Gamma}}{\frac{TL^3}{E\Gamma}} = 0.0208 \quad \text{II.1.56}$$

The expressions for the true values of f_1 and f_2 are

$$f_1 = \frac{\tanh \frac{\lambda L}{2}}{2\lambda L} \quad \text{and} \quad f_2 = \left[\frac{1}{4(\lambda L)^2} - \frac{\tanh \frac{\lambda L}{2}}{2(\lambda L)^3} \right] \quad \text{II.1.57}$$

Using equations II.1.57 the variation of f_1 and f_2 with λL in the range $0 < \lambda L < 1.5$ is shown graphically in Fig. II.7 and compared with the constant approximate values.

From this analysis, it is seen that as λL increases, the true value of the coefficients f_1 and f_2 decrease. The errors at $\lambda L = 1$, expressed as a percentage of the true values are approximately +8.25% for f_1 and +9.50% for f_2 . Thus, the approximate solution tends to give higher values of bi-moment and angle of twist and when used for practical design problems will yield conservative results.

This approach to the analysis of torsional behaviour cannot be used for beam sections, such as angles or tees, for which the torsion bending constant is zero, since by definition, the bi-moment will also be zero. The torsional behaviour of these sections in the linear small displacement range can be analysed using the St. Venant torque/angle of twist relationship,

$$T = GC \frac{d\beta}{dz} \quad \text{II.1.58}$$

II.2 Nonlinear Large Displacement Flexural-Torsional Behaviour of Thin-Walled Open Section Beams

In the analysis of large displacement flexural-torsional behaviour of thin-walled open sections, it is necessary to allow for additional effects in the formulation of the basic differential equations of bending moment and torque equilibrium. These effects are

- (i) components of moment and torque due to axial displacement
- (ii) changes in the St. Venant torsional rigidity due to initial axial bending stress
- (iii) components of torque due to the longitudinal stress system of the 'shortening effect'
- (iv) components of torque due to the displacements of the points of application of the loads.

The first of these conditions is catered for by considering the differential equations of equilibrium of bending moment and torque relative to the displaced

axes of the member. Thus, for a positive system of axes, ox , oy and oz as shown in Fig. II.8, where oz is the longitudinal axis through the shear centres, the values of bending moments and torque at any section z , relative to the displaced axes ox' , oy' and oz' , due to applied bending moments, $+M_x$ and $+M_y$, and torque $+M_z$, are given by

$$M_{x'} = M_x \cos \beta + M_y \sin \beta - M_z \frac{d\bar{u}}{dz}$$

$$M_{y'} = M_y \cos \beta - M_x \sin \beta - M_z \frac{d\bar{v}}{dz}$$

$$M_{z'} = M_z + M_x \frac{d\bar{u}}{dz} + M_y \frac{d\bar{v}}{dz} \quad \text{II.2.1}$$

In deriving these equations, the approximations

$$\tan \frac{d\bar{u}}{dz} = \frac{d\bar{u}}{dz} \quad \text{and} \quad \tan \frac{d\bar{v}}{dz} = \frac{d\bar{v}}{dz} \quad \text{have been used.}$$

This leads to the other approximations of

$$\sin \frac{d\bar{u}}{dz} = \frac{d\bar{u}}{dz}, \quad \cos \frac{d\bar{u}}{dz} = 1, \quad \sin \frac{d\bar{v}}{dz} = \frac{d\bar{v}}{dz} \quad \text{and} \quad \cos \frac{d\bar{v}}{dz} = 1$$

These approximations are considered acceptable, for although the angle of twist is large, the flexural displacements are still of the order where $\frac{d\bar{u}}{dz}$ and $\frac{d\bar{v}}{dz} \ll 1$. The values of the bending moments $M_{x'}$, and $M_{y'}$, and torque $M_{z'}$, obtained from equations II.2.1 can now be substituted into the appropriate

differential equations of equilibrium for bending moments and torque about the displaced axes, thus

$$\begin{aligned} EI_x \frac{d^2 v}{dz^2} &= -M_{x'} = -M_x \cos \beta - M_y \sin \beta + M_z \frac{d\bar{u}}{dz} \\ EI_y \frac{d^2 u}{dz^2} &= M_{y'} = M_y \cos \beta - M_x \sin \beta - M_z \frac{d\bar{v}}{dz} \\ GC \frac{d\beta}{dz} - EI \frac{d^3 \beta}{dz^3} &= M_{z'} = M_z + M_x \frac{d\bar{u}}{dz} + M_y \frac{d\bar{v}}{dz} \end{aligned} \quad \text{II.2.2}$$

The deflections v and u which appear in the first two of equations II.2.2 are taken to be in the direction of the displaced axes oy' and ox' respectively. The values of the deflections \bar{u} and \bar{v} , relative to the undisplaced axes ox and oy in terms of u and v , can be seen from Fig. II.9 to be given by the expressions

$$\begin{aligned} \bar{u} &= u \cos \beta - v \sin \beta \\ \bar{v} &= u \sin \beta + v \cos \beta \end{aligned} \quad \text{II.2.3}$$

For initial axial bending stress the coefficient of the St. Venant torsional rigidity term becomes, according to the present sign convention

$$\left(GC - \frac{K_y M_{y'}}{I_y} + \frac{K_x M_{x'}}{I_x} \right) \quad \text{II.2.4}$$

where K is the geometrical constant of the section

defined by GOODIER^{22,27} as

$$K_x = \iint (y - y_g)^2 R^2 dx dy \quad \text{and} \quad K_y = \iint (x - x_g)^2 R^2 dx dy \quad \text{II.2.5}$$

and $R^2 = x^2 + y^2$ where (x, y) are co-ordinates for a system of axes with the origin at the shear centre.

As already noted, the constant K vanishes if,

- (i) the section has two axes of symmetry,
- (ii) the section has point symmetry, for example, a zed section,
- (iii) the section has one axis of symmetry and the bending moment vector is in the same direction, that is, the axis of symmetry is normal to the plane of bending.

Additional torque action is developed by the longitudinal stress system due to the 'shortening effect', especially if large angles of twist obtain. The expression for this torque, derived by GREGORY¹⁹, in terms of the present sign convention, is as shown below and should be included in the differential equation of torque equilibrium,

$$\frac{1}{2} E \left(\frac{d\beta}{dz} \right)^3 \left(K_c - \frac{I_c^2}{A} - \frac{K_y^2}{I_y} - \frac{K_x^2}{I_x} \right) \quad \text{II.2.6}$$

where the constant K_c is given by the expression

$$K_c = \iint R^4 dx dy \quad \text{and} \quad R^2 = x^2 + y^2 \quad \text{II.2.7}$$

As before (x, y) are co-ordinates for a system of axes with the shear centre as origin.

The last effect to be considered is the torque produced by the displacement of the load points. This torque, referred to as T_D will depend on the relative displacements of the points of application of the loads and, as illustrated in Fig. 10, for the case of a load P at mid-span, its value at any section z , where

$0 \leq z < \frac{L}{2}$ is given by the expression

$$T_{Dz} = \frac{P}{2} (\bar{u}_L - \bar{u}_z) \quad \text{II.2.8}$$

$0 \leq z < \frac{L}{2}$

The generalised differential equations of bending moment and torque can now be formulated by including the expressions II.2.4, II.2.6 and II.2.8 in the last of equations II.2.2, thus

$$\begin{aligned} EI_x \frac{d^2 \bar{v}}{dz^2} &= -M_x \cos \beta - M_y \sin \beta + M_z \frac{d\bar{u}}{dz} \\ EI_y \frac{d^2 \bar{u}}{dz^2} &= M_y \cos \beta - M_x \sin \beta - M_z \frac{d\bar{v}}{dz} \\ \left(GC - \frac{K_y M_y'}{I_y} + \frac{K_x M_x'}{I_x} \right) \frac{d\beta}{dz} - EI' \frac{d^3 \beta}{dz^3} + \frac{1}{2} E \left(\frac{d\beta}{dz} \right)^3 &\left(K_c - \frac{I_c^2}{A} - \frac{K_y^2}{I_y} - \frac{K_x^2}{I_x} \right) \\ &= M_z + M_x \frac{d\bar{u}}{dz} + M_y \frac{d\bar{v}}{dz} + T_{Dz} \end{aligned} \quad \text{II.2.9}$$

The solution of these equations for particular combinations of bending moment and torque is examined in the next section.

II.3 Particular Solutions of the Generalised Differential Equations of Bending Moment and Torque Equilibrium

The generalised differential equations II.2.9, for equilibrium of bending moment and torque relative to the displaced axes of a beam, comprise a system of nonlinear differential equations which are effectively of seventh order. No mathematical techniques, available at present, give generalised solutions for such a system of equations. However, numerical solutions can be obtained in specific cases by techniques such as numerical integration, Rayleigh-Ritz or Galerkin. In the present analysis, approximate solutions for equations II.2.9 are obtained by a simplified single term Galerkin approach.

The analysis considers beams of monosymmetrical open cross-section of the type indicated in Fig. II.11. The beams are subjected to combinations of bending moment and torque which are symmetrically disposed about the mid-span position of the beam. This loading produces a maximum angle of twist at the mid-span position. The origin of the axes x , y and z coincides with the shear centre position of the cross-section and the axis of cross-sectional symmetry

lies along the x-axis. The bending moment and torque are applied in the $y\zeta$ and xy planes respectively as illustrated in Fig. II.12. The sign convention for bending moment, torque, deflections and angle of twist, used in the analyses corresponds to that adopted in the derivation of the generalised differential equations as indicated in Fig. II.8.

Four separate solutions, using different approximations for $\sin \beta$ and $\cos \beta$, and assuming nonlinear and linear forms of variation of β with ζ , are obtained. In each case, the two dependent variables u and v , are considered in terms of the third dependent variable β .

The boundary conditions used in obtaining the solutions correspond to the ends of the beam being considered as

- (i) simply supported with respect to bending moment, that is,

$$u = v = 0, \quad \frac{d^2 u}{d\zeta^2} = \frac{d^2 v}{d\zeta^2} = 0$$

- (ii) free to warp but restrained from twisting with respect to torsion,

$$\text{that is, } \beta = 0, \quad \frac{d^2 \beta}{d\zeta^2} = 0$$

Additional boundary conditions for the problem arise

due to the symmetry of loading, that is, at $z = \frac{L}{2}$

$$\frac{du}{dz} = \frac{dv}{dz} = \frac{d\beta}{dz} = 0$$

In the particular problem considered in this analysis, the x-axis is an axis of symmetry of the beam cross-section and thus $K_x = 0$. In addition, the applied bending moment is in the yz plane only, that is

$M_y = 0$, and since there are no concentrated loads

$T_{Dz} = 0$. The generalised differential equations

II.2.9 as applied to this problem can be written as

$$\begin{aligned} EI_x \frac{d^2 v}{dz^2} &= -M_x \cos \beta + M_z \frac{d\bar{u}}{dz} \\ EI_y \frac{d^2 u}{dz^2} &= -M_x \sin \beta - M_z \frac{d\bar{v}}{dz} \\ \left[GC - \frac{K_y (-M_x \sin \beta - M_z \frac{d\bar{v}}{dz})}{I_y} \right] \frac{d\beta}{dz} &- EI \frac{d^3 \beta}{dz^3} \\ + \frac{1}{2} E \left(\frac{d\beta}{dz} \right)^3 \left(K_c - \frac{I_c^2}{A} - \frac{K_y^2}{I_y} \right) &= M_z + M_x \frac{d\bar{u}}{dz} \end{aligned} \quad \text{II.3.1}$$

These equations can be further simplified by assuming

that $M_z \frac{d\bar{u}}{dz}$ and $M_z \frac{d\bar{v}}{dz}$ are small in comparison with

$M_x \cos \beta$ and $M_x \sin \beta$ and can be neglected. This

approximation is examined in Appendix VIII.2. Equations

II.3.1 can then be presented as

$$EI_x \frac{d^2 v}{dz^2} = -M_x \cos \beta$$

$$EI_y \frac{d^2 u}{dz^2} = -M_x \sin \beta$$

$$\begin{aligned} & \left(Gc + \frac{K_y M_x \sin \beta}{I_y} \right) \frac{d\beta}{dz} - EI' \frac{d^3 \beta}{dz^3} \\ & + \frac{1}{2} E \left(\frac{d\beta}{dz} \right)^3 \left(K_c - \frac{I_c^2}{A} - \frac{K_y^2}{I_y} \right) = M_z + M_x \frac{d\bar{u}}{dz} \end{aligned} \quad \text{II.3.2}$$

To solve equations II.3.2 by a simplified one term Galerkin technique, it is necessary to assume a form of variation of β with z in terms of β_0 , the maximum angle of twist at the mid-span position. This form must satisfy the boundary conditions for the problem that is, at $z = 0$, $\beta = 0$, $z = L$, $\beta = 0$ and at $z = \frac{L}{2}$ $\frac{d\beta}{dz} = 0$.

These conditions are satisfied by assuming a sine variation for β with z , thus

$$\beta_z = \beta_0 \sin \frac{\pi z}{L} \quad \text{II.3.3}$$

It is now possible to express $\frac{d\beta}{dz}$ and $\frac{d^3\beta}{dz^3}$ in terms of β_0 thus

$$\frac{d\beta}{dz} = \frac{\pi}{L} \beta_0 \cos \frac{\pi z}{L} \quad \text{and} \quad \frac{d^3\beta}{dz^3} = -\left(\frac{\pi}{L}\right)^3 \beta_0 \cos \frac{\pi z}{L} \quad \text{II.3.4}$$

The last of equations II.3.2 can now be written as

$$\begin{aligned} & \left[GC + \frac{K_y M_x \sin(\beta_0 \sin \frac{\pi z}{L})}{I_y} \right] \left(\frac{\pi}{L} \beta_0 \cos \frac{\pi z}{L} \right) \\ & + E \Gamma \left(\frac{\pi}{L} \right)^3 \beta_0 \cos \frac{\pi z}{L} + \frac{1}{2} E \left(\frac{\pi}{L} \right)^3 \beta_0^3 \cos^3 \frac{\pi z}{L} \left(K_c - \frac{I_c^2}{A} - \frac{K_y^2}{I_y} \right) \\ & = M_z + M_x \frac{d\bar{u}}{dz} \end{aligned} \quad \text{II.3.5}$$

To obtain the solution of equation II.3.5 by the Galerkin method, the derivative $\frac{d\bar{u}}{dz}$ must be expressed as a function of β_0 and z . This can be achieved by direct integration of the first two of equations II.3.2 in which β is replaced by $\beta_0 \sin \frac{\pi z}{L}$. These equations are then

$$\begin{aligned} EI_x \frac{d^2 v}{dz^2} &= -M_x \cos(\beta_0 \sin \frac{\pi z}{L}) \\ EI_y \frac{d^2 u}{dz^2} &= -M_x \sin(\beta_0 \sin \frac{\pi z}{L}) \end{aligned} \quad \text{II.3.6}$$

To facilitate the integration of equations II.3.6 sine and cosine can be expanded into their series forms, thus

$$\begin{aligned} \cos(\beta_0 \sin \frac{\pi z}{L}) &= 1 - \frac{(\beta_0 \sin \frac{\pi z}{L})^2}{2!} + \frac{(\beta_0 \sin \frac{\pi z}{L})^4}{4!} \\ &\quad - \frac{(\beta_0 \sin \frac{\pi z}{L})^6}{6!} + \dots \end{aligned}$$

$$\sin\left(\beta_0 \sin \frac{\pi z}{L}\right) = \beta_0 \sin \frac{\pi z}{L} - \frac{(\beta_0 \sin \frac{\pi z}{L})^3}{3!} + \frac{(\beta_0 \sin \frac{\pi z}{L})^5}{5!} - \frac{(\beta_0 \sin \frac{\pi z}{L})^7}{7!} + \dots \quad \text{II.3.7}$$

Using the first terms of the sine and cosine series, equations II.3.6 become

$$\begin{aligned} EI_x \frac{d^2 v}{dz^2} &= -M_x \\ EI_y \frac{d^2 u}{dz^2} &= -M_x \beta_0 \sin \frac{\pi z}{L} \end{aligned} \quad \text{II.3.8}$$

Integrating equation II.3.8 directly and using the boundary conditions $z=0$, $u=v=0$ and $z=\frac{L}{2}$,

$\frac{du}{dz} = \frac{dv}{dz} = 0$ the following expressions are obtained for u and v ,

$$\begin{aligned} u &= \frac{M_x}{EI_y} \left(\frac{L}{\pi}\right)^2 \beta_0 \sin \frac{\pi z}{L} \\ v &= \frac{M_x}{2EI_x} (Lz - z^2) \end{aligned} \quad \text{II.3.9}$$

In the previous section, it was shown that

$$\bar{u} = u \cos \beta - v \sin \beta \quad \text{II.3.10}$$

If the first term approximations of sine and cosine series are used, equation II.3.10 becomes

$$\bar{u} = u - v\beta \quad \text{II.3.11}$$

and replacing β by $\beta_0 \sin \frac{\pi z}{L}$ and substituting the results II.3.9 for u and v , the following expression for \bar{u} is obtained,

$$\bar{u} = \frac{M_x}{EI_y} \left(\frac{L}{\pi} \right)^2 \beta_0 \sin \frac{\pi z}{L} - \frac{M_x}{2EI_x} (Lz - z^2) \beta_0 \sin \frac{\pi z}{L} \quad \text{II.3.12}$$

Thus the derivative $\frac{d\bar{u}}{dz}$ is obtained as

$$\begin{aligned} \frac{d\bar{u}}{dz} = & \frac{M_x}{EI_y} \cdot \frac{L}{\pi} \beta_0 \cos \frac{\pi z}{L} - \frac{M_x}{2EI_x} \cdot \frac{\pi}{L} (Lz - z^2) \beta_0 \cos \frac{\pi z}{L} \\ & - \frac{M_x}{2EI_x} (L - 2z) \beta_0 \sin \frac{\pi z}{L} \end{aligned} \quad \text{II.3.13}$$

Equation II.3.5 can now be written in an appropriate Galerkin integral equation form, allowing for the symmetry of the problem, thus

$$\begin{aligned} & 2 \int_0^{\frac{L}{2}} \left\{ \left[GC + \frac{K_y M_x \sin(\beta_0 \sin \frac{\pi z}{L})}{I_y} \right] \left(\frac{\pi}{L} \beta_0 \cos \frac{\pi z}{L} \right) \right. \\ & + EI \left(\frac{\pi}{L} \right)^3 \beta_0 \cos \frac{\pi z}{L} + \frac{1}{2} E \left(\frac{\pi}{L} \right)^3 \beta_0^3 \cos^3 \frac{\pi z}{L} \left(K_c - \frac{I_c^2}{A} - \frac{K_y^2}{I_y} \right) - M_z \\ & - M_x \left[\frac{M_x}{EI_y} \cdot \frac{L}{\pi} \beta_0 \cos \frac{\pi z}{L} - \frac{M_x}{2EI_x} \cdot \frac{\pi}{L} (Lz - z^2) \beta_0 \cos \frac{\pi z}{L} \right. \\ & \left. \left. - \frac{M_x}{2EI_x} (L - 2z) \beta_0 \sin \frac{\pi z}{L} \right] \right\} \frac{d\beta}{d\beta_0} dz = 0 \end{aligned}$$

$$\text{II.3.14}$$

Substituting $\beta_0 \sin \frac{\pi z}{L}$ for $\sin(\beta_0 \sin \frac{\pi z}{L})$ in the K_y term and replacing $\frac{d\beta}{d\beta_0}$ by the appropriate derivative, that is

$$\beta = \beta_0 \sin \frac{\pi z}{L} \quad \text{hence} \quad \frac{d\beta}{d\beta_0} = \sin \frac{\pi z}{L} \quad \text{II.3.15}$$

equation II.3.14 can be written in the following form, thus

$$\begin{aligned} & \int_0^{\frac{L}{2}} \left\{ \frac{\pi}{L} G C \beta_0 \sin \frac{\pi z}{L} \cos \frac{\pi z}{L} + \frac{\pi}{L} \cdot \frac{K_{yy} M_x}{I_y} \beta_0^2 \sin^2 \frac{\pi z}{L} \cos \frac{\pi z}{L} \right. \\ & + \left(\frac{\pi}{L} \right)^3 E \Gamma \beta_0 \sin \frac{\pi z}{L} \cos \frac{\pi z}{L} + \frac{1}{2} \left(\frac{\pi}{L} \right)^3 E \left(K_c - \frac{I_c^2}{A} - \frac{K_{yy}}{I_y} \right) \beta_0^3 \sin \frac{\pi z}{L} \cos^3 \frac{\pi z}{L} \\ & - M_z \sin \frac{\pi z}{L} - M_x \left[\frac{M_x}{E I_y} \cdot \frac{L}{\pi} \beta_0 \sin \frac{\pi z}{L} \cos \frac{\pi z}{L} \right. \\ & - \frac{M_x}{2 E I_x} \cdot \frac{\pi}{L} \beta_0 (L z - z^2) \sin \frac{\pi z}{L} \cos \frac{\pi z}{L} \\ & \left. \left. - \frac{M_x}{2 E I_x} \beta_0 (L - 2 z) \sin^2 \frac{\pi z}{L} \right] \right\} dz = 0 \end{aligned} \quad \text{II.3.16}$$

The following polynomial expression for M_z at $z = \frac{L}{2}$ that is, half the applied torque at mid-span, in terms of β_0 is obtained by solving equation II.3.16, thus

$$M_z = a_1 \beta_0 + b_1 \beta_0^2 + c_1 \beta_0^3 \quad \text{II.3.17}$$

$z = \frac{L}{2}$

where

$$\begin{aligned}
 a_1 &= 1.571 \frac{GC}{L} + 15.528 \frac{E\Gamma}{L^3} \\
 &\quad - 0.159 \frac{M_x^2 L}{EI_y} + 0.254 \frac{M_x^2 L}{EI_x} \\
 b_1 &= 1.047 \frac{K_y M_x}{LI_y} \\
 c_1 &= 3.881 \frac{E}{L^3} \left(K_c - \frac{I_c^2}{A} - \frac{K_y^2}{I_y} \right)
 \end{aligned}$$

II.3.18

A second solution for equations II.3.2 for the same combination of bending moment and torque is presented in Appendix VIII.1. A similar method of analysis is employed, but, in substituting for $\sin \beta$ and $\cos \beta$ the first two terms of their series form are used, that is,

$$\begin{aligned}
 \sin \beta &= \beta - \frac{\beta^3}{3!} \\
 \cos \beta &= 1 - \frac{\beta^2}{2!}
 \end{aligned}$$

II.3.19

The expression obtained for M_z at $z = \frac{L}{2}$ in terms of β_0 is of the following polynomial form, thus

$$M_z = a_2 \beta_0 + b_2 \beta_0^2 + c_2 \beta_0^3 + d_2 \beta_0^4 + e_2 \beta_0^5$$

$z = \frac{L}{2}$

II.3.20

where

$$a_2 = 1.571 \frac{GC}{L} + 15.528 \frac{E\Gamma}{L^3}$$

$$-0.159 \frac{M_x^2 L}{EI_y} + 0.254 \frac{M_x^2 L}{EI_x}$$

$$b_2 = 1.047 \frac{K_y M_x}{LI_y}$$

$$c_2 = 3.881 \frac{E}{L^3} \left(K_c - \frac{I_c^2}{A} - \frac{K_y^2}{I_y} \right)$$

$$+ 0.142 \frac{M_x^2 L}{EI_y} - 0.146 \frac{M_x^2 L}{EI_x}$$

$$d_2 = -0.1047 \frac{K_y M_x}{LI_y}$$

$$e_2 = -0.0158 \frac{M_x^2 L}{EI_y} + 0.0174 \frac{M_x^2 L}{EI_x}$$

II.3.21

As before, the value of M_3 at $z = \frac{L}{2}$ obtained from equation II.3.20, corresponds to half the applied torque at that position.

Equations II.3.17 and II.3.20 refer particularly to problems where the torsional behaviour is non-uniform and where the torsion bending constant Γ for the beam cross-section is non-zero. In such cases, the variation of β with z is nonlinear. If the beam cross-section is of the form where the flanges all intersect at the one point, such as an angle or tee section, there is no flange warping during

torsion and for these sections $\Gamma' = 0$. In such cases, the torsional behaviour is uniform except at high values of bending moment and approximate solutions for equations II.3.2 can be obtained by assuming a linear variation of β with z , that is $\frac{d\beta}{dz} =$ a constant, thus

$$\beta_z = \beta_0 \frac{2z}{L} \quad 0 \leq z < \frac{L}{2} \quad \text{II.3.22}$$

Two solutions for equations II.3.2, assuming a linear variation of β and following a similar analytical procedure as used to obtain the solutions II.3.17 and II.3.20, are detailed in Appendix VIII.1. In the first solution, $\sin \beta$ and $\cos \beta$ are replaced by β and 1 respectively, and in the second, the first two terms of the sine and cosine series are used. The relationships found for M_z at $z = \frac{L}{2}$ in terms of β_0 are as follows,

$$(i) \quad \sin \beta = \beta \quad \cos \beta = 1$$

$$M_z = a_3 \beta_0 + b_3 \beta_0^2 + c_3 \beta_0^3 \quad \text{II.3.23}$$

$$z = \frac{L}{2}$$

where

$$a_3 = \frac{2GC}{L} - 0.125 \frac{M_x^2 L}{EI_y} + 0.292 \frac{M_x^2 L}{EI_x}$$

$$b_3 = 1.333 \frac{K_y M_x}{L I_y}$$

$$c_3 = 4 \frac{E}{L^3} \left(K_c - \frac{I_c^2}{A} - \frac{K_y^2}{I_y} \right)$$

II.3.24

$$(ii) \quad \sin \beta = \beta - \frac{\beta^3}{3!} \quad \cos \beta = 1 - \frac{\beta^2}{2!}$$

$$M_3 = a_4 \beta_o + b_4 \beta_o^2 + c_4 \beta_o^3 + d_4 \beta_o^4 + e_4 \beta_o^5$$

$\beta = \frac{L}{2}$

II.3.25

where

$$a_4 = \frac{2GC}{L} - 0.125 \frac{M_x^2 L}{EI_y} + 0.292 \frac{M_x^2 L}{EI_x}$$

$$b_4 = 1.333 \frac{K_y M_x}{L I_y}$$

$$c_4 = 4 \frac{E}{L^3} \left(K_c - \frac{I_c^2}{A} - \frac{K_y^2}{I_y} \right) + 0.132 \frac{M_x^2 L}{EI_y} - 0.217 \frac{M_x^2 L}{EI_x}$$

$$d_4 = -0.133 \frac{K_y M_x}{L I_y}$$

$$e_4 = -0.0119 \frac{M_x^2 L}{EI_y} + 0.0436 \frac{M_x^2 L}{EI_x}$$

II.3.26

The values of M_3 at $\beta = \frac{L}{2}$ found from equations II.3.23 and II.3.25 correspond to half the torque applied at the mid-span position.

Equations II.3.17, II.3.20, II.3.23 and II.3.25 describe nonlinear torque/angle of twist equilibrium

paths. Typical forms of these paths for an extruded brass angle section, predicted by equation II.3.25, are illustrated in Fig. II.13. It can be seen that the nonlinearity of the paths increases as the bending moment is increased and, as indicated by the M_3 , M_4 , M_5 and M_6 graphs, unstable equilibrium paths can obtain. The significance of the unstable behaviour range is discussed later in the analysis of the problem of flexural-torsional instability of thin-walled open section beams.

The torque/angle of twist equilibrium paths for one particular bending moment predicted by each of the four solutions, are illustrated in Fig. II.14. These graphs show that whilst the forms of the paths are similar there are significant quantitative differences between the various solutions. A detailed study of the applications and limitations of each solution is presented in Chapter IV where values predicted by the different solutions are compared with a range of experimentally determined torque/angle of twist relationships.

II.4 Flexural-Torsional Instability of Thin-Walled Open Section Beams

The torque/angle of twist relationships obtained from the analysis presented in the previous section, can be used to derive an expression for the value of bending moment that initiates flexural-torsional instability.

Referring to Fig. II.15, it can be seen that, as the bending moment is increased, the turning point on the torque/angle of twist equilibrium path, which defines the start of the unstable range of behaviour, occurs at smaller values of torque and angle of twist. Thus, as the bending moment is increased, it is theoretically possible to obtain an equilibrium path in which the turning point coincides with the origin, as illustrated by the path for bending moment M_c . This indicates that, at this value of bending moment, the beam is torsionally unstable and a flexural-torsional failure mode may obtain.

The slope of the equilibrium path at any point is given by the derivative $\frac{dM_3}{d\beta_0}$ and at a turning point, this slope will be zero, that is

$$\frac{dM_3}{d\beta_0} = 0$$

II.4.1

Thus if

$$M_3 = a\beta_o + b\beta_o^2 + c\beta_o^3 + \dots$$

then $\frac{dM_3}{d\beta_o} = a + 2b\beta_o + 3c\beta_o^2 + \dots$ II.4.2

If the turning point is to coincide with the origin of the equilibrium path, then $\frac{dM_3}{d\beta_o} = 0$ at $\beta_o = 0$. By substituting these values into equation II.4.2, it can be seen that, for the condition of instability, the coefficient a must be zero.

Expressions for the coefficient a were obtained in the analysis presented in section II.3. In one case the variation of the angle of twist β with z was assumed to be sinusoidal whilst for the second solution this variation was considered to be linear.

In the present analysis the beam is subjected to bending moment only and the angular deformation which obtains is due to torque components of the bending moment about the displaced axes of the beam as given by the term $M_x \frac{d\bar{u}}{dz}$. This torque action varies with z and thus the resulting torsional behaviour will be non-uniform even if the beam section is of a form which does not exhibit the warping deformation usually associated with non-uniform torsion. Thus the variation of the angle of twist β with z will be nonlinear and

the appropriate expression for the coefficient a is considered to be that found from the analysis based on the sinusoidal distribution of twist.

From equations II.3.21 the expression for the coefficient a is

$$a_2 = 1.571 \frac{GC}{L} + 15.528 \frac{E\Gamma}{L^3} - 0.159 \frac{M_x^2 L}{EI_y} + 0.254 \frac{M_x^2 L}{EI_x} \quad \text{II.4.3}$$

and if $a_2 = 0$, then

$$\begin{aligned} \frac{M_x^2 L}{E} \left(\frac{0.159}{I_y} - \frac{0.254}{I_x} \right) \\ = 1.571 \frac{GC}{L} + 15.528 \frac{E\Gamma}{L^3} \end{aligned} \quad \text{II.4.4}$$

and thus

$$(M_x)_c = \sqrt{\frac{EI_y \left(9.875 \frac{GC}{L^2} + 97.75 \frac{E\Gamma}{L^4} \right)}{1 - 1.6 \frac{I_y}{I_x}}} \quad \text{II.4.5}$$

or, in terms of π/L equation II.4.5 becomes

$$(M_x)_c = \frac{\pi}{L} \sqrt{\frac{EI_y \left(GC + \frac{\pi^2}{L^2} E\Gamma \right)}{1 - \frac{3\pi^2 - 4}{16} \cdot \frac{I_y}{I_x}}} \quad \text{II.4.6}$$

If the beam cross-section is of a form for which the torsion bending constant J is zero, such as an angle or tee section, then equation II.4.6 can be written as

$$(M_x)_c = \frac{\pi}{L} \sqrt{\frac{EI_y GC}{1 - \frac{3\pi^2 - 4}{16} \cdot \frac{I_y}{I_x}}} \quad \text{II.4.7}$$

The following assumptions are made in using equations II.4.5, II.4.6 and II.4.7 for the evaluation of critical bending moment for flexural-torsional failure.

- (i) the beam cross-section has a value of I_x greater than I_y
- (ii) the ox axis is an axis of symmetry or point symmetry of the beam cross-section
- (iii) the bending moment is applied in the yz plane, that is, in the plane of greater flexural rigidity.

CHAPTER III

EXPERIMENTAL INVESTIGATIONS

The programme of experimental work was planned to provide physical substantiation of the theoretical analyses presented for linear and nonlinear, stable and unstable flexural-torsional behaviour of thin-walled open section beams. The tests performed are classified into four main groups as follows:

- (i) stable behaviour - linear torque/
angle of twist equilibrium paths -
angles of twist up to 0.15 radian
- (ii) stable behaviour - nonlinear
torque/angle of twist equilibrium
paths - angles of twist up to
1.0 radian
- (iii) stable and unstable behaviour -
nonlinear torque/angle of twist
equilibrium paths - angles of
twist up to 1.5 radian
- (iv) flexural-torsional failure due
to applied bending moment.

In the first three groups of tests, the specimens were subjected to combinations of bending moment and torque that produced stress values within the elastic limit of the specimen material.

III.1 Stable Behaviour - Linear Torque/Angle of Twist Equilibrium Paths - Small Displacements

A thin-walled mild steel lipped channel section was subjected to a range of different combinations of bending moment and torque. The experimental values of longitudinal stress distribution and angles of twist were compared with the corresponding values predicted by the approximate theoretical analysis.

The dimensions of the lipped channel section used in this group of tests are shown in Fig. III.1. The values of GC and EI found for this beam were $0.01905 \times 10^6 \text{ lbf in}^2$ and $134 \times 10^6 \text{ lbf in}^4$ respectively and using a test span of $6' - 0''$, $\lambda L = 0.86$.

Details of the experimental rig in which the beam was tested are shown in Fig. III.2. The design requirements of this rig were based on the desired support conditions of the beam with respect to bending and to torsion, that is,

- (i) simply supported for bending actions
- (ii) free to warp but with angular deformation restrained for torque actions.

These conditions were achieved by supporting the beam in thin aluminium alloy diaphragms as illustrated in Fig. III.3. These diaphragms were held in 'anti-torque' frames which rested on the main test bench. The frame at one end was provided with a set of roller bearings and its counterpart at the other end was attached to a knife edge, prepared from a short length of T-section. To prevent angular deformation at the ends of the test beam, the extremities of the anti-torque frames were attached to cross-beams forming part of the main test bench.

Various combinations of bending moment and torque were applied to the beam by suspending weights from different positions on the aluminium discs clamped to the web of the beam by the screw jacks and spreader bar arrangement, illustrated in Fig. III.4. The position of the rectangular hole cut in the disc was such that the centre of the disc coincided with the centroid of the beam cross-section.

This loading arrangement made it possible to load the beam in a vertical plane containing the shear centre and thus obtain the condition of bending with no torsion relative to the shear centre axis. By moving the load away from this position, values of

torque about the shear centre with the same value of bending moment, could be applied simultaneously by the one system of loading.

The distribution of longitudinal strain at three cross-sections of the beam was measured using electrical resistance strain gauges attached in pairs to either side of the web, flanges and lips of the section, placed as indicated in Fig. III.5. The location of the gauged cross-sections relative to one end of the beam is also shown in Fig. III.5. Each pair of gauges was connected in series and strains due to local bending deformations were thus self cancelling and were not recorded. Readings from the strain gauges were recorded on a multi-channel battery operated strain bridge.

Angles of twist were measured by the reflected image technique. The variation of this deformation along the span of the beam was obtained by recordings at eleven equally spaced positions along the span. The mirrors required for this system of angular deformation measurement, were attached to the web of the beam at the point of intersection with the horizontal axis of symmetry of the cross-section.

The test programme was arranged to give both

symmetrical and unsymmetrical distributions of bending moment and torque about the shear centre axis. The load positions are detailed in Fig. III.6. In each case the loads were applied in six different vertical planes, one of which contained the shear centre. The positions of these load planes are indicated in Fig. III.7. Thus, the complete test programme allowed for eighteen different combinations of bending moment and torque relative to the shear centre axis, including three cases of zero torque.

III.2 Stable Behaviour - Nonlinear Torque/Angle of Twist Equilibrium Paths - Large Displacements

This aspect was investigated initially in the stable behaviour range by a series of tests on a 1.5" x 0.75" x 0.064" mild steel cold formed channel section beam.

The tests were performed in a modified version of the experimental rig used for the small displacement investigation of the larger lipped channel section beam. The test arrangement is shown in Fig. III.8. As before, the beam was held in diaphragm supports at each end of the test span. In this case, however, the loads were applied at the ends of the beam outwith the test span. This created a four point load system which could produce a constant value of bending moment over the test span as was considered in the theoretical analysis. In order to obtain the condition of bending with zero torque, the loads had to be applied in the vertical plane through the shear centre. This was achieved by an aluminium disc and pin arrangement clamped to the web of the beam as shown in Fig. III.9. The bending moment loads were suspended from the pin which, in turn, coincided with the shear centre of the beam cross-section.

Torque was applied to the beam at the mid-span position using the disc and pulley system as illustrated in Fig. III.10. In this arrangement, the centre of the disc coincided with the shear centre position and thus, the torque was applied about the shear centre axis. The direction of the applied torque could be reversed by interchanging the pulley brackets and cable system.

The support conditions for the test span were considered to be

- (i) simply supported for bending actions
- (ii) free to warp but with angular deformation restrained for torque actions.

In the tests, the angle of twist at the mid-span position was measured by an adjustable vernier protractor and level bubble, attached to the torque application disc. The horizontal and vertical deflections of the shear centre at the mid-span position were measured by dial gauges connected to the shear centre pin of the torque application disc by thin wire.

The test programme was designed so as to obtain

torque/angle of twist equilibrium paths at the mid-span position for different applied bending moments, including the case of zero bending moment. The specimen was twisted in both the positive and negative directions and at each increment of torque, the angle of twist and the deflections of the shear centre at the mid-span position were recorded.

The form of the applied loading on the test span is shown in Fig. III.11. The values of M_x for which torque/angle of twist equilibrium paths were measured, were 500, 750 and 1000 in lbf. The direction of the bending moment at any section was negative according to the present sign convention.

III.3 Stable and Unstable Behaviour - Nonlinear Torque/Angle of Twist Equilibrium Paths - Large Displacements

The typical form of a torque/angle of twist equilibrium path in the stable and unstable ranges, as predicted by the theoretical analysis, is shown in Fig. III.12. In this graph, it is seen that for certain values of torque, the corresponding value of twist is not unique, for example, torque T_1 corresponds to three angles of twist β_1 , β_2 and β_3 . This type of equilibrium path cannot be obtained by the usual procedure of applying increments of torque and measuring the corresponding angles of twist. If this technique were employed, the stable path would be followed up to the turning point a , after which any further increase in the torque would cause the beam to twist through to the position b . The portion of the path below the line ab would not be measured.

However, for any angle of twist, the corresponding value of torque is unique. This condition can be utilised in the development of an experimental technique for measuring the complete equilibrium path. In this technique, a controlled deformation loading system is used whereby increments

of angular displacement are applied and the corresponding values of torque recorded.

The arrangement of the experimental test rig designed for this form of controlled deformation loading is shown in Fig. III.13(a). The load conditions were similar to those used in the small channel investigation, that is, a four point load system producing constant applied bending moment over the test span, with a torque action at the mid-span position. The beam was held in gimbal supports, as shown in Fig. 13(b), which allowed rotation about the x and y axes but prevented angular deformation, that is, rotation about the z -axis. The portion of the beam between the gimbal supports was treated as the test span. Thus the gimbal supports replaced the diaphragm arrangements used for the channel tests. This new form of support was adopted so as to provide a more stable test arrangement since any disturbance of the test beam when loaded in the unstable range, could upset the equilibrium of the system.

In order to obtain the simply supported conditions for bending actions, as considered in the theoretical analysis, the gimbal support at one end of the test span rested on rollers. Thin-walled equal

angle sections were used as test beams. This form of cross-section was selected for two reasons.

- (i) The shear centre of an angle is located at the same point irrespective of the flange size, that is, at the apex of the angle. This condition made it possible for the one form of opening to be cut in the loading discs and the central plates of the gimbal supports. This opening allowed for a range of angle sizes with the apex coinciding with the centre of the disc or plate in each case.
- (ii) The flanges of an angle section intersect at one point and for this form of thin-walled section the torsion bending constant is zero. This implies that warping deformations do not obtain and any restraint of such deformations that might be provided by the clamping arrangement in the central plate of the gimbal support, does not have to be considered. Thus, the support

conditions for torque action
are consistent with those
assumed for the theoretical
analysis.

Extruded brass angle sections were used as test specimens. This material was selected so that the desired large displacement behaviour could be obtained at relatively low values of bending moment, torque and corresponding stresses.

The bending moment loads were applied at the extreme ends of the test beam by means of an aluminium disc, wire loop and pulley wheel as shown in Fig. III.13(c). This arrangement ensured that the load acted through the centroid of the disc at all times. The disc was clamped to the angle section so that the shear centre of the angle coincided with the centroid of the disc. In this way, the loading was in a plane containing the shear centre and pure bending actions only were applied over the test span length of the beam.

The controlled deformation equipment used for measuring the torque/angle of twist equilibrium paths at the mid-span position is shown in Fig. III.14. The system comprised a cable continuous round seven pulley

wheels and attached at each end to opposite extremities of a diameter of an aluminium disc clamped to the mid-span section of the test beam. The centroid of the disc coincided with the shear centre of the angle section. By moving the pulley wheel P_1 in the direction as indicated in Fig. III.14, a rotation of the aluminium disc was produced. The increment of angular deformation was proportional to the movement of the pulley wheel. A secondary pulley system S was also provided, by which torques could be applied in the opposite direction to that of the main pulley system. The pulley wheel P_2 was used to apply weight to counterbalance the load effect of the torque disc and its attachments.

Angular deformation of the mid-span section was measured by a low-start torque potentiometer attached to the torque disc. The free end of the potentiometer brush spindle carried a steel spline pendulum and as the disc rotated this pendulum remained vertical. This produced, in effect, a rotation of the potentiometer brush equal to the angular displacement of the disc. The change in signal from the potentiometer was metered on an ultra-violet galvanometer recorder.

The torque for any angular displacement was evaluated from the product of the disc diameter and the cable force. This force was measured using a specially prepared spring steel dynamometer connected into the main pulley cable system as shown in Fig. III.14. Four electrical resistance strain gauges were attached to the dynamometer at positions of maximum strain and formed a complete bridge circuit. The change in signal from this bridge, which was proportional to the cable force producing the strain in the dynamometer, was fed into a second channel of the ultra-violet galvanometer recorder. The dynamometer was fitted with a spring, as shown in the figure, to prevent deformations large enough to produce a nonlinear load/strain calibration. The stiffness of the spring used depended on the maximum cable forces to be measured in any particular test.

The sensitivity of both the twist and torque measuring devices was controlled by varying the current voltage supplied to them. Both devices were calibrated prior to the start of each test run.

Surface strains of the test beam at selected positions were measured using electrical resistance strain gauges. The gauges were of the foil type, $\frac{1}{4}$ in

gauge length and 110 ohm resistance, and were attached in the form of 45° rosettes in the positions as indicated in Fig. III.15. The readings from the strain gauges were recorded by means of a 100-channel data logging system which gave printed records of results. The maximum rate of recording provided by the system was 10 channels per second. The block layout of this system is shown in Fig. III.16 and the actual equipment is shown in Fig. III.17. The horizontal and vertical deflections of the mid-span section of the test specimen were measured by dial gauges attached by wires to a pin fixed on the horizontal diameter of the disc behind the apex of the angle. Using the dial gauge readings in conjunction with the corresponding measured angle of twist the position and orientation of the mid-span section could be determined.

The theoretical analysis has indicated that when the beam is subjected to combined bending and torsion, the form of the torque/angle of twist equilibrium path varies with the direction of twist. It has also been shown that at large values of bending moment the torque/angle of twist equilibrium path may be of the type illustrated in Fig. III.18. It can be seen from

this graph that in the unstable range of behaviour the direction of the torque may be reversed for the same direction of twist.

The test procedure adopted, enabled the measurement of the equilibrium path for both directions of twist and allowed for the possible condition of torque reversal at large applied bending moments. This procedure is illustrated in Fig. III.19. The beam, with the bending moment loads applied, was initially twisted in the negative torque direction using the secondary pulley system. Increments of angular deformation in the positive direction were then applied starting from this initially twisted position. Recordings of torque, angle of twist, deflections and strains were made at each increment of deformation.

This test procedure effectively displaced the base line of the torque/angle of twist equilibrium path. To obtain the appropriate interpretation of the results, that is, where the origin of the path corresponded to the axis of symmetry of the angle lying in the horizontal plane, the base line had to be raised by an amount equal to the value of the initially applied negative torque. The point of intersection of this new base line with the equilibrium path, corresponded to the

appropriate origin, as shown in Fig. III.19. In the case of torque reversal, the test could be performed with the main cable system always in tension by applying an initial negative torque greater than the magnitude of the torque reversal. The test equipment is shown in Fig. III.20.

The full experimental programme comprised a series of tests on equal angle sections with flange sizes of 1, 1.5 and 2 in. and thicknesses ranging from 0.0375 to 0.0846 in. Individual tests were performed a number of times, to check the repeatability of the experimental system.

Details of the material and section properties of each specimen are given in Appendix VIII.4. The experimental techniques used for measuring the combined material and section properties EI_x , EI_y and GC , are described in Appendix VIII.3.

III.4 Flexural-Torsional Failure of Thin-Walled Open Section Beams due to Applied Bending Moment

In order to obtain experimental values of bending moments causing flexural-torsional failure of thin-walled open sections, a series of tests were performed on a range of thin-walled, cold rolled steel, equal angle section beams. The angle section was selected so that the tests could be carried out in the experimental rig used for the tests on the brass angle sections.

The angle specimens were held in the gimbal supports and were tested by applying increments of load at the extreme ends of the beam outwith the test span, until failure, defined as the maximum load carrying capacity, occurred. The loads were applied by the disc and pulley arrangements used in the previous group of tests. Thus, as before, the test span was subjected to a constant value of bending moment in the plane of greater flexural rigidity containing the shear centre. Torque actions were not applied to the beam.

The horizontal and vertical deflections and angle of twist of the mid-span section were measured at each increment of load. These measurements were obtained

by clamping the torque disc of the controlled deformation system to the mid-span section and employing the dial gauges and potentiometer device used in the previous investigation. As before, the position and orientation of the mid-span section could be determined by analysing the dial gauge readings in conjunction with the corresponding angle of twist. The main and secondary pulley systems were not connected to the torque disc. The single pulley system used to counterbalance the load effects of the torque disc and its attachments was included in setting up the test equipment. The test rig, with an angle specimen in its position at failure, is shown in Fig. III.21.

The complete experimental programme comprised tests on angle sections with flange sizes of 1, 1.5 and 2 in, five specimens of each size being tested. All the sections were nominally 16 S.W.G. in wall thickness. Details of the material and section properties of each specimen are given in Appendix VIII.4.

CHAPTER IV

COMPARISON OF THEORETICAL AND EXPERIMENTAL RESULTS

The experimental investigations have been considered under four principal test groupings and the comparison of the theoretical and experimental results is presented under the same headings. Unless otherwise indicated the comparison is presented in graphical form showing experimental results plotted as points with respect to the corresponding theoretical values shown as a full line. The complete experimental results are given in Appendix VIII.5.

IV.1 Stable Behaviour - Linear Torque/Angle of Twist Equilibrium Paths - Small Displacements

The experimentally determined distributions of angle of twist and longitudinal stress in the lipped channel section agree well with the corresponding theoretical values. The analysis used for calculating these theoretical values was based on the analogy between the problems of simple bending and restrained torsion of beams discussed in Chapter II, section 1, and, since $\lambda L < 1$, the St. Venant torsional rigidity GC was neglected.

Angle of Twist

Typical variations of angle of twist with applied torque, for each of the three different load

cases, are shown in Fig. IV.1. The experimental values show a linear torque/angle of twist relationship. In cases (I) and (II), where the measured twist is at a position of applied torque, the experimental observations tend to be slightly higher than the corresponding theoretical values. This condition is not so apparent in case (III) where the position of the measured twist was some distance from the loaded sections. This would appear to imply a localised load effect. The distributions of twist along the length of the beam for the maximum applied torque in each load case is shown in Fig. IV.2. It can be seen that the general tendency is as before, for the measured twists to be slightly greater than the predicted values at or near the applied load and torque positions. The distributions of angle of twist along the beam span for the complete range of applied torques for all load cases are shown in Graphs/1/3,4 and 5 in Appendix VIII.5.

Longitudinal Stresses

The variation of longitudinal stress with applied torque at different positions on a cross-section is shown for a typical case in Fig. IV.3. It can be seen that the relationship between the change in longitudinal stress and applied torque is linear. The

maximum changes in stress occur at the junctions of the web and flanges and at the edge of the lips. This condition is consistent with the distribution of the 'sectorial co-ordinate' which has maximum values at these positions, as illustrated in Fig. IV.4.

The results presented in Fig. IV.3 are shown isometrically in Fig. IV.5 where the typical form of longitudinal stress distribution, associated with restrained warping behaviour, is more clearly illustrated. The distributions of longitudinal stress in the upper flange at the three strain gauged sections, for case (I) loading with maximum applied torque, are shown in Fig. IV.6. As expected from the theoretical analysis, these distributions are proportional to the corresponding values of moment and bi-moment at each section. The complete detailed results of the stress distribution investigation for all combinations of bending moment and torque, at the three strain gauged sections are shown in Graphs/1/8 to 16 inclusive, in Appendix VIII.5.

It can be stated that, in general, the experimentally determined distributions of longitudinal stress in the channel agree closely with the predicted

values. These latter values have been calculated from the expressions presented in the theoretical analysis (equations II.1.6), that is

$$\sigma_z = \frac{M_x \cdot y}{I_x} + \frac{B \cdot \omega}{r} \quad \text{IV.1.1}$$

IV.2 Stable Behaviour - Nonlinear Torque/Angle of Twist Equilibrium Paths - Large Displacements

The tests performed in this section of the experimental investigation were devoted to the measurement of angle of twist and shear centre displacements at the mid-span position of a small channel section beam.

Angle of Twist

In the first instance the beam was subjected to a concentrated torque action at the mid-span position and the corresponding angles of twist at mid-span were recorded. The results are shown in Fig. IV.7. It can be seen that the experimental values show a linear torque angle of twist relationship and agree closely with the values calculated from the expression given in the theoretical analysis (equation II.1.21), that is,

at $z = \frac{L}{2}$

$$\beta_{z=\frac{L}{2}} = -\frac{T \tanh \frac{\lambda L}{2}}{2 E \Gamma \lambda^3} + \frac{TL}{4 E \Gamma \lambda^2} \quad \text{IV.2.1}$$

The corresponding theoretical values of β obtained from the approximate solution, which neglects the

St. Venant torsional rigidity GC that is, at $z = \frac{L}{2}$

$$\beta = \frac{TL^3}{48EI}$$

$$\beta = \frac{L}{2}$$

IV.2.2

are also shown in Fig. IV.7. For this case, the approximate analysis yields values of twist much larger than the experimental values. This result is to be expected since, for the small channel used,

$\lambda L = 12.7$ and, as shown in Fig. IV.8, the true value of the angle of twist coefficient f_2 ($= \beta \cdot \frac{EI}{TL^3}$) for this value of λL is 0.00126 compared with the approximate solution value which is constant at 0.0208 .

The torque/angle of twist relationship at the mid-span position, when the beam is subjected to a constant bending moment $M_x = 1000$ in lbf over the entire test span is shown in Fig. IV.9. This relationship is nonlinear and consequently, as is shown, it does not agree with values predicted by the linear solution for β , given by equation IV.2.1. Theoretical values of torque and corresponding angle of twist at the mid-span position obtained from the single term Galerkin solutions of the generalised differential equations of bending moment and torque equilibrium (equations II.2.9), are also illustrated in Fig. IV.9. The experimental observations agree closely with the theoretical values given by the solution which

considered the first two terms of the sine and cosine series. In the case of the solution where only the first terms of the sine and cosine series were employed, good agreement with experimental values obtains up to angles of twist of approximately 0.25 radian.

The test results for the combined loading case also illustrate the predicted variation of the torque/angle of twist relationship with the direction of twist. Thus, for a positive angle of twist of 0.4 radian at mid-span, the corresponding applied torque is approximately 39 in lbf, whilst for the same angle of twist in the negative direction, the applied torque is approximately 54 in lbf. The results of similar tests for values of bending moment M_x of 500 and 750 in lbf are shown in Graph/2/4 in Appendix VIII.5.

Shear Centre Displacement

The predicted path of the shear centre at the mid-span position for both positive and negative torques, at bending moments M_x of 500 and 1000 in lbf are shown in Fig. IV.10. The theoretical values of deflection in the displaced axial direction x' and y' , at different angles of twist at mid-span, were found from the solution of the first two of equations II.2.9.

The experimental observations show good agreement in form with the predicted values, but tend to deviate quantitatively at angles of twist above approximately 0.4 radian.

This deviation is also observed in the results of similar flexural-torsional tests on the brass angle section beams. In the analysis of these tests, presented in the following section, a possible explanation of the discrepancy between the measured and predicted deflections is discussed.

The small channel section tests, which have been discussed, were undertaken only as a preliminary study of nonlinear flexural-torsional behaviour. The more detailed experimental investigation of both stable and unstable nonlinear flexural-torsional behaviour was accomplished using the brass angle sections and the controlled twist testing technique.

IV.3 Stable and Unstable Behaviour - Nonlinear Torque/Angle of Twist Equilibrium Paths - Large Displacements.

In the tests performed on the brass angle section beams, measurements of torque, angle of twist, deflection and strain were recorded. The specimens were subjected to different values of bending moment M_x constant over the entire test span. The torque/angle of twist equilibrium paths and the vertical and horizontal deflections were measured at the mid-span section and the strains near the edge of both flanges, on each face, were recorded at a section 12 inches from the mid-span position. The results of these tests are shown in Graphs/3/1 to 18 inclusive in Appendix VIII.5.

Angle of Twist

The torque/angle of twist equilibrium paths illustrated the predicted nonlinear forms as shown for a typical case in Fig. IV.11. The variation of the torque/angle of twist relationship with the direction of twist is also observed. Theoretical values were obtained from the solution which considered the first two terms of the sine and cosine series, that is, equation II.3.20 in which the variation of β with z was assumed to be sinusoidal and equation II.3.25 which

was based on a linear variation of β with z . It has been noted that for an angle section subjected to pure torsion, warping displacement does not obtain and theoretically the value of the torsion bending constant is zero. Thus, a linear variation of β with z is to be expected, that is, $\frac{d\beta}{dz}$ is constant. However, in the presence of bending actions, the axial displacement of the beam gives rise to torque components due to the applied bending moments, namely, $M_x \cdot \frac{d\bar{u}}{dz}$ and $M_y \cdot \frac{d\bar{v}}{dz}$ as indicated in the last of equations II.2.9. These components effectively produce the condition of a beam subjected to a varying distributed torque along the span. In this situation $\frac{d\beta}{dz}$ is no longer constant and the solution assuming a linear variation of β with z would not apply.

If the applied bending moment is small, then the additional torque components will be correspondingly low and the overall torsional behaviour will remain predominantly uniform. As the bending moment increases, the additional torque components become larger and more pronounced relative to the applied torque. At this stage the torsional behaviour will tend to be non-uniform and a theoretical solution based on the sinusoidal variation of β with z might yield more acceptable results.

This condition is illustrated in the typical results shown in Fig. IV.11. At the lowest value of applied bending moment of 200 in lbf, the experimental results agree well with the values predicted by the solution which assumed a linear variation of β with ζ . In the case of the maximum applied bending moment of 400 in lbf, the experimental observations agree with the values predicted from the solution based on a sinusoidal variation of β with ζ . The measured values for the intermediate applied bending moment of 300 in lbf tend to lie between the theoretical paths corresponding to the two assumed forms of variation of β with ζ .

The approximate limit of application of the linear variation solution can be assessed, for the present group of test results, in relation to the value of critical bending moment M_c for flexural-torsional instability. The value of M_c for each specimen has been calculated from equation II.4.7. It can be seen that the linear variation solution generally yields acceptable results for applied bending moments in the range $0 \leq M_x < 0.4 M_c$. The experimentally determined torque/angle of twist equilibrium paths for the 1 inch specimens A.1 and A.2 (Graphs/3/1 and 2, Appendix VIII.5) show a tendency to deviate from the

appropriate theoretical path when the applied bending moment M_x is in the range $0.8 M_c < M_x < M_c$. In this range, the effect of any initial irregularities in the specimen would be most pronounced and could give rise, at least in part, to the observed deviation. It is to be noted, however, that the form of these paths, is still as predicted. In particular, the paths for bending moments approaching the critical value indicate that the turning point, defining the limit of the stable behavioural range, tends to coincide with the origin. This condition is consistent with the analytical approach used in the derivation of the expression for critical bending moment given by equation II.4.5.

In the preliminary investigation using the small channel section, it was shown that the solution based on the first terms only of the sine and cosine series was limited to angles of twist in the range $0 < \beta < 0.25$ radian approximately. This limitation is also observed in the results of the angle section tests. This is illustrated in Fig. IV.12, which gives the results of a typical test for which a theoretical solution based on a sinusoidal variation of β with z was applicable. It can be seen that, for the complete range of measurement, the experimental observations agree with

the theoretical values found from the solution based on the first two terms of the sine and cosine series. Agreement with the corresponding theoretical values obtained from the solution based on the first terms only of the sine and cosine series is again limited to angles of twist in the range $0 < \beta < 0.25$ radian approximately. A similar limitation of the range of applicability of the solution using the first terms of the sine and cosine series is also found in the analysis based on a linear variation of β with z as illustrated in Graph/3/20 in Appendix VIII.5.

The experimentally determined torque/angle of twist equilibrium paths also illustrate the necessity for including all the additional torque effects in the generalised differential equation of torque equilibrium, that is, the last of equations II.2.9. A typical experimental path is shown in Fig. IV.13 where the value of the applied bending moment corresponds to $0.78 M_c$. In this case, the appropriate theoretical solution is based on a sinusoidal variation of β with z . It can be seen that the form of the theoretical path predicted by the solution in which the K term is the only additional effect considered, does not agree with the experimental observations. The alternative theoretical path found from the solution

which considered all the additional effects agrees well with the measured values. The difference between such theoretical solutions is not so pronounced at values of bending moment less than $0.4 M_c$ where the solution is based on a linear variation of β with ϕ , as illustrated in Graph/3/22 in Appendix VIII.5. This would indicate that, apart from the K term, the predominant additional effect is that arising from the torque components of the applied bending moment, due to axial displacement.

The remaining additional effect, that is the longitudinal stress system arising from the 'shortening effect', would appear to be of less importance, particularly in the range of angular deformation considered in the present test group. This hypothesis is further illustrated in the results of a torque test at zero applied bending moment shown in Fig. IV.14. In this test, the experimental values indicate a linear torque/angle of twist relationship in the range $0 < \beta < 1.3$ radian approximately and good agreement with theoretical values found from the simple expression

$$\beta = \frac{TL}{4GC} \quad \text{IV.3.1}$$

is obtained. At values of twist greater than 1.3 radian, the apparent increase in torsional rigidity due

to the longitudinal stress system of the 'shortening effect' can be observed, although it is still relatively small.

Shear Centre Displacement

The comparisons between the experimentally observed and predicted paths of the shear centre, that is, the apex of the angle at the mid-span position, are shown in Graphs/3/7 to 12 inclusive in Appendix VIII.5. A typical case is illustrated in Fig. IV.15 where, as in the case of the small channel tests, the values of deflection in the direction of the displaced axes x' and y' were found from the first two of equations II.2.9. The experimental observations again show good agreement in form with the predicted values but tend to deviate quantitatively at angles of twist above approximately 0.4 radian.

A possible explanation of this deviation is suggested by the results of the torsion test with zero bending moment previously discussed in relation to the 'shortening effect'. In this test the position of the mid-span section was recorded at each increment of torque and corresponding twist. The relative positions of torque disc pin, apex and centroid of the angle section at different angles of twist are shown in

Fig. IV.16. It can be seen that, as assumed in the theoretical analysis, the section twists initially about the shear centre, that is, the apex. However, the position of the centre of twist does not remain fixed and deviates from the apex at an angle of twist of approximately 0.4 radian.

This would introduce additional body rotation effects not considered in the theoretical analysis for the deflection path and could explain the observed deviation in the test results.

Longitudinal Stresses

The values of stress obtained from the analysis of the strain gauge rosette readings at each increment of twist agreed closely with predicted values for each specimen as shown in Graphs/3/13 to 18 inclusive, in Appendix VIII.5. A typical case is shown in Fig. IV.17. The theoretical values of stress were found by determining the angle of twist β_3 at the strain gauged section in terms of the value at mid-span, using the relationship

$$\beta_3 = \beta_0 \sin \frac{\pi z}{L} \quad \text{IV.3.2}$$

and then computing the longitudinal stresses due to the bending moment components $M_x \cos \beta_3$ and $M_x \sin \beta_3$.

using simple bending theory. The appropriate algebraic sum of the resulting stresses is compared with the measured values. The agreement between the experimental and theoretical stresses illustrate that, as expected, warping stresses do not obtain in the angle section. The results would also indicate that longitudinal stresses due to the 'shortening effect' are negligible in the range of angular deformation obtaining in the present group of tests.

IV.4 Flexural-Torsional Failure of Thin-Walled Open Section Beams due to Applied Bending Moment

In this group of tests, three series of mild steel equal angle section beams were tested to failure under the action of pure bending moment constant over the entire test span. The three different flange sizes considered were 1, $1\frac{1}{2}$ and 2 inches and all the specimens were nominally 16 S.W.G. in thickness.

In each test the deflections and angle of twist of the mid-span section were recorded for every increment of applied bending moment. These results were then used to plot the true path of the mid-span section in the xy plane, as illustrated for a typical test in Fig. IV.18. It can be seen that the displacement of the mid-span section is initially in the vertical direction only. As the bending moment is increased horizontal deflection and angular deformation develop. This form of deformation behaviour is consistent with that expected from specimens which have initial irregularities. If such imperfections were not present then, theoretically the beam deformations for this type of loading would be restricted to deflection in the vertical plane only. In the present series of tests this plane corresponds

to that containing the minor principal axis of the beam.

The relationships between the applied bending moment and the horizontal deflection of the apex and the angle of twist, at the mid-span section for the same typical test are shown graphically in Fig. IV.19. The curves are seen to approximate to rectangular hyperbolae and using the inverse plot technique developed by SOUTHWELL³⁶, the approximate straight line relationships, $\delta H \propto \frac{\delta H}{M}$ and $\delta \beta \propto \frac{\delta \beta}{M}$ are obtained as shown in Fig. IV.20. The slope of these lines was taken as defining the value of critical bending moment causing flexural-torsional instability. In this way two values of critical bending moment were determined experimentally for each specimen. It is to be noted that the slope of the $\delta H \propto \frac{\delta H}{M}$ line is apparently independent of the point on the axis of symmetry of the beam cross-section for which the horizontal deflection is taken. This is shown in Fig. IV.21 where lines corresponding to the horizontal deflection of both the apex and the centroid are shown and are seen to be parallel.

The experimentally determined values of critical bending moment are shown for each specimen in columns .

SPECIMEN		COLLAPSE M	EXPERIMENTAL INVERSE PLOT M_c		THEORETICAL M_c			
			$\delta H \propto \frac{\delta H}{M}$	$\delta \beta \propto \frac{\delta \beta}{M}$	PRANDTL MICHELL	REISSNER	GOODIER	PRESENT THESIS EQN. II.4.7
		(1)	(2)	(3)	(4)	(5)	(6)	(7)
1"x1"x16 SWG	A.1	960	890	905	760	880	1440	985
	A.2	965	950	935	755	870	1405	980
	A.3	1060	870	900	710	820	1330	915
	A.4	1090	860	840	705	810	1300	905
	A.5	1090	1030	865	705	810	1300	905
1½"x1½"x16 SWG	B.1	2460	2460	2400	1700	1940	1310	2160
	B.2	2460	2440	2415	1710	1950	1325	2190
	B.3	1980	2025	2060	1440	1645	1000	1820
	B.4	1950	1975	1865	1465	1675	1045	1840
	B.5	1980	1950	2080	1515	1730	1075	1920
2"x2"x16 SWG	C.1	4730	5130	5400	3540	4060	1710	4530
	C.2	4965	5510	5180	3560	4105	1700	4600
	C.3	4600	5420	5600	3560	4105	1725	4600
	C.4	2385	4420	2380	2940	3380	1275	3750
	C.5	2285	3180	2460	2945	3380	1280	3750

All values are given in in lbf

TABLE IV.1

2 and 3 of Table IV.1. This table also shows theoretically computed values of critical bending moment using the expressions presented by Prandtl, Michell, Reissner and Goodier and also using equation II.4.7 derived in this thesis.

On examination of these values it can be seen that,

- (i) the experimentally determined values of M_c obtained from $\delta H \propto \frac{\delta H}{M}$ and $\delta \beta \propto \frac{\delta \beta}{M}$ are generally closely comparable and
- (ii) of the theoretically predicted M_c values the one found from equation II.4.7 gives the best agreement with the experimental values.

The collapse moment values are shown in column 1 of the same table. Comparison of these values with the experimentally and the relevant theoretically determined values of critical bending moment shows, with the exception of tests C4 and C5, acceptable correspondence. This implies that for the specimens in the dimensions proportion range, that is, width to thickness and depth to length, covered by the test programme, the value of M_c obtained theoretically from equation II.4.7 may be

taken as representing the maximum load carrying capacity. The post critical load carrying capacity margin of the sections investigated is obviously minimal and in fact, due to the effect of initial irregularities already discussed, collapse loads in some cases tend to be slightly lower than the corresponding experimentally predicted values.

In sections C4 and C5 the mode of failure was different to that of all the other test specimens. This was manifested by the angle of twist developed in these sections being such as to result in a progressive reduction in the effective torsional rigidity, culminating in a snap through failure. This condition is clearly illustrated by the divergence of the critical bending moment values predicted from the experimental results, based on horizontal deflection and angle of twist respectively.

CHAPTER V

PRACTICAL DESIGN APPLICATIONS

It has been shown that if a thin-walled open section beam is loaded in a plane not containing the shear centre, the resulting longitudinal stress system can only be determined by considering both bending and torsion effects. In practical design analysis this form of flexural-torsional behaviour will be in the small displacement range and the distribution of stresses can be evaluated by the methods presented in Chapter II, section 1. The various factors which have to be considered in this approach to flexural-torsional analysis are indicated in the following calculations for the safe load values of a thin-walled open section beam carrying a uniformly distributed load.

The beam section considered is a 10 in x 2 in x 14 S.W.G. ($t = 0.08$ in) channel section as shown in Fig. V.1 and has a span of 8 ft. The end conditions are considered to be simply supported with respect to bending and free to warp but restrained from twisting with respect to torsion. It is assumed that the compression flange of the beam has adequate lateral support.

The load carried by the beam is considered to be uniformly distributed across the width of the flange and is treated as a concentrated load per unit

length of the beam acting through the mid-point of the flange as illustrated in Fig. V.1. The bending and torsion effects of this loading are considered separately in the calculations which follow.

(1) Maximum longitudinal stress σ_{b3} due to bending

Maximum bending moment

$$M_x = \frac{wL^2}{8}$$

and if w is in lbf/in and L in ft then

$$M_x = \frac{144}{8} wL^2 \text{ in lbf}$$

The value of the appropriate section modulus is

$Z_{xx} = 2.804 \text{ in}^3$ and for $L = 8$ ft the maximum stress in the upper flange due to bending is given by the expression

$$\sigma_{b3} = -\frac{144 \cdot w \cdot (8)^2}{8 \times 2.804} = -411 \cdot w \quad \text{lbf/in}^2$$

where the negative sign indicates compressive stress.

(2) Maximum longitudinal stress σ_{T3} due to torsion

The approximate method of analysis which neglects the St. Venant torsional rigidity GC gives the maximum value of bi-moment B for this case as

$$B = \frac{mL^2}{8}$$

For w in lbf/in, the uniformly distributed torque m

about the shear centre is seen from Fig. V.1 to be given by the expression

$$m = w \left(e + \frac{d}{2} \right) \text{ in lbf/in}$$

The shear centre distance e for a thin-walled channel section is found from the expression

$$e = d \cdot \frac{3 \frac{d}{h}}{1 + 6 \frac{d}{h}} \quad (\text{reference 37 p.133})$$

In this case $d = 2$ in, $h = 10$ in and hence

$e = 0.545$ in. The value of m is therefore $w(0.545 + 1)$, that is $1.545w$ in lbf/in and for $L = 8$ ft the maximum bi-moment is

$$B = \frac{144}{8} (1.545w)(8)^2 = 1780w \text{ in}^2 \text{ lbf}$$

The value of the torsion bending constant Γ for a thin-walled channel section is found from the expression

$$\Gamma = \frac{t h^2 d^3}{12} \cdot \frac{2 + \frac{3d}{h}}{1 + 6 \frac{d}{h}} \quad (\text{reference 37 p.133})$$

which gives in this case $\Gamma = 6.303 \text{ in}^6$. The maximum values of longitudinal stress in a channel section due to torsion occur at the junction of the web and flange and at the free edge of the flange. The values of the sectorial co-ordinate ω for these two positions are

(i) web to flange junction (upper)

$$\omega_i = -\left(e \times \frac{h}{2}\right) = -(0.545 \times 5) = -2.725 \text{ in}^2$$

(ii) free edge of flange (upper)

$$\begin{aligned}\omega_{ii} &= +[(d-e) \times \frac{h}{2}] = +[(2-0.545) \times 5] \\ &= +7.275 \text{ in}^2\end{aligned}$$

The longitudinal stresses due to torsion at these positions are given by the expression

$$\sigma_{T3} = \frac{B_{max.} \omega}{r}$$

Thus for position (i)

$$\sigma_{T3} = \frac{1780 \omega (-2.725)}{6.303} = -768 \omega \text{ lbf/in}^2$$

and for position (ii)

$$\sigma_{T3} = \frac{1780 \omega (+7.275)}{6.303} = +2050 \omega \text{ lbf/in}^2$$

where the negative and positive signs indicate compressive and tensile stress respectively.

(3) Maximum longitudinal stress σ_{L3} due to bending and torsion

The total maximum longitudinal stress is given by the expression

$$\sigma_{L3} = \sigma_{b3} + \sigma_{T3}$$

Thus for position (i)

$$\sigma_{L3} = -411w - 768w = -1179w \text{ lbf/in}^2$$

and for position (ii)

$$\sigma_{L3} = -411w + 2050w = +1639w \text{ lbf/in}^2$$

Thus in this case the final maximum longitudinal stress due to bending and torsion occurs at the free edge of the flange.

(4) Safe load evaluation

The maximum permissible value of stress in bending, for thin-walled sections is given in Addendum No. 1 (1961) to BS 449 : 1959, as $0.65 Y_s$ which for a yield stress of $Y_s = 14 \text{ tonf/in}^2$ gives a permissible value of 9.1 tonf/in^2 or $20,400 \text{ lbf/in}^2$. This value of stress must be equal to the maximum longitudinal stress σ_{L3} due to bending and torsion, thus

$$1639w = 20,400$$

hence $w = 12.5 \text{ lbf/in}$ or 150 lbf/ft .

As indicated in Chapter II, section 1, the approximate method of analysis which neglects the St. Venant torsional rigidity, overestimates the maximum value of the bi-moment and corresponding

longitudinal stresses. Thus in using the approximate analysis the safe load will be underestimated.

The difference between the true and approximate values of the bi-moment depends on the type of loading and support conditions of the beam and can be related in any particular case, to the value of the beam parameter λL . The value of this parameter for the beam at present under consideration can be found as follows.

For a thin-walled channel section the torsion constant C is found from the expression

$$C = \frac{1}{3} (h + 2d) t^3$$

which in this case gives $C = 0.00239 \text{ in}^4$. Taking

$$E = 30 \times 10^6 \text{ lbf/in}^2 \text{ and } G = 12 \times 10^6 \text{ lbf/in}^2$$

then

$$\lambda = \sqrt{\frac{GC}{EI}} = \sqrt{\frac{12 \times 10^6 \times 0.00239}{30 \times 10^6 \times 6.303}} = 0.0123 \text{ in}^{-1}$$

and $\lambda L = 0.0123 \times 8 \times 12 = 1.18$

The true value of the bi-moment can be found by multiplying the approximate value by a correction factor α which will be related to the value of λL , the type of loading and the support conditions of the

beam. The variation of this correction factor with λL for a uniformly distributed torque on a simply supported beam is shown graphically in Fig. V.2.

This graph has been prepared by comparing the true and approximate values of the bi-moment coefficient f_1 , defined in Chapter II, section 1. Thus for a uniformly distributed torque

$$\text{approximate } B_{\max.} = \frac{mL^2}{8} \text{ and}$$

$$\text{true } B_{\max.} = \frac{m}{\lambda^2} \left(\frac{\cosh \lambda L - 1}{\sinh \lambda L} \cdot \sinh \frac{\lambda L}{2} - \cosh \frac{\lambda L}{2} + 1 \right)$$

and since for this case $f_1 = \frac{B}{mL^2}$ then

$$\text{approximate } f_1 = 0.125 \text{ and}$$

$$\text{true } f_1 = \frac{1}{(\lambda L)^2} \left(\frac{\cosh \lambda L - 1}{\sinh \lambda L} \cdot \sinh \frac{\lambda L}{2} - \cosh \frac{\lambda L}{2} + 1 \right)$$

The correction factor is found from the expression

$$\alpha = \frac{f_1 \text{ true}}{f_1 \text{ approximate}}$$

For the beam at present under consideration $\lambda L = 1.18$ and the correction factor $\alpha = 0.88$.

The maximum longitudinal stresses due to torsion are directly proportional to the maximum bi-moment value. Thus to obtain the true value of these stresses the approximate values already found can be multiplied by the correction factor α .

Thus for position (i)

$$\sigma_{T_3} = -768w \times 0.88 = -676w \text{ lbf/in}^2$$

and for position (ii)

$$\sigma_{T_3} = +2050w \times 0.88 = +1805w \text{ lbf/in}^2$$

The total maximum stresses at these positions thus become

$$(i) \quad \sigma_{L_3} = \sigma_{b_3} + \sigma_{T_3} = -411w - 676w = -1087w \text{ lbf/in}^2$$

$$(ii) \quad \sigma_{L_3} = \sigma_{b_3} + \sigma_{T_3} = -411w + 1805w = +1394w \text{ lbf/in}^2$$

As before the final maximum longitudinal stress due to bending and torsion occurs at the free edge of the flange and the safe load is found from the expression

$$1394w = 20,400$$

hence $w = 14.6 \text{ lbf/in or } 175 \text{ lbf/ft}$

If the bending stresses only are considered then the apparent safe load is calculated from the

expression

$$411w = 20,400$$

hence $w = 49.6 \text{ lbf/in}$ or 595 lbf/ft

The results of the present analysis are summarised in the following table.

ANALYSIS	SAFE LOAD
Bending and torsion - approximate bi-moment	150 lbf/ft
Bending and torsion - true bi-moment	175 lbf/ft
Bending only	595 lbf/ft

For the present analysis it can be seen that by taking into account the longitudinal stresses due to torsion the safe load is reduced to less than one third of the value based on bending stresses alone. The difference between the safe loads found from the approximate and true bi-moment analyses is, in this case, significant and as expected the approximate bi-moment approach gives rise to a conservative estimate of the safe load.

In the suggested safe load tables for thin-walled channel sections presented in Appendix VIII.6, the values given have been obtained by the present method of analysis using the true bi-moment value. However, in cases where $\lambda L < 1$ the difference between the safe loads based on the true and approximate bi-moment values will be small. This condition is more often encountered when lipped thin-walled open sections are used. For these sections the increase in the torsion bending constant J' due to the lip is greater than the corresponding increase in the torsion constant C . This gives rise to smaller values of λ and increases the range of spans for which $\lambda L < 1$.

The advantages of the approximate bi-moment analysis are more obvious when the structures considered are of indeterminate form such as continuous beams or rigid jointed frames. Thus in the case of a continuous beam the closed solution approach to the bi-moment distribution due to concentrated or uniformly distributed torques would involve laborious mathematical techniques of analysis.

However if the approximate method of solution is adopted, the resulting analogy between the problems of restrained torsion and plane bending, discussed in

Chapter II, section 1, can be applied to the analysis. In this way the approximate bi-moment distribution can be obtained by any of the methods used for the analysis of bending moment distribution, simply by replacing loads W or w by torques T or m and flexural rigidity EI by warping rigidity Er' . The results of such an analysis are illustrated by the bending moment and bi-moment diagrams for a two span continuous beam carrying uniformly distributed load actions, as shown in Fig. V.3.

The problem of flexural-torsional behaviour is not restricted to thin-walled open sections and will also obtain for conventional hot rolled sections of open form or for any section subjected to combined bending and torque actions. It is to be noted that in the safe load tables for hot rolled channel sections, presented in several structural engineering handbooks, the values quoted are based only on flexural stress analysis and no account has been taken of the possible torsion effects. The results of the present investigation have shown that longitudinal stresses due to torsion are of considerable magnitude and should be included in the safe load analysis.

CHAPTER VI

SUMMARY AND CONCLUSIONS

In the review of published literature it has been shown that the existing solutions for flexural-torsional behaviour of thin-walled open section beams, have been limited generally to small displacement problems. Although individual investigations have been carried out on the additional effects associated with large displacement behaviour, no single solution has been presented, in which all such effects are included.

The theoretical analysis of small displacement problems presented in this investigation has been based on the work of VLASOV. Solutions of closed form have been obtained for selected combinations of bending moment and torque. The application and limitations of an approximate method of analysis have been studied in relation to the practical design aspects of thin-walled open section structures.

The problem of large displacement flexural-torsional behaviour has been examined theoretically and the appropriate equations of bending moment and torque equilibrium have been established. In these equations the following additional effects have been included

- (i) Components of bending moment and torque due to axial displacement.
- (ii) Initial axial stress due to applied bending moments.
- (iii) Longitudinal stresses due to the 'shortening effect'.
- (iv) Components of torque due to load point displacement.

Approximate solutions have been found for these nonlinear equations for particular combinations of bending moment and torque, by a single term Galerkin technique. The results obtained from these solutions enabled the prediction of both stable and unstable nonlinear torque/angle of twist equilibrium paths in the elastic range of behaviour. Further analysis of these equilibrium paths has lead to the derivation of an expression for the critical value of bending moment producing flexural-torsional collapse.

A range of experimental work has been carried out on thin-walled channel and angle section beams. In the tests, small and large displacement behaviour and flexural-torsional failure of thin-walled beams due to bending moment has been examined. As predicted, the behaviour has been found to vary from linear to

nonlinear and stable to unstable according to the displacement range, the value of the beam parameter λL and the relative magnitudes of the applied bending moments and torques. The controlled deformation technique of testing which has been developed has enabled the measurement of strain and deformation in the elastic nonlinear unstable range of flexural-torsional behaviour. So far as the author is aware this form of behaviour has not been recorded experimentally in any previous investigation. The results obtained from the experimental investigation have substantiated the theoretical analyses which have been presented for flexural-torsional deformation and corresponding stress actions.

The principal findings of the present investigation can be summarised as follows.

- (1) The small displacement flexural-torsional behaviour of thin-walled open section beams for which the parameter $\lambda L < 1$, is linear and stable. The analysis of deformations and stresses in this range of behaviour can be obtained by considering the bending moment and torque actions separately.
- (2) The evaluation of the angles of twist and longitudinal stresses due to torsion, in

the small displacement range can be based on either the true or approximate bi-moment analysis, depending on the value of the beam parameter λL . If $\lambda L > 1$, the true bi-moment analysis should be used and if $\lambda L < 1$, then the approximate solution which always gives rise to conservative values of deformation and stress, will usually be acceptable. This latter approach would appear to be of considerable use in the formulation of a rational design procedure for structures composed of thin-walled open section members.

- (3) The flexural-torsional behaviour of thin-walled open section beams for which the parameter $\lambda L \gg 1$ can vary from linear to nonlinear and stable to unstable depending on the displacement range and the relative magnitudes of the applied bending moments and torques. The analysis of this form of behaviour must be based on the more general theory which takes account of the additional effects such as axial displacement and initial axial stress.
- (4) The maximum load carrying capacity with respect to bending of a thin-walled open section beam under flexural-torsional conditions, would appear to depend on the direction of the twist which develops as failure approaches. If the beam twists in a direction corresponding to increasing

effective torsional rigidity, then the bending moment causing collapse is adequately predicted by the assessment of critical bending moment. Failure, in the form of 'snap through' torsional buckling can occur at bending moment values less than the critical if the twist develops in the direction corresponding to a decreasing effective torsional rigidity.

ACKNOWLEDGEMENTS

The author wishes to express his thanks to Professor A.S.T. Thomson, Head of the Department of Mechanical Engineering at the University of Strathclyde, Glasgow, for the use of the facilities of the Department.

Thanks are also due to Professor R.M. Kenedi, Research Professor in Bio-Engineering at the University, for his continued interest and guidance during the period of this investigation. The author would also like to express his thanks to the Cold Rolled Sections Association for sponsoring the research programme.

Martin M. Black.

CHAPTER VII

BIBLIOGRAPHY AND AUTHOR INDEX

VII.1 Bibliography

1. BACH, C.

'Versuche uber die tatsachliche
Widerstandsfahigkeit von Balken mit
[- formigen Querschnitt'
Zeit d. Vereins deutscher Ingenieure, 1909,
p. 1790, 1910, p. 382.

2. MAILLART, R.

'Zur Frage der Biegung'
Schweiz. Bauztg., 1921, vol. 77, No. 18,
p. 195.

3. SEELY, F.G., PUTNAM, W.J. and SCHWALBE, W.L.

'The torsional effect of transverse bending
loads on channel beams'
Univ. Illinois, Engineering Experiment
Station, Bulletin No. 211, July, 1930.

4. TIMOSHENKO, S.P.

'Theory of bending, torsion and buckling of
thin walled members of open cross section'
Jnl. Franklin Inst., 1945, vol. 239,
Nos. 3, 4 and 5.

5. VLAZOV, V.Z.

Thin Walled Elastic Beams
Translation, Israel Program for Scientific
Translations, Jerusalem, 1961.

6. COULOMB, C.A.
Histoire de l'Academie
1784, p. 229, (Paris, 1787).
7. ST. VENANT, B.
'De la Torsion des Prismes'
Mems. Savants Etrangers, 1855, vol. XIV,
p. 233.
8. PRANDTL, L.
'Zur Torsion von Prismatischen Staben'
Physik. Zeit., 1903, vol. 4, p. 758.
9. GRIFFITH, A.A. and TAYLOR, G.I.
'The use of soap films in solving torsion
problems'
Proc. Inst. Mech. Eng., 1917, p. 755.
10. TIMOSHENKO, S.P.
Strength of Materials, Part II, Advanced
Theory and Problems
Third Edition, 1956, p. 239. (Van Nostrand,
New York).
11. TIMOSHENKO, S.P.
'On the stability in plane bending of an
I-beam'
Bull. Polytech. Inst. St. Petersburg,
1905 and 1906, vols. 4 and 5.

12. WEBER, C.

'Übertragung des Drehmomentes in Balken
mit doppelflanschigem Querschnitt'
Zeit. Angew. Math. u. Mech., 1926, vol. 6,
No. 2, p. 85.

13. REISSNER, E.

'On torsion with variable twist'
Oestr. Ing. - Archiv., 1955, vol. 9,
Nos. 2 and 3, p.218.

14. GOODIER, J.N. and BARTON, M.V.

'Effects of web deformation on the torsion
of I-beams'
Trans. A.S.M.E., 1944, vol. 66, p. A-35.

15. YOUNG, T.

A course of lectures on natural philosophy
and the mechanical arts
London, 1807.

16. WEBER, C.

'Die Lehre der Verdrehungsfestigkeit'
Forscharb. Ing. Wes., 1921, No. 249, p. 60.

17. CULLIMORE, M.S.G.

'The shortening effect, a nonlinear feature
of pure torsion'
Res. Eng. Struct., Colston Papers, 1949,
p. 153 (Butterworth, London).

18. GREGORY, M.
'Elastic torsion of members of thin open cross section'
Aust. Jnl. Appl. Sci., 1961, vol. 12,
No. 2, p. 174.
19. WILBERFORCE, L.R. and CAMPBELL, A.
'On vibration galvanometers with unifilar torsional control'
Proc. Phys. Soc. (London), 1913, vol. 25,
p. 203.
20. BUCKLEY, J.C.
'Bifilar property of twisted strips'
Phil. Mag., 1914, vol. 28, p. 778.
21. WAGNER, H.
'Torsion and buckling of open sections'
N.A.C.A., Tech. Mem. No. 807, 1936.
22. GOODIER, J.N.
'Elastic torsion in the presence of initial axial stress'
Trans. A.S.M.E., 1950, vol. 72, p. 383.
23. WINTER, G., LANSING, W. and McCALLEY, R.B.
'Performance of laterally loaded channel beams'
Res. Eng. Struct., Colston Papers, 1949,
p. 49 (Butterworth, London).

24. TERRINGTON, J.S.

'The calculation of bending and torsional effects in girders'

Jnl. Inst. Struct. Eng., January, 1958.

25. PETTERSSON, O.

'Combined bending and torsion of simply supported beams of bisymmetrical cross section'

Trans. Roy. Inst. Tech. (Stockholm), 1949, No. 29.

26. DOHRENWEND, C.O.

'Action of deep beams under combined vertical, lateral and torsional loads'

Trans. A.S.M.E., 1941, vol. 63, p. A-130.

27. ENGEL, H.L. and GOODIER, J.N.

'Measurements of torsional stiffness changes and instability due to tension, compression and bending'

Jnl. Appl. Mech., December, 1953, p. 553.

28. PRANDTL, L.

'Kipperscheinungen'

Doctoral Dissertation, Munich, 1899.

29. MICHELL, A.G.M.

'Elastic stability of long beams under transverse forces'

Phil. Mag., 1899, vol. 48, p. 298.

30. REISSNER, H.

'Uber die Stabilitat der Biegung'
Archiv. d. Math. u. Phys., 1904, vol. 7,
(Sitzungsb. Berl. Math. Ges. 1904, p. 53).

31. GOODIER, J.N.

'Some observations on elastic stability'
Proc. First National Congress of Applied
Mechanics, 1951, (A.S.M.E.)

32. TIMOSHENKO, S.P.

'Einige Stabilitatsprobleme der
Elastizitatstheorie'
Zeit. Math. Physik, 1910, vol. 58, p. 337.

33. TIMOSHENKO, S.P.

Theory of Elastic Stability
First Edition, 1936, p. 239. (McGraw-Hill,
New York).

34. RICHARDS, N.E.

'The strength of open sections in
compression and bending'
Council for Scientific and Industrial
Research, Australia, Division of Aeronautics,
Report S.M. 94, May, 1947.

35. CHILVER, A.H.

'Structural problems in the use of
cold-formed steel sections'

Proc. Inst. Civil Engs., October, 1961,
vol. 20, p. 233.

36. SOUTHWELL, R.V.

'On the analysis of experimental
observations in problems of elastic
stability'

Proc. Roy. Soc. (London), April, 1932,
vol. 135, ser. A, p. 601.

37.

Handbook of Aeronautics, No. 1 -
Structural Principles and Data
Fourth Edition, 1952 (Pitman).

VII.2 Author Index

Name	Reference No.	Page
BACH, C.	1	1
BARTON, M.V.	14	13
BUCKLEY, J.C.	20	18
CAMPBELL, A.	19	17
CHILVER, A.H.	35	41
COULOMB, C.A.	6	9
CULLIMORE, M.S.G.	17	16, 44
DOHRENWEND, C.O.	26	28
ENGEL, H.L.	27	31, 44
GOODIER, J.N.	14, 22, 27, 31	13, 18, 29, 31, 35, 39, 44, 45, 69
GREGORY, M.	18	16, 33, 44, 45, 69
GRIFFITH, A.A.	9	11
LANSING, W.	23	24, 43
MCCALLEY, R.B.	23	24, 43
MAILLART, R.	2	1
MICHELL, A.G.M.	29	34, 45
PETTERSSON, O.	25	28
PRANDTL, L.	8, 28	10, 34, 45

Name	Reference No.	Page
PUTNAM, W.J.	3	2
REISSNER, E.	13	13
REISSNER, H.	30	34, 45
RICHARDS, N.E.	34	41
ST. VENANT, B.	7	9
SCHWALBE, W.L.	3	2
SEELY, F.B.	3	2
SOUTHWELL, R.V.	36	128
TAYLOR, G.I.	9	11
TERRINGTON, J.S.	24	27, 43, 45
TIMOSHENKO, S.P.	4, 10, 11, 32, 33	6, 11, 12, 22, 36, 40, 42, 43, 45
VLAZOV, V.Z.	5	8, 13, 19, 40, 42, 43, 45, 48, 145
WAGNER, H.	21	18
WEBER, C.	12, 16	13, 14, 44
WILBERFORCE, L.R.	19	17
WINTER, G.	23	24, 43, 45
YOUNG, T.	15	14

CHAPTER VIII

APPENDICES

APPENDIX VIII.1

Theoretical Solutions

The method used to obtain an approximate single term Galerkin solution to the generalised differential equations of bending moment and torque equilibrium (equations II.2.9) has been described in Chapter II, section 3. In that section one solution for a particular combination of bending moment and torque on a beam was presented and the results of three alternative solutions for the same problem were quoted. Details of these alternative solutions are given in this Appendix.

The appropriate differential equations of bending moment and torque equilibrium for the problem considered have been shown in Chapter II, section 3, to be

$$\begin{aligned}
 EI_x \frac{d^2 v}{dz^2} &= - M_x \cos \beta \\
 EI_y \frac{d^2 u}{dz^2} &= - M_x \sin \beta \\
 \left(GC + \frac{K_y M_x \sin \beta}{I_y} \right) \frac{d\beta}{dz} - EI \frac{d^3 \beta}{dz^3} + \frac{1}{2} E \left(\frac{d\beta}{dz} \right)^2 \left(K_c - \frac{I_c^2}{A} - \frac{K_y^2}{I_y} \right) \\
 &= M_z + M_x \frac{d\bar{u}}{dz}
 \end{aligned}$$

CASE I

Assuming a sinusoidal variation of β with z ,
that is

$$\beta_z = \beta_0 \sin \frac{\pi z}{L}$$

and substituting

$$\sin \beta = \beta - \frac{\beta^3}{3!}$$

$$\cos \beta = 1 - \frac{\beta^2}{2!}$$

then equations A.1.1 can be written as

$$EI_x \frac{d^2 v}{dz^2} = -M_x \left[1 - \frac{(\beta_0 \sin \frac{\pi z}{L})^2}{2!} \right]$$

$$EI_y \frac{d^2 u}{dz^2} = -M_x \left[\beta_0 \sin \frac{\pi z}{L} - \frac{(\beta_0 \sin \frac{\pi z}{L})^3}{3!} \right]$$

$$\left\{ GC + \frac{K_y M_x \left[\beta_0 \sin \frac{\pi z}{L} - \frac{(\beta_0 \sin \frac{\pi z}{L})^3}{3!} \right]}{I_y} \right\} \left(\frac{\pi}{L} \beta_0 \cos \frac{\pi z}{L} \right)$$

$$- EI \left(-\frac{\pi^3}{L^3} \beta_0 \cos \frac{\pi z}{L} \right) + \frac{1}{2} E \left(\frac{\pi}{L} \beta_0 \cos \frac{\pi z}{L} \right)^3 \left(K_c - \frac{I_c^2}{A} - \frac{K_y^2}{I_y} \right)$$

$$= M_z + M_x \frac{d\bar{u}}{dz}$$

A.1.2

To obtain the solution for the last of equations A.1.2

by the Galerkin method, the derivative $\frac{d\bar{u}}{dz}$ must be expressed as a function of β_0 and z .

Integrating directly, the first two of equations A.1.2 and using the boundary conditions

$$z=0, \quad u=v=0 \quad \text{and} \quad z=\frac{L}{2}, \quad \frac{du}{dz} = \frac{dv}{dz} = 0$$

gives the following expressions for u and v .

$$\begin{aligned} u = & -\frac{M_x}{EI_y} \left(-\beta_0 \frac{L^2}{\pi^2} \sin \frac{\pi z}{L} + \frac{1}{6} \beta_0^3 \frac{L^2}{\pi^2} \sin \frac{\pi z}{L} \right. \\ & \left. + \frac{1}{54} \beta_0^3 \frac{L^2}{\pi^2} \sin^3 \frac{\pi z}{L} - \frac{1}{18} \beta_0^3 \frac{L^2}{\pi^2} \sin \frac{\pi z}{L} \right) \\ v = & -\frac{M_x}{EI_x} \left(\frac{1}{2} z^2 - \frac{1}{8} \beta_0^2 z^2 - \frac{1}{16} \beta_0^2 \frac{L^2}{\pi^2} \cos \frac{2\pi z}{L} \right) \\ & + \frac{M_x L}{EI_x} z \left(\frac{1}{2} - \frac{1}{8} \beta_0^2 \right) - \frac{1}{16} \frac{M_x}{EI_x} \beta_0^2 \frac{L^2}{\pi^2} \end{aligned} \quad \text{A.1.3}$$

The horizontal deflection \bar{u} relative to the undisplaced axes is given by the expression

$$\bar{u} = u \cos \beta - v \sin \beta$$

that is, in terms of β_0 ,

$$\begin{aligned} \bar{u} = & u \left[1 - \frac{(\beta_0 \sin \frac{\pi z}{L})^2}{2!} \right] \\ & - v \left[\beta_0 \sin \frac{\pi z}{L} - \frac{(\beta_0 \sin \frac{\pi z}{L})^3}{3!} \right] \end{aligned} \quad \text{A.1.4}$$

Substituting the expressions for u and v given by equations A.1.3 into equation A.1.4 and differentiating with respect to z , the following expression for $\frac{d\bar{u}}{dz}$ is obtained,

$$\begin{aligned} \frac{d\bar{u}}{dz} = & - \frac{M_x L^2}{EI_y} \left[-\frac{\beta_o}{\pi^2} \frac{\pi}{L} \cos \frac{\pi z}{L} + \frac{1}{6} \frac{\beta_o^3}{\pi^2} \frac{\pi}{L} \cos \frac{\pi z}{L} + \right. \\ & \left. \frac{1}{54} \frac{\beta_o^3}{\pi^2} \frac{3\pi}{L} \sin^2 \frac{\pi z}{L} \cos \frac{\pi z}{L} - \frac{1}{18} \frac{\beta_o^3}{\pi^2} \frac{\pi}{L} \cos \frac{\pi z}{L} \right] + \\ & \frac{M_x L^2}{EI_y} \left[-\frac{1}{2} \frac{\beta_o^3}{\pi^2} \frac{3\pi}{L} \sin^2 \frac{\pi z}{L} \cos \frac{\pi z}{L} + \frac{1}{12} \frac{\beta_o^5}{\pi^2} \frac{3\pi}{L} \sin^2 \frac{\pi z}{L} \cos \frac{\pi z}{L} + \right. \\ & \left. \frac{1}{108} \frac{\beta_o^5}{\pi^2} \frac{5\pi}{L} \sin^4 \frac{\pi z}{L} \cos \frac{\pi z}{L} - \frac{1}{36} \frac{\beta_o^5}{\pi^2} \frac{3\pi}{L} \sin^2 \frac{\pi z}{L} \cos \frac{\pi z}{L} \right] + \\ & \frac{M_x}{EI_x} \left[\frac{1}{2} \beta_o \left(\frac{\pi}{L} z^2 \cos \frac{\pi z}{L} + 2z \sin \frac{\pi z}{L} \right) - \frac{1}{8} \beta_o^3 \left(\frac{\pi}{L} z^2 \cos \frac{\pi z}{L} + 2z \sin \frac{\pi z}{L} \right) - \right. \\ & \left. \frac{1}{16} \beta_o^3 \frac{L^2}{\pi^2} \left(\frac{\pi}{L} \cos \frac{\pi z}{L} \cos \frac{2\pi z}{L} - \frac{4\pi}{L} \sin^2 \frac{\pi z}{L} \cos \frac{\pi z}{L} \right) - \right. \\ & \left. \frac{1}{2} L \beta_o \left(\frac{\pi}{L} z \cos \frac{\pi z}{L} + \sin \frac{\pi z}{L} \right) + \frac{1}{8} L \beta_o^3 \left(\frac{\pi}{L} z \cos \frac{\pi z}{L} + \sin \frac{\pi z}{L} \right) + \right. \\ & \left. \frac{1}{16} \beta_o^3 \frac{L}{\pi} \cos \frac{\pi z}{L} \right] - \frac{M_x}{EI_x} \left[\frac{1}{12} \beta_o^3 \left(\frac{3\pi}{L} z^2 \sin^2 \frac{\pi z}{L} \cos \frac{\pi z}{L} + 2z \sin^3 \frac{\pi z}{L} \right) - \right. \\ & \left. \frac{1}{48} \beta_o^5 \left(\frac{3\pi}{L} z^2 \sin^2 \frac{\pi z}{L} \cos \frac{\pi z}{L} + 2z \sin^3 \frac{\pi z}{L} \right) - \right. \\ & \left. \frac{1}{96} \beta_o^5 \frac{L^2}{\pi^2} \left(\frac{3\pi}{L} \cos \frac{2\pi z}{L} \sin^2 \frac{\pi z}{L} \cos \frac{\pi z}{L} - \frac{4\pi}{L} \sin^4 \frac{\pi z}{L} \cos \frac{\pi z}{L} \right) - \right. \end{aligned}$$

$$\begin{aligned}
& \frac{1}{12} L \beta_0^3 \left(\frac{3\pi}{L} z \sin^2 \frac{\pi z}{L} \cos \frac{\pi z}{L} + \sin^3 \frac{\pi z}{L} \right) + \\
& \left[\frac{1}{48} L \beta_0^5 \left(\frac{3\pi}{L} z \sin^2 \frac{\pi z}{L} \cos \frac{\pi z}{L} + \sin^3 \frac{\pi z}{L} \right) + \frac{1}{96} \beta_0^5 \frac{L^2}{\pi^2} \frac{3\pi}{L} \sin^2 \frac{\pi z}{L} \cos \frac{\pi z}{L} \right] \\
& = F_I(\beta_0, z)
\end{aligned}$$

A.1.5

The last of equations A.1.2 can now be written in an appropriate Galerkin integral equation form allowing for the symmetry of the problem, thus

$$\begin{aligned}
& 2 \int_0^{\frac{L}{2}} \left\{ GC + \frac{K_y M_x \left[\beta_0 \sin \frac{\pi z}{L} - \frac{(\beta_0 \sin \frac{\pi z}{L})^3}{3!} \right]}{I_y} \right\} \left(\frac{\pi}{L} \beta_0 \cos \frac{\pi z}{L} \right) + \\
& E \Gamma \frac{\pi^3}{L^3} \beta_0 \cos \frac{\pi z}{L} + \frac{1}{2} E \left(\frac{\pi}{L} \beta_0 \cos \frac{\pi z}{L} \right)^3 \left(K_c - \frac{I_c^2}{A} - \frac{K_y^2}{I_y} \right) - \\
& M_z - M_x \left[F_I(\beta_0, z) \right] \left(\frac{d\beta}{d\beta_0} \right) dz = 0
\end{aligned}$$

A.1.6

Equation A.1.6 can be solved by substituting $\sin \frac{\pi z}{L}$ for $\frac{d\beta}{d\beta_0}$ and integrating. This procedure yields the following polynomial expression for M_z at $z = \frac{L}{2}$ in terms of β_0 , thus

$$\begin{aligned}
M_z &= a_2 \beta_0 + b_2 \beta_0^2 + c_2 \beta_0^3 + d_2 \beta_0^4 + e_2 \beta_0^5 \\
& \quad \text{where} \\
a_2 &= 1.571 \frac{GC}{L} + 15.528 \frac{E \Gamma}{L^3} - 0.159 \frac{M_x^2 L}{EI_y} + 0.254 \frac{M_x^2 L}{EI_x}
\end{aligned}$$

$$b_2 = 1.047 \frac{K_y M_x}{L I_y}$$

$$c_2 = 3.881 \frac{E}{L^3} \left(K_c - \frac{I_c^2}{A} - \frac{K_y^2}{I_y} \right) + 0.142 \frac{M_x^2 L}{E I_y} - 0.146 \frac{M_x^2 L}{E I_x}$$

$$d_2 = -0.1047 \frac{K_y M_x}{L I_y}$$

$$e_2 = -0.0158 \frac{M_x^2 L}{E I_y} + 0.0174 \frac{M_x^2 L}{E I_x}$$

A.1.7

CASE II

Assuming a linear variation of β with z ,
that is

$$\beta_z = \beta_0 \frac{2z}{L}$$

and substituting

$$\sin \beta = \beta$$

$$\cos \beta = 1$$

then equations A.1.1 can be written as

$$E I_x \frac{d^2 v}{dz^2} = -M_x$$

$$E I_y \frac{d^2 u}{dz^2} = -M_x \beta_0 \frac{2z}{L}$$

$$\left[G C - \frac{K_y M_x \left(\beta_0 \frac{2z}{L} \right)}{I_y} \right] \left(\frac{2\beta_0}{L} \right) + \frac{1}{2} E \left(\frac{2\beta_0}{L} \right)^3 \left(K_c - \frac{I_c^2}{A} - \frac{K_y^2}{I_y} \right)$$

$$= M_z + M_x \frac{d\bar{u}}{dz}$$

A.1.8

As before, the solution of the last of equations A.1.8 by the Galerkin method requires the derivative $\frac{d\bar{u}}{dz}$ to be expressed as a function of β_0 and z .

Integrating directly the first two of equations A.1.8 and using the boundary conditions

$$z=0, \quad u=v=0 \quad \text{and} \quad z=\frac{L}{2}, \quad \frac{du}{dz} = \frac{dv}{dz} = 0$$

gives the following expressions for u and v .

$$\begin{aligned} u &= \frac{M_x}{EI_y} \beta_0 \left(\frac{Lz}{4} - \frac{z^3}{3L} \right) \\ v &= \frac{M_x}{2EI_x} (Lz - z^2) \end{aligned} \quad \text{A.1.9}$$

The horizontal deflection \bar{u} relative to the undisplaced axes is given by the expression

$$\bar{u} = u \cos \beta - v \sin \beta$$

that is, in terms of β_0

$$\bar{u} = u - v \beta_0 \frac{2z}{L} \quad \text{A.1.10}$$

Substituting the expressions for u and v given by equations A.1.9, into equation A.1.10 and differentiating with respect to z the following expression for $\frac{d\bar{u}}{dz}$ is obtained

$$\frac{d\bar{u}}{dz} = \frac{M_x}{EI_y} \beta_0 \left(\frac{L}{4} - \frac{z^2}{L} \right) - \frac{M_x}{EI_x} \beta_0 \left(2z - 3 \frac{z^2}{L} \right) \quad \text{A.1.11}$$

The last of equations A.1.8 can now be written in an appropriate Galerkin integral equation form allowing for the symmetry of the problem, thus

$$2 \int_0^{\frac{L}{2}} \left\{ \left[GC + \frac{K_y M_x (\beta_0 \frac{2z}{L})}{I_y} \right] \left(\frac{2\beta_0}{L} \right) + \frac{1}{2} E \left(\frac{2\beta_0}{L} \right) \left(K_c - \frac{I_c^2}{A} - \frac{K_y^2}{I_y} \right) - M_z \right. \\ \left. - M_x \left[\frac{M_x}{EI_y} \beta_0 \left(\frac{L}{4} - \frac{z^2}{L} \right) - \frac{M_x}{EI_x} \beta_0 \left(2z - \frac{3z^2}{L} \right) \right] \right\} \left(\frac{d\beta}{d\beta_0} \right) dz = 0 \quad \text{A.1.12}$$

Equation A.1.12 can be solved by substituting $2 \frac{z}{L}$ for $\frac{d\beta}{d\beta_0}$ and integrating. This procedure yields the following polynomial expression for M_z at $z = \frac{L}{2}$ in terms of β_0 , thus

$$M_z = a_3 \beta_0 + b_3 \beta_0^2 + c_3 \beta_0^3$$

$z = \frac{L}{2}$

where

$$a_3 = 2 \frac{GC}{L} - 0.125 \frac{M_x^2 L}{EI_y} + 0.292 \frac{M_x^2 L}{EI_x}$$

$$b_3 = 1.333 \frac{K_y M_x}{L I_y}$$

$$c_3 = 4 \frac{E}{L^3} \left(K_c - \frac{I_c^2}{A} - \frac{K_y^2}{I_y} \right) \quad \text{A.1.13}$$

CASE III

Assuming a linear variation of β with z that is

$$\beta_z = \beta_0 \frac{2z}{L}$$

and substituting

$$\sin \beta = \beta - \frac{\beta^3}{3!}$$

$$\cos \beta = 1 - \frac{\beta^2}{2!}$$

then equations A.1.1 can be written as

$$\begin{aligned} EI_x \frac{d^2 v}{dz^2} &= -M_x \left[1 - \frac{(\beta_0 \frac{2z}{L})^2}{2!} \right] \\ EI_y \frac{d^2 u}{dz^2} &= -M_x \left[\beta_0 \frac{2z}{L} - \frac{(\beta_0 \frac{2z}{L})^3}{3!} \right] \\ \left\{ GC + \frac{K_y M_x \left[\beta_0 \frac{2z}{L} - \frac{(\beta_0 \frac{2z}{L})^3}{3!} \right]}{I_y} \right\} \left(\frac{2\beta_0}{L} \right) + \frac{1}{2} E \left(\frac{2\beta_0}{L} \right)^3 \left(K_c - \frac{I_c^2}{A} - \frac{K_y^2}{I_y} \right) \\ &= M_z + M_x \frac{d\bar{u}}{dz} \end{aligned} \quad \text{A.1.14}$$

As before, the solution of the last of equations A.1.14 by the Galerkin method requires the derivative $\frac{d\bar{u}}{dz}$ to be expressed as a function of β_0 and z .

Integrating directly the first two of equations A.1.14 and using the boundary conditions

$$z=0, \quad u=v=0 \quad \text{and} \quad z=\frac{L}{2}, \quad \frac{du}{dz} = \frac{dv}{dz} = 0$$

gives the following expressions for u and v .

$$\begin{aligned} u &= \frac{M_x}{EI_y} \left[\beta_0 \left(\frac{Lz}{4} - \frac{z^3}{3L} \right) + \beta_0^3 \left(\frac{z^5}{15L^3} - \frac{Lz}{48} \right) \right] \\ v &= \frac{M_x}{EI_x} \left[\frac{1}{2} (Lz - z^2) + \frac{1}{3} \beta_0^2 \left(\frac{z^4}{L^2} - \frac{Lz}{2} \right) \right] \end{aligned} \quad \text{A.1.15}$$

The horizontal deflection u relative to the undisplaced axes is given by the expression

$$\bar{u} = u \cos \beta - v \sin \beta$$

that is, in terms of β_0

$$\bar{u} = u \left[1 - \frac{(\beta_0 \frac{2z}{L})^2}{2!} \right] - v \left[\beta_0 \frac{2z}{L} - \frac{(\beta_0 \frac{2z}{L})^3}{3!} \right] \quad \text{A.1.16}$$

Substituting the expressions for u and v given by equations A.1.15, into equation A.1.16 and differentiating with respect to z , the following expression for $\frac{d\bar{u}}{dz}$ is obtained

$$\begin{aligned} \frac{d\bar{u}}{dz} = & \frac{M_x}{EI_y} \left[\beta_0 \left\{ \left(\frac{L}{4} - \frac{z^2}{L} \right) - \left(\frac{3\beta_0^2 z^2}{2L} - \frac{10\beta_0^2 z^4}{3L^3} \right) \right\} + \beta_0^3 \left\{ \left(\frac{z^4}{3L^3} - \frac{L}{48} \right) - \right. \right. \\ & \left. \left(\frac{14\beta_0^2 z^6}{15L^5} - \frac{\beta_0^2 z^2}{8L} \right) \right\} \right] - \frac{M_x}{EI_x} \left[\frac{1}{2} \left\{ (4\beta_0 z - \frac{6\beta_0 z^3}{L}) - \right. \right. \\ & \left. \left(\frac{16\beta_0^3 z^3}{3L^2} - \frac{20\beta_0^3 z^4}{3L^3} \right) \right\} + \frac{1}{3} \beta_0^2 \left\{ \left(\frac{10\beta_0 z^4}{L^3} - 2\beta_0 z \right) - \right. \\ & \left. \left(\frac{28\beta_0^3 z^6}{3L^5} - \frac{8\beta_0^3 z^3}{3L^2} \right) \right\} \right] \\ = & F_{III}(\beta_0, z) \end{aligned} \quad \text{A.1.17}$$

The last of equations A.1.14 can now be written in an appropriate Galerkin integral equation form allowing for the symmetry of the problem thus,

$$2 \int_0^{\frac{L}{2}} \left\{ GC + \frac{K_{yy} M_x \left[\beta_0 \frac{2z}{L} - \frac{(\beta_0 \frac{2z}{L})^3}{3!} \right] \right\} \left(\frac{2\beta_0}{L} \right) + \frac{1}{2} E \left(\frac{2\beta_0}{L} \right)^3 \left(K_c - \frac{I_c^2}{A} - \frac{K_{yy}^2}{I_y} \right) - M_z - M_x \left[F_{III}(\beta_0, z) \right] \left(\frac{d\beta}{d\beta_0} \right) dz = 0 \quad A.1.18$$

Equation A.1.18 can be solved by substituting $\frac{2z}{L}$ for $\frac{d\beta}{d\beta_0}$ and integrating. This procedure yields the following polynomial expression for M_z at $z = \frac{L}{2}$ in terms of β_0 , thus

$$M_z = a_4 \beta_0 + b_4 \beta_0^2 + c_4 \beta_0^3 + d_4 \beta_0^4 + e_4 \beta_0^5 \quad z = \frac{L}{2}$$

where

$$\begin{aligned} a_4 &= \frac{2GC}{L} - 0.125 \frac{M_x^2 L}{EI_y} + 0.292 \frac{M_x^2 L}{EI_x} \\ b_4 &= 1.333 \frac{K_{yy} M_x}{LI_y} \\ c_4 &= \frac{4E}{L^3} \left(K_c - \frac{I_c^2}{A} - \frac{K_{yy}^2}{I_y} \right) + 0.132 \frac{M_x^2 L}{EI_y} - 0.217 \frac{M_x^2 L}{EI_x} \\ d_4 &= -0.133 \frac{K_{yy} M_x}{LI_y} \\ e_4 &= -0.0119 \frac{M_x^2 L}{EI_y} + 0.0436 \frac{M_x^2 L}{EI_x} \end{aligned} \quad A.1.19$$

APPENDIX VIII.2

Effect of Neglecting Bending Moment Components

$$\underline{M_3 \frac{d\bar{u}}{dz} \quad \text{and} \quad M_3 \frac{d\bar{v}}{dz} .}$$

It has been shown in Chapter II, section 2, that the equations of bending moment equilibrium about the displaced axes of a beam subjected to bending and torsion can be written as

$$\begin{aligned} M_{x'} &= M_x \cos \beta + M_y \sin \beta - M_3 \frac{d\bar{u}}{dz} \\ M_{y'} &= M_y \cos \beta - M_x \sin \beta - M_3 \frac{d\bar{v}}{dz} \end{aligned} \quad \text{A.2.1}$$

If $M_y = 0$, equations A.2.1 are reduced to

$$\begin{aligned} M_{x'} &= M_x \cos \beta - M_3 \frac{d\bar{u}}{dz} \\ M_{y'} &= -M_x \sin \beta - M_3 \frac{d\bar{v}}{dz} \end{aligned} \quad \text{A.2.2}$$

Dividing by M_x equations A.2.2 become

$$\begin{aligned} \frac{M_{x'}}{M_x} &= \cos \beta - \frac{M_3}{M_x} \frac{d\bar{u}}{dz} \\ \frac{M_{y'}}{M_x} &= -\sin \beta - \frac{M_3}{M_x} \frac{d\bar{v}}{dz} \end{aligned} \quad \text{A.2.3}$$

Assuming that the variation of \bar{u} , \bar{v} and β with z is sinusoidal then, in terms of the maximum

displacements \bar{u}_0 , \bar{v}_0 and β_0 at the centre of the span, the displacements at any section z can be written as

$$\bar{u}_z = \bar{u}_0 \sin \frac{\pi z}{L}$$

$$\bar{v}_z = \bar{v}_0 \sin \frac{\pi z}{L}$$

$$\beta_z = \beta_0 \sin \frac{\pi z}{L}$$

A.2.4

Using these relationships, equations A.2.3 can be expressed as

$$\frac{M_x'}{M_x} = \cos(\beta_0 \sin \frac{\pi z}{L}) - \frac{M_z}{M_x} \bar{u}_0 \frac{\pi}{L} \cos \frac{\pi z}{L}$$

$$\frac{M_y'}{M_x} = -\sin(\beta_0 \sin \frac{\pi z}{L}) - \frac{M_z}{M_x} \bar{v}_0 \frac{\pi}{L} \cos \frac{\pi z}{L}$$

A.2.5

In the experimental work described in the present thesis, the maximum values of β_0 , $\frac{M_z}{M_x}$ and \bar{u}_0 or \bar{v}_0 which obtained were 1.4 radian, 0.2 and $\frac{L}{65}$ in respectively. For these maximum values, equations A.2.5 become,

$$\frac{M_x'}{M_x} = \cos(1.4 \sin \frac{\pi z}{L}) - 0.2 \frac{\pi}{65} \cos \frac{\pi z}{L}$$

$$\frac{M_y'}{M_x} = -\sin(1.4 \sin \frac{\pi z}{L}) - 0.2 \frac{\pi}{65} \cos \frac{\pi z}{L}$$

A.2.6

The numerical values of the terms on the right hand sides of equations A.2.6 in the range $0 \leq z < \frac{L}{2}$ are

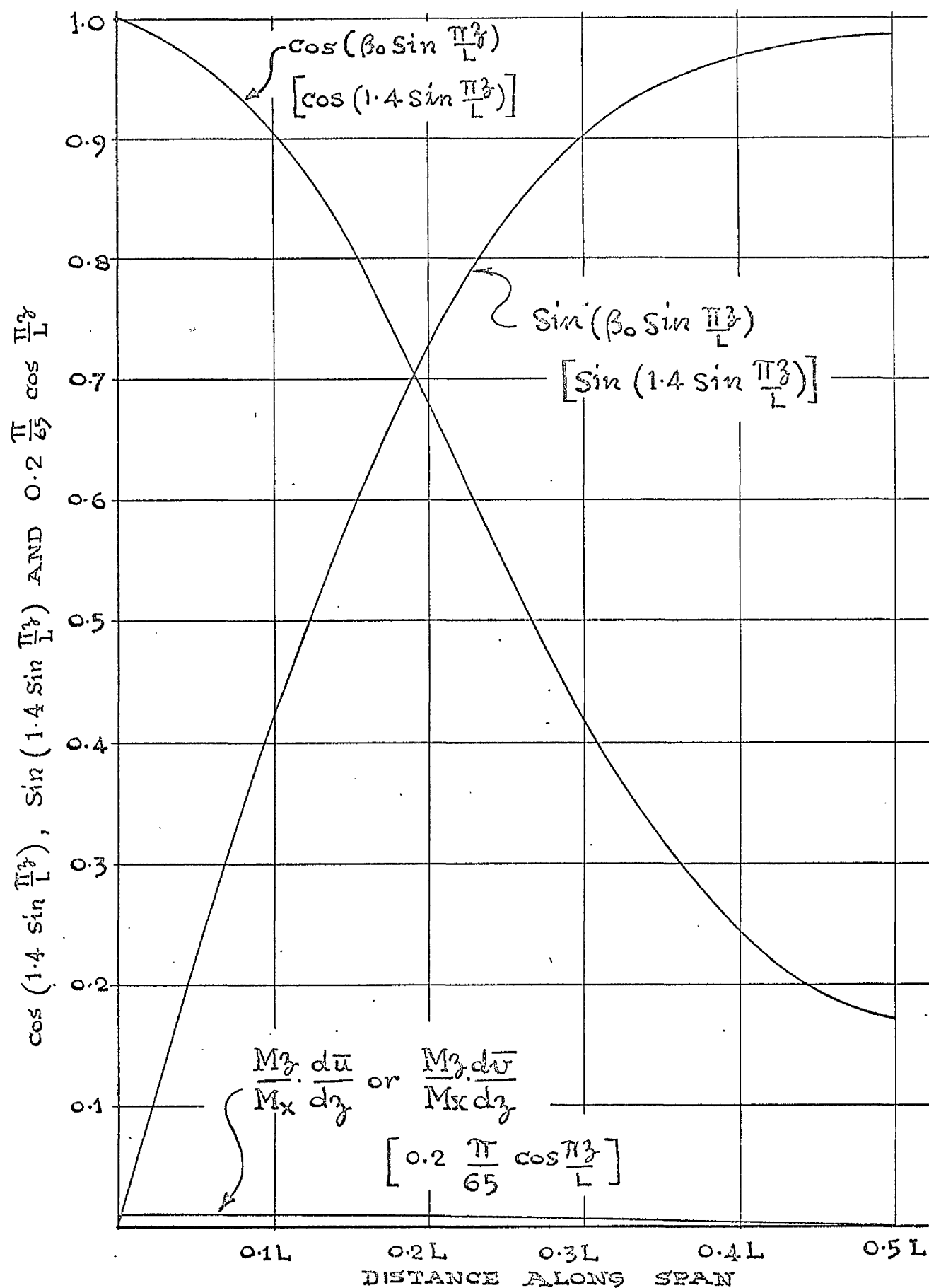


FIG. A.2.1. RELATIVE MAGNITUDES OF $\sin(\beta_0 \sin \frac{\pi z}{L})$
 $\cos(\beta_0 \sin \frac{\pi z}{L})$, $\frac{M_z}{M_x} \frac{d\bar{u}}{dz}$ AND $\frac{M_z}{M_x} \frac{d\bar{v}}{dz}$

shown graphically in Fig. A.2.1. It can be seen that for this range, the term $0.2 \frac{\pi}{65} \cos \frac{\pi z}{L}$ is negligible in comparison with the terms $\cos(1.4 \sin \frac{\pi z}{L})$ and $\sin(1.4 \sin \frac{\pi z}{L})$. Thus for the maximum torque/bending moment ratio and displacements, equations A.2.2 can be approximated to

$$M_{x'} = M_x \cos \beta$$

$$M_{y'} = -M_x \sin \beta$$

A.2.7

APPENDIX VIII.3

Experimental Measurement of the Flexural and Torsional Rigidities of the Brass and Steel Angle Section

Specimens

The extruded brass angle sections used for the experimental investigation were found to have small variations in the cross-sectional dimensions. In an attempt to allow for these variations the flexural and torsional rigidities of each specimen were found from pure bending and torsion tests.

(1) Flexural rigidities

In the case of the flexural rigidities, the angles were tested by a four-point loading system as shown in Fig. A.3.1. The deflection at mid-span was recorded for different values of applied bending moment constant over the test span. The test span length was the same as that adopted for the combined bending and torsion tests.

The value of the flexural rigidity was calculated from the expression

$$EI = \frac{M \alpha^2}{2h} \quad \text{A.3.1}$$

where M was the applied bending moment, h the

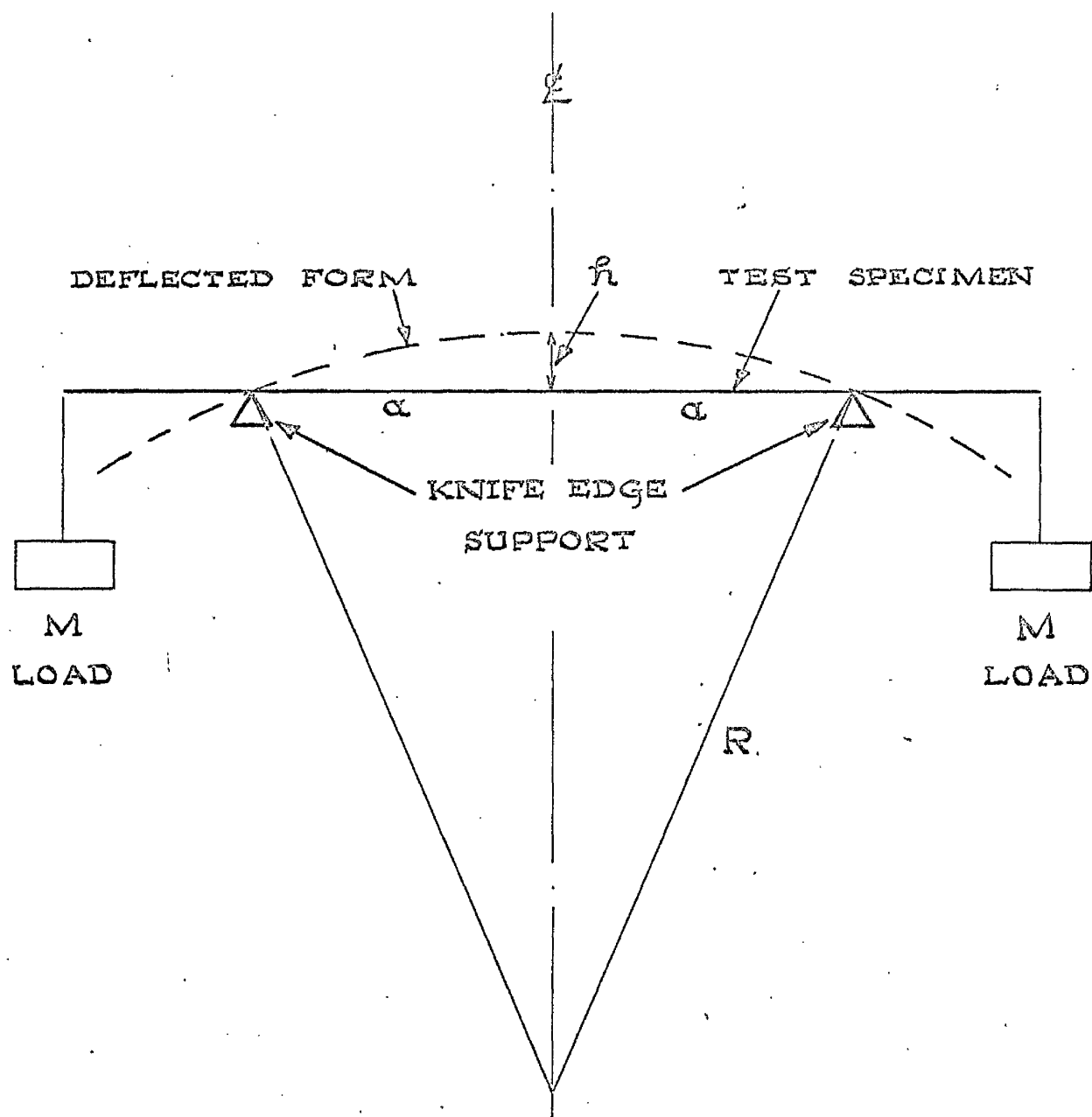


FIG. A.3.1. EXPERIMENTAL MEASUREMENT OF FLEXURAL RIGIDITY.

corresponding deflection at mid-span and a was the half span length.

For EI_y the angle was placed toes down on simple knife edge supports and for EI_x it was held in the gimbal supports of the main test rig and loaded by the aluminium disc and pulley arrangement.

(2) Torsional rigidity

The value of the torsional rigidity for each specimen was found from two different forms of test. In the first, the specimen was held in the gimbal supports and increments of torque were applied at mid-span. The corresponding angles of twist were recorded and the straight line torque/angle of twist relationship obtained. The value of GC was found from the expression

$$GC = \frac{TL}{4\beta_0} \quad \text{A.3.2}$$

where T was the applied torque at mid-span, β_0 the corresponding angle of twist at mid-span and L the distance between the gimbal supports.

The second experimental method used to determine GC was based on the torsional oscillation of the angle section. The specimen was suspended vertically from a

fixed support and a plate of known inertia was attached to the free end. The plate was displaced through a small angle in the horizontal plane and released. The frequency of the resulting torsional oscillations was measured and knowing the length between the fixed support and the plate, the value of GC could be calculated from the expression

$$GC = I_o (2\pi)^2 f^2 L \quad A.3.3$$

where I_o was the appropriate plate inertia, f the frequency of the torsional oscillations and L was the length between the fixed support and the plate.

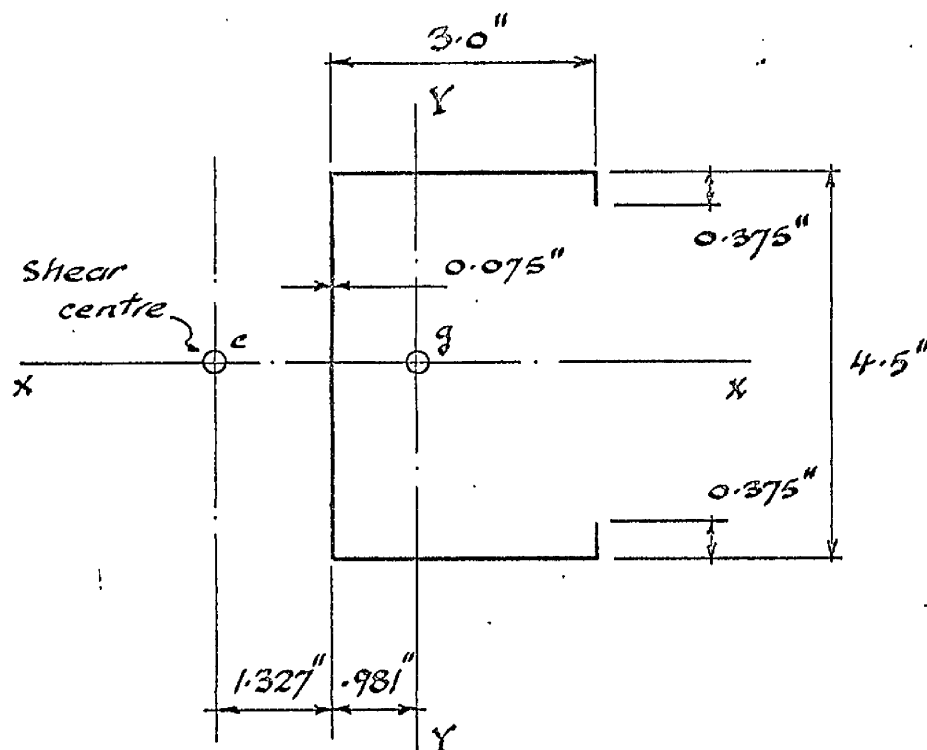
The values of GC found from the two methods were closely comparable.

These experimental methods for determining the flexural and torsional rigidities were also adopted for the mild steel angle sections used in the tests to failure under applied bending moment only.

APPENDIX VIII.4

Details of Test Specimens(I) Lipped Channel Section

(Test Group 1)



SECTION PROPERTIES

I_x	2.83 in ⁴
I_y	0.89 in ⁴
C	1.56×10^{-3} in ⁴
Γ	4.47 in ⁶

MATERIAL PROPERTIES

E	29.8×10^6 lbf/in ²
G	12.2×10^6 lbf/in ²

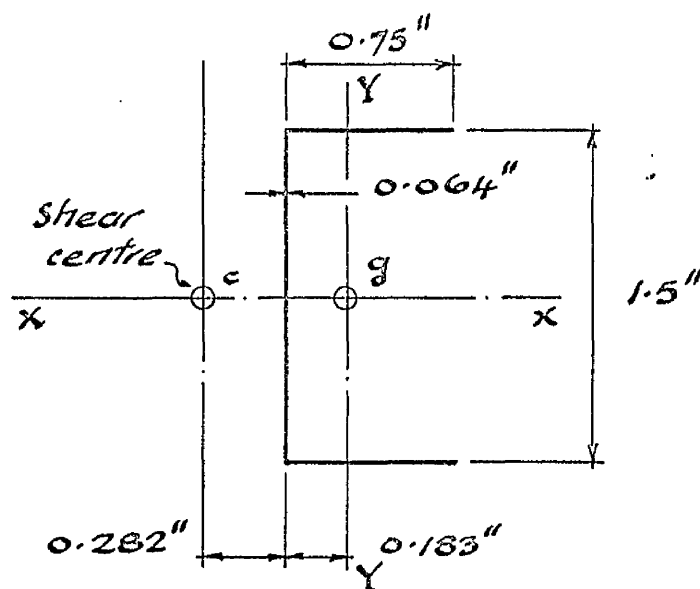
$$\lambda = \sqrt{\frac{GC}{E\Gamma}} = 0.01195 \text{ in}^{-1}$$

hence λL for test beam

$$= 0.01195 \times 72 = 0.86.$$

(II) Channel Section

(Test Group 2)



SECTION PROPERTIES

I_x	0.061 in^4
I_y	0.009 in^4
C	$0.262 \times 10^{-3} \text{ in}^4$
J	$3.56 \times 10^{-3} \text{ in}^6$
A	0.179 in^2
I_c	0.109 in^4
K_y	0.016 in^5
K_c	0.107 in^6

MATERIAL PROPERTIES

E	$30.9 \times 10^6 \text{ lbf/in}^2$
G	$13.0 \times 10^6 \text{ lbf/in}^2$

$$\lambda = \sqrt{\frac{GC}{EI}}$$

$$= 0.176 \text{ in}^{-1}$$

hence λL for test beam

$$= 0.176 \times 72 = 12.7$$

(III) Brass Angle Sections (Test Group 3)

SPECIMEN	AVERAGE FLANGE BREADTH	AVERAGE FLANGE THICKNESS	GC	$\frac{EI_x}{10^5}$	$\frac{EI_y}{10^5}$	$\frac{E}{10^6}$
	in	in	lbf in ²	lbf in ²	lbf in ²	lbf/in ²
A.1	1.007	0.0480	455	2.288	0.5685	15.28
A.2	1.008	0.0382	250	1.845	0.4660	15.23
A.3	1.007	0.0640	1070	3.142	0.7776	16.06
B.1	1.496	0.0846	2340	13.58	3.338	15.50
C.1	2.001	0.0665	1620	25.91	5.987	14.22
C.2	1.998	0.0588	1180	22.22	5.822	15.54

SPECIMEN	A	I_y	K_c	I_c	K_y
	in ²	in ⁴	in ⁶	in ⁴	in ⁵
A.1	0.0945	0.00372	0.0176	0.0305	0.00528
A.2	0.0757	0.00306	0.0145	0.0248	0.00427
A.3	0.1249	0.00484	0.0225	0.0400	0.00681
B.1	0.2460	0.0218	0.220	0.179	0.0446
C.1	0.2620	0.0421	0.787	0.342	0.118
C.2	0.2320	0.0374	0.696	0.303	0.104

(IV) Mild Steel Angle Sections (Test Group 4)

SPECIMEN		$\frac{EI_x}{10^5}$	$\frac{EI_y}{10^5}$	GC	K_y	I_y
		lbf in ²	lbf in ²	lbf in ²	in ⁵	in ⁴
1"x1"x16 SWG	A.1	5.818	1.443	2135	0.00754	0.00509
	A.2	5.769	1.436	2080	0.00754	0.00509
	A.3	5.552	1.361	1965	0.00742	0.00503
	A.4	5.524	1.358	1920	0.00742	0.00503
	A.5	5.483	1.353	1915	0.00742	0.00503
1½"x1½"x16 SWG	B.1	20.62	4.851	3115	0.0406	0.0171
	B.2	20.71	5.016	3150	0.0406	0.0171
	B.3	19.42	4.513	2405	0.0382	0.0159
	B.4	19.65	4.521	2515	0.0382	0.0159
	B.5	19.61	4.642	2595	0.0382	0.0159
2"x2"x16 SWG	C.1	53.61	13.03	5045	0.130	0.0441
	C.2	53.53	13.28	5015	0.130	0.0441
	C.3	53.05	13.19	5080	0.130	0.0441
	C.4	50.02	12.02	3795	0.123	0.0413
	C.5	50.41	12.03	3805	0.123	0.0413

APPENDIX VIII.5

Graphical Presentation of the
Comparison of Theoretical and
Experimental Results

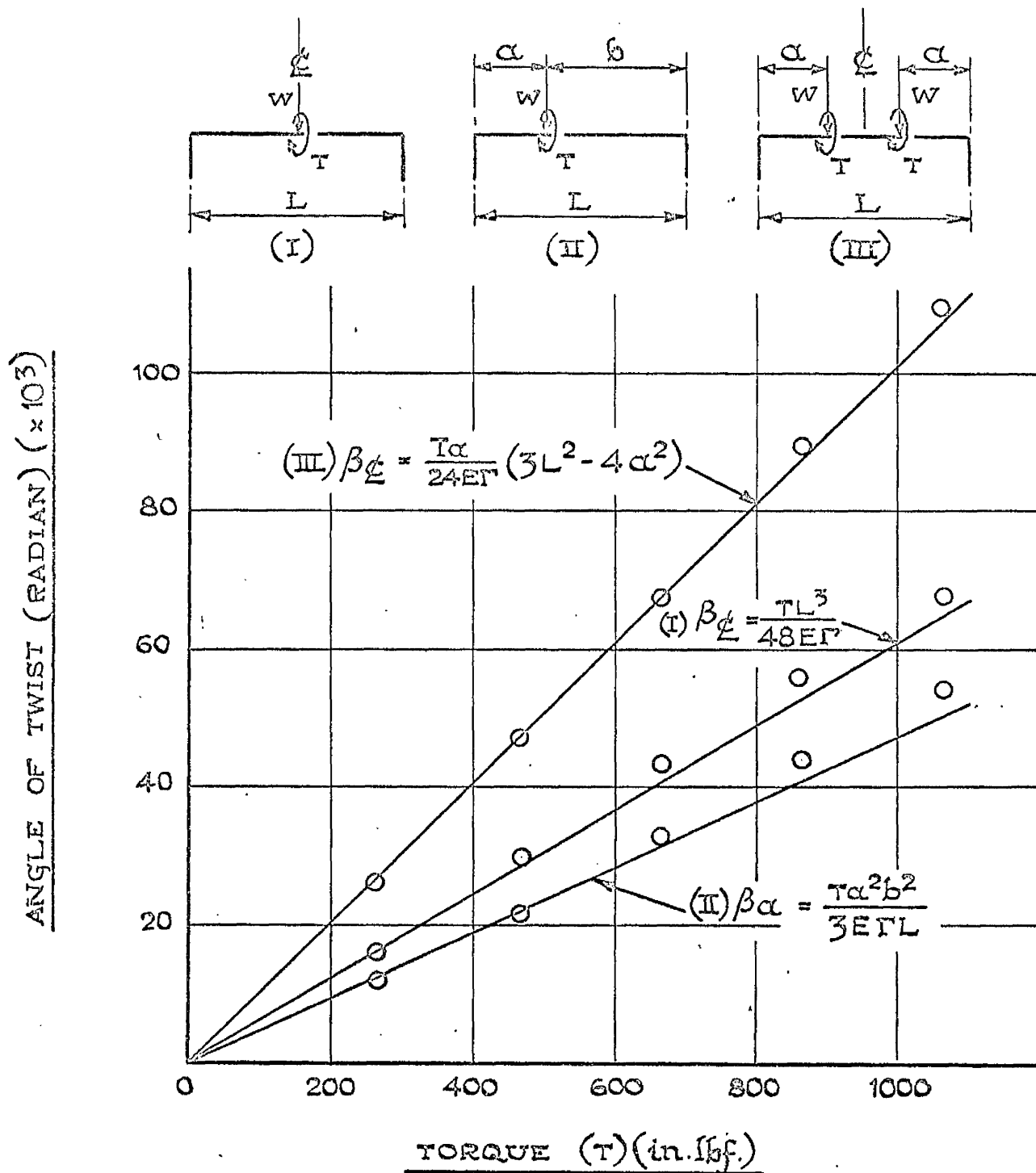
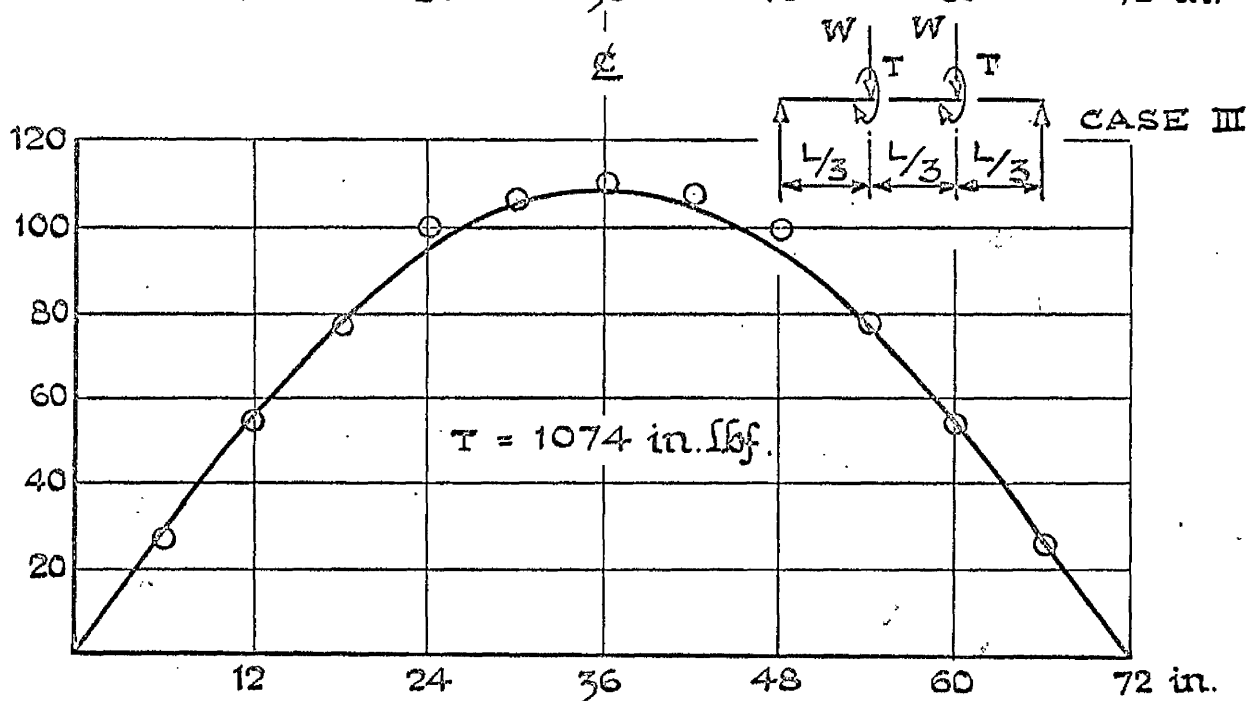
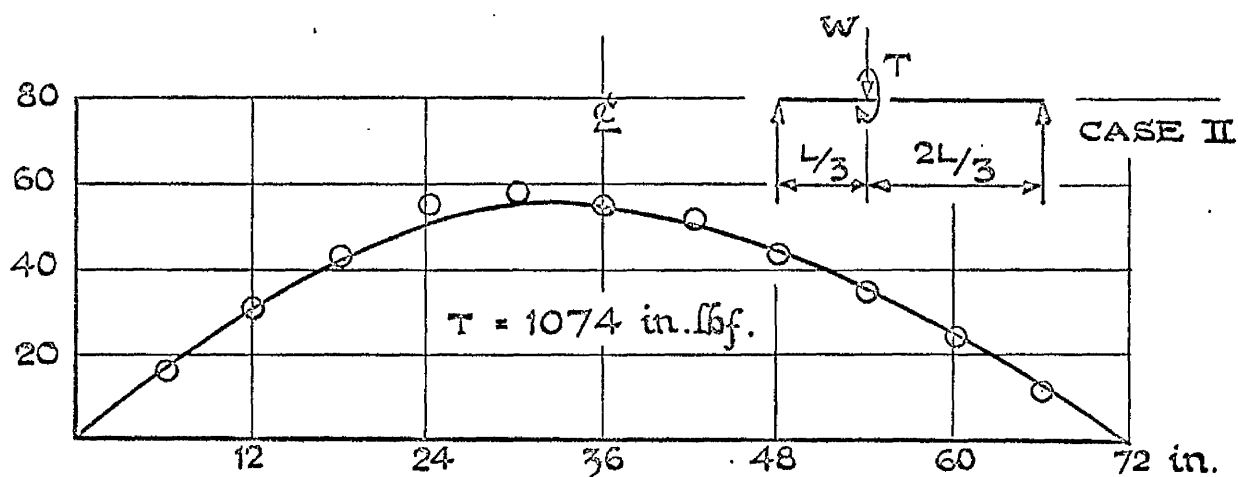
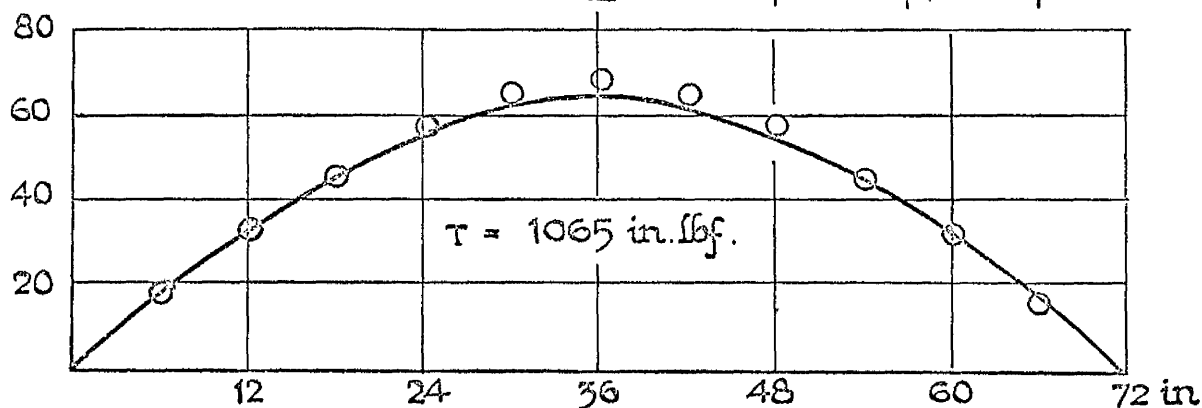
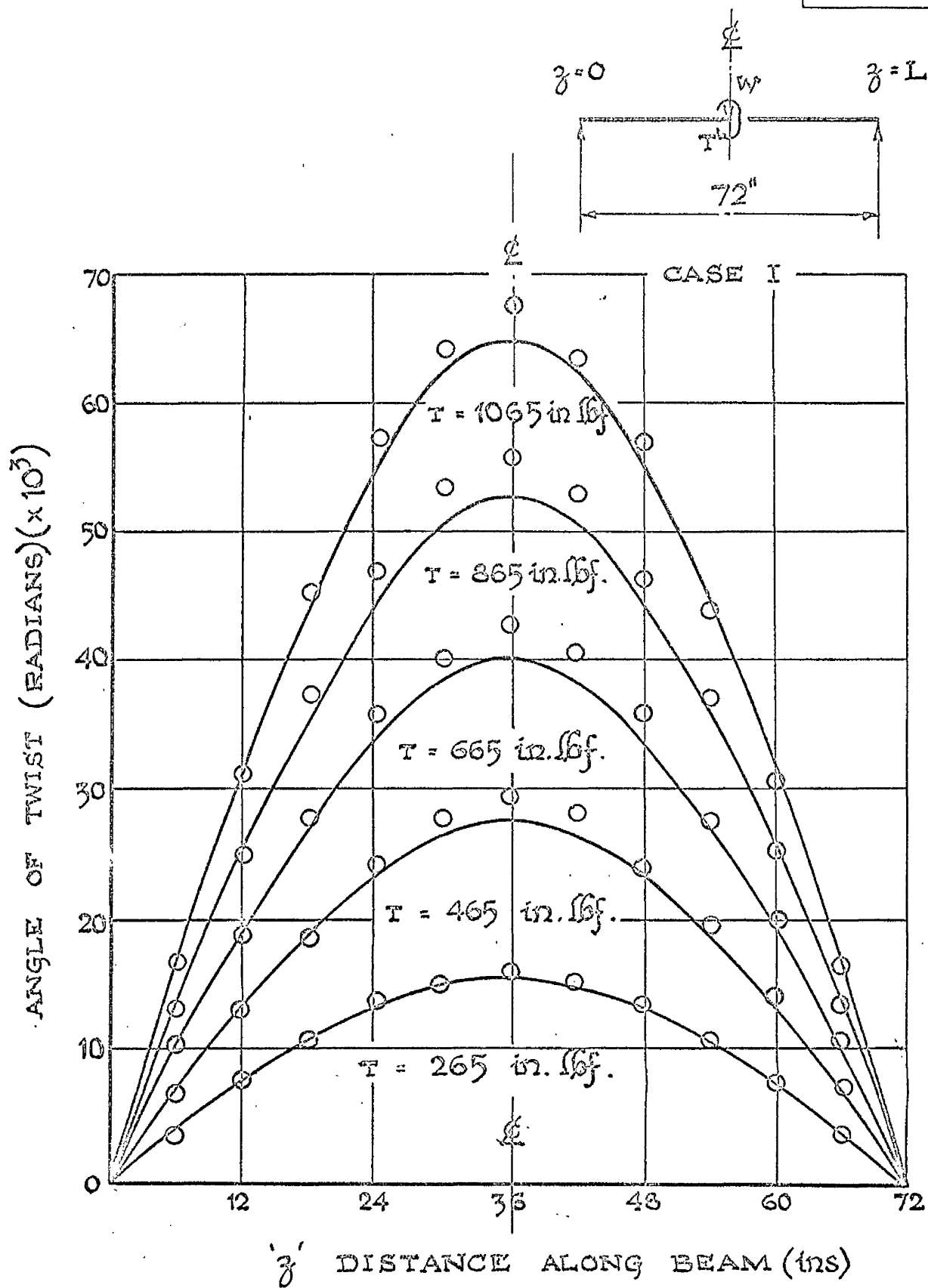


FIG. IV. 1. TYPICAL TORQUE / ANGLE OF TWIST RELATIONSHIPS FOR SMALL DISPLACEMENT BEHAVIOUR .

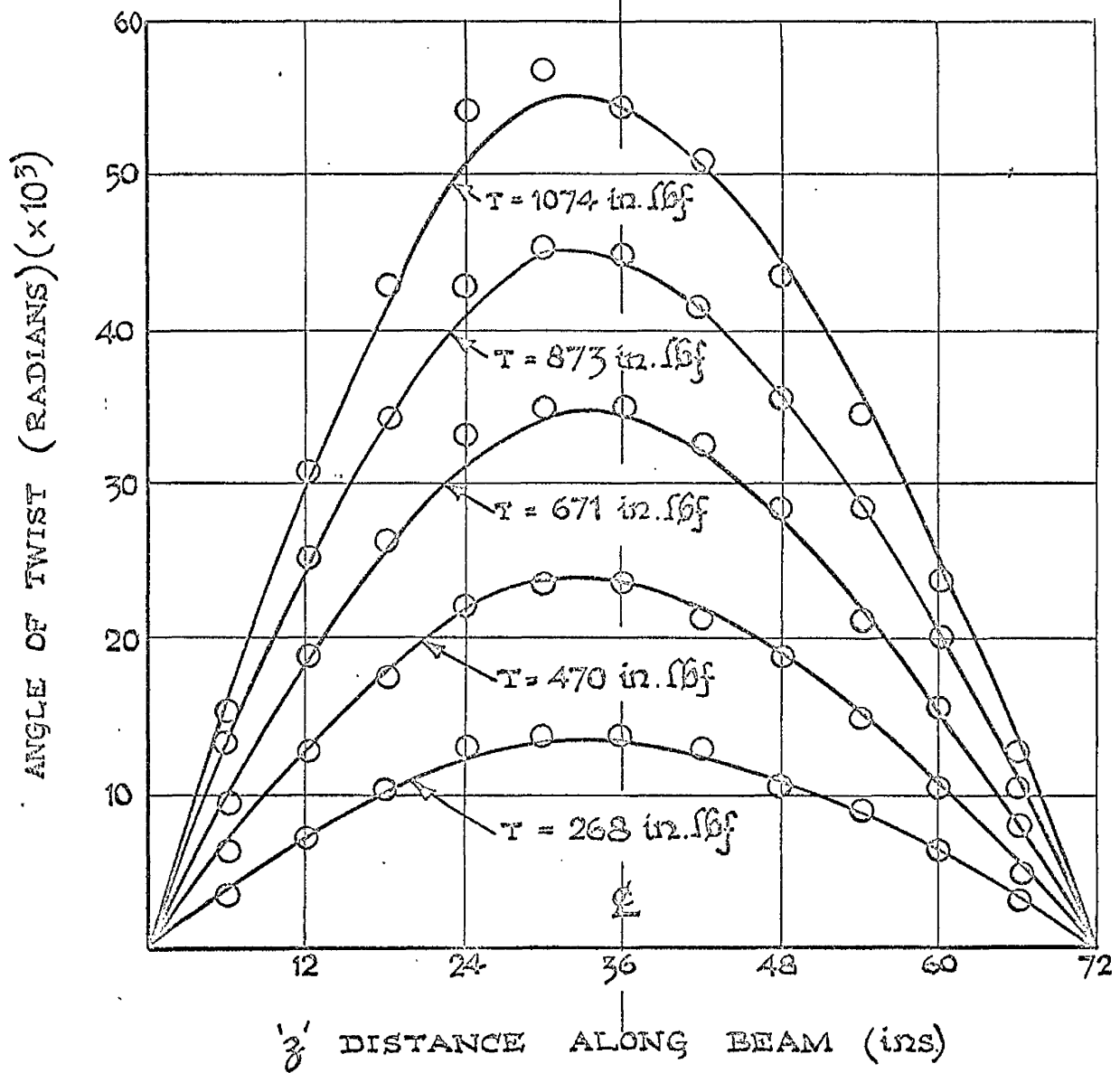
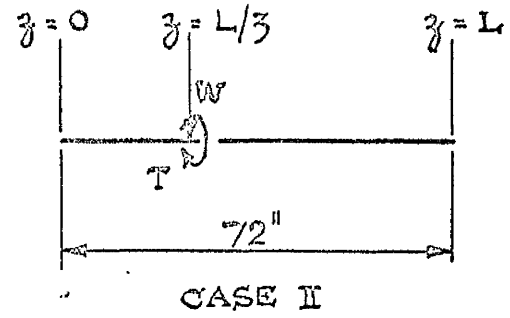


3' DISTANCE ALONG BEAM.

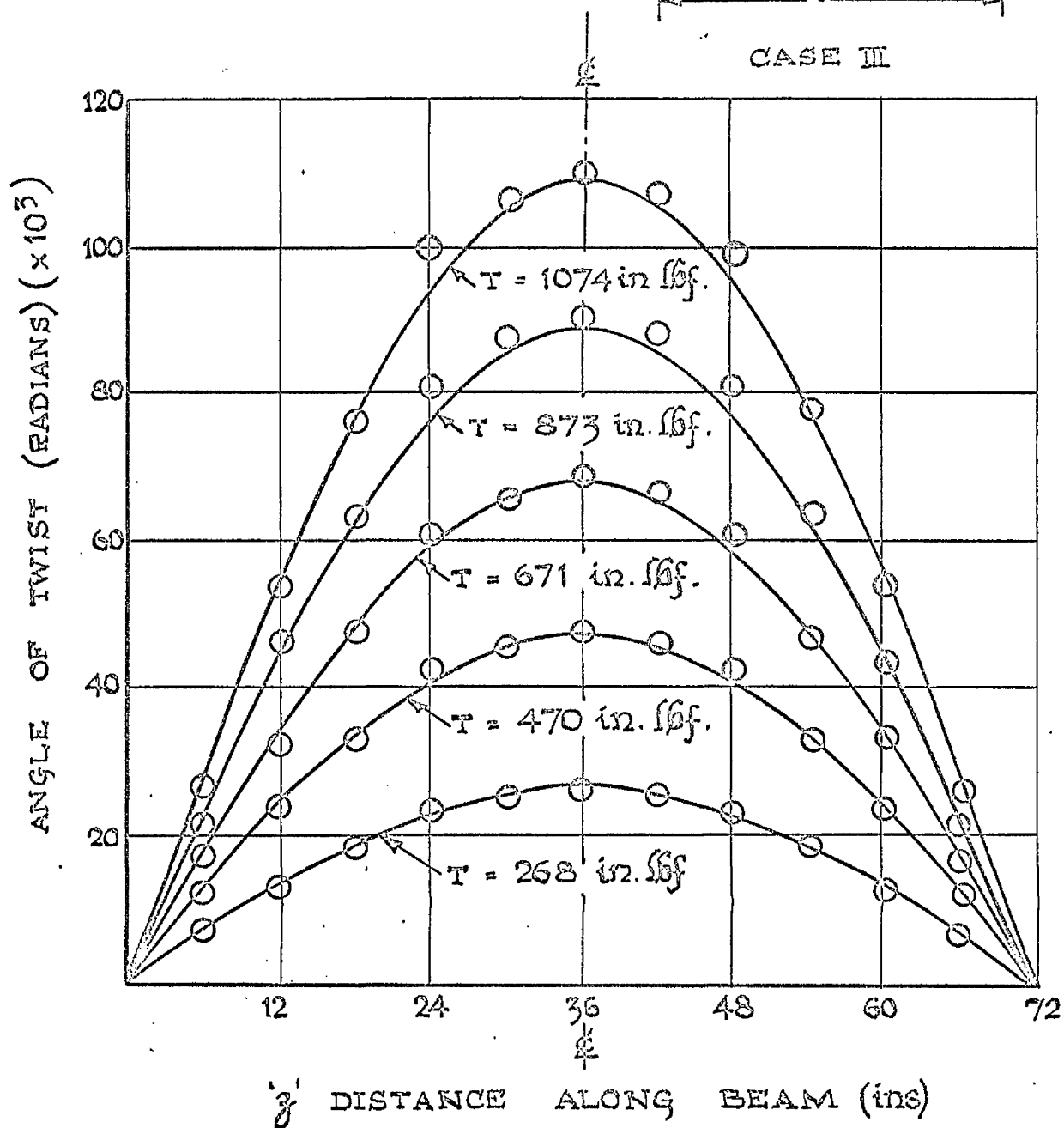
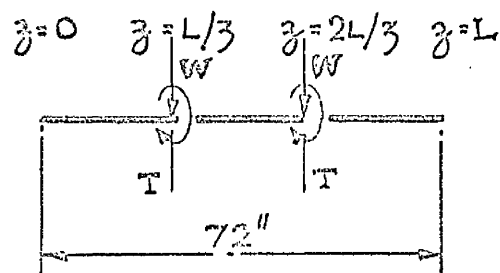
FIG. IV. 2. TYPICAL DISTRIBUTIONS OF ANGLE OF TWIST OVER TEST SPAN.



DISTRIBUTIONS OF ANGLE OF TWIST
OVER TEST SPAN.



DISTRIBUTIONS OF ANGLE OF TWIST
OVER TEST SPAN.



DISTRIBUTIONS OF ANGLE OF TWIST OVER TEST SPAN.

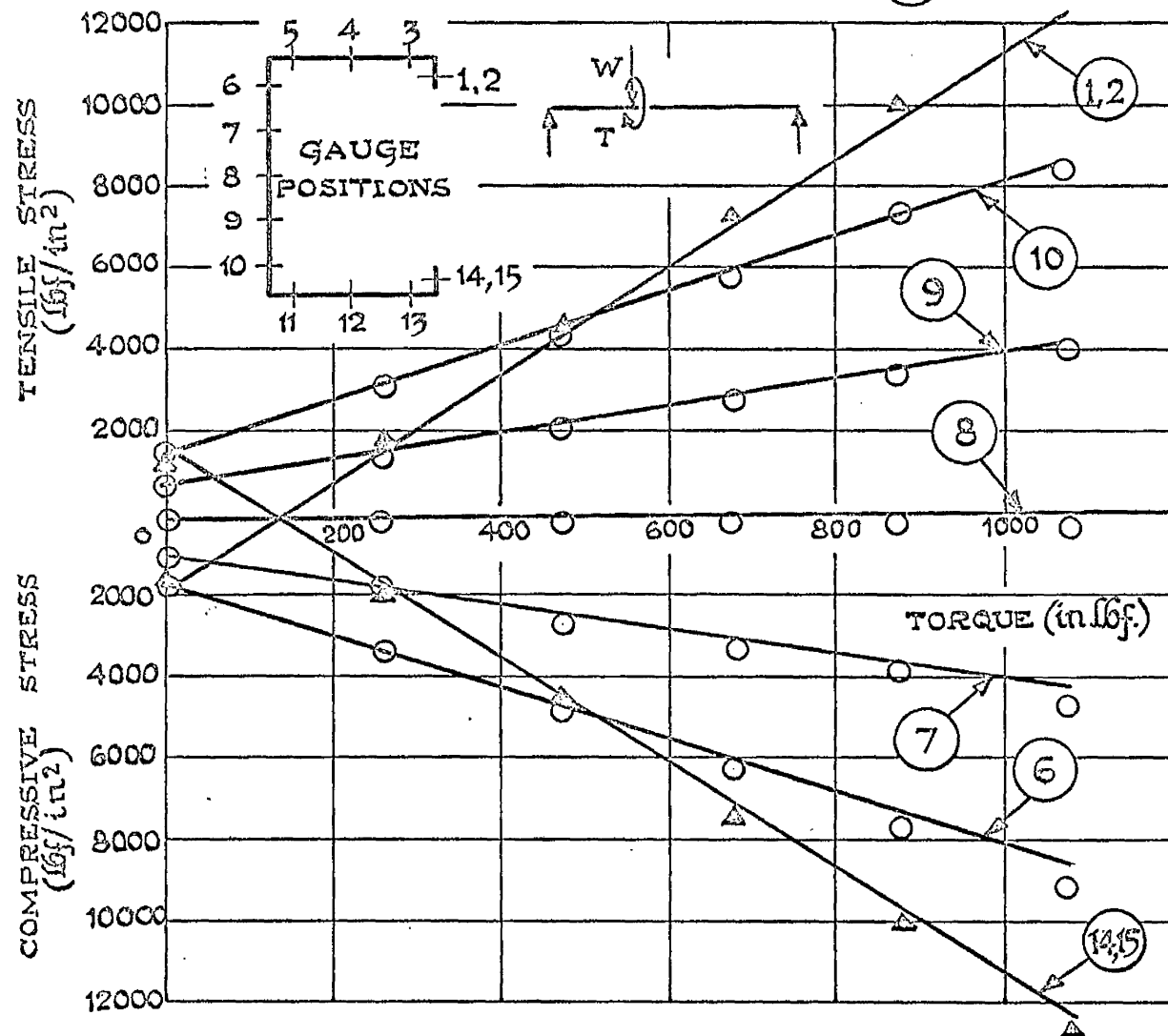
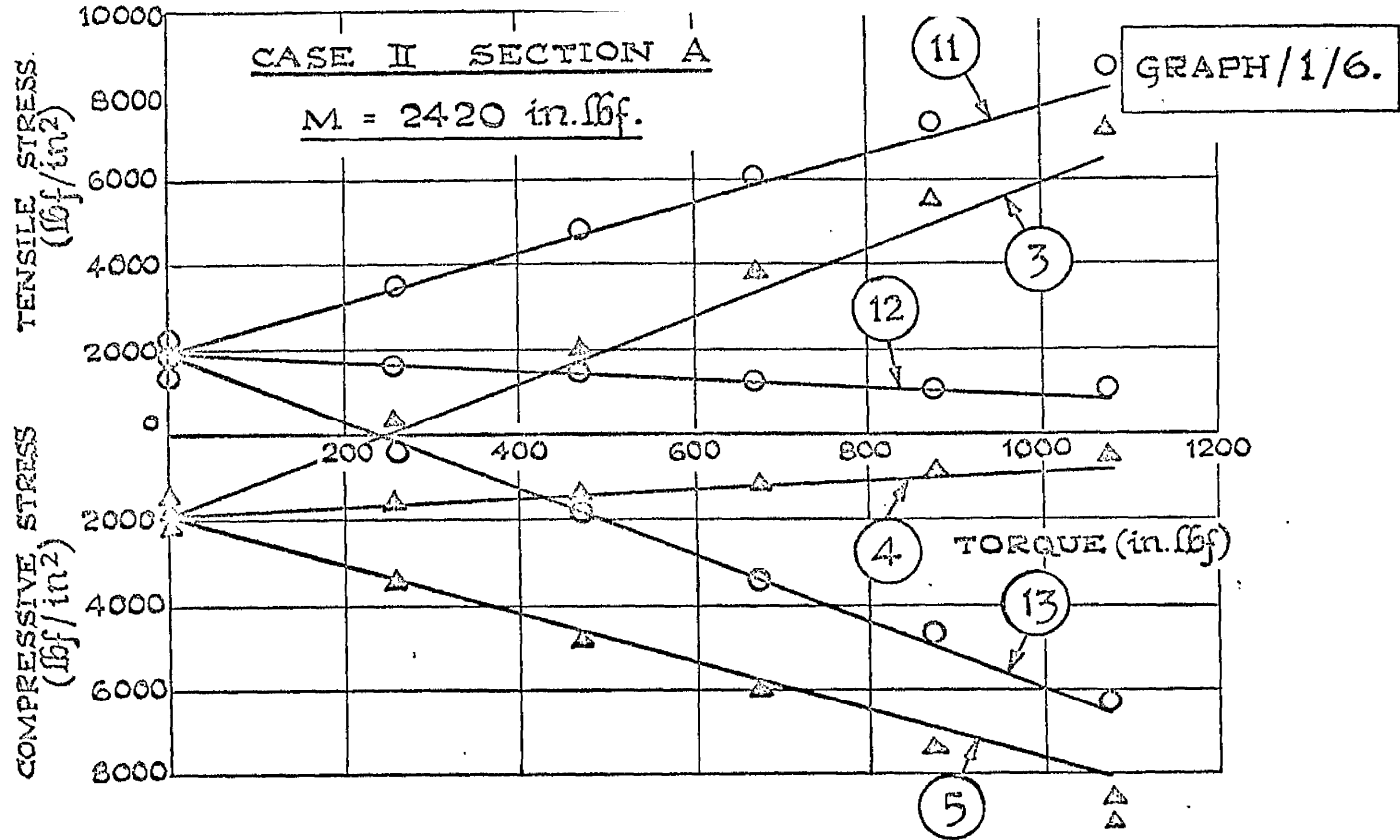
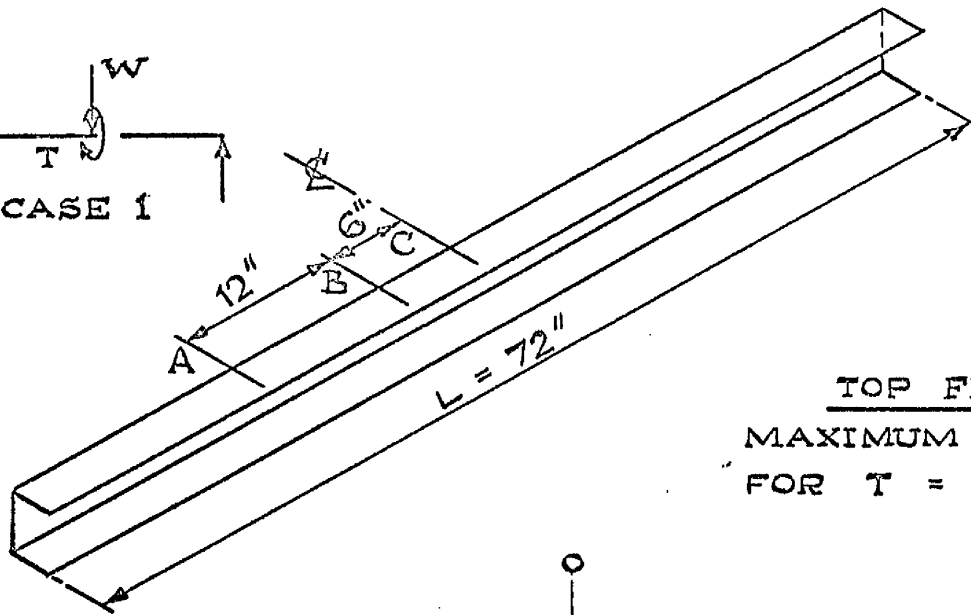
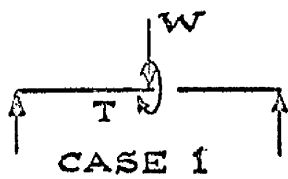


FIG. IV. 3. VARIATION OF LONGITUDINAL STRESS WITH TORQUE.



TOP FLANGE.
MAXIMUM STRESSES
FOR $T = 1068 \text{ in.}\cdot\text{lb}_f$.

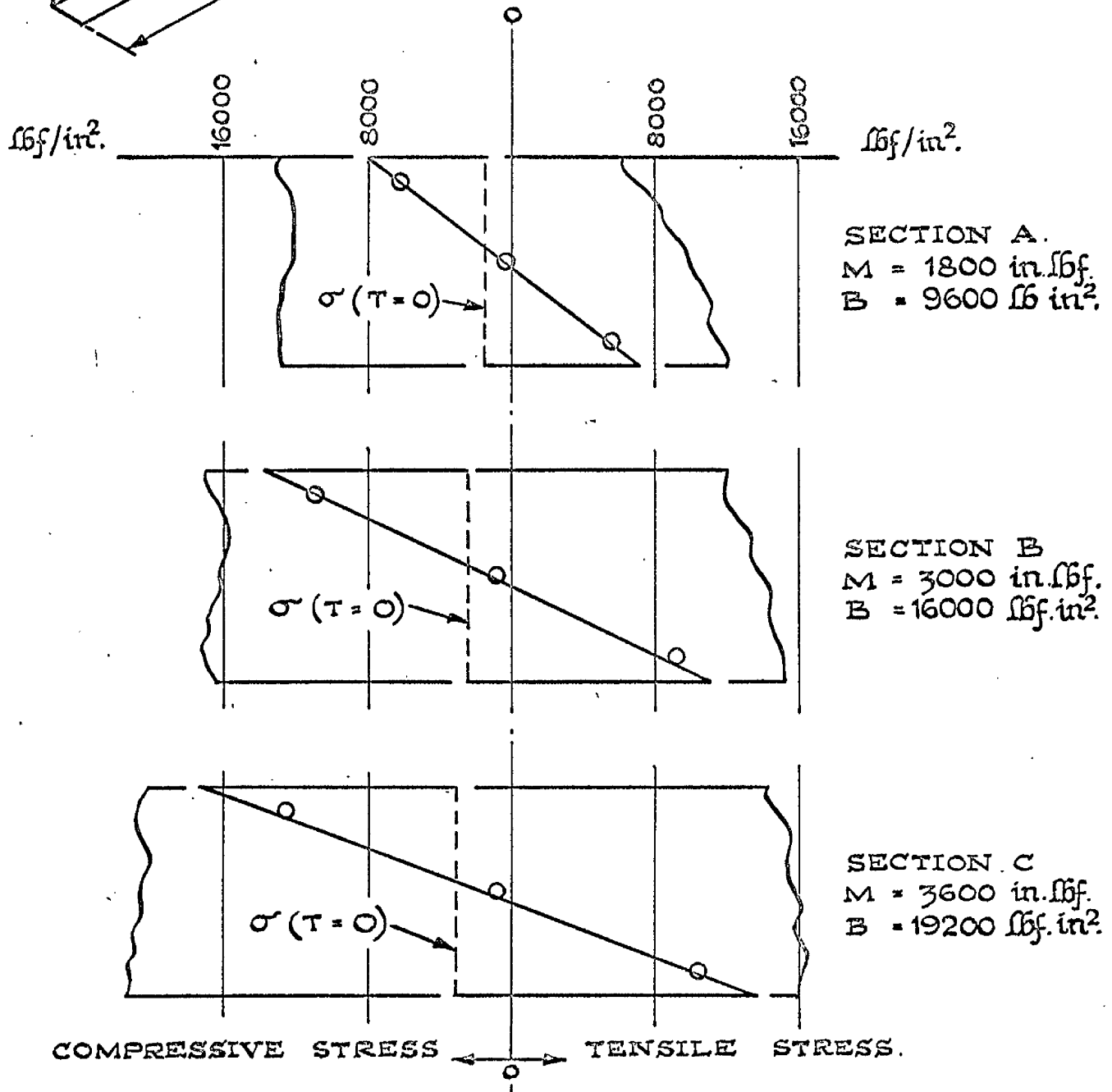
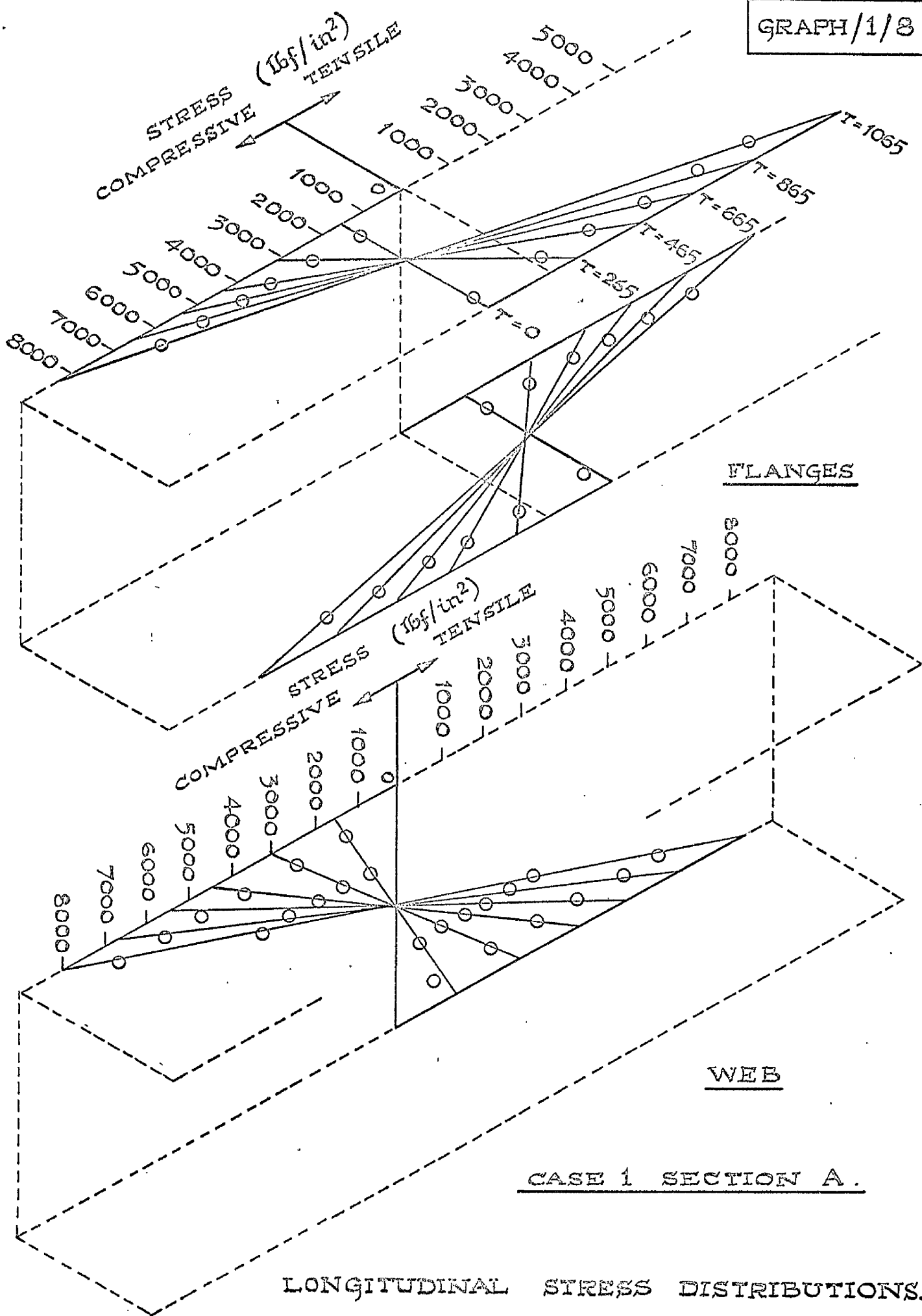
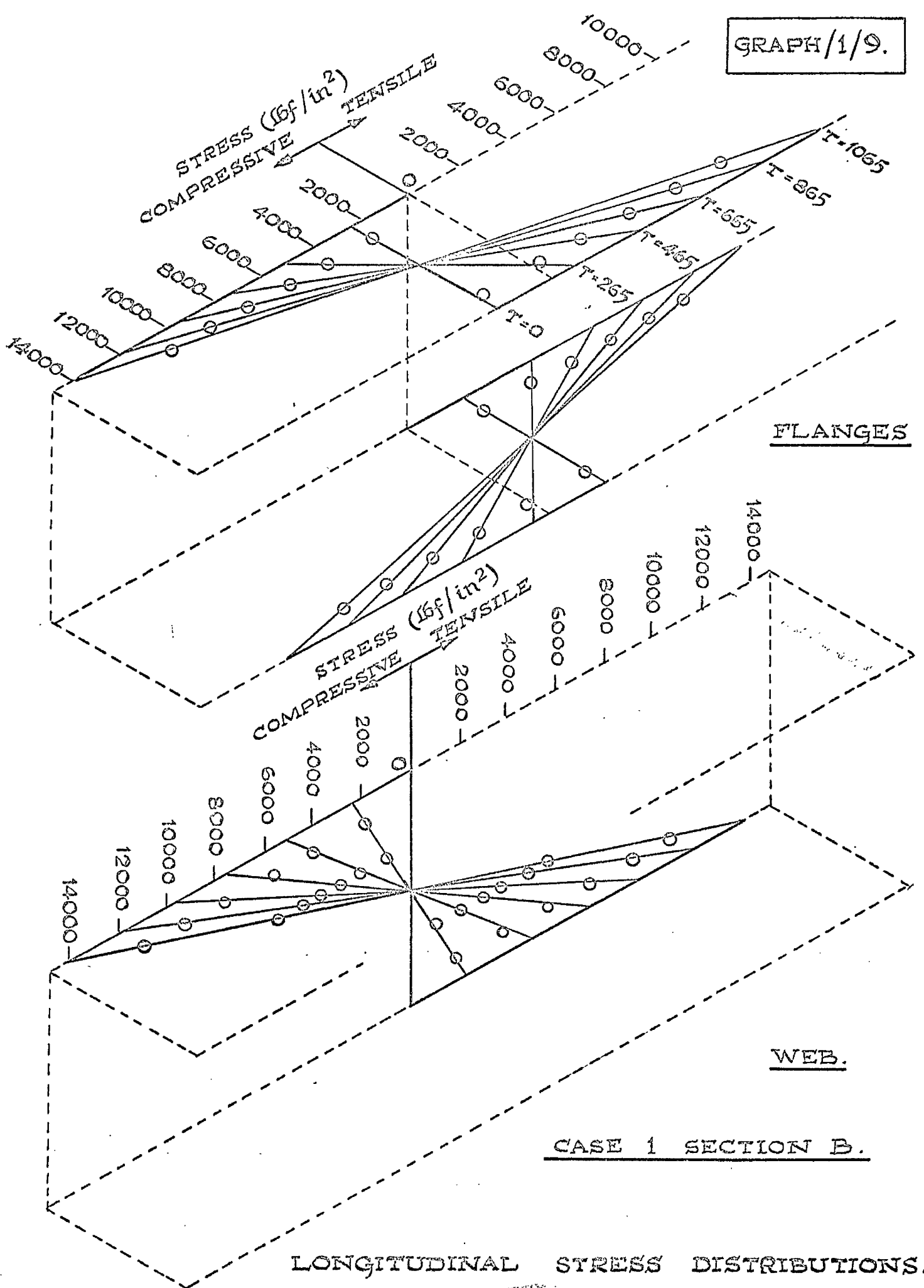
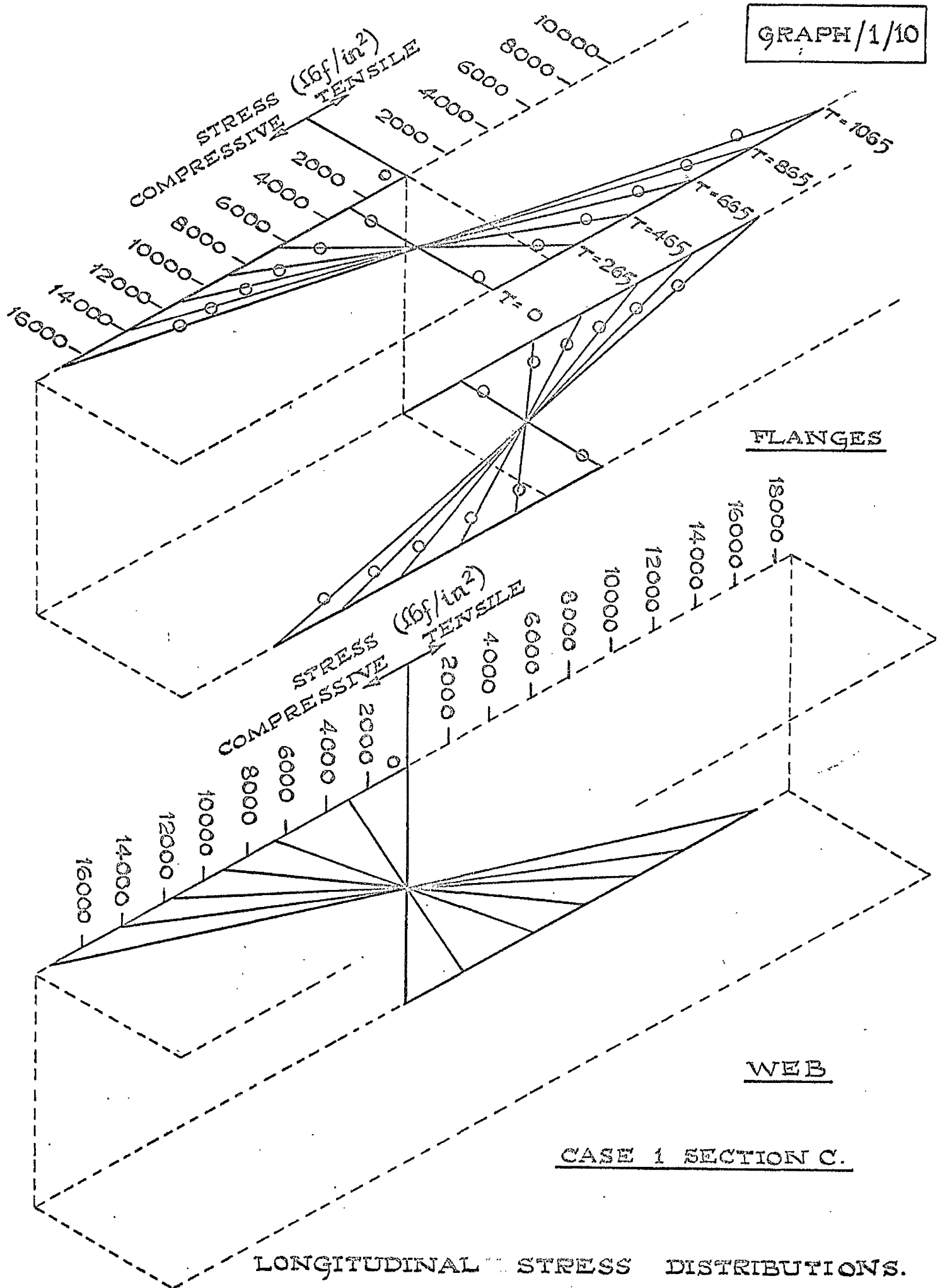


FIG. IV. 6. LONGITUDINAL STRESS DISTRIBUTIONS
AT DIFFERENT CROSS - SECTIONS.







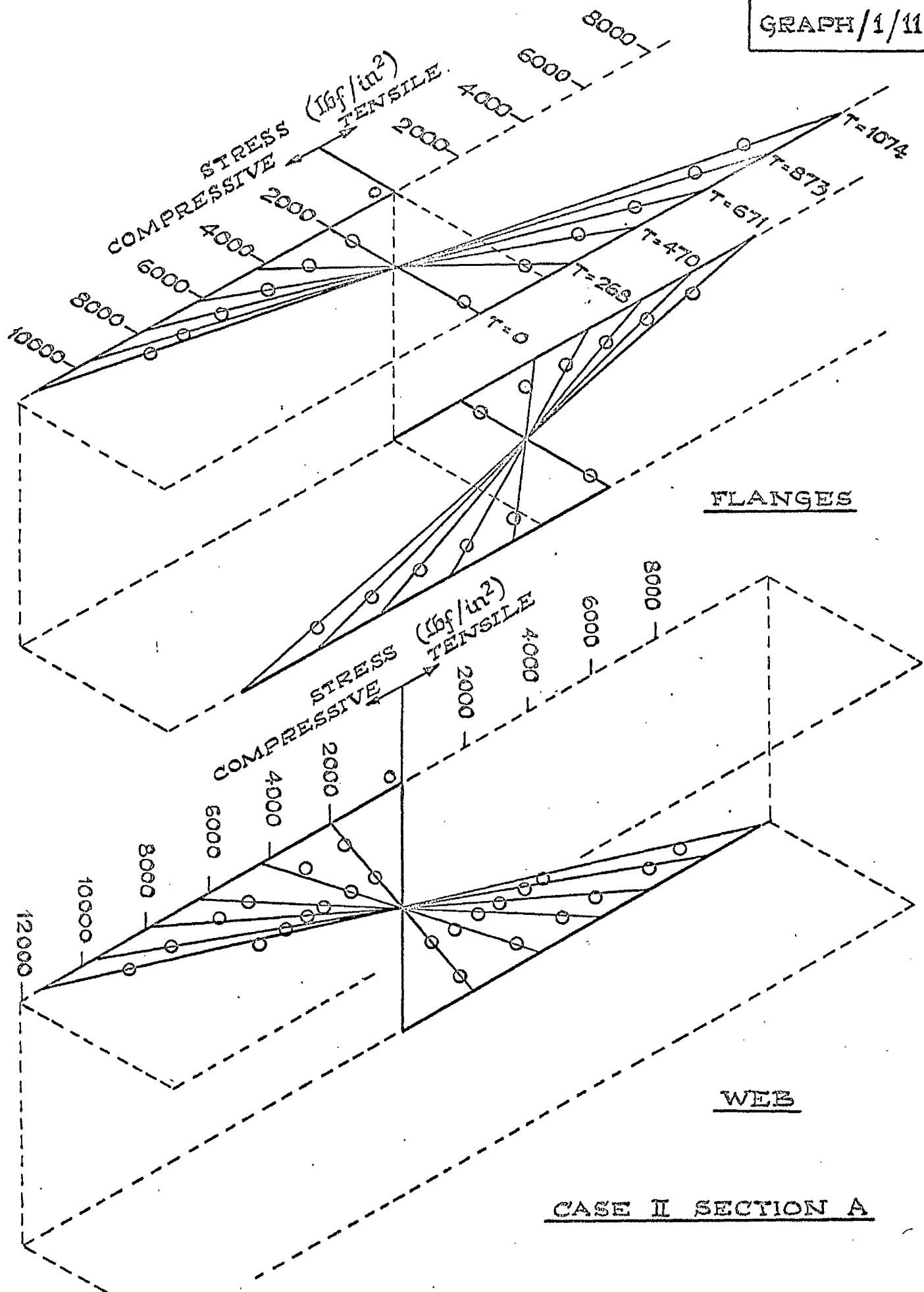
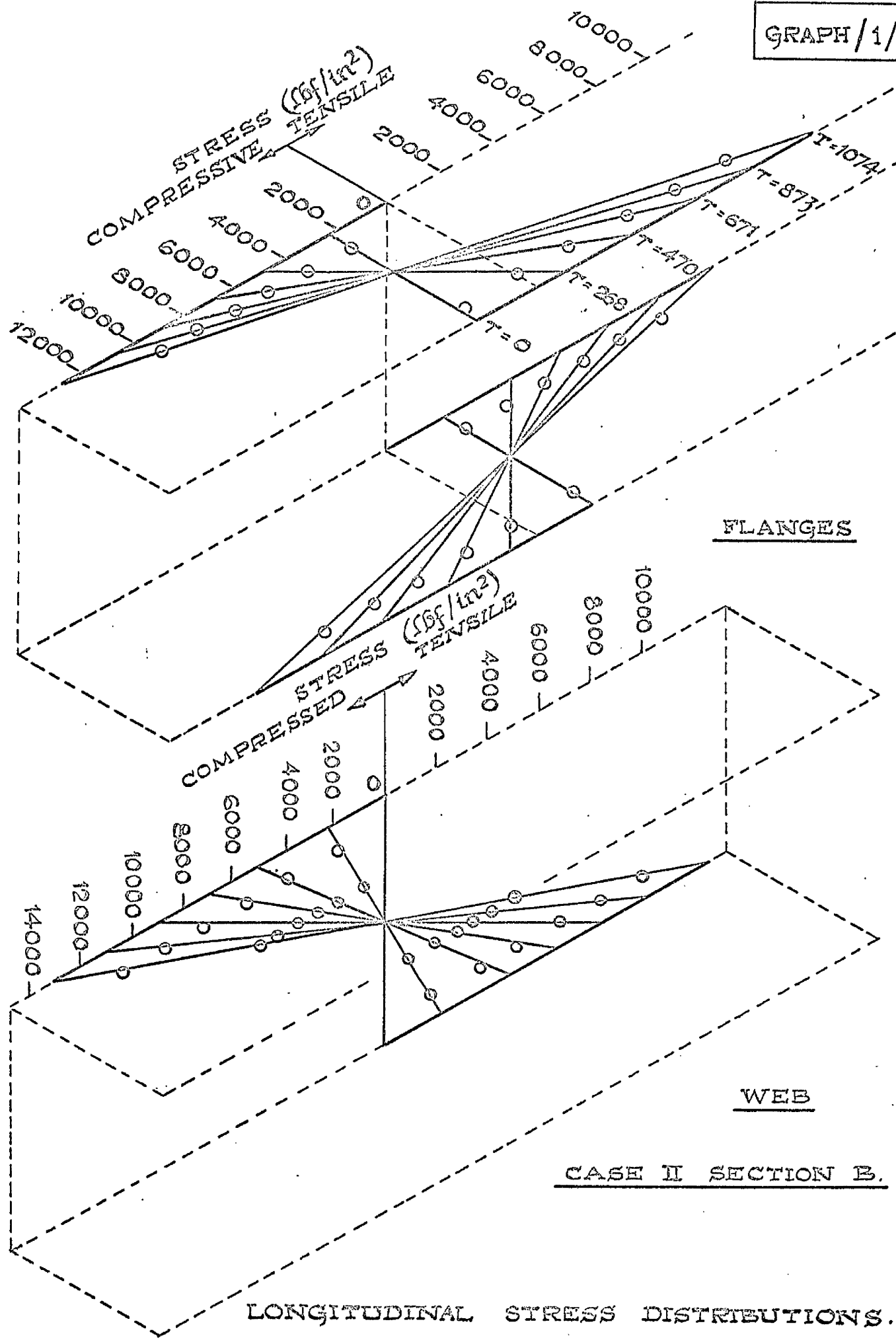
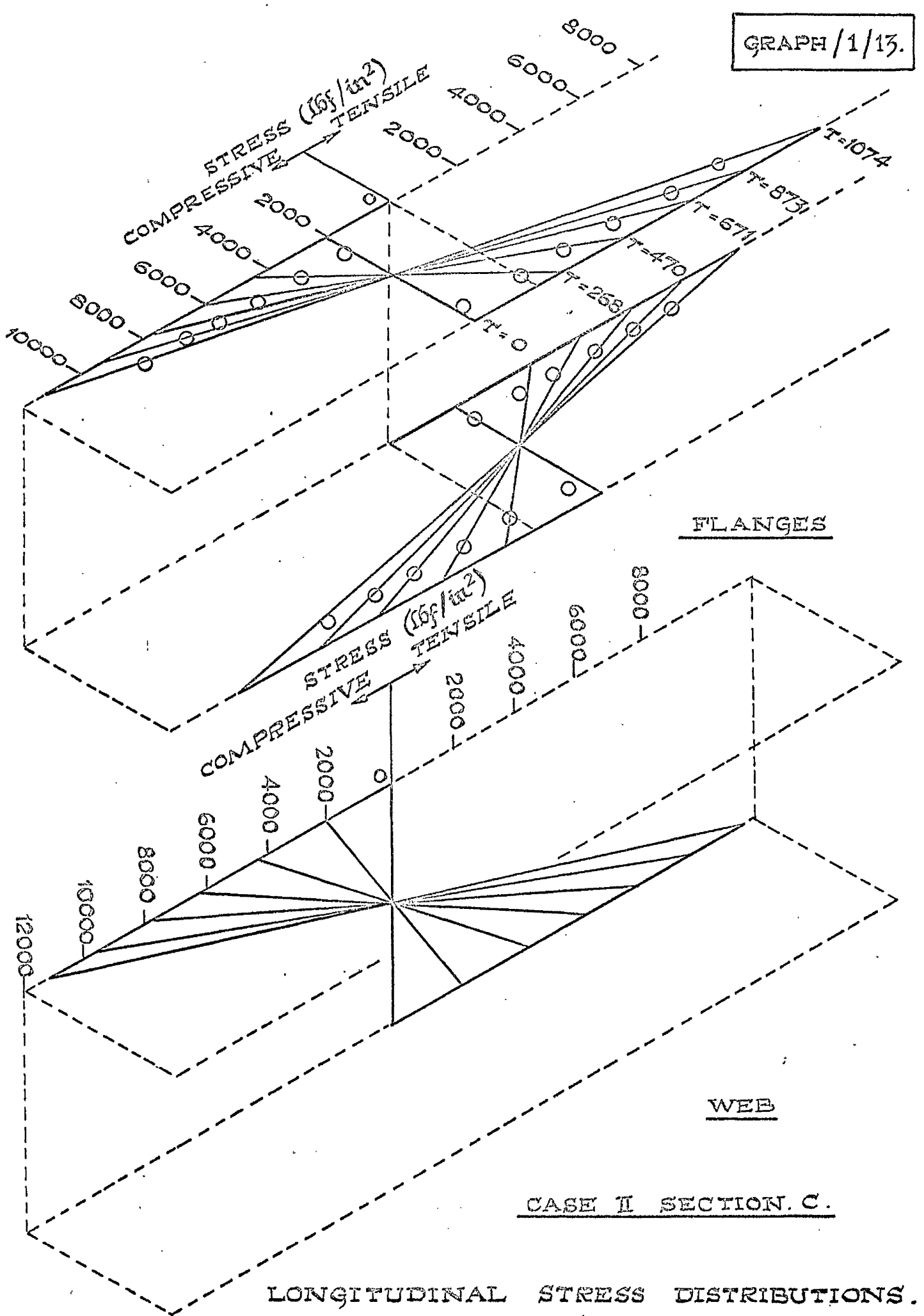


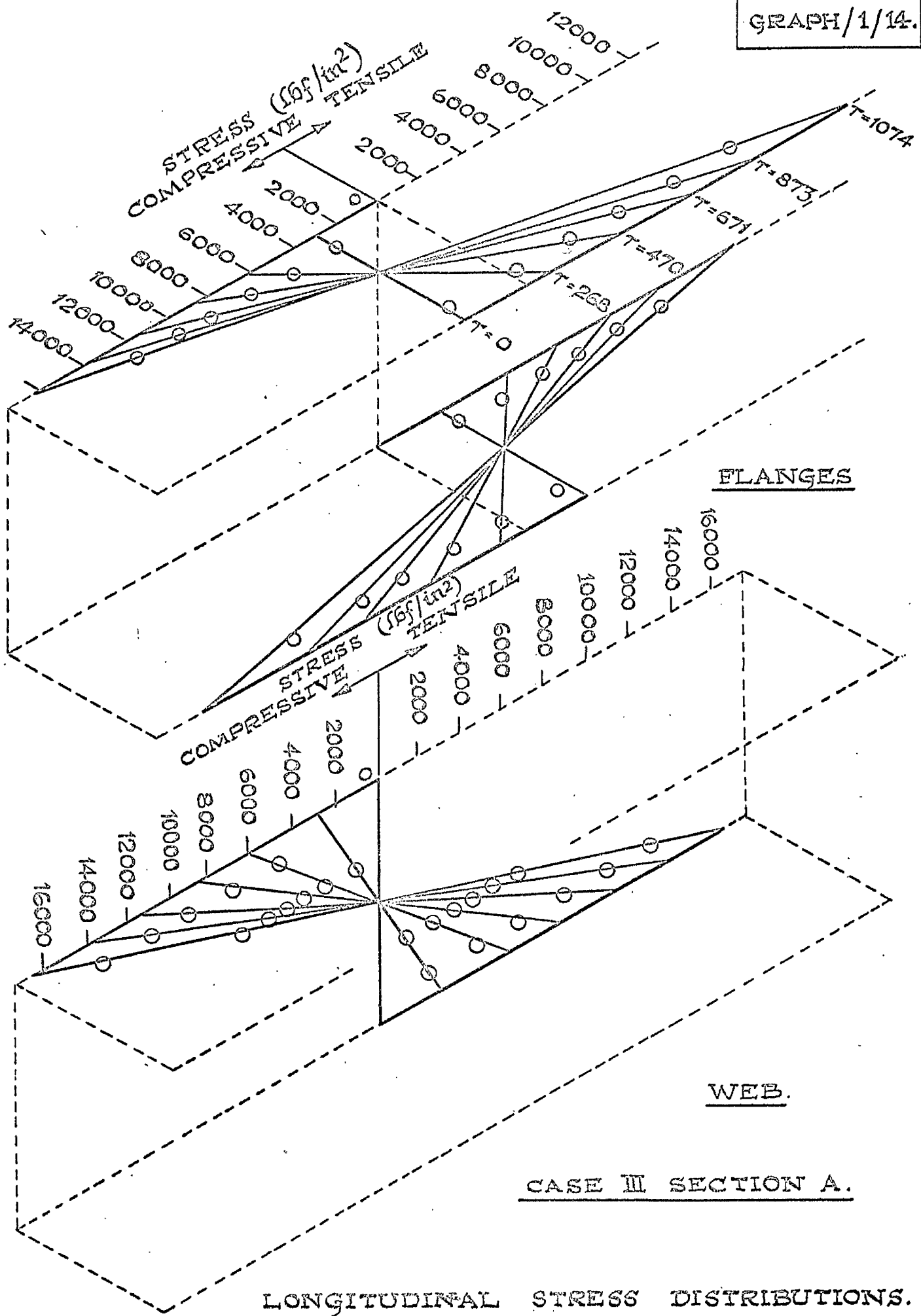
FIG. IV.5. LONGITUDINAL STRESS DISTRIBUTIONS.

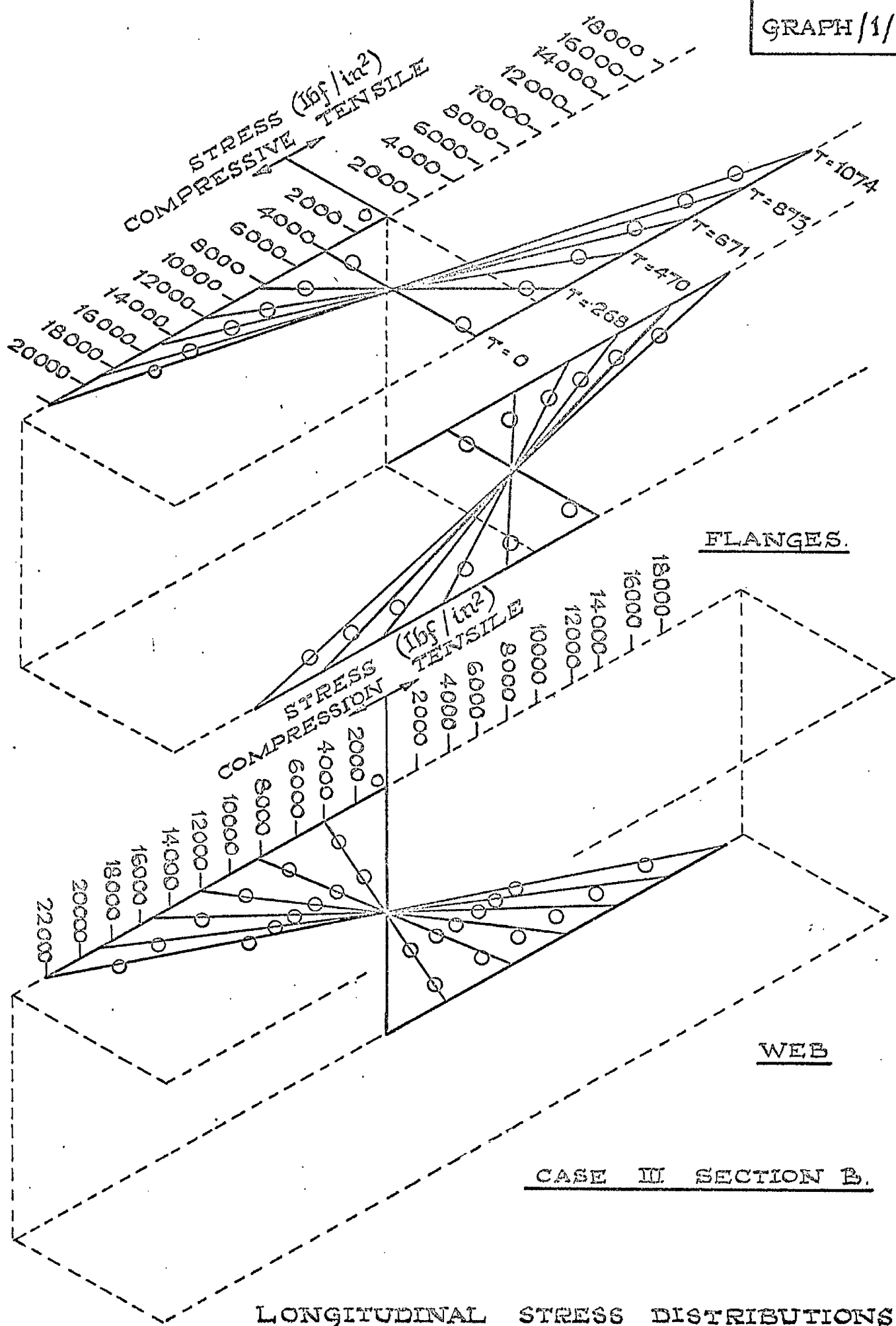


CASE II SECTION B.

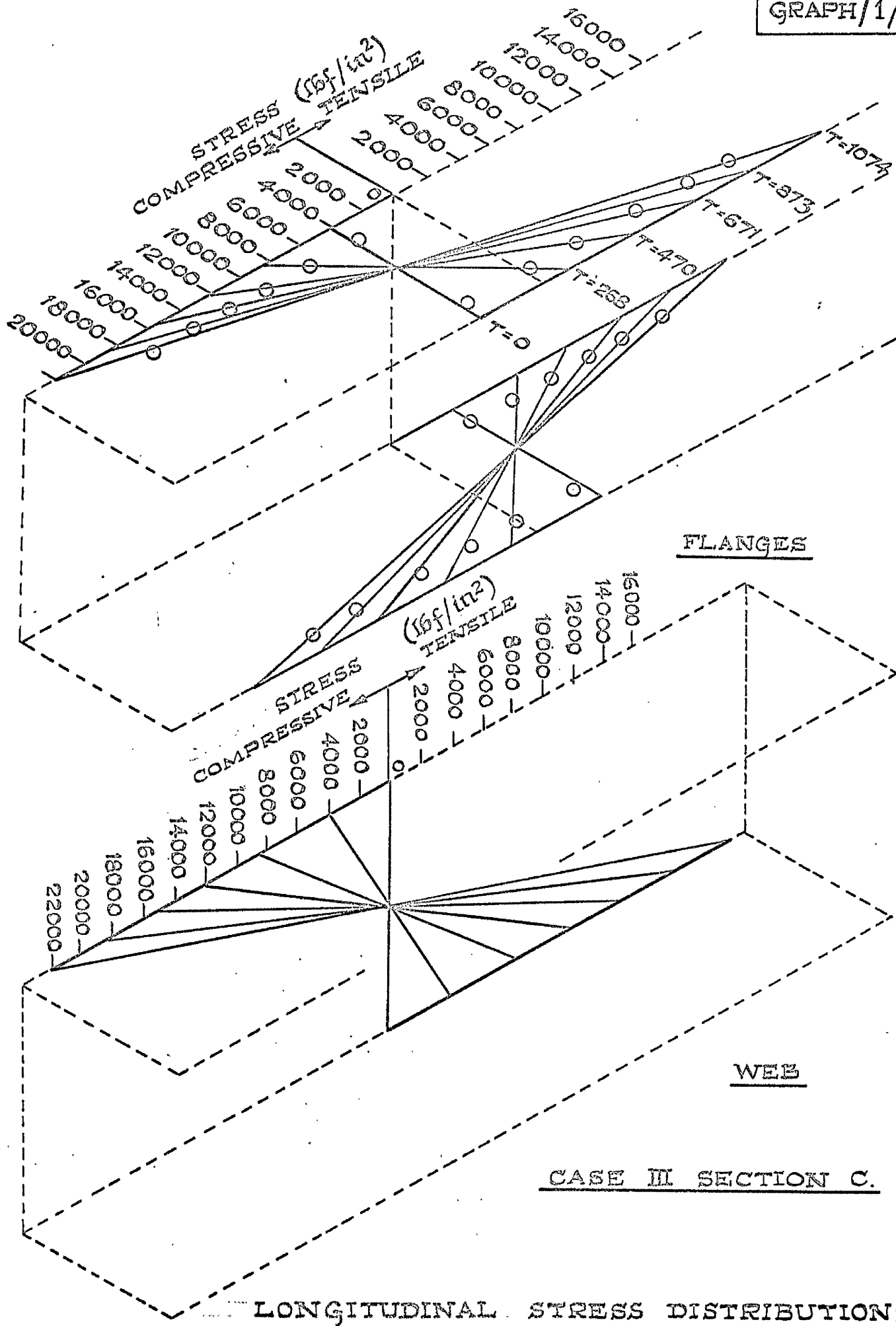
LONGITUDINAL STRESS DISTRIBUTIONS.







LONGITUDINAL STRESS DISTRIBUTIONS.



CASE III SECTION C.

LONGITUDINAL STRESS DISTRIBUTIONS.

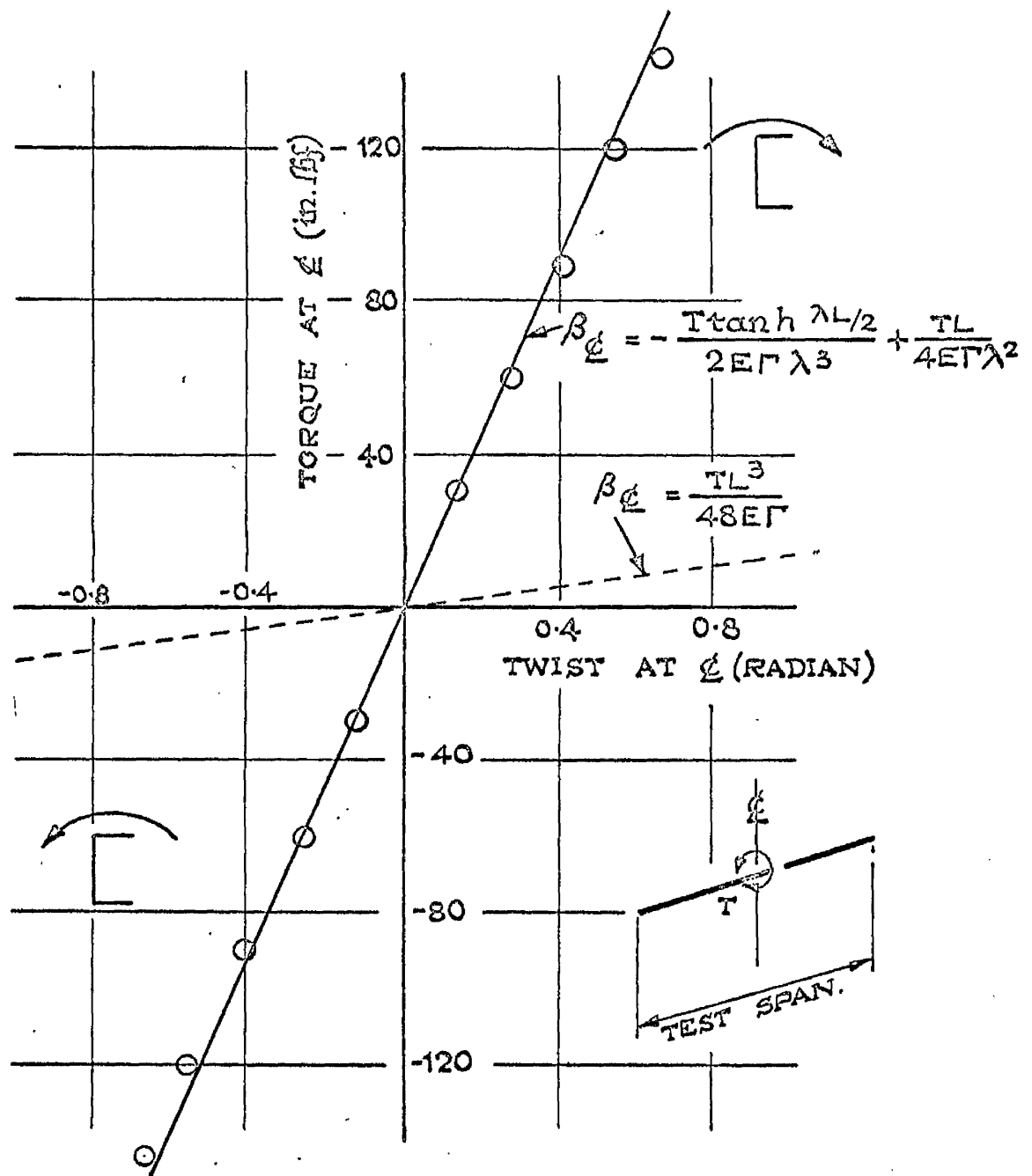


FIG. IV. 7. TORQUE / ANGLE OF TWIST RELATIONSHIP
- LARGE DISPLACEMENT BEHAVIOUR.

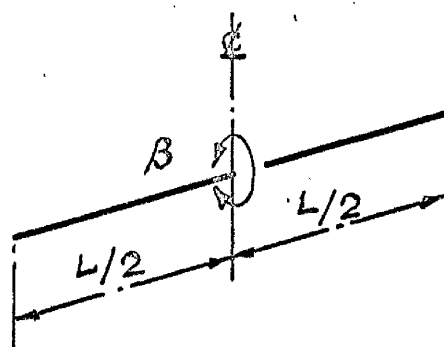
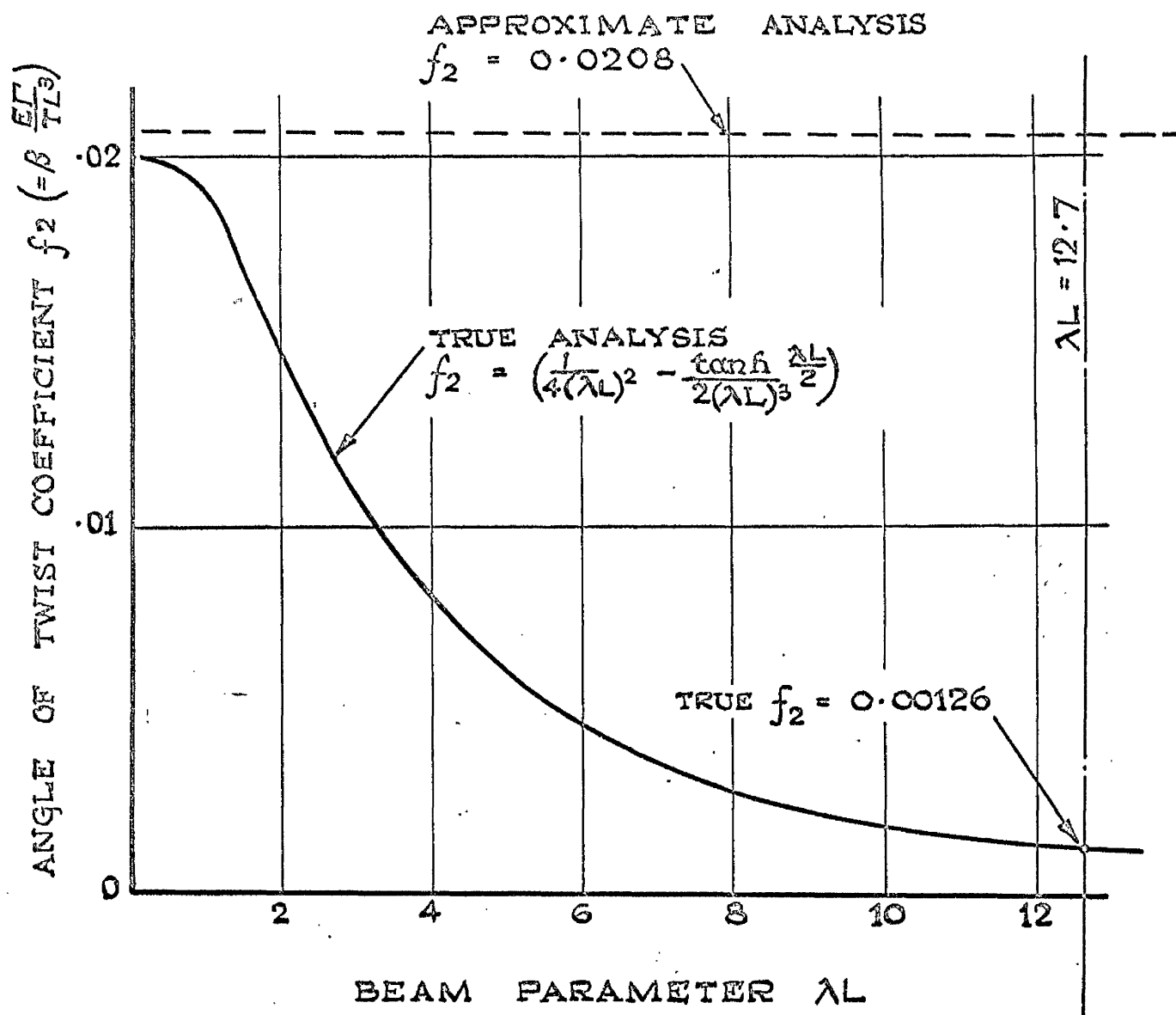


FIG. IV. 8. VARIATION OF ANGLE OF TWIST COEFFICIENT f_2 WITH BEAM PARAMETER λL .

THEORETICAL SOLUTIONS

(a) EQUATION IV. 2.1.

(b) EQUATION II. 3.20.

(c) EQUATION II. 3.17.

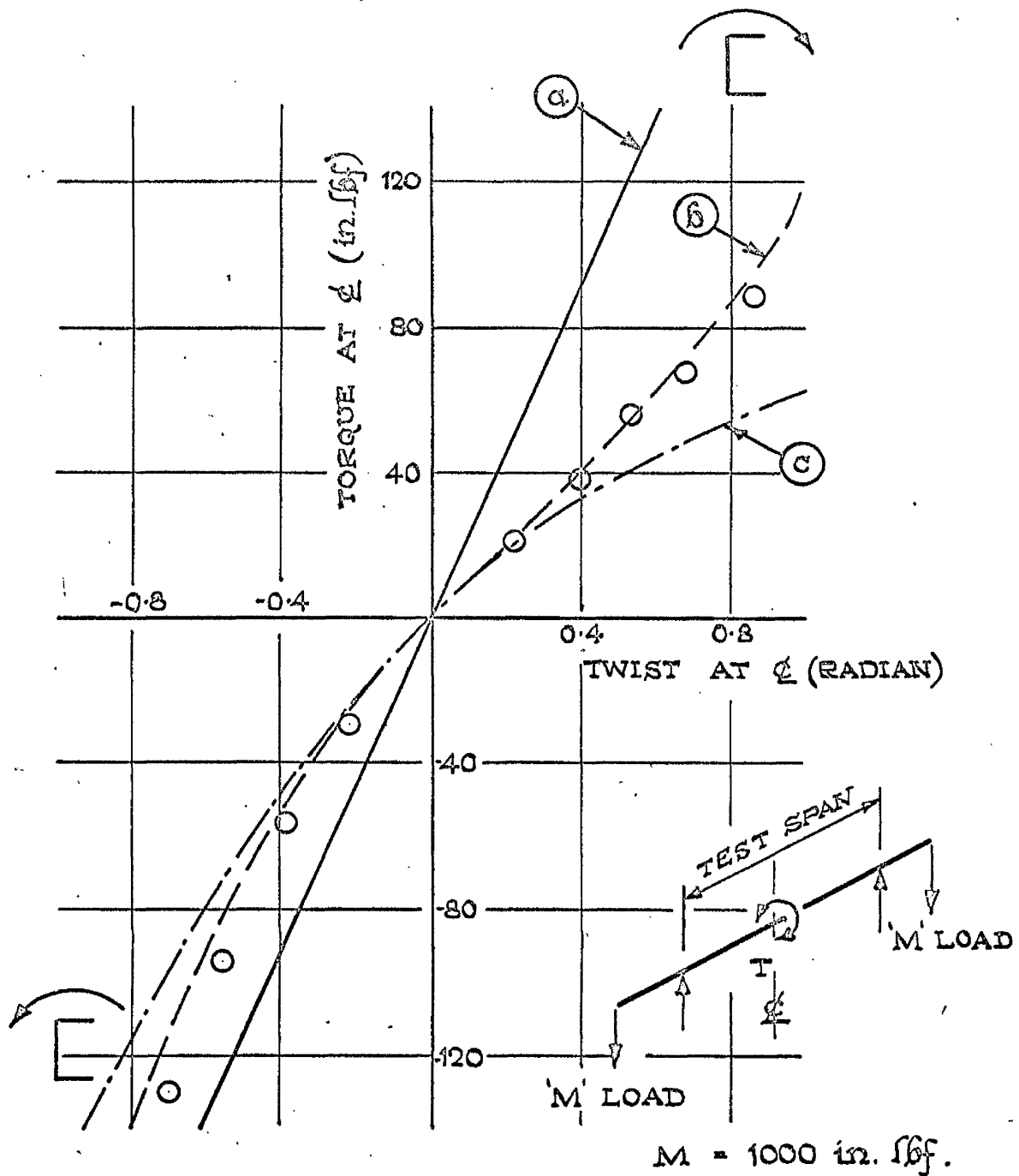
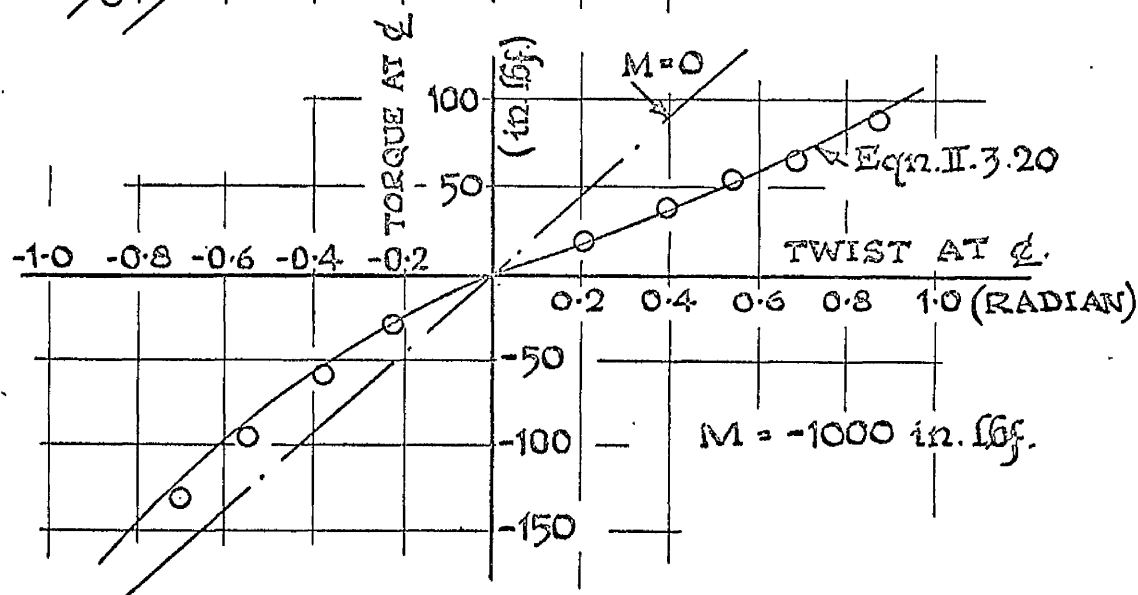
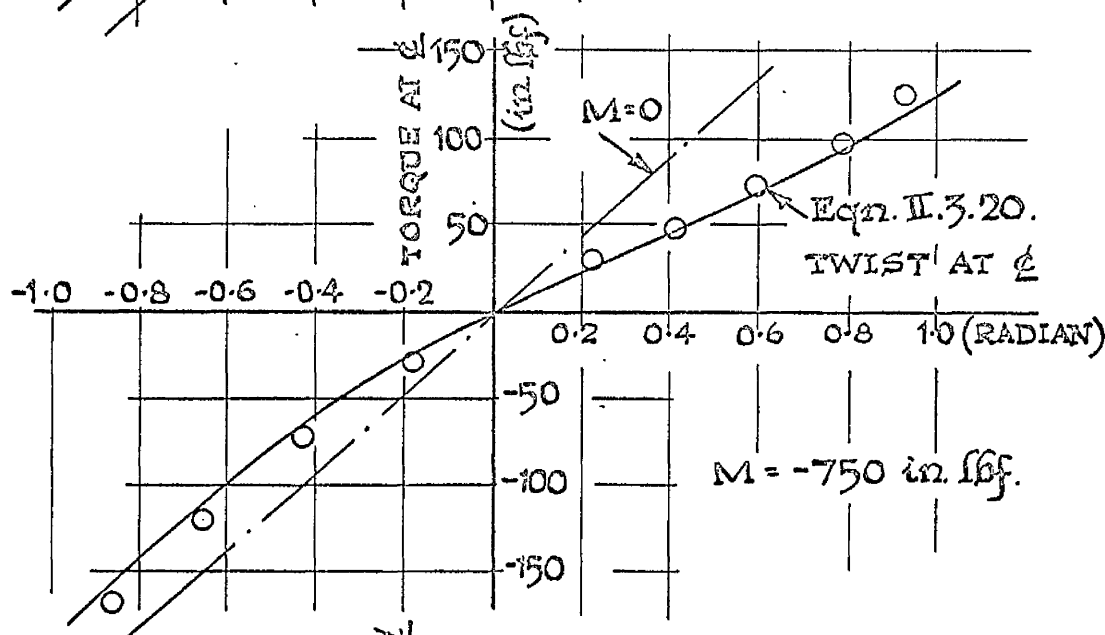
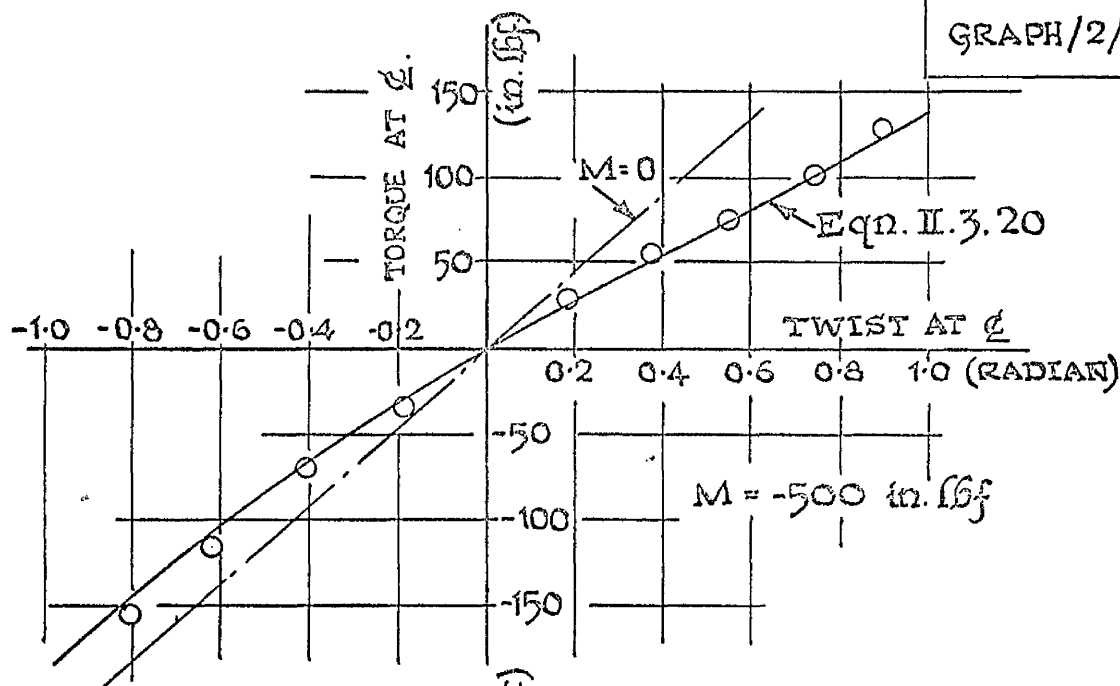


FIG. IV. 9. TORQUE / ANGLE OF TWIST RELATIONSHIP
FOR COMBINED BENDING AND TORSION



NONLINEAR TORQUE / ANGLE OF TWIST
EQUILIBRIUM PATHS - SMALL CHANNEL SECTION.

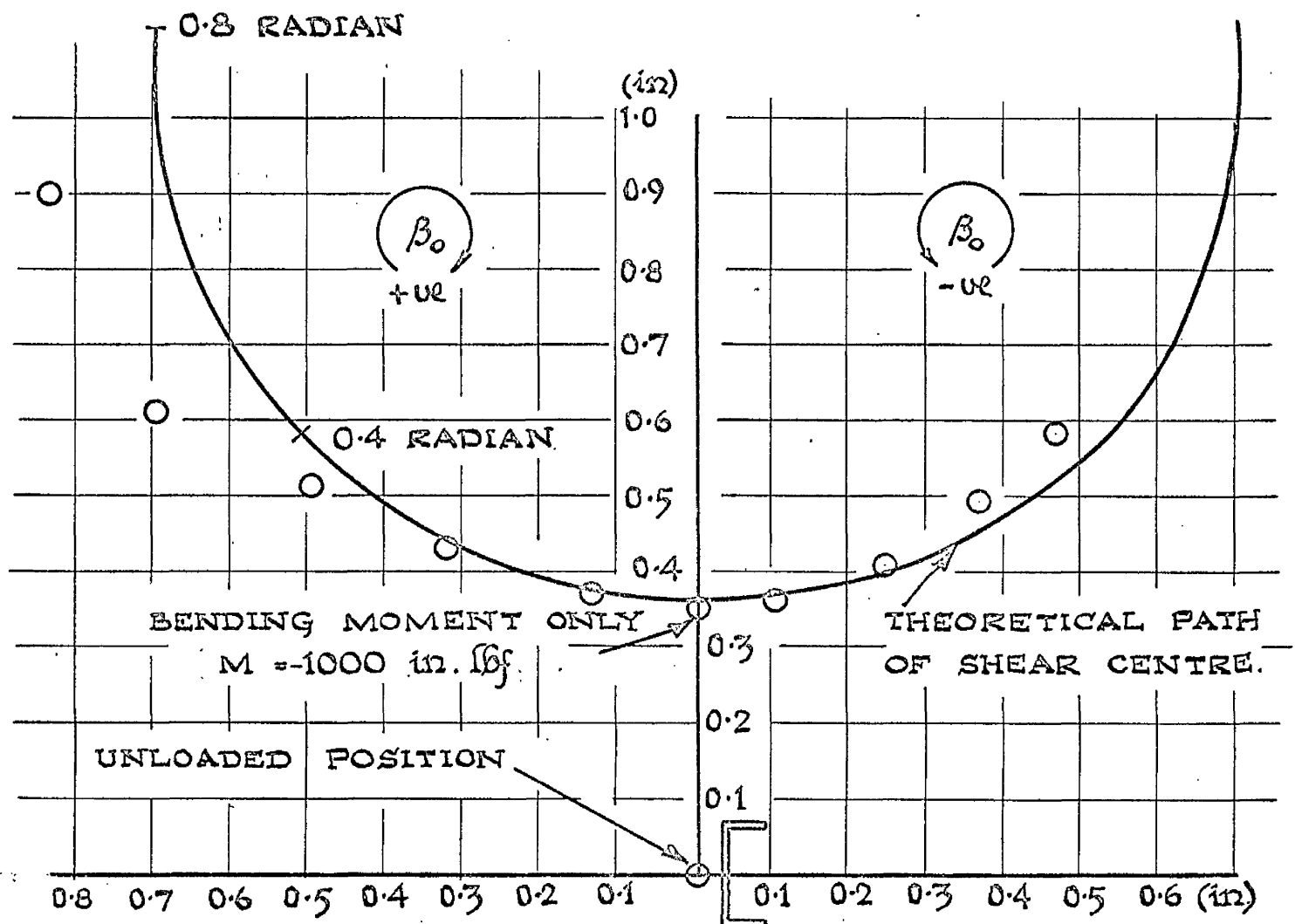
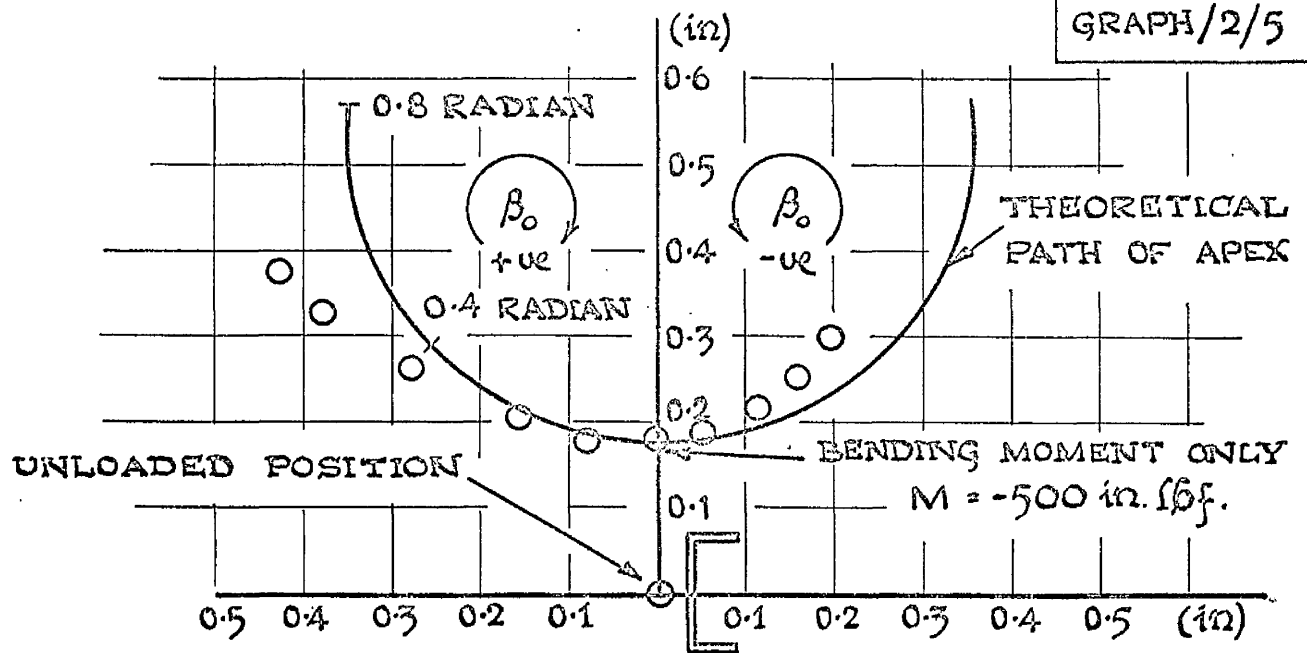
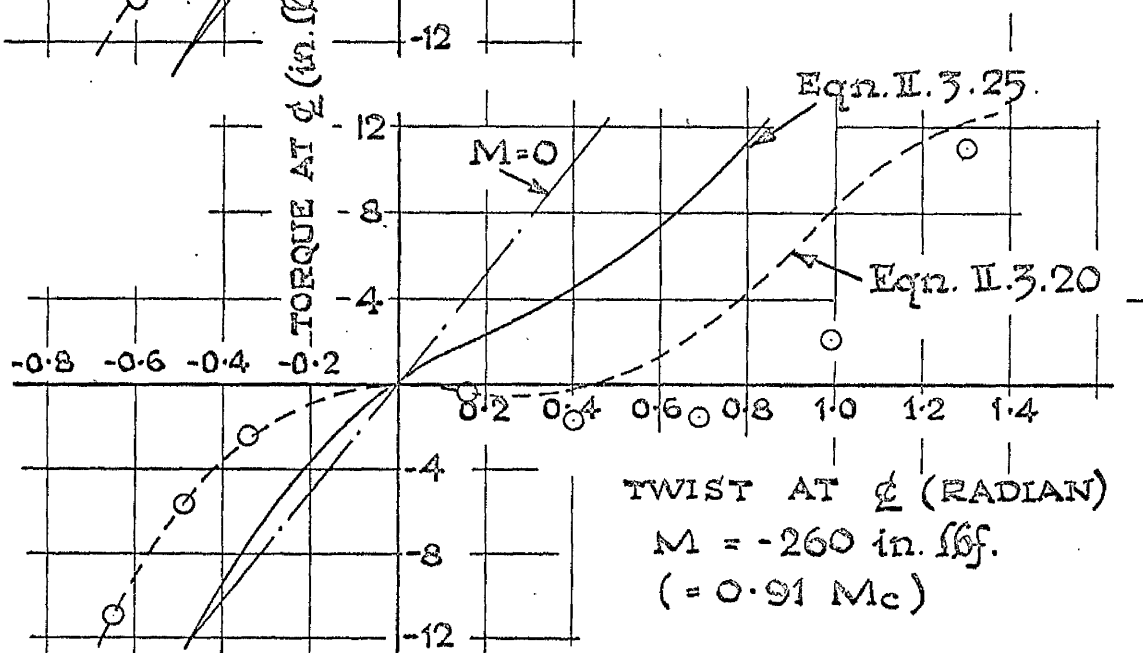
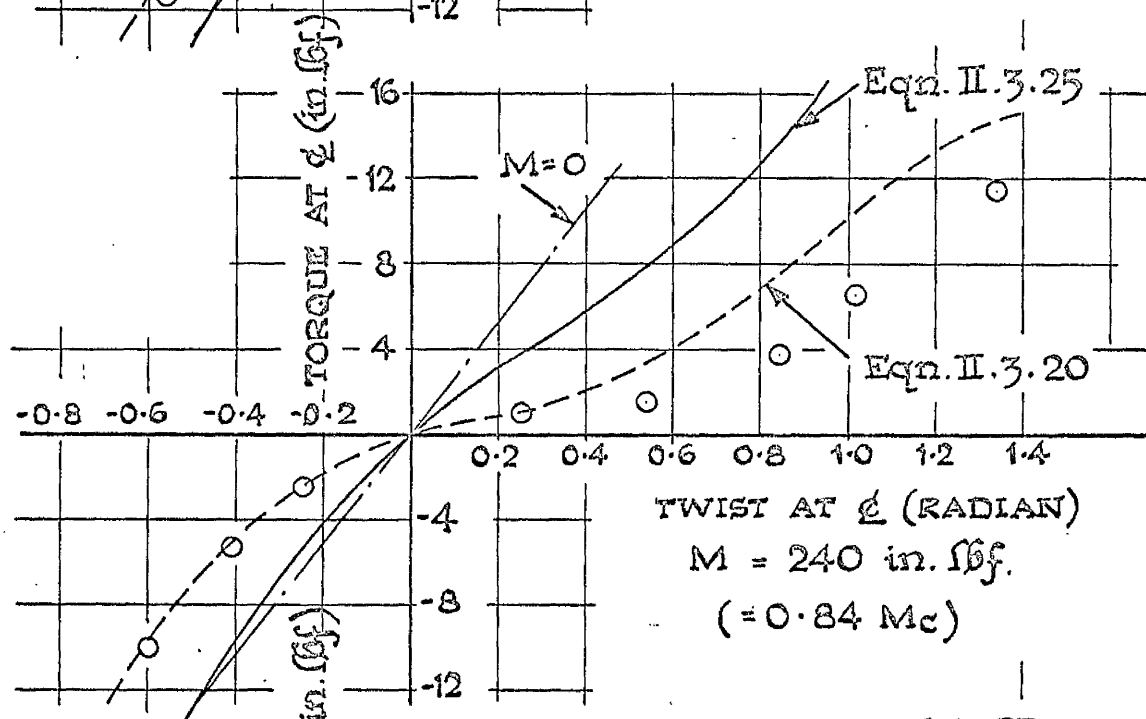
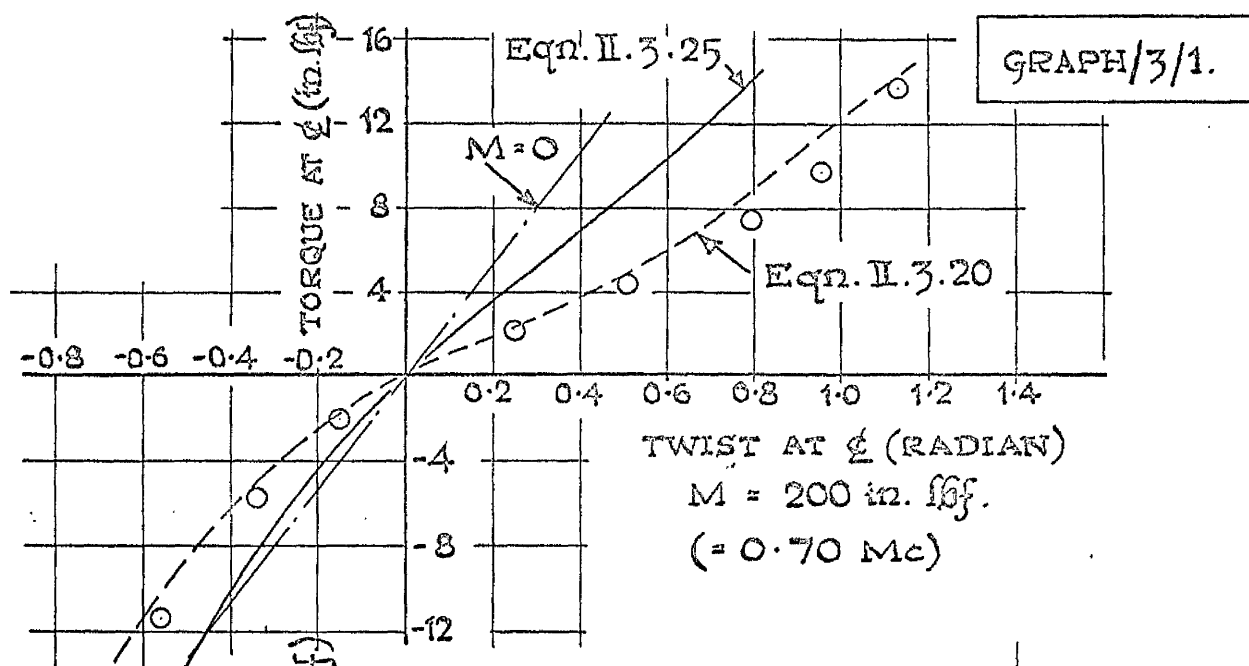
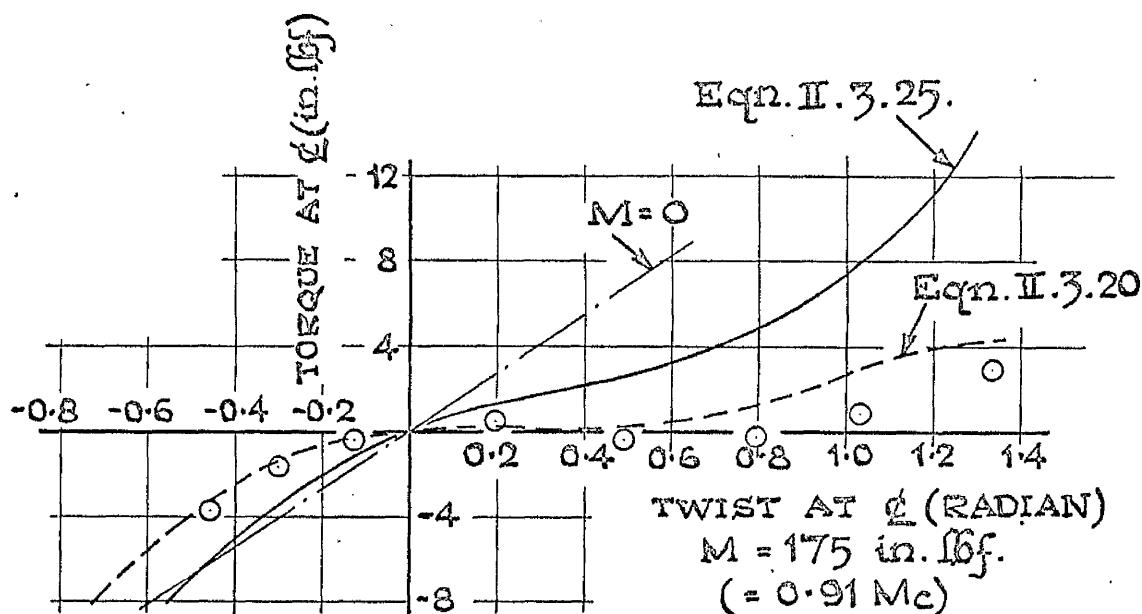
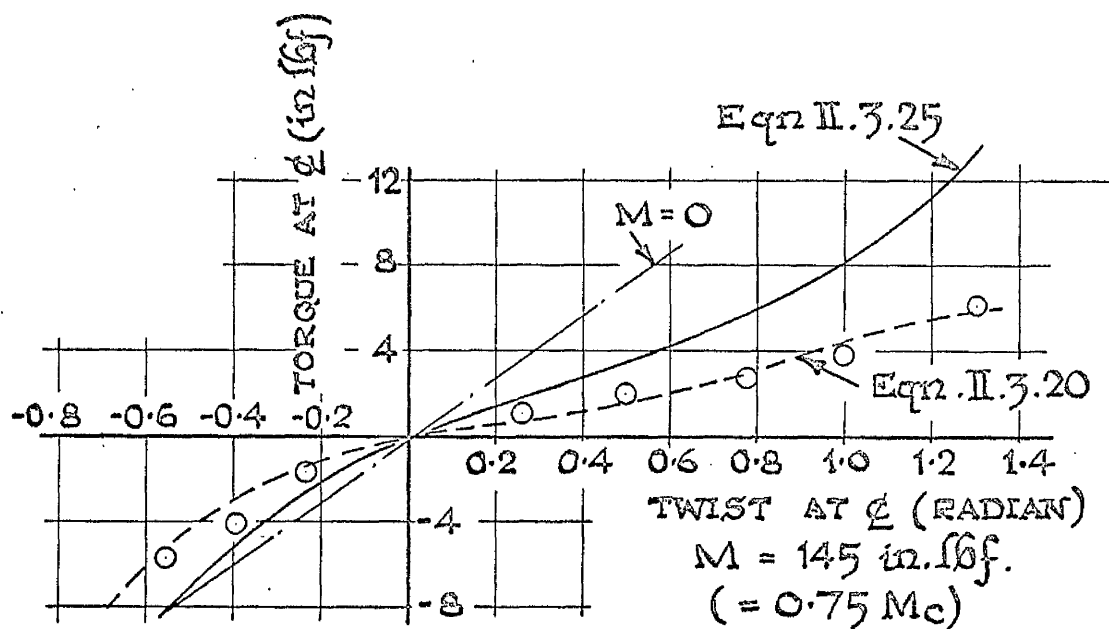
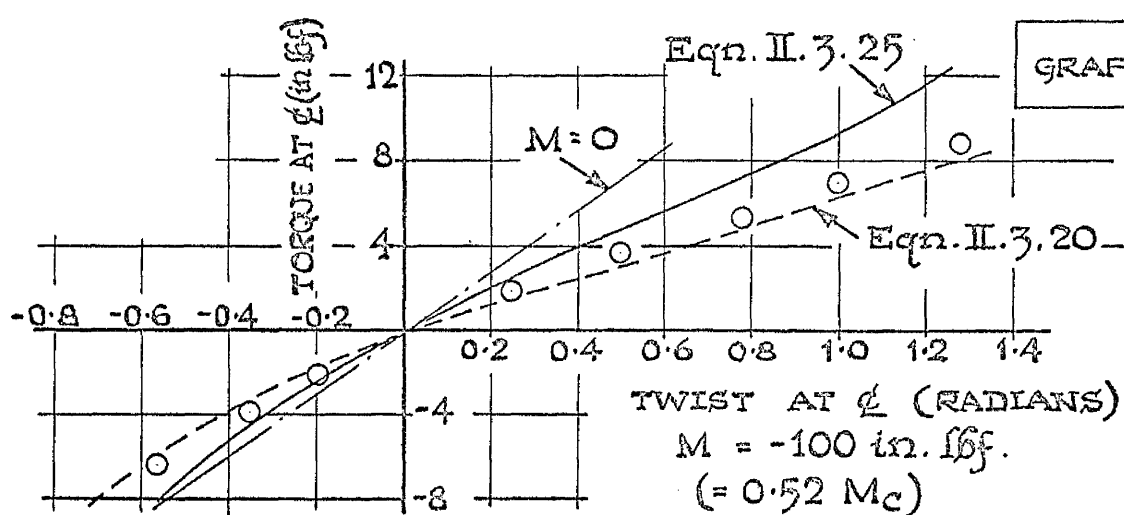


FIG. IV.10. SHEAR CENTRE DISPLACEMENT PATH AT MID-SPAN. (SMALL CHANNEL BEAM.)



NONLINEAR TORQUE / ANGLE OF TWIST
EQUILIBRIUM PATHS (SPECIMEN A.1.)



NON - LINEAR TORQUE / ANGLE OF TWIST
 EQUILIBRIUM PATHS (SPECIMEN A2)

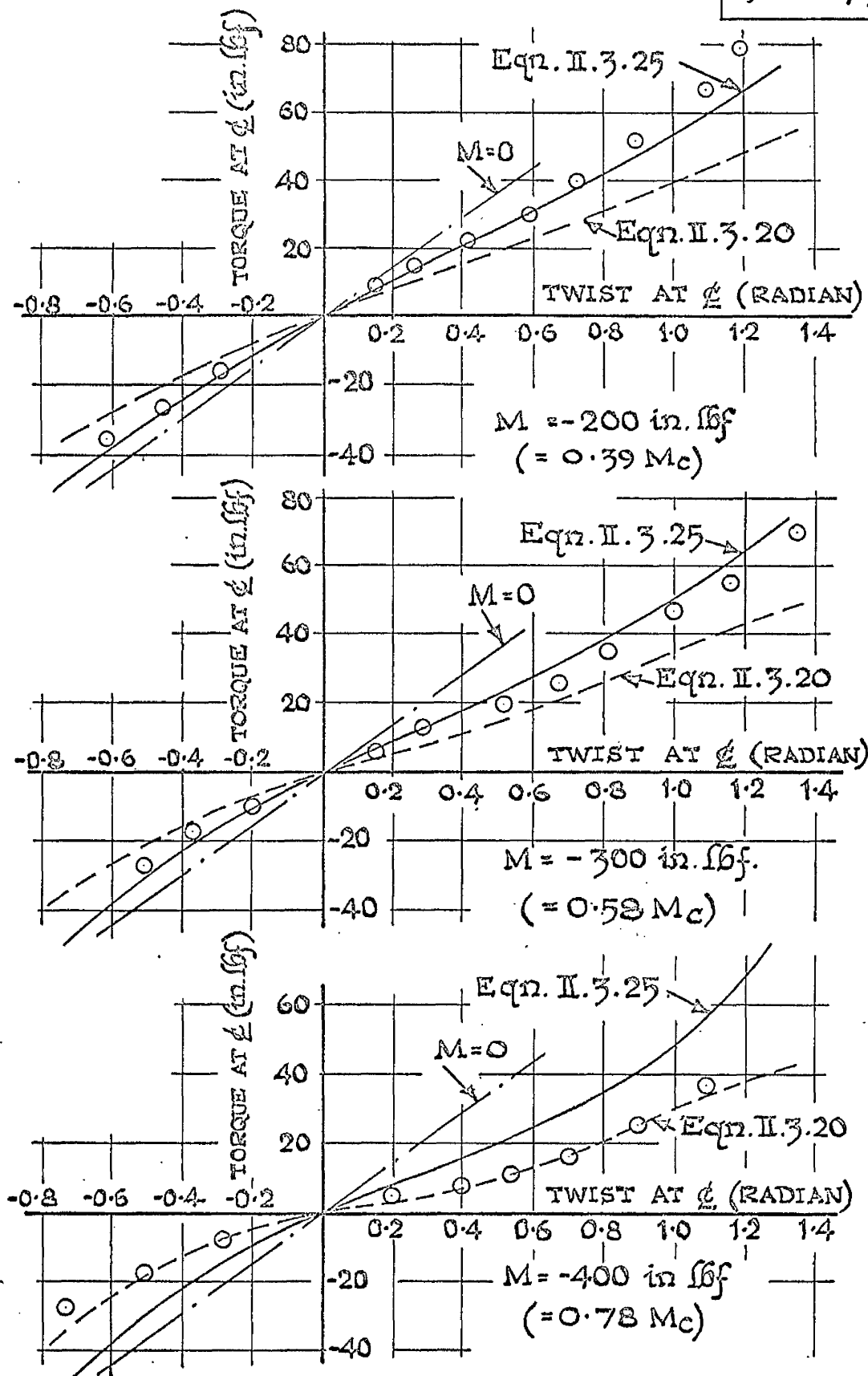
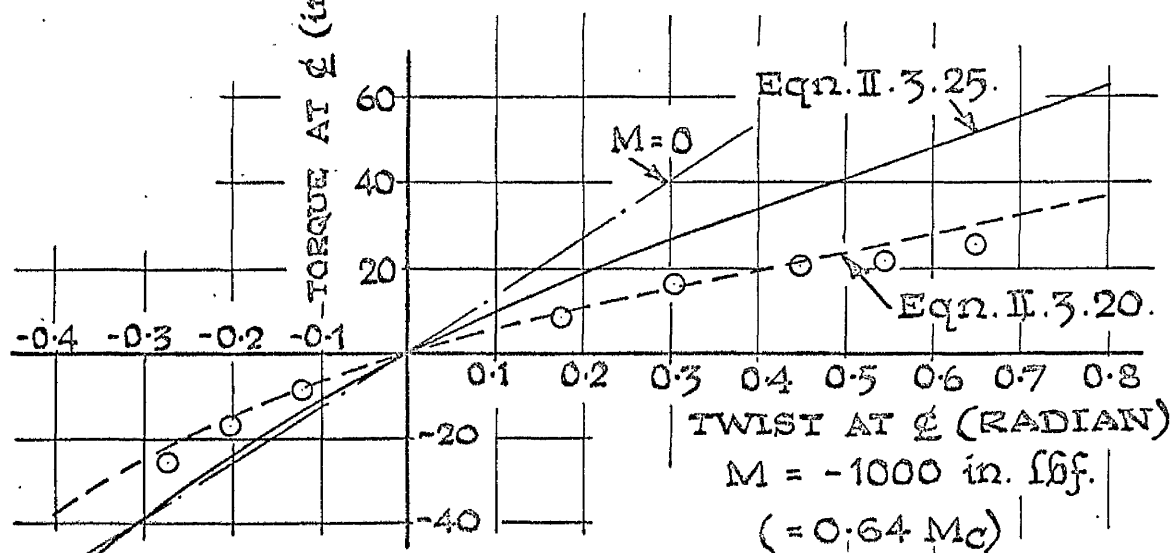
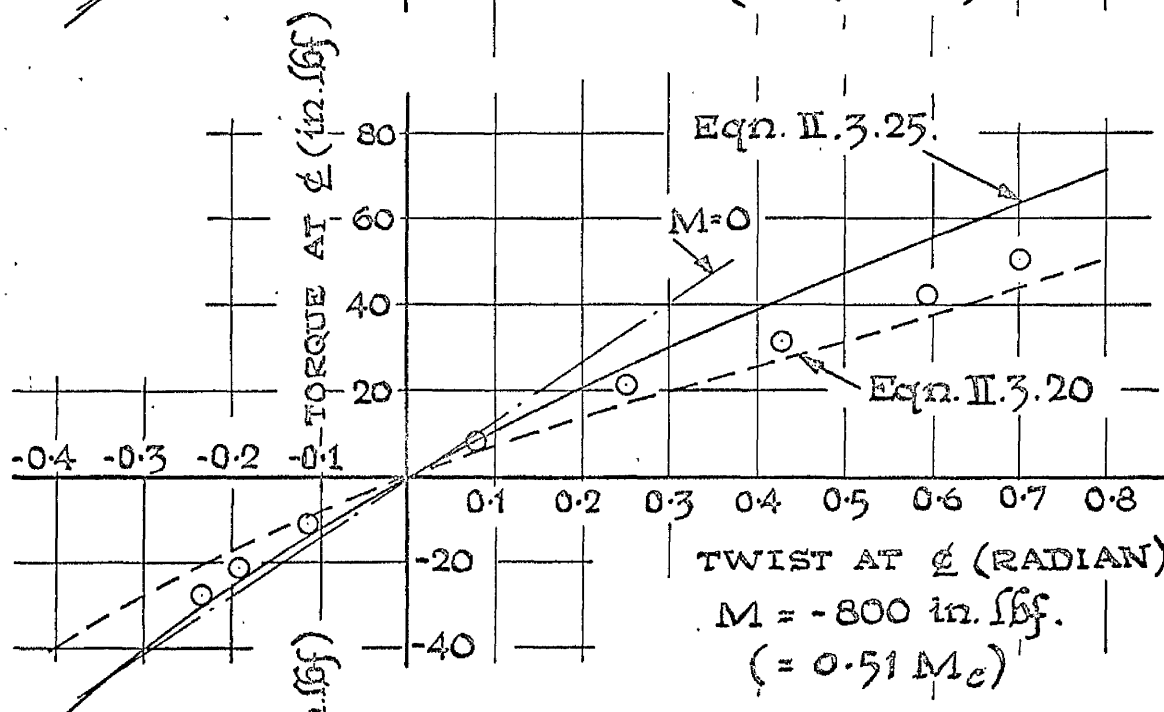
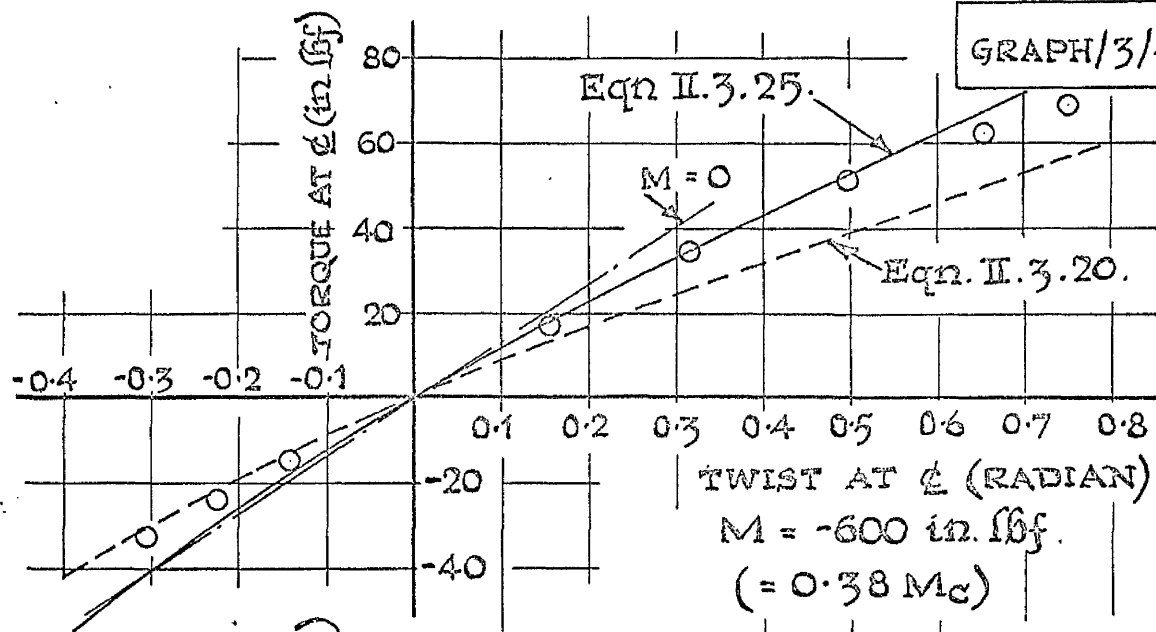
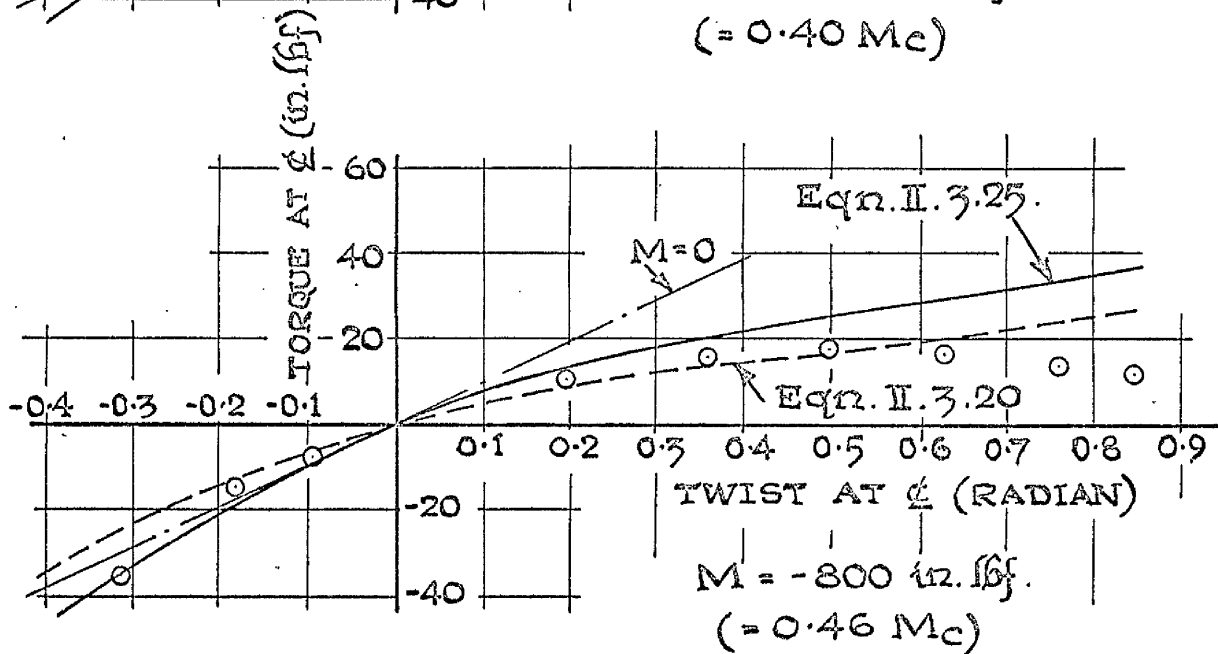
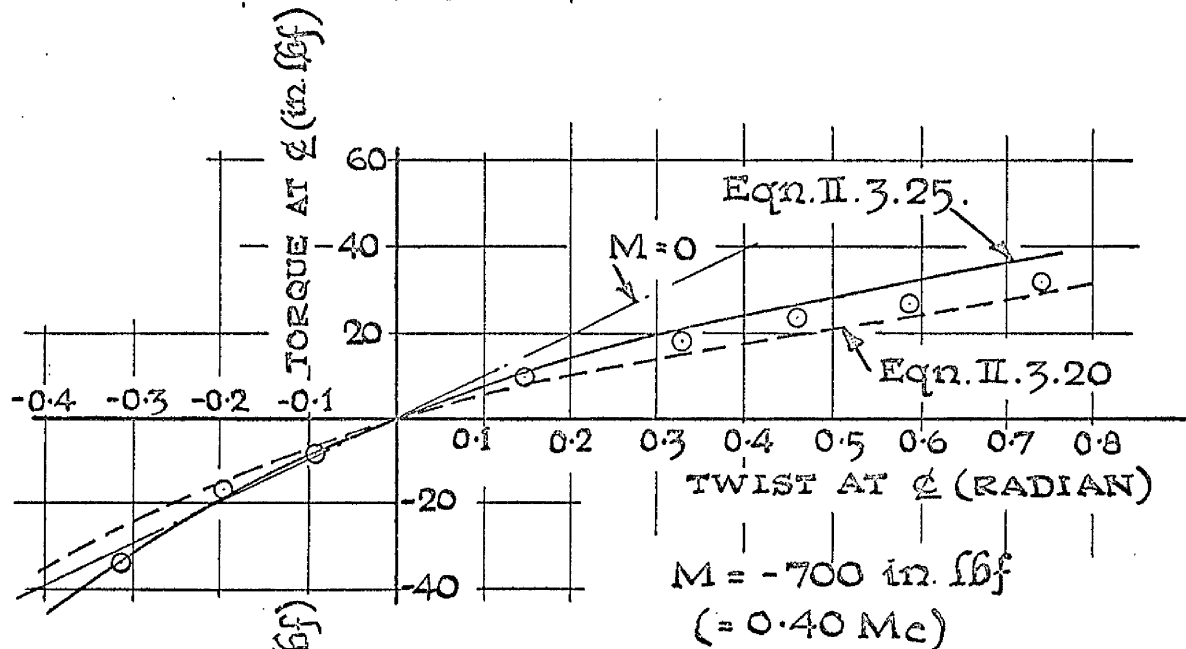
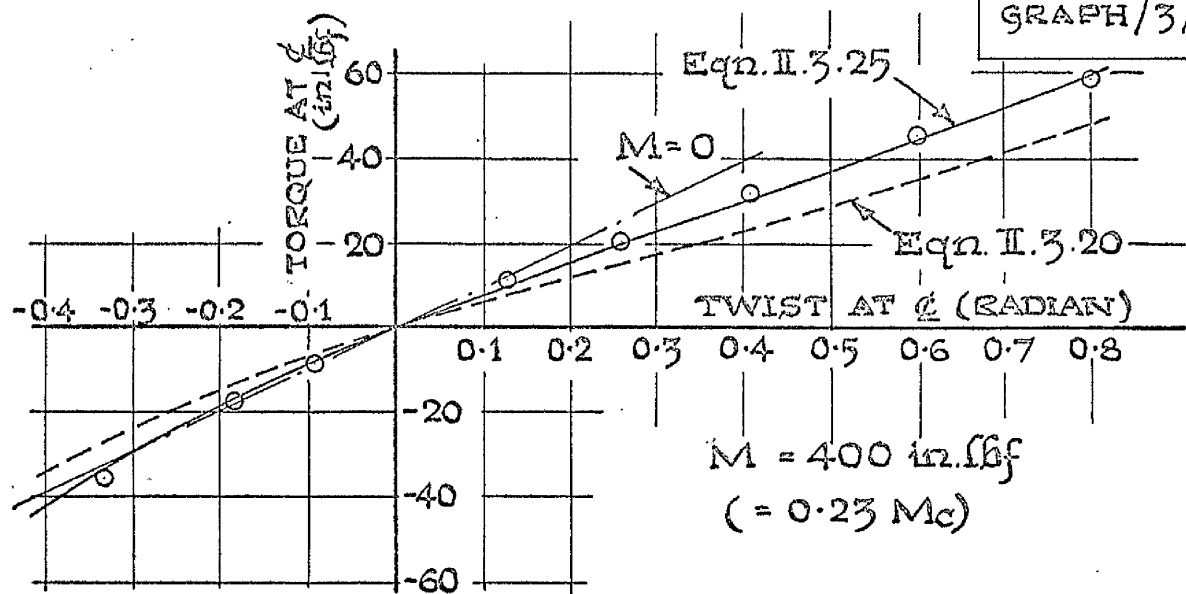


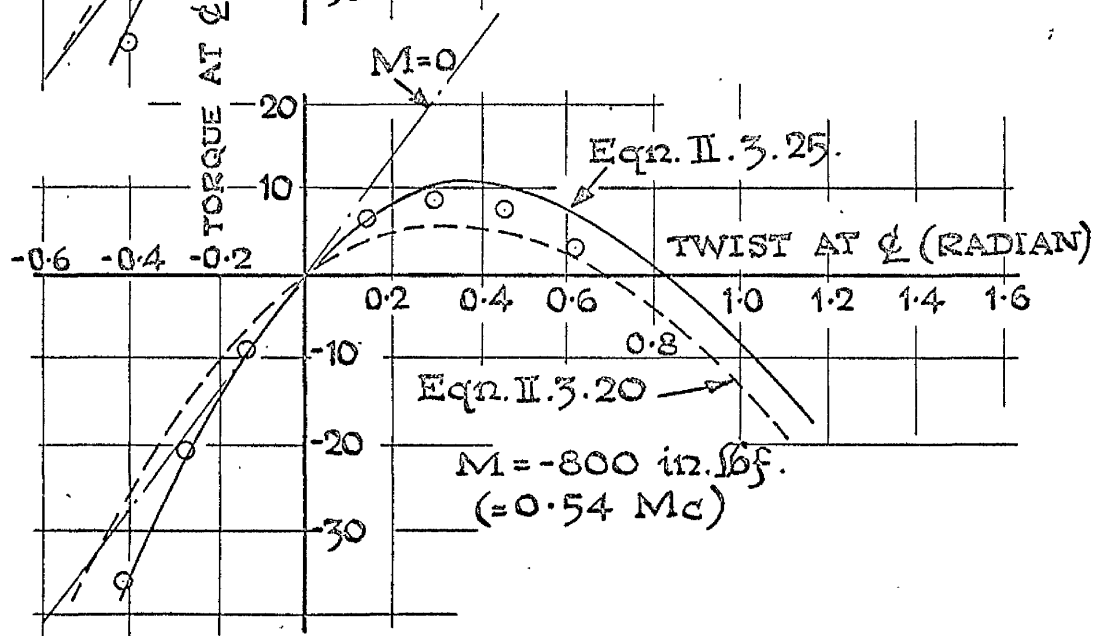
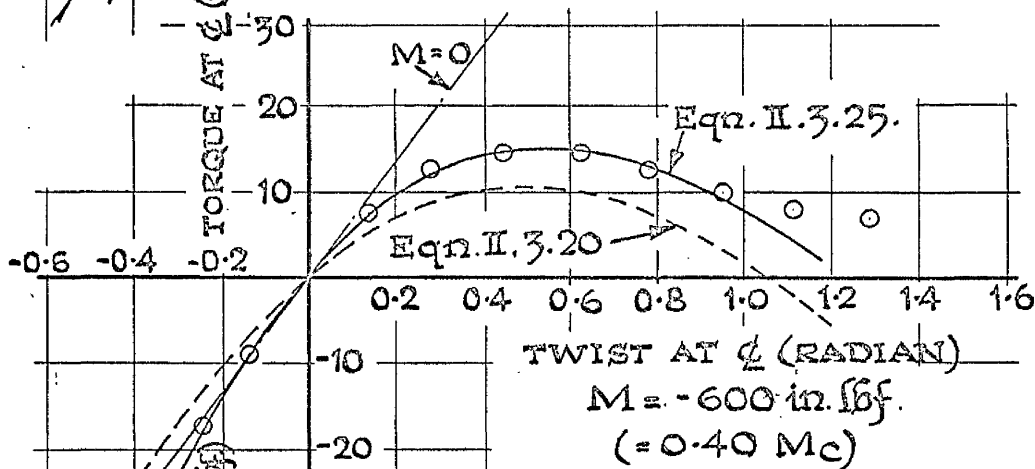
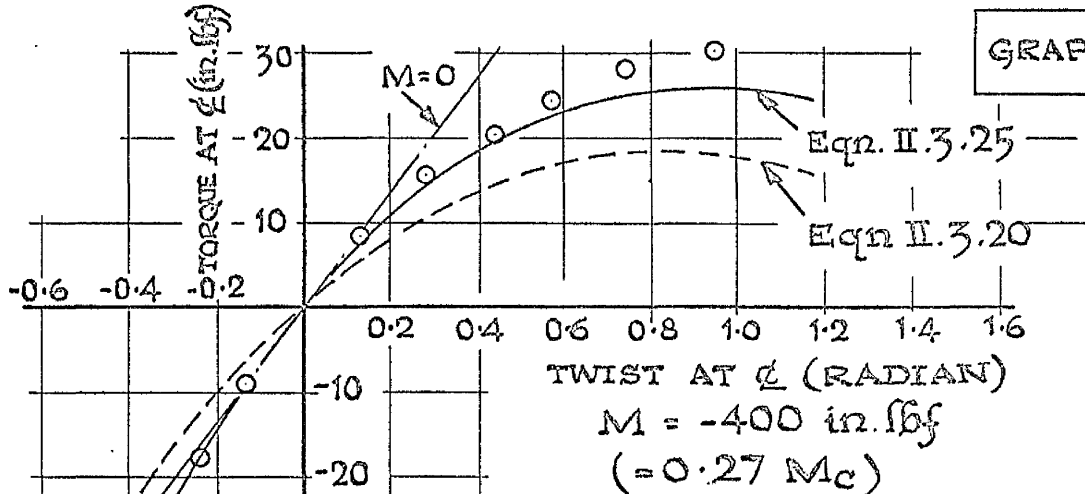
FIG. IV. 11. NONLINEAR TORQUE/ANGLE OF TWIST
EQUILIBRIUM PATHS (SPECIMEN A3)



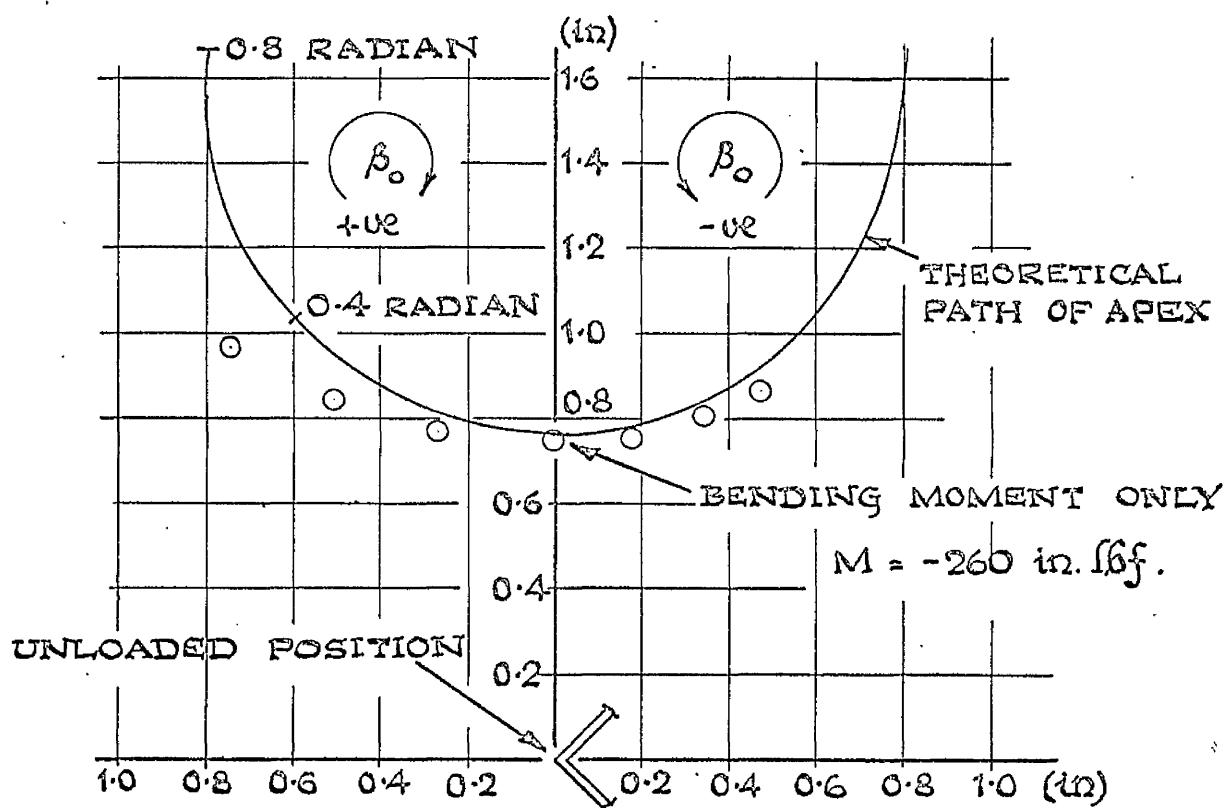
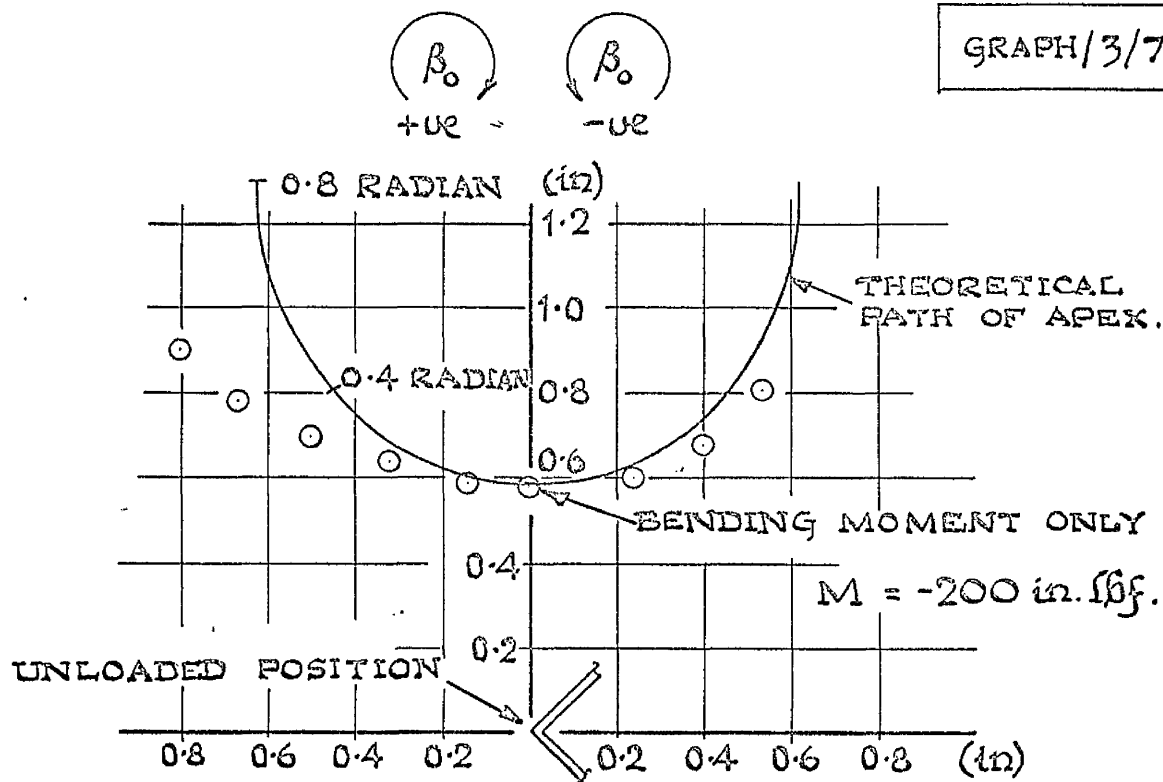
NONLINEAR TORQUE/ANGLE OF TWIST
EQUILIBRIUM PATHS. (SPECIMEN B.1)



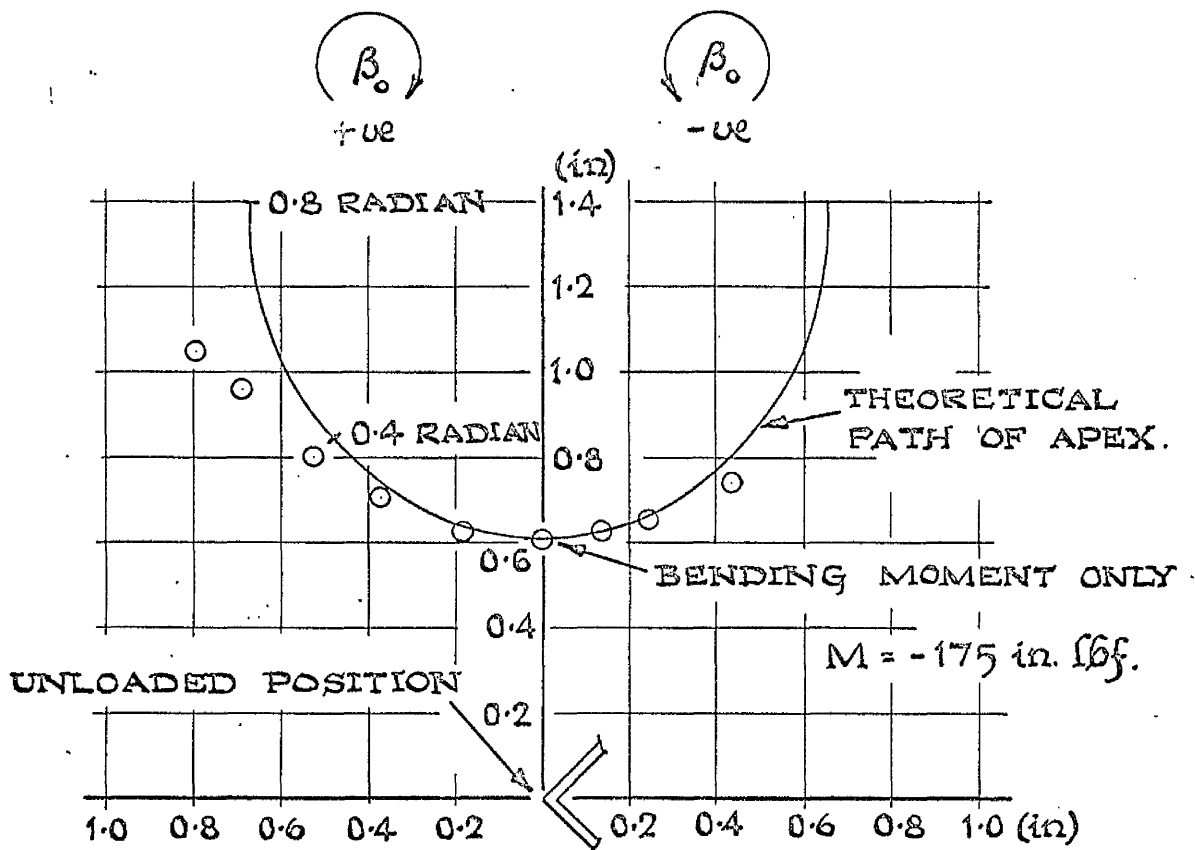
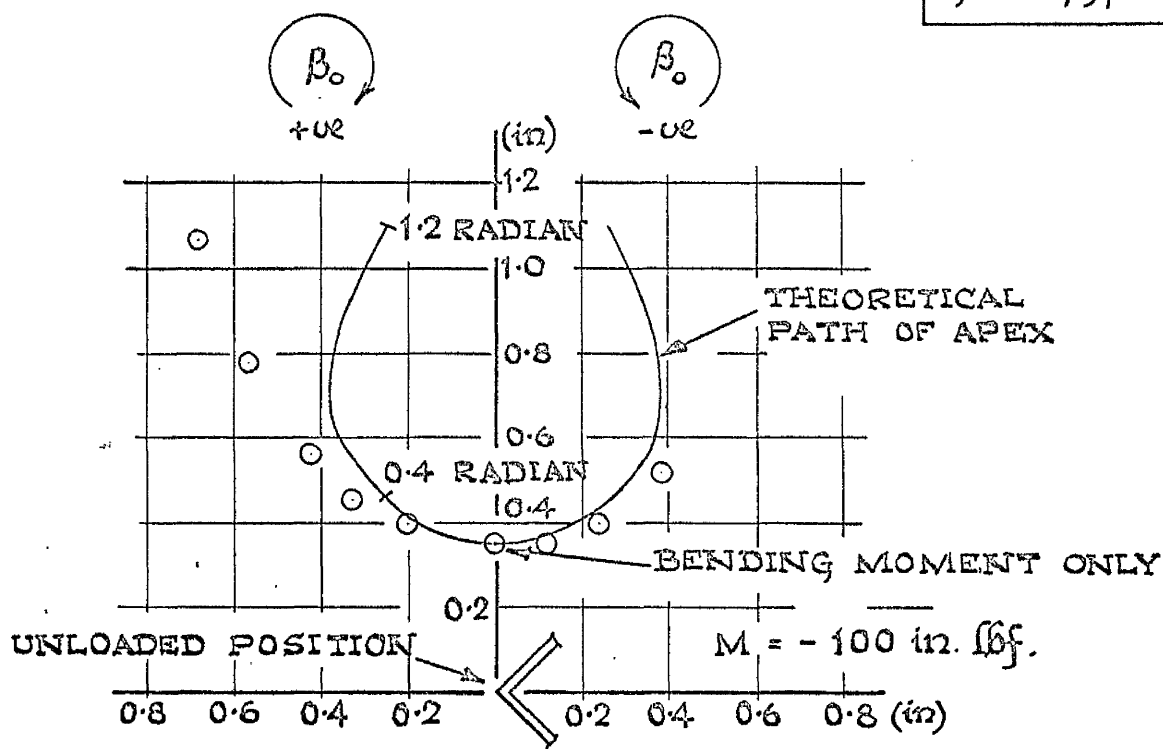
NONLINEAR TORQUE/ANGLE OF TWIST
EQUILIBRIUM PATHS (SPECIMEN C1)



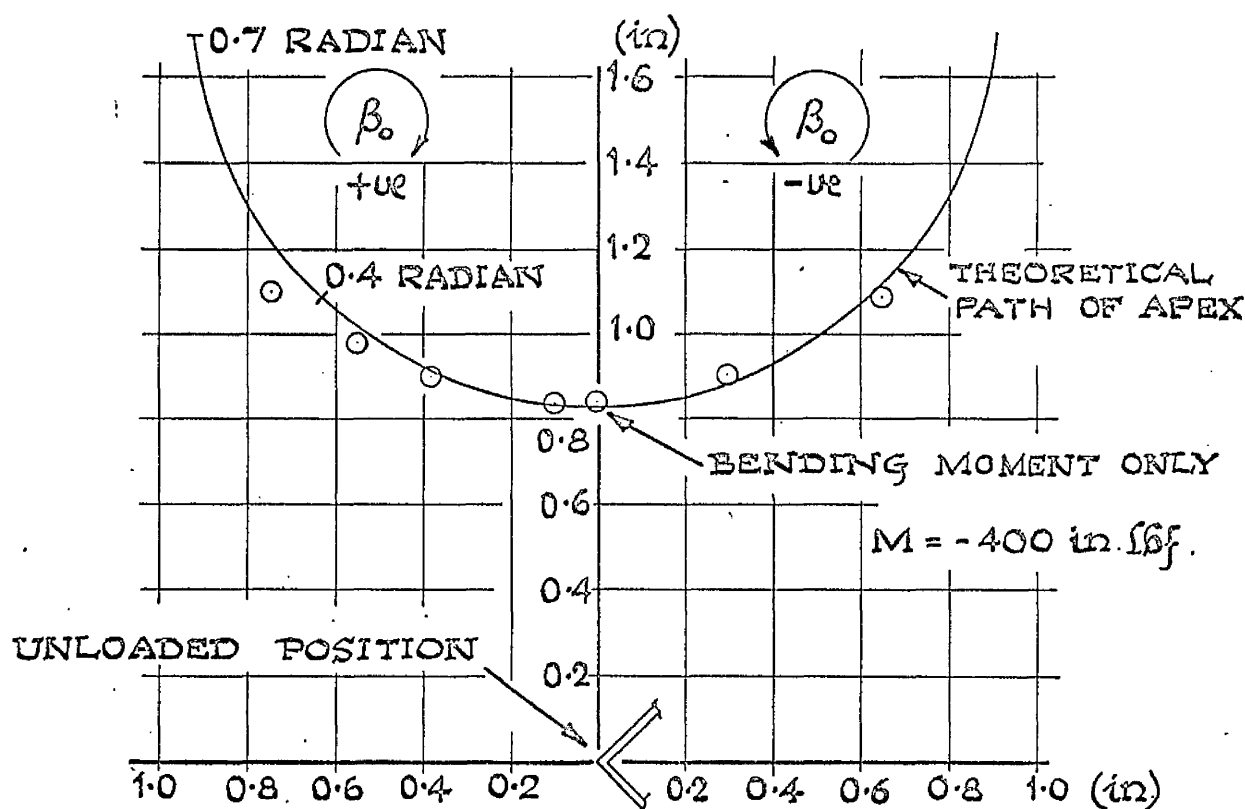
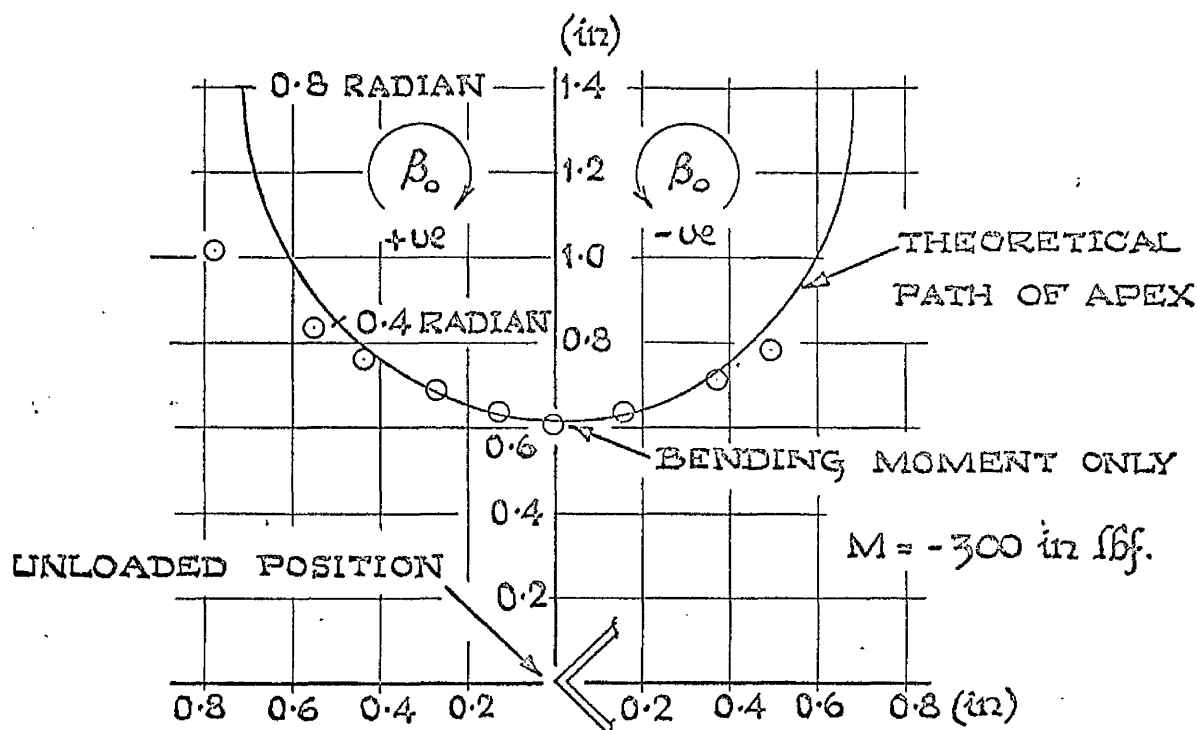
NONLINEAR TORQUE / ANGLE OF TWIST
 EQUILIBRIUM PATHS (SPECIMEN C.2)



SHEAR CENTRE (APEX) DISPLACEMENT
PATHS AT MID-SPAN. (SPECIMEN A1)



SHEAR CENTRE (APEX) DISPLACEMENT PATHS
AT MID - SPAN. (SPECIMEN A2.)



SHEAR CENTRE (APEX) DISPLACEMENT
PATHS AT MID-SPAN (SPECIMEN A.3.)

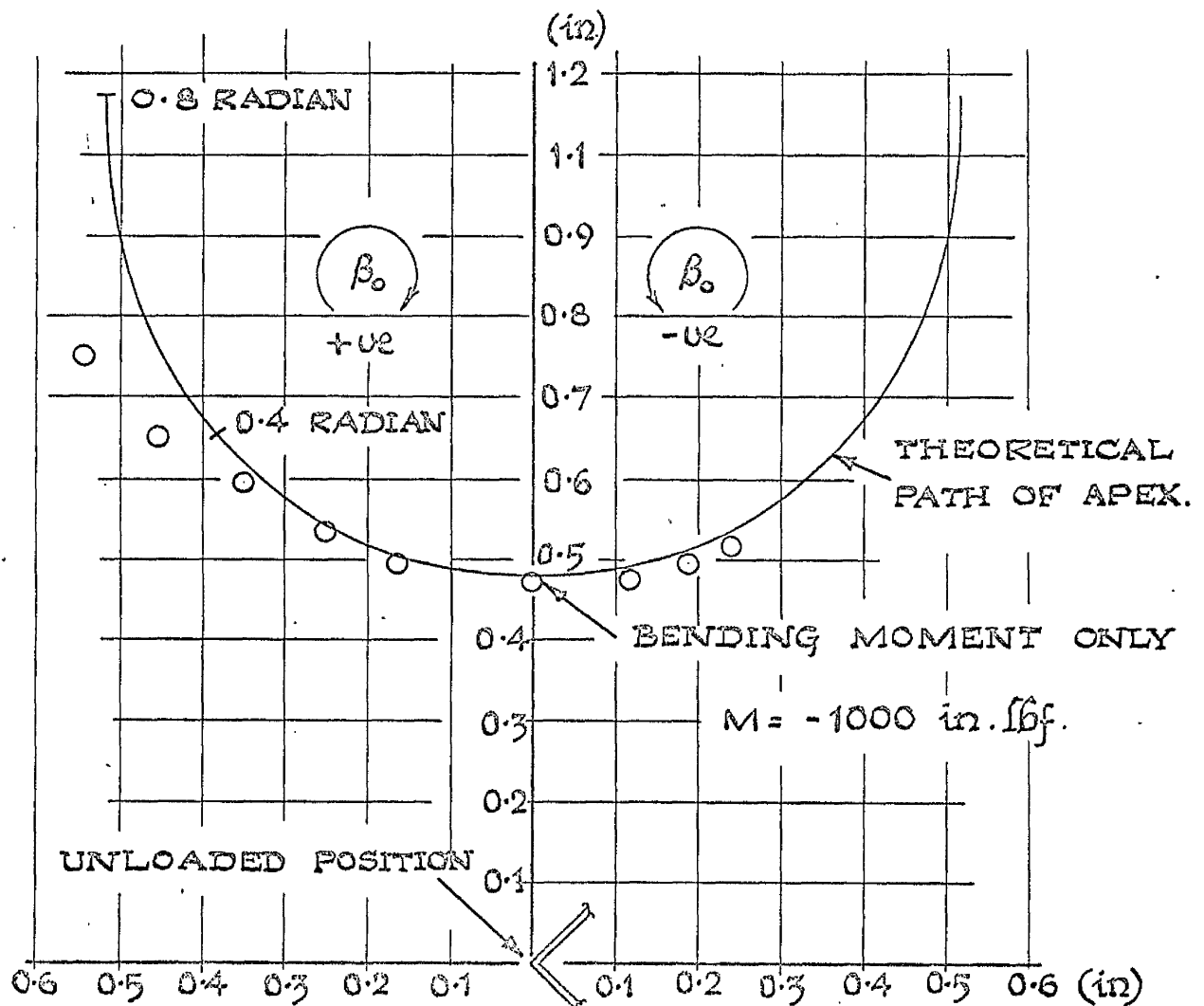
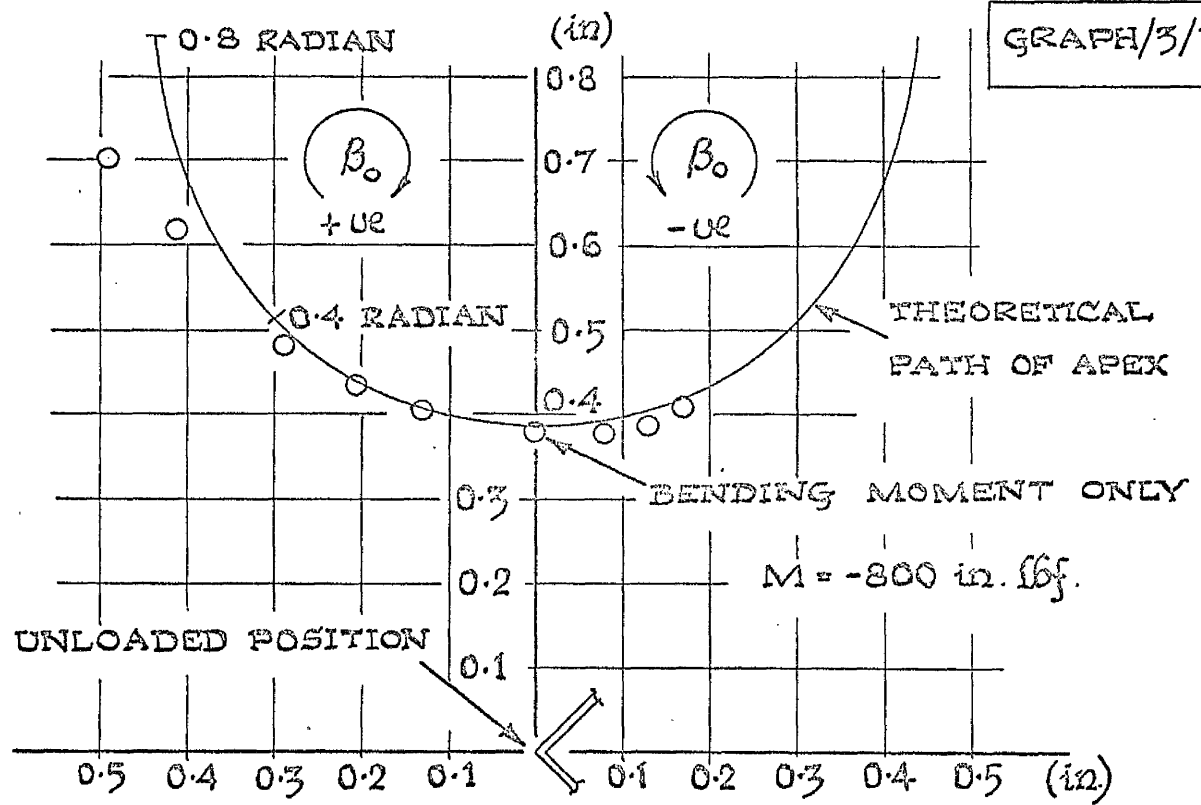
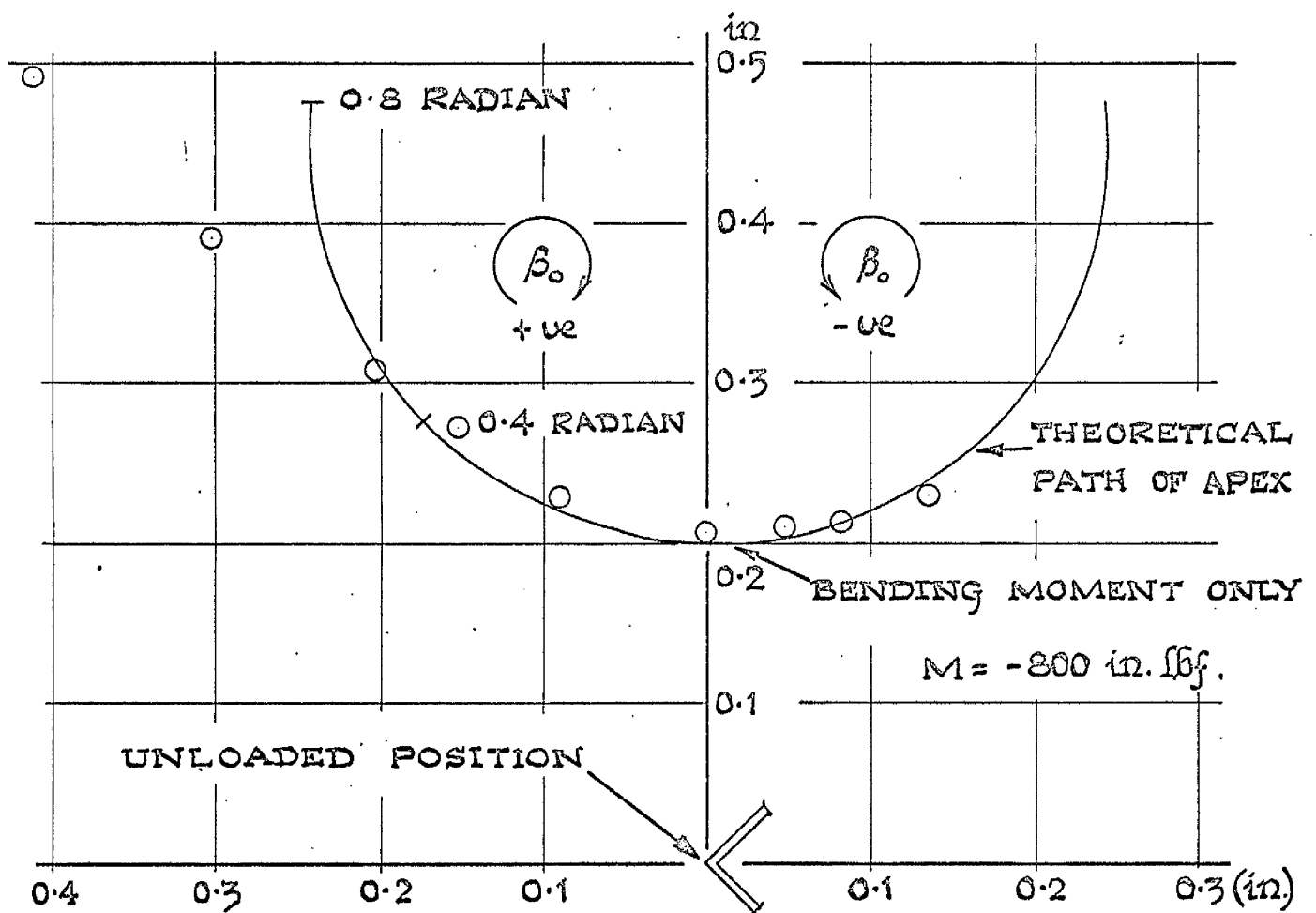
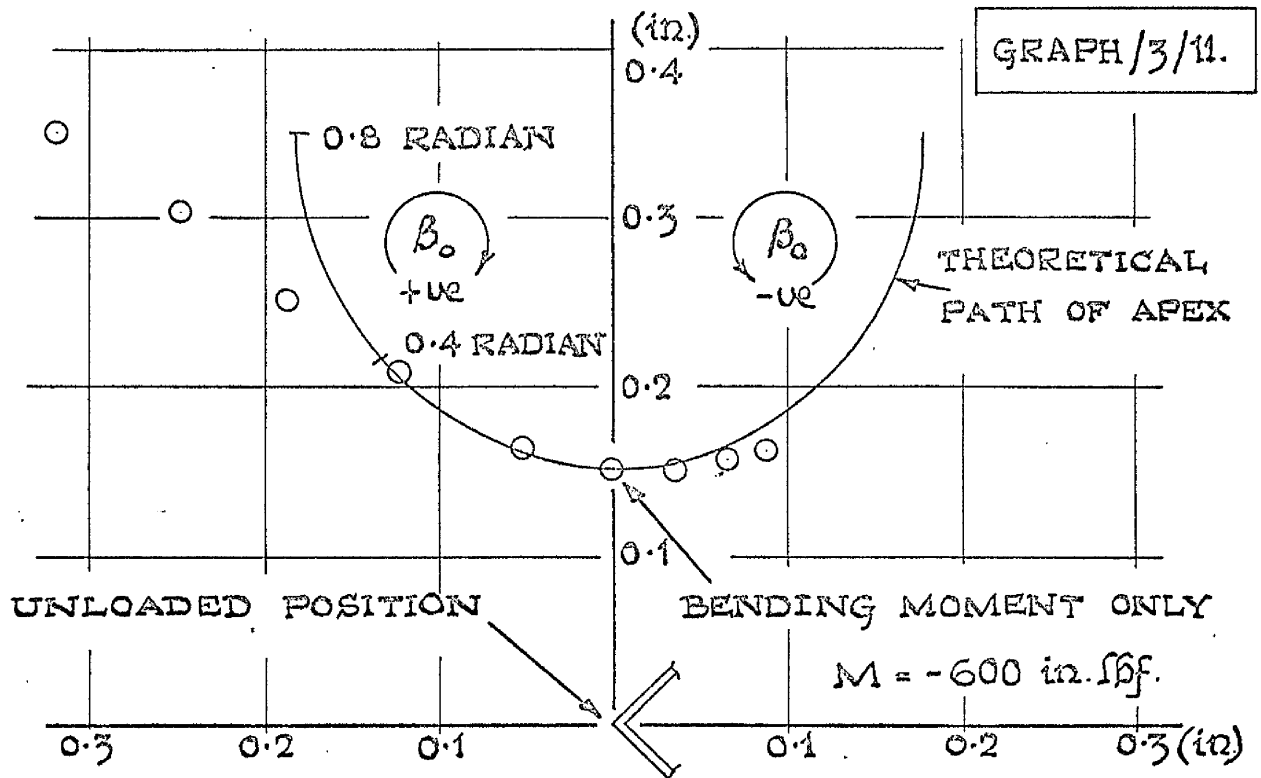
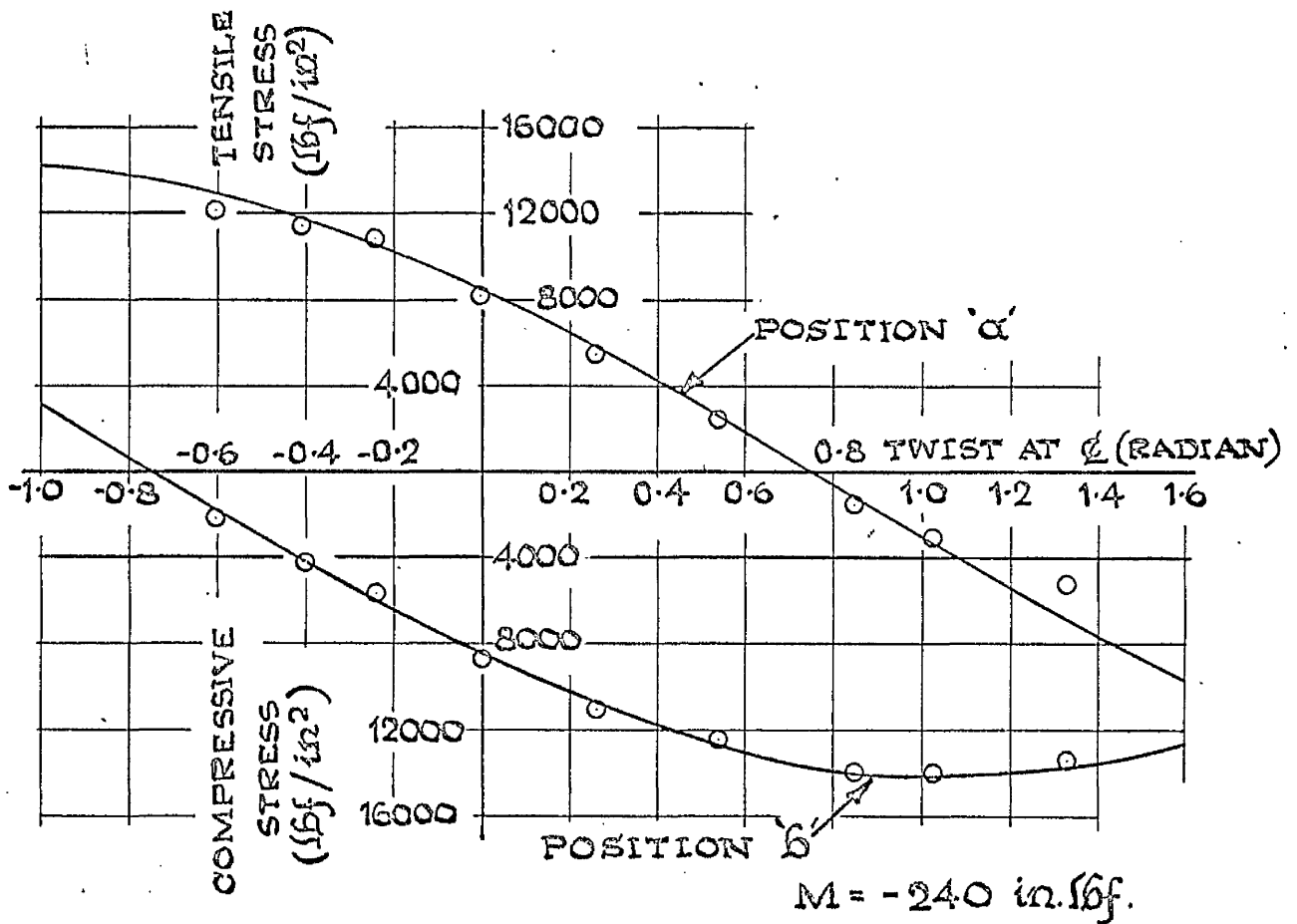
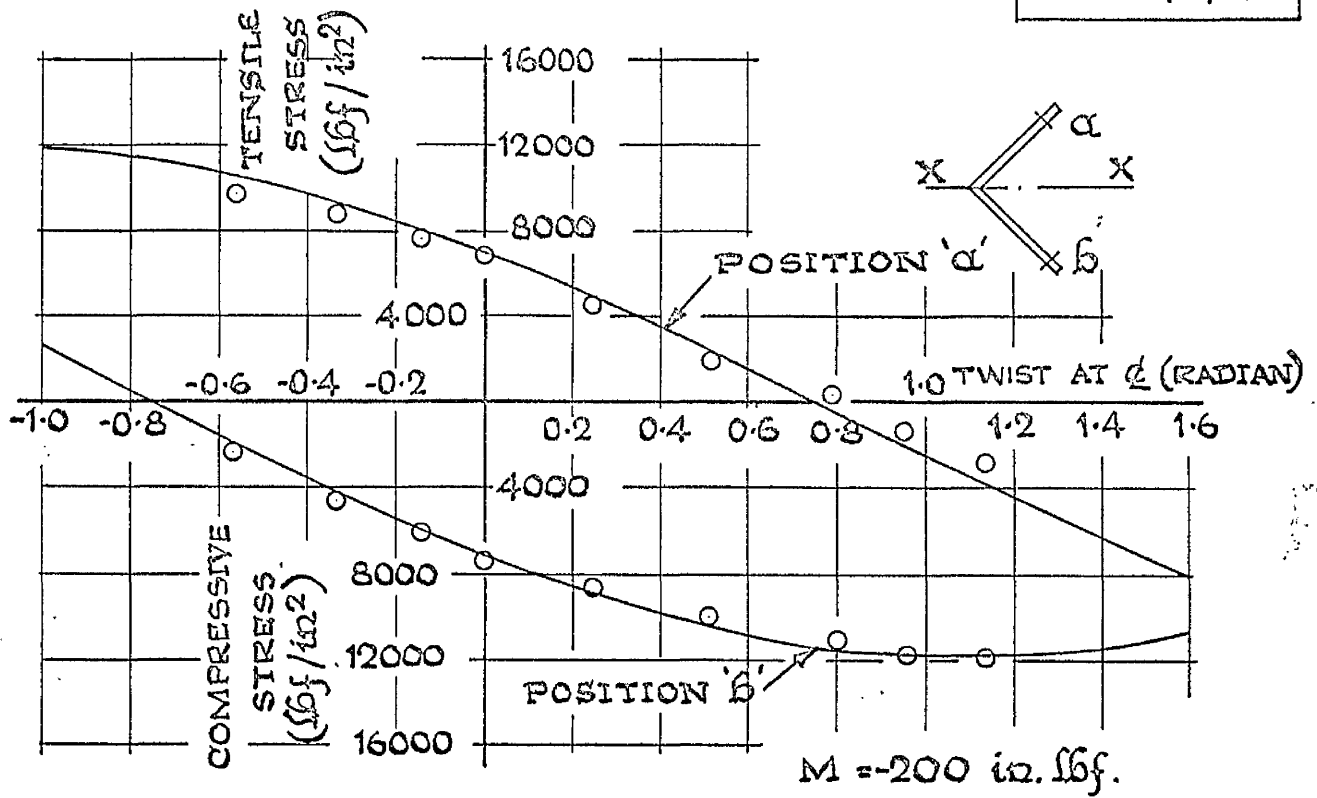


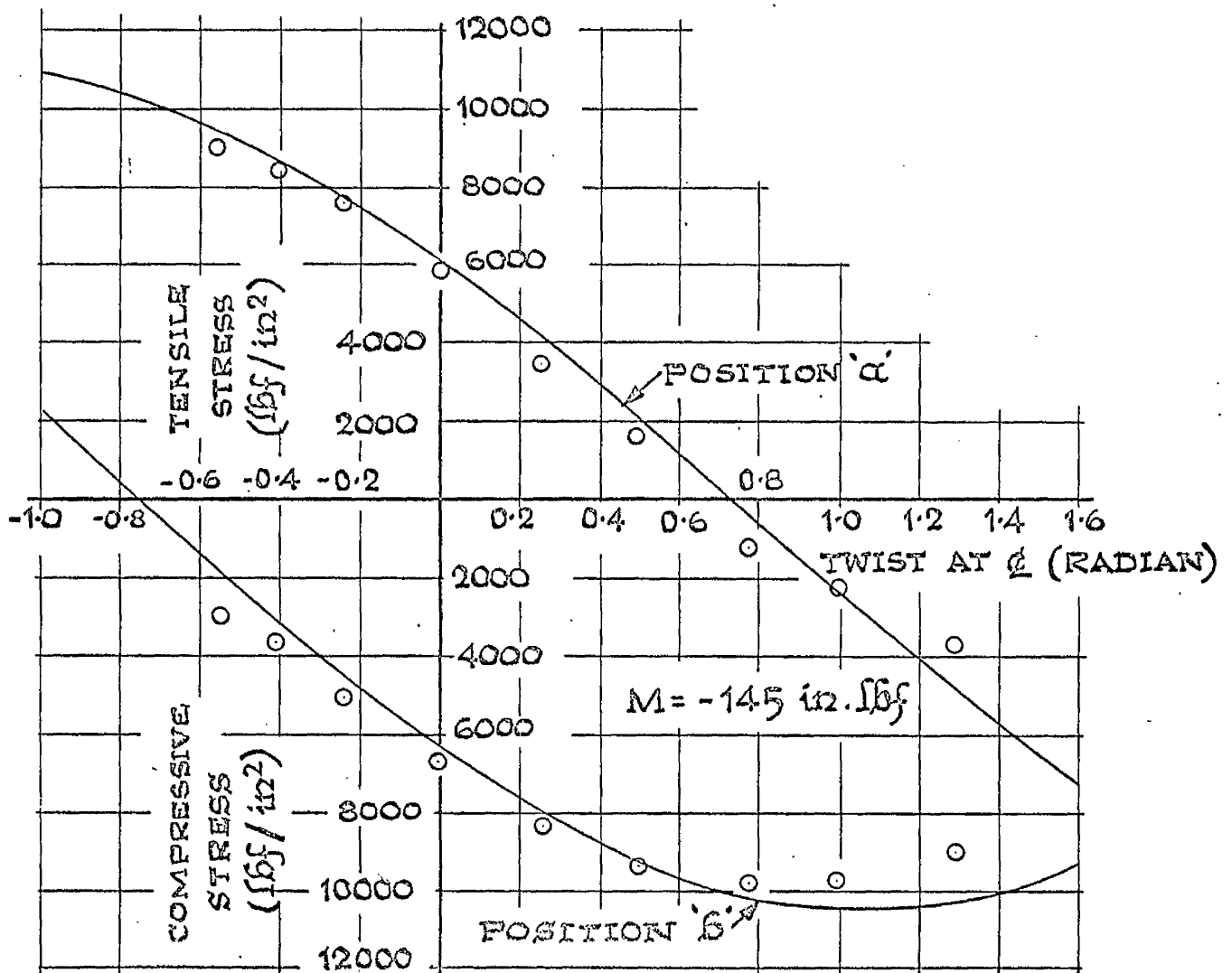
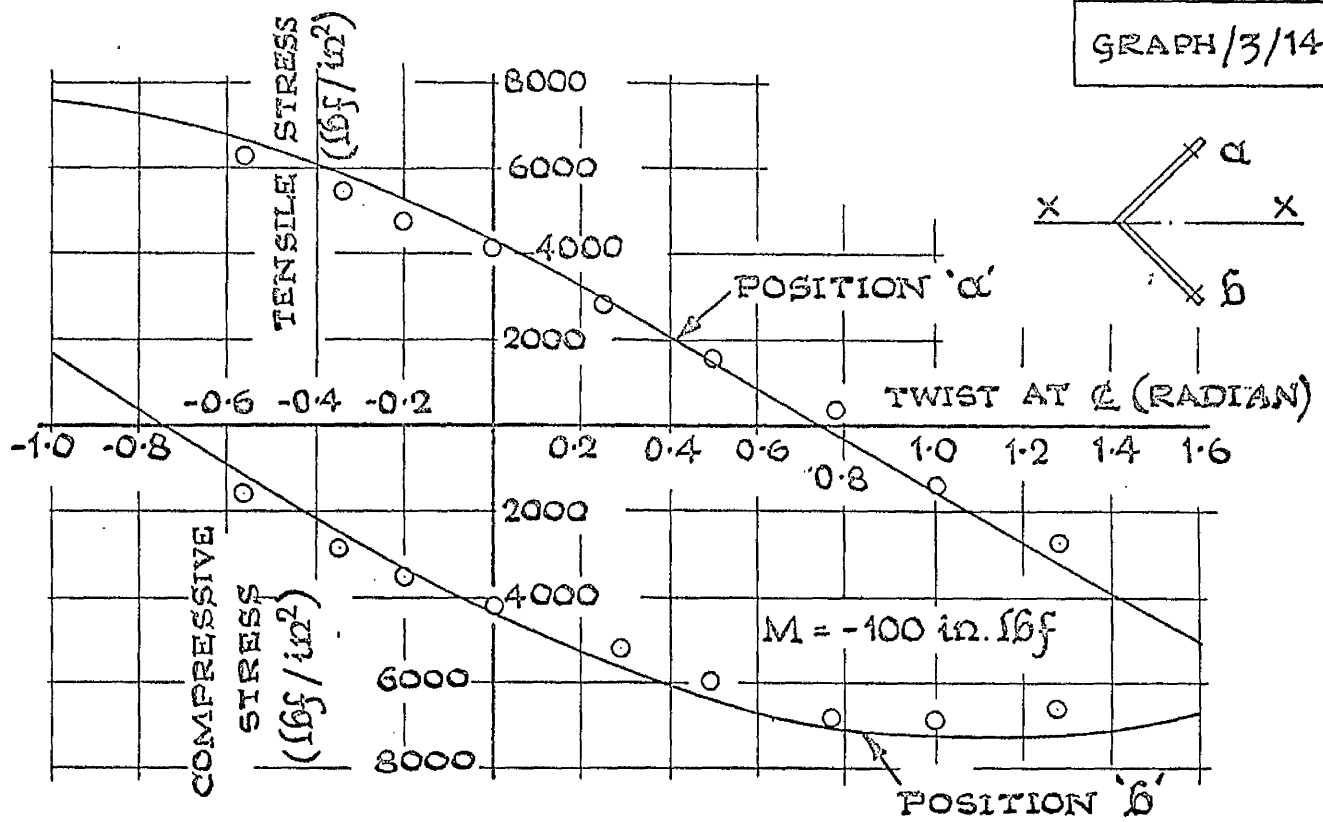
FIG. IX. 15. SHEAR CENTRE (APEX) DISPLACEMENT PATHS AT MID-SPAN (SPECIMEN BI.)



SHEAR CENTRE (APEX) DISPLACEMENT PATHS
AT MID - SPAN (SPECIMEN C.1.)



VARIATION OF LONGITUDINAL STRESS WITH ANGLE OF TWIST. (SPECIMEN A1.)



VARIATION OF LONGITUDINAL STRESS WITH ANGLE OF TWIST (SPECIMEN A.2.)

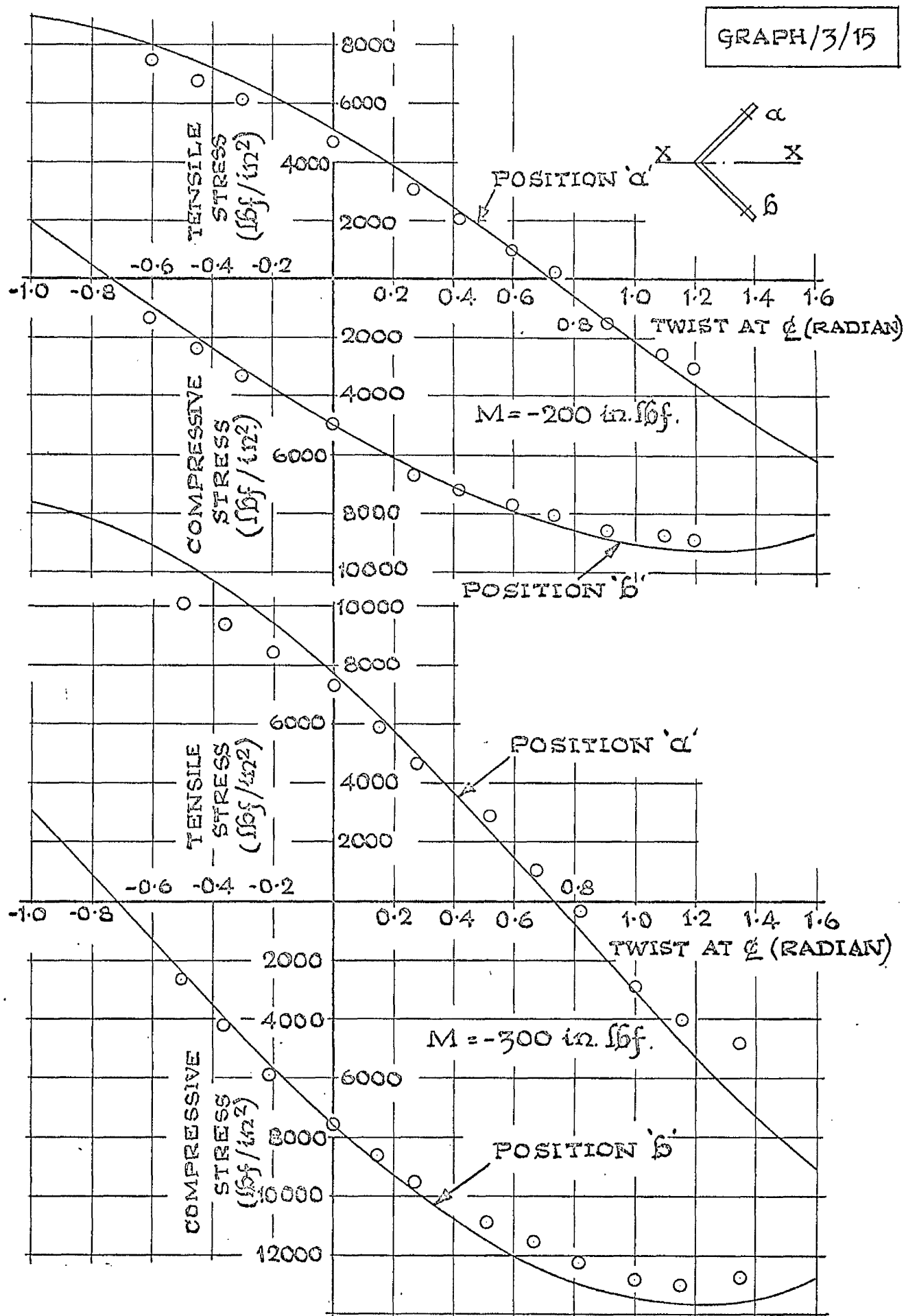
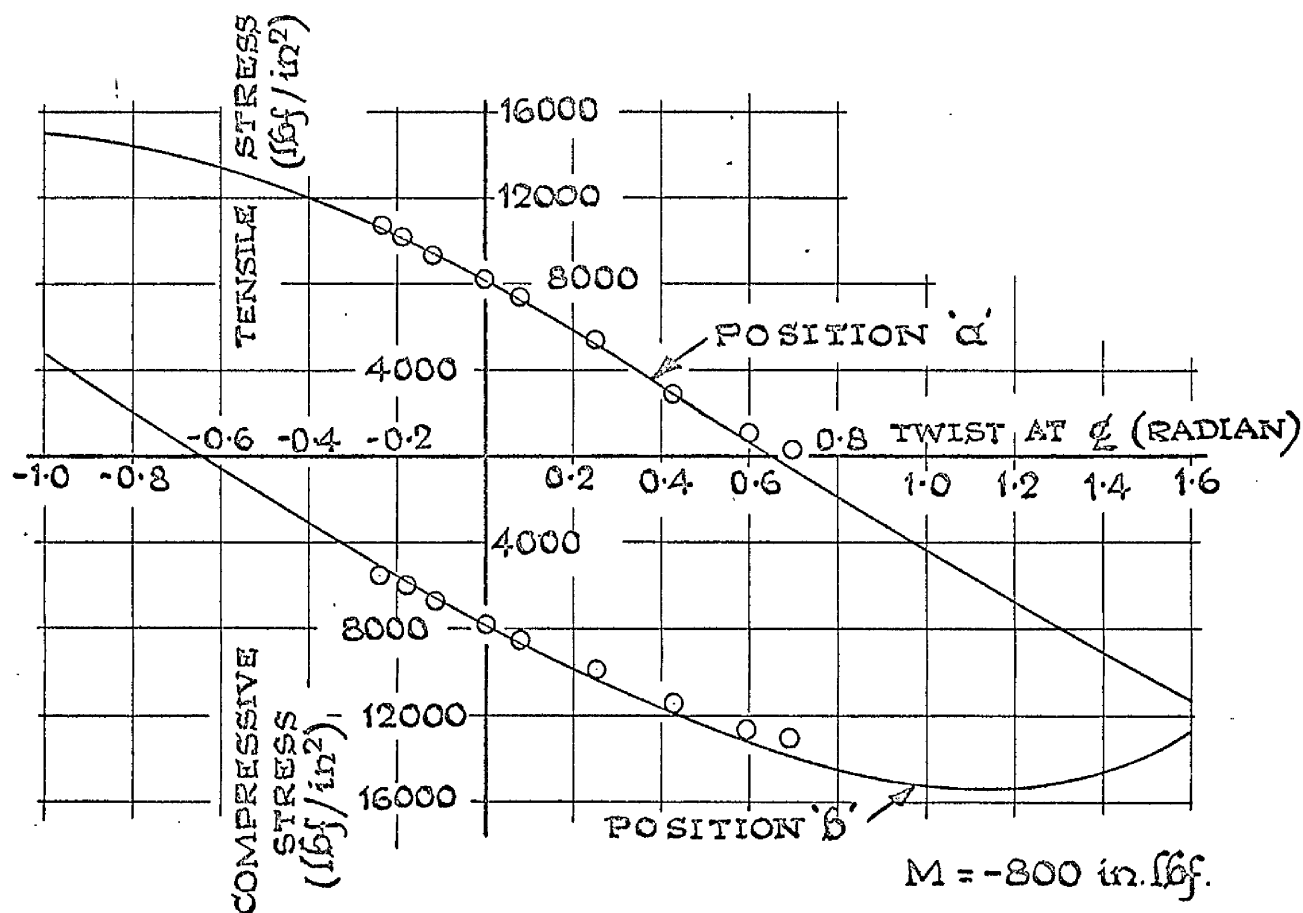
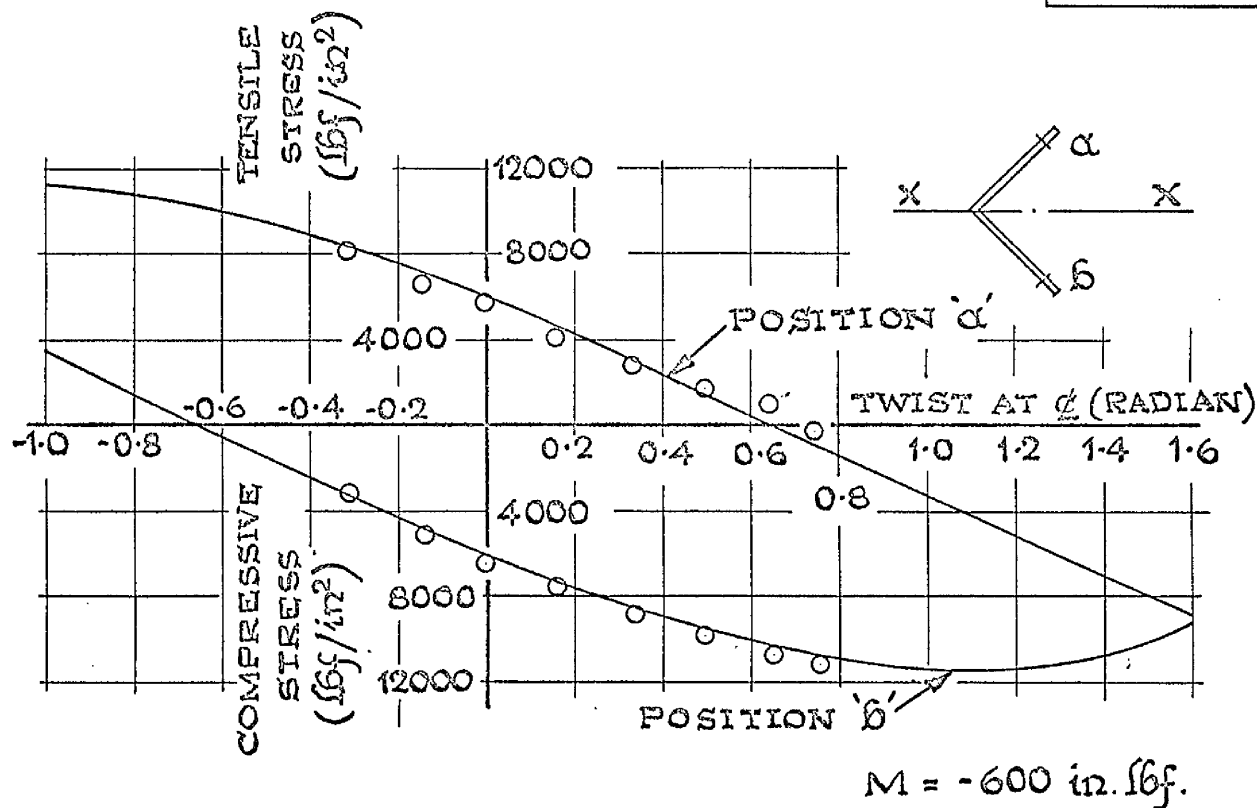
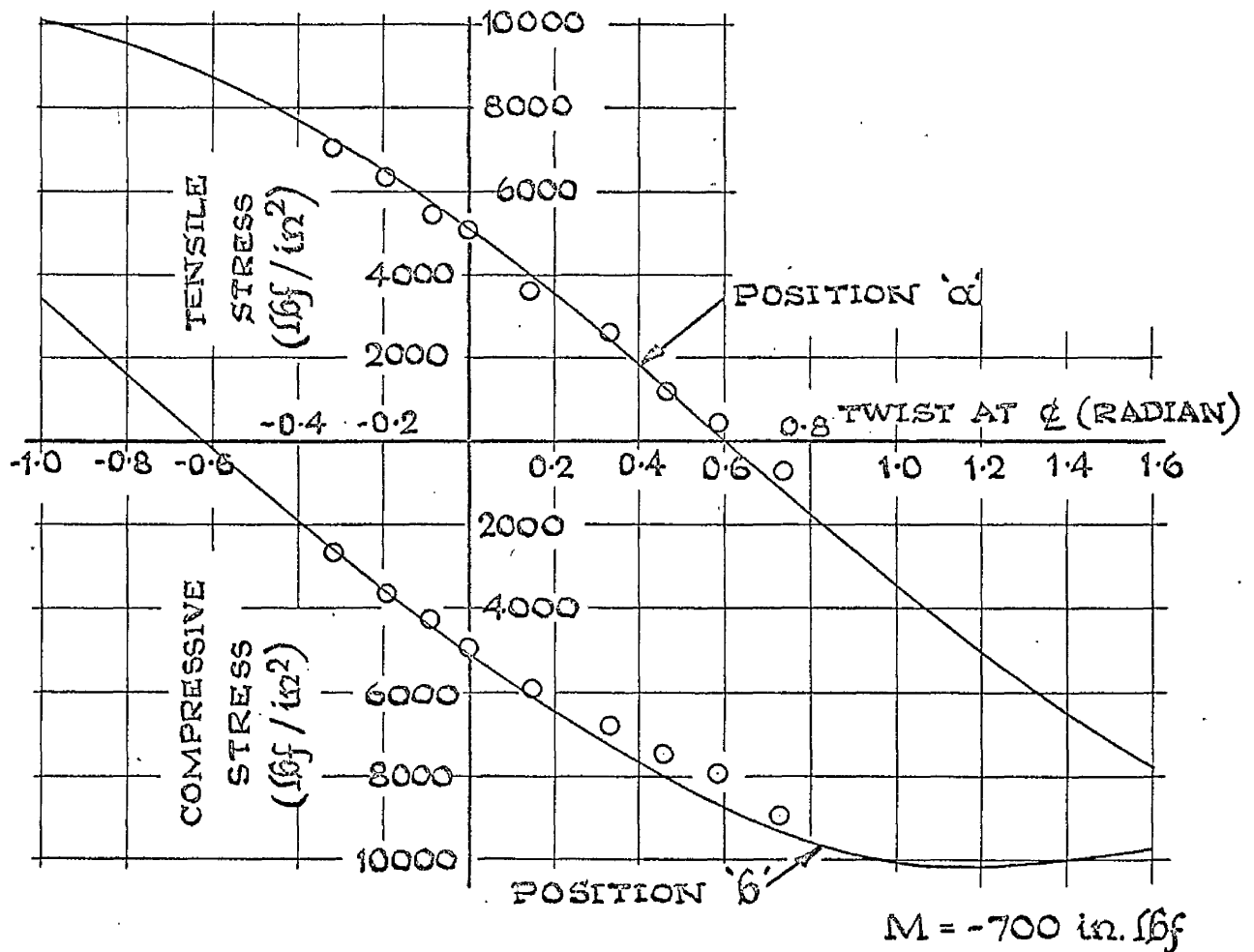
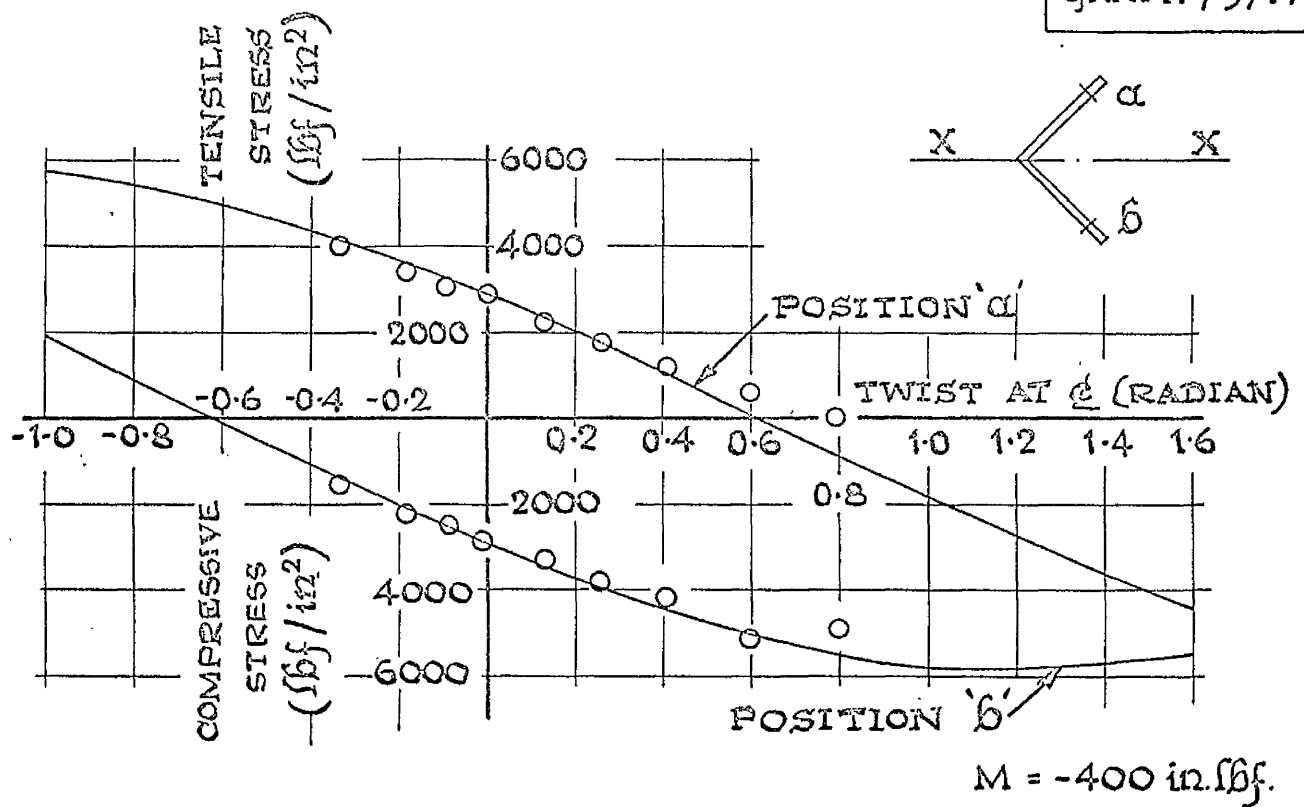


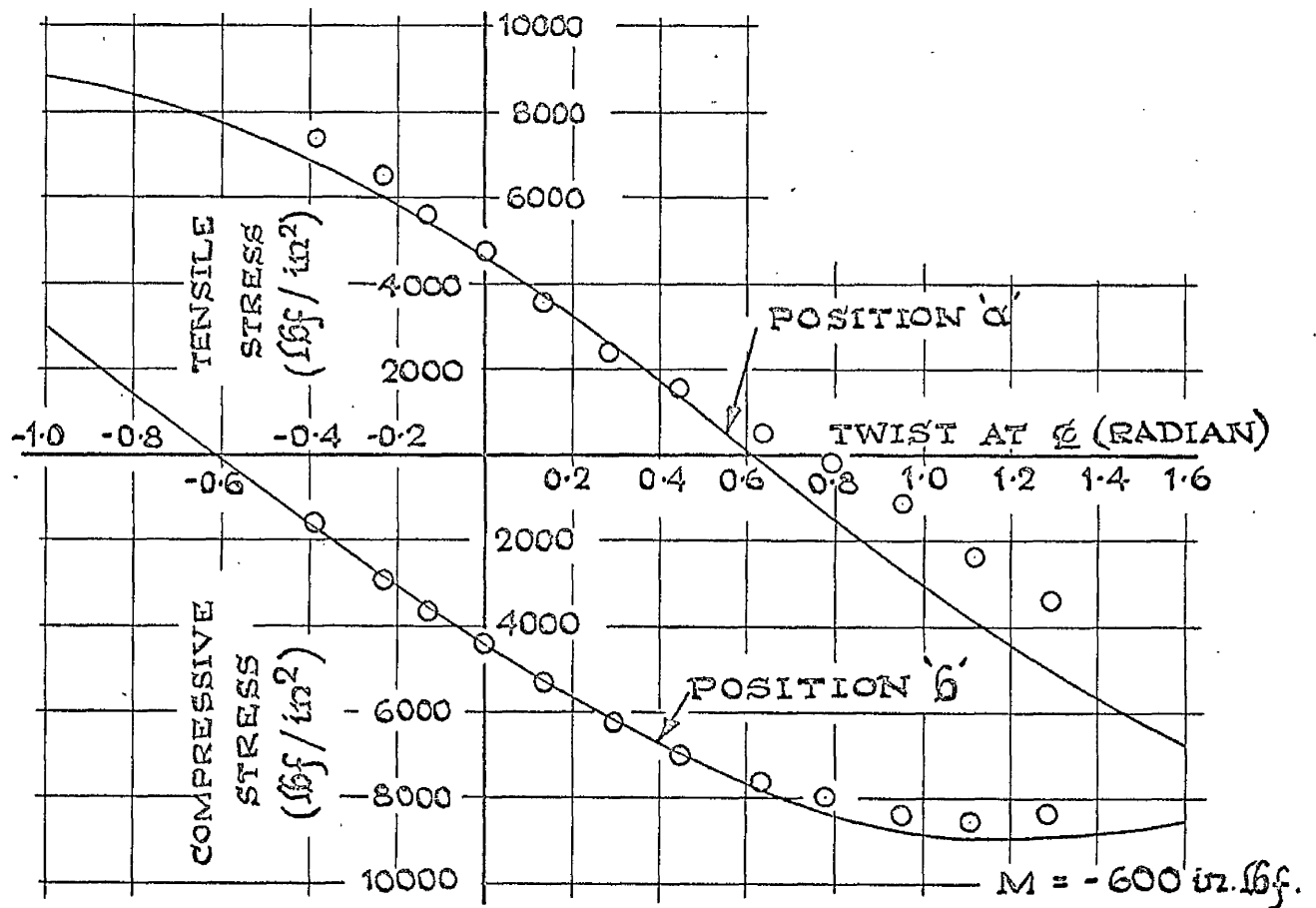
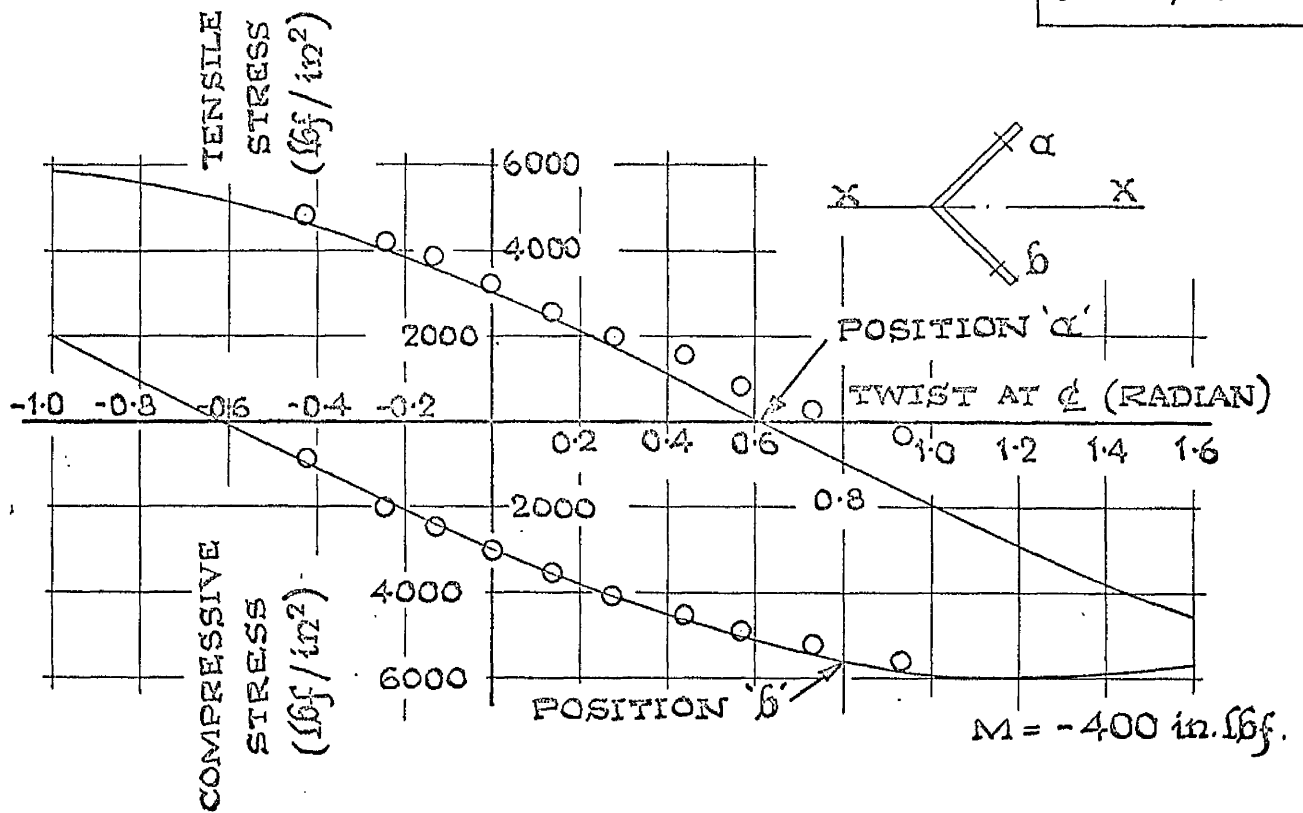
FIG IV.17. VARIATION OF LONGITUDINAL STRESS WITH ANGLE OF TWIST. (SPECIMEN A3).



VARIATION OF LONGITUDINAL STRESS
WITH ANGLE OF TWIST (SPECIMEN B1.)



VARIATION OF LONGITUDINAL STRESS WITH ANGLE OF TWIST. (SPECIMEN C.1.)



VARIATION OF LONGITUDINAL STRESS
WITH ANGLE OF TWIST. (SPECIMEN C2.)

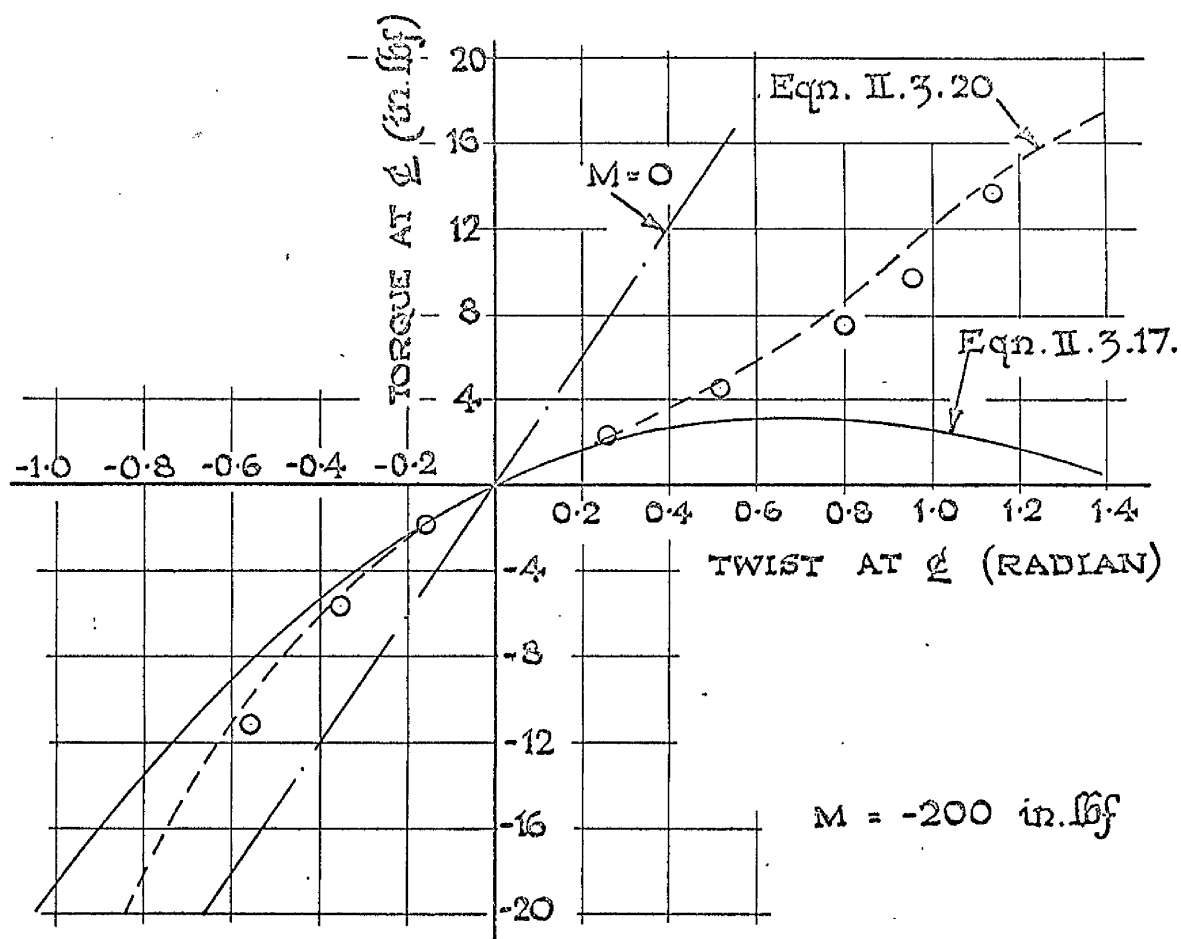
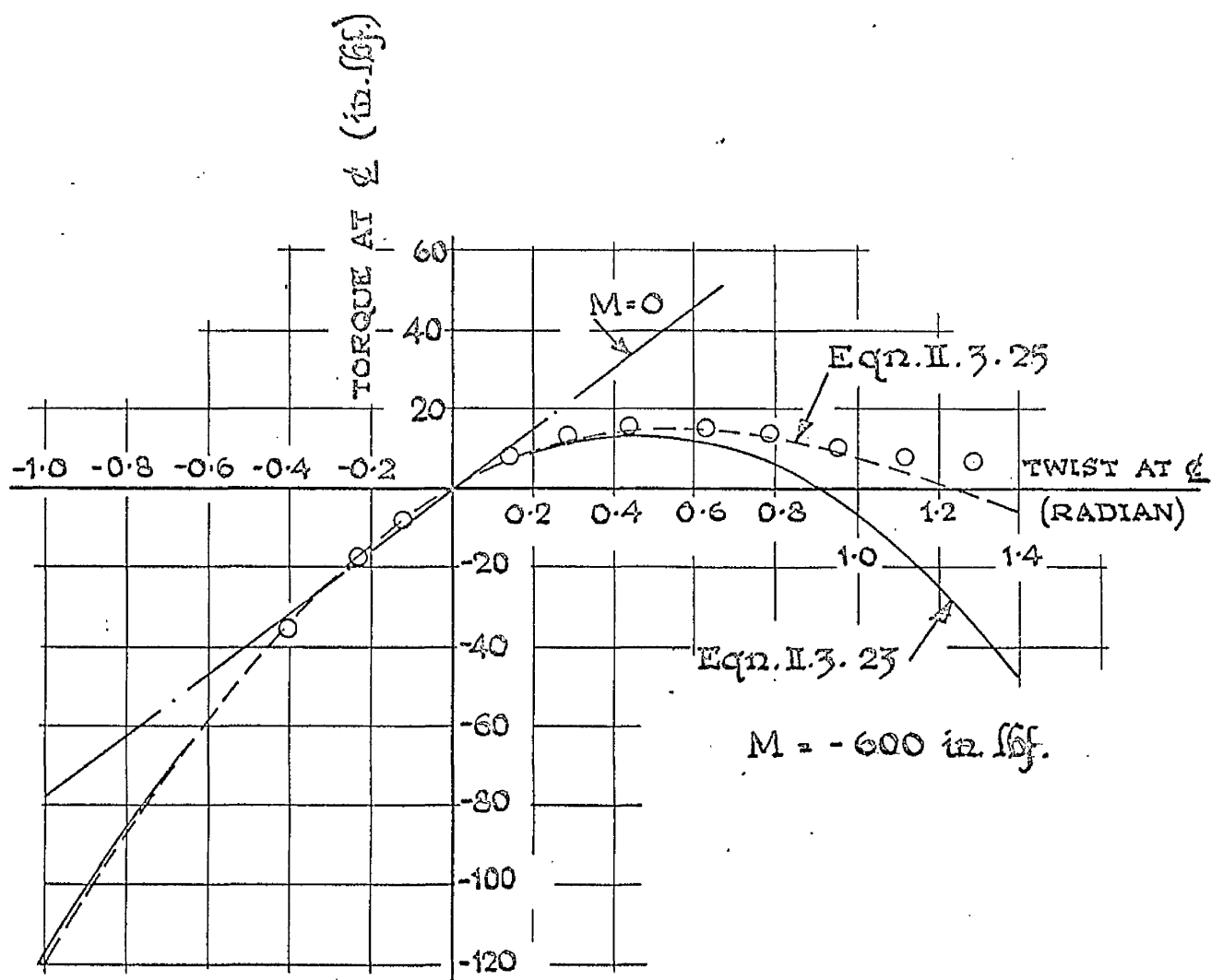


FIG. IV.12. TORQUE / ANGLE OF TWIST EQUILIBRIUM PATHS - COMPARISON OF SOLUTIONS FOR ONE AND TWO TERMS OF SINE AND COSINE SERIES (SPECIMEN A.1.)



TORQUE / ANGLE OF TWIST EQUILIBRIUM PATHS
 - COMPARISON OF SOLUTIONS FOR ONE AND
 TWO TERMS OF SINE AND COSINE SERIES
 (SPECIMEN C.2.)

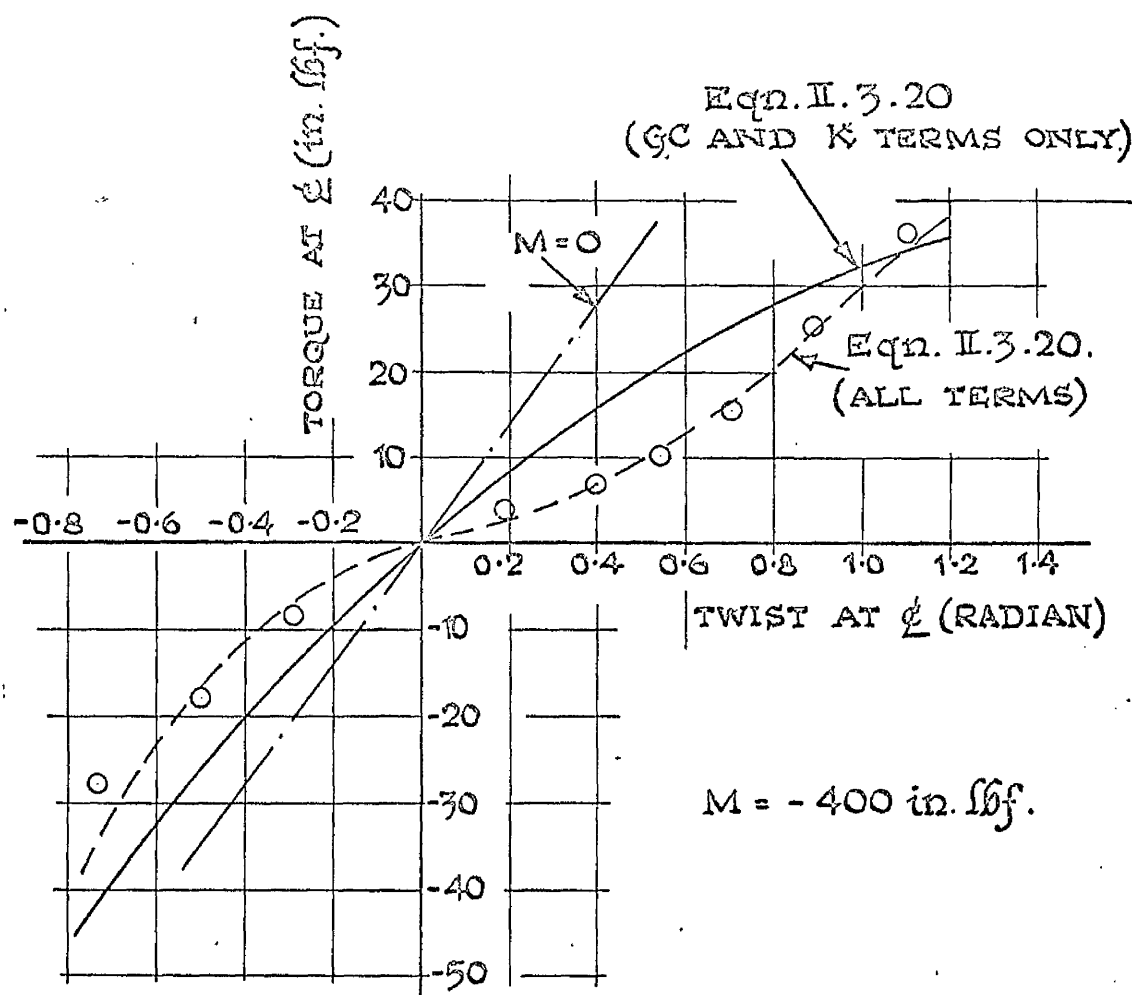
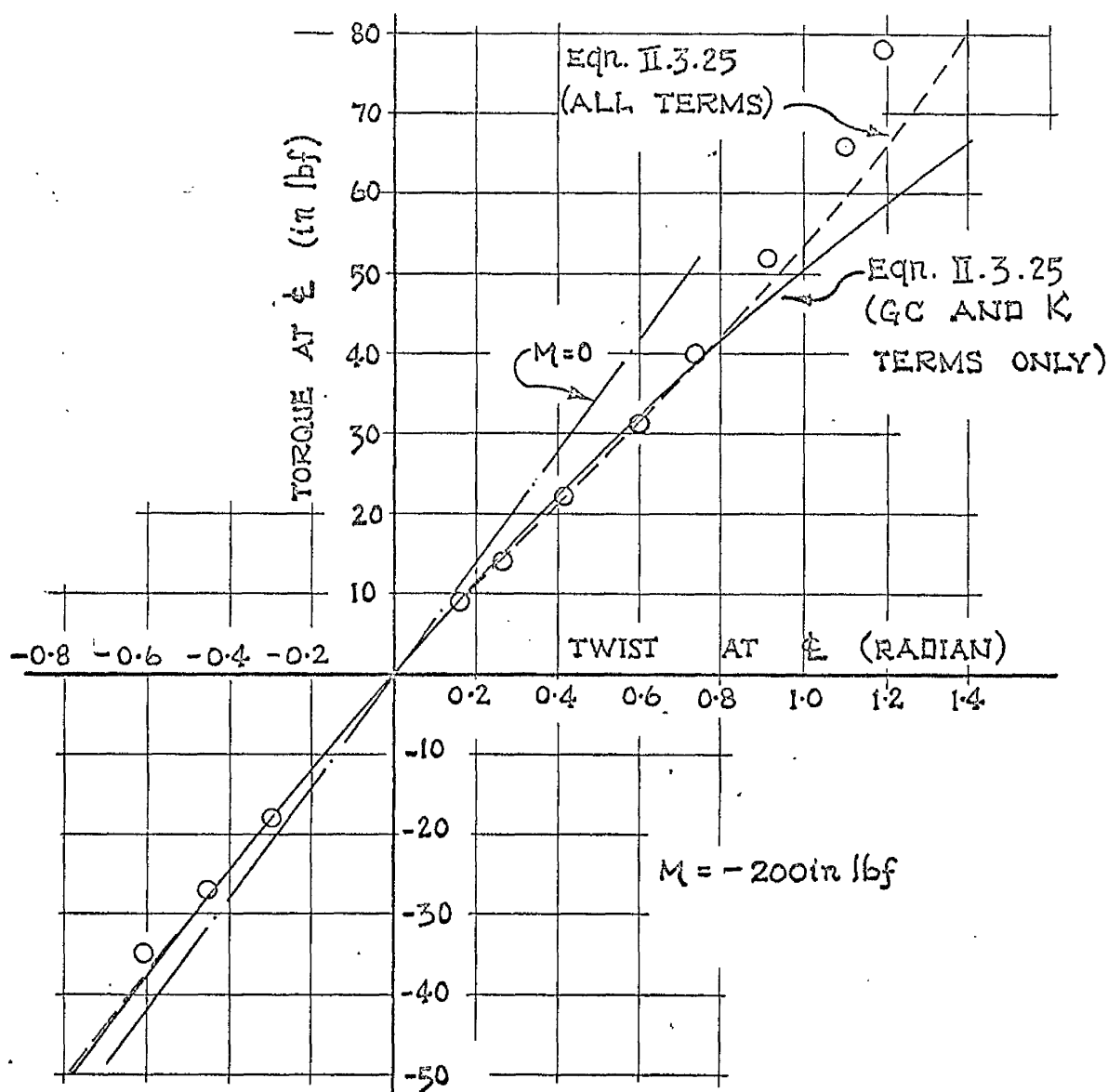


FIG. IV. 13. TORQUE / ANGLE OF TWIST EQUILIBRIUM PATHS - COMPARISON OF THEORETICAL SOLUTIONS WITH AND WITHOUT ALL ADDITIONAL EFFECTS. (SPECIMEN A.3)



TORQUE / ANGLE OF TWIST EQUILIBRIUM
 PATHS - COMPARISON OF THEORETICAL
 SOLUTIONS WITH AND WITHOUT ALL
 ADDITIONAL EFFECTS (SPECIMEN A.3)

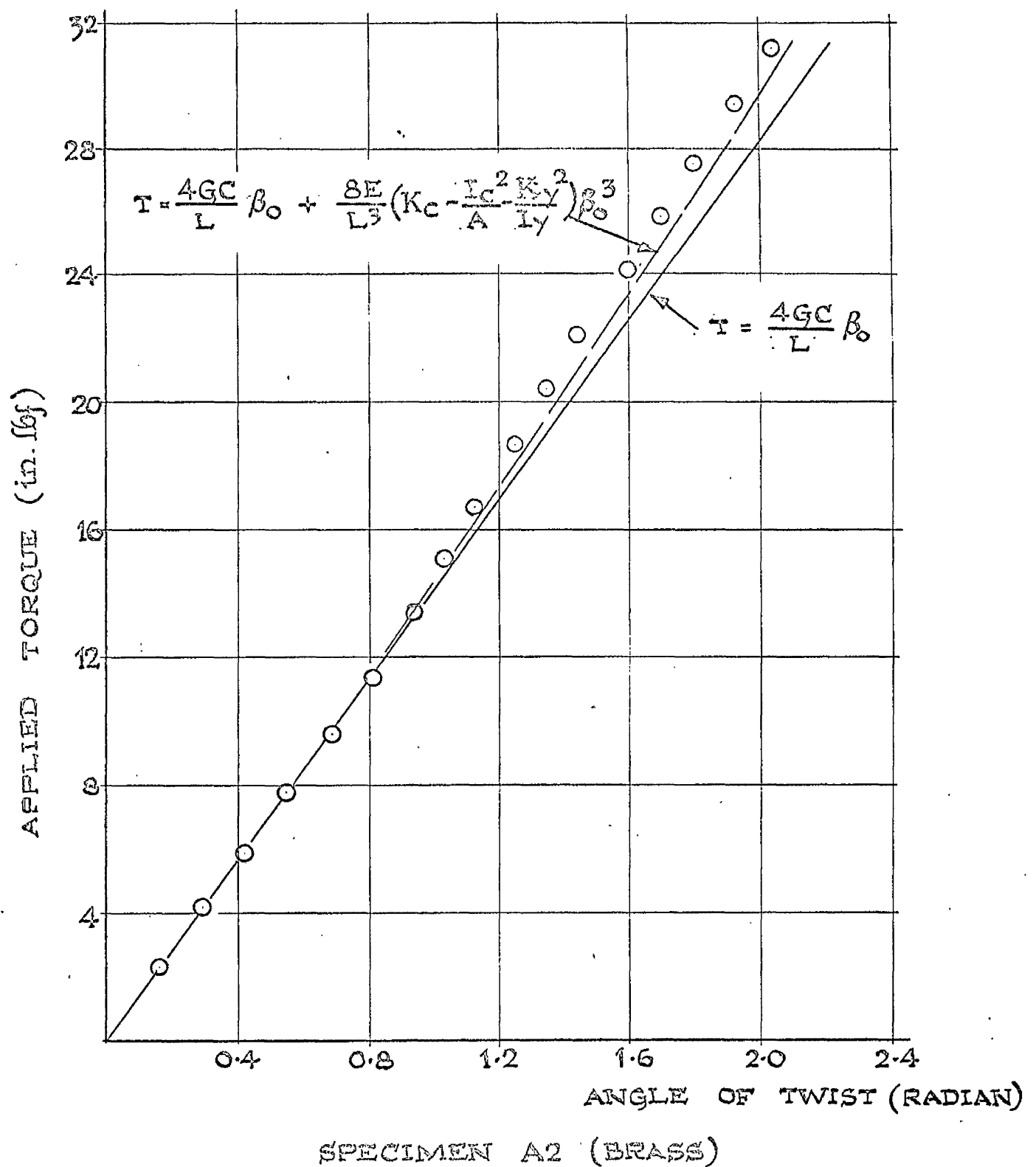
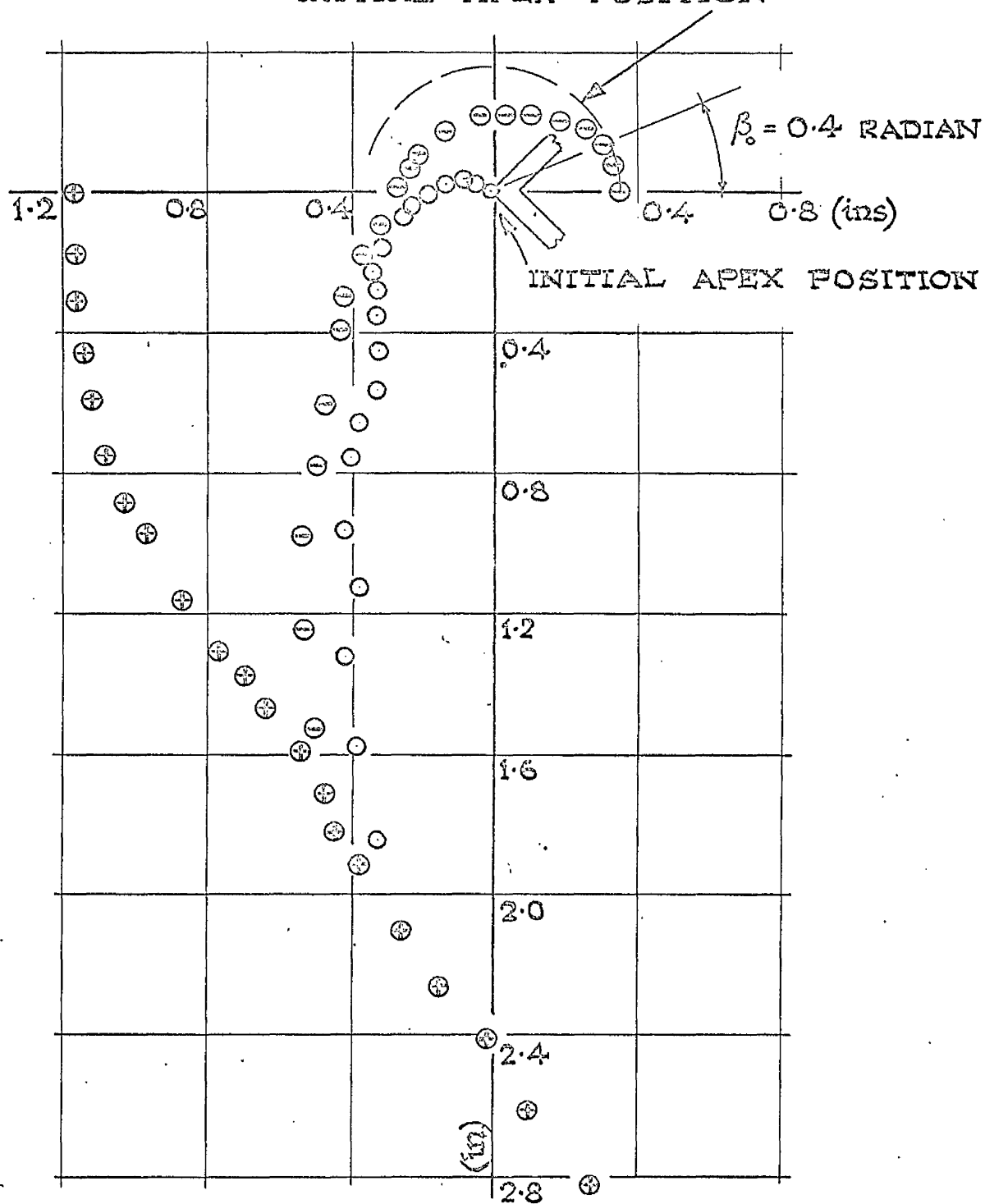


FIG. IV. 14. TORQUE / ANGLE OF TWIST
EQUILIBRIUM PATHS AT MID-SPAN
SECTION FOR APPLIED TORQUE ONLY

⊕ DISC PIN

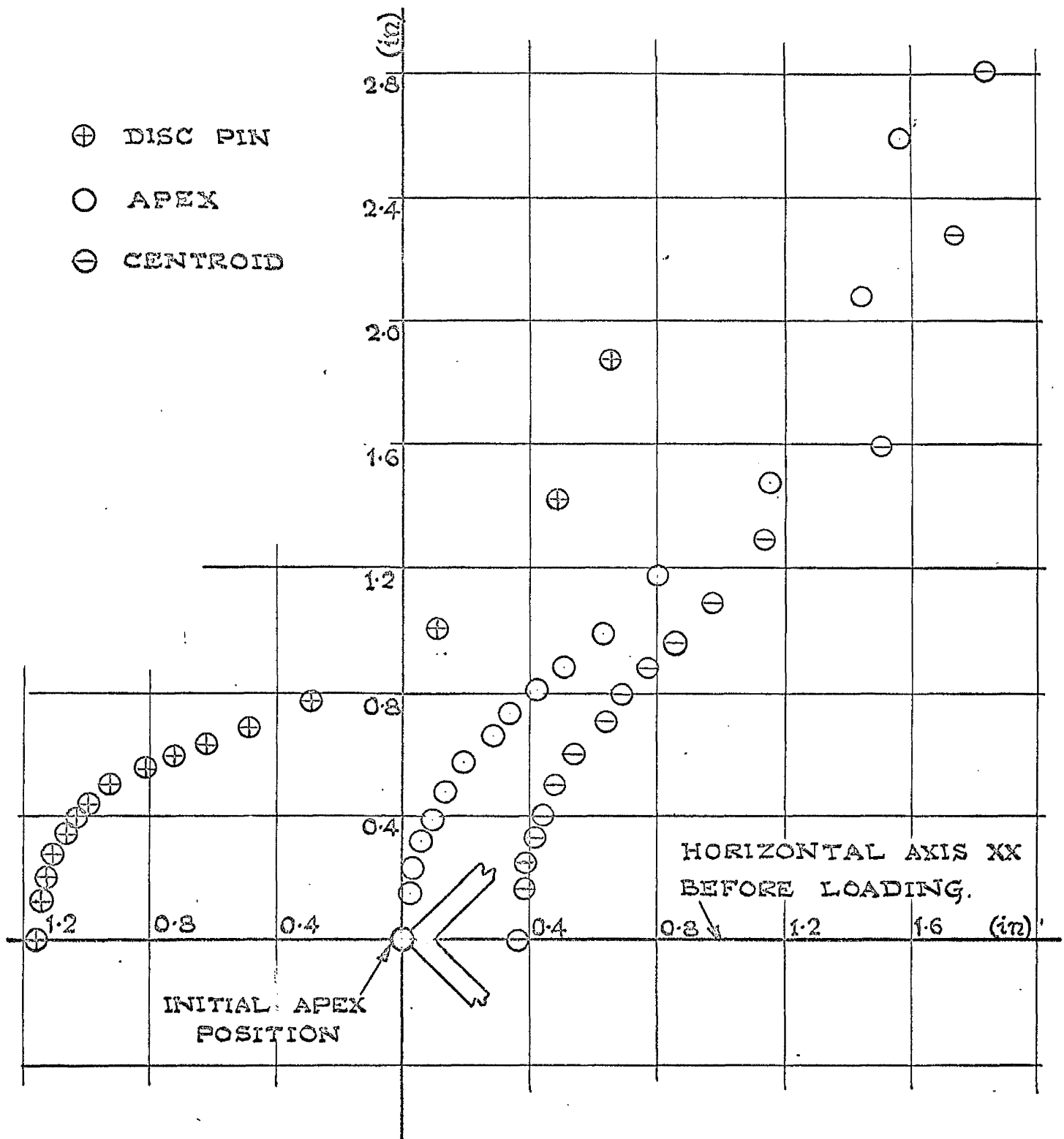
○ APEX

⊖ CENTROID

CENTROID PATH FOR
CENTRE OF TWIST AT
INITIAL APEX POSITION

SPECIMEN A2 (BRASS)

FIG. IV. 16. DISC PIN AND ANGLE APEX
AND CENTROID PATH AT MID-
SPAN FOR APPLIED TORQUE ONLY



SPECIMEN A1.

PATHS FOLLOWED BY DISC PIN AND ANGLE
APEX AND CENTROID DURING TEST TO FAILURE

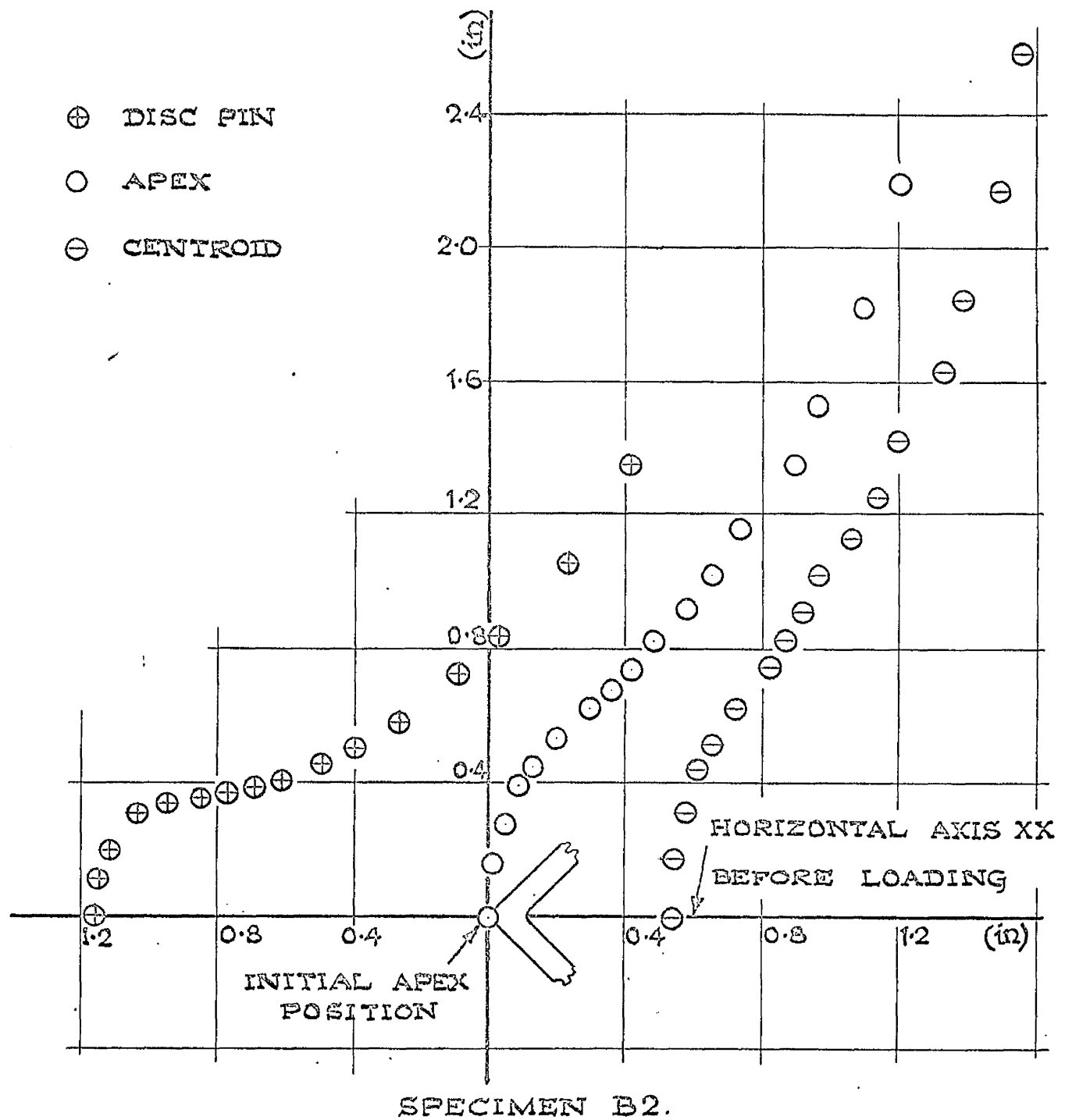
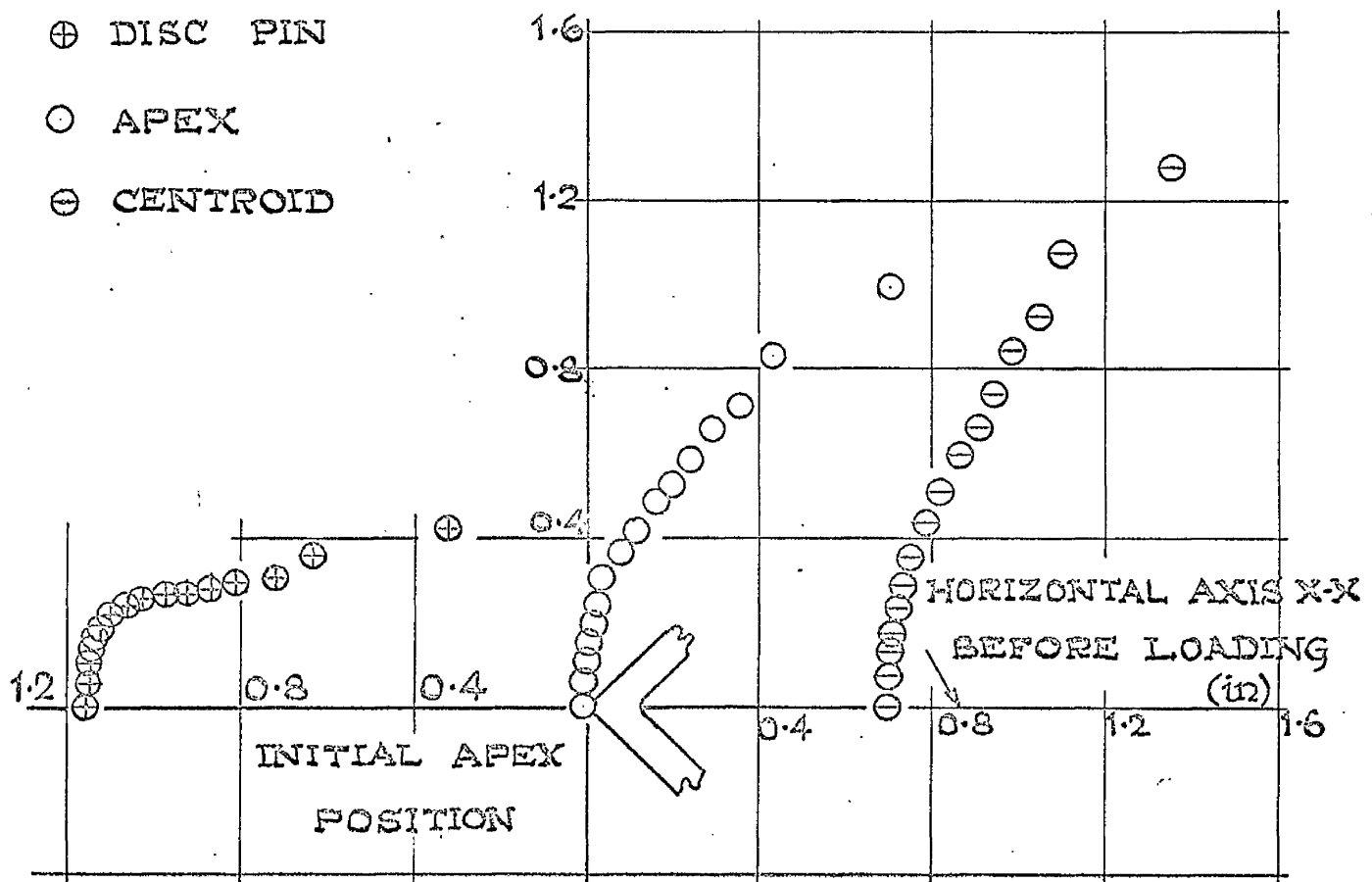


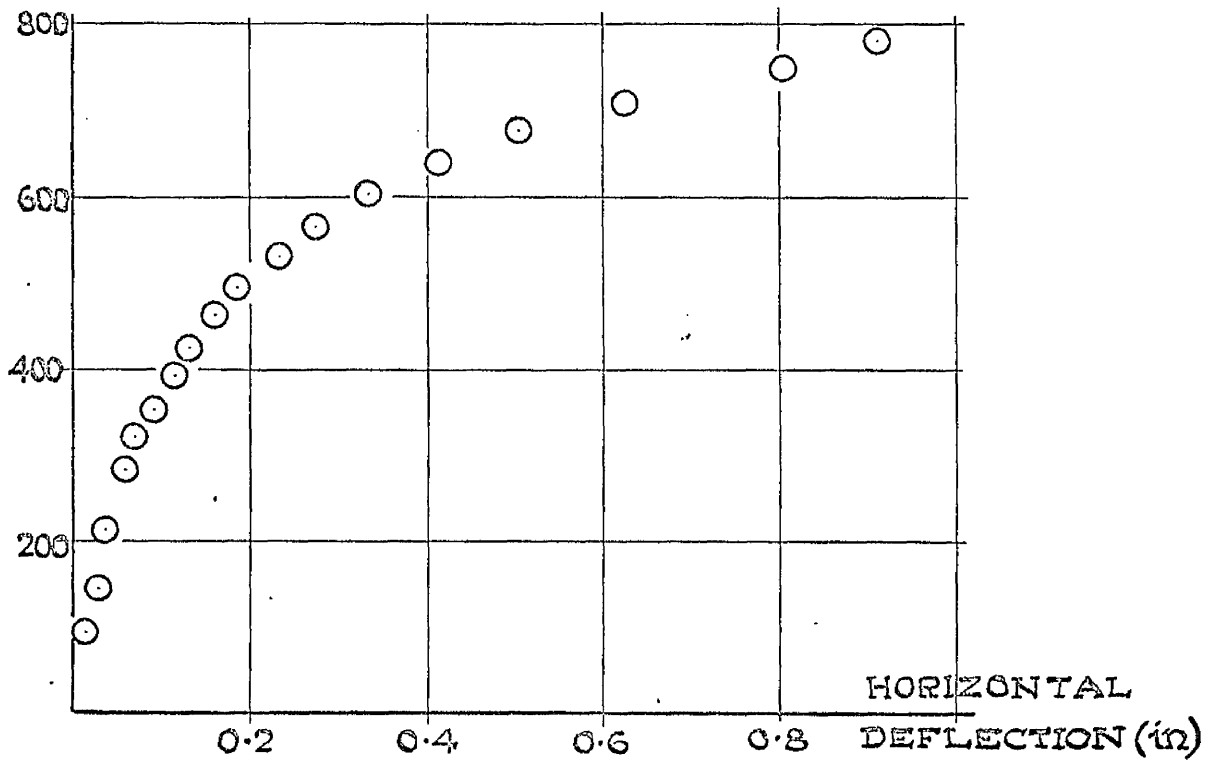
FIG. IV. 18. PATHS FOLLOWED BY DISC PIN AND
ANGLE APEX AND CENTROID DURING
TEST TO FAILURE.



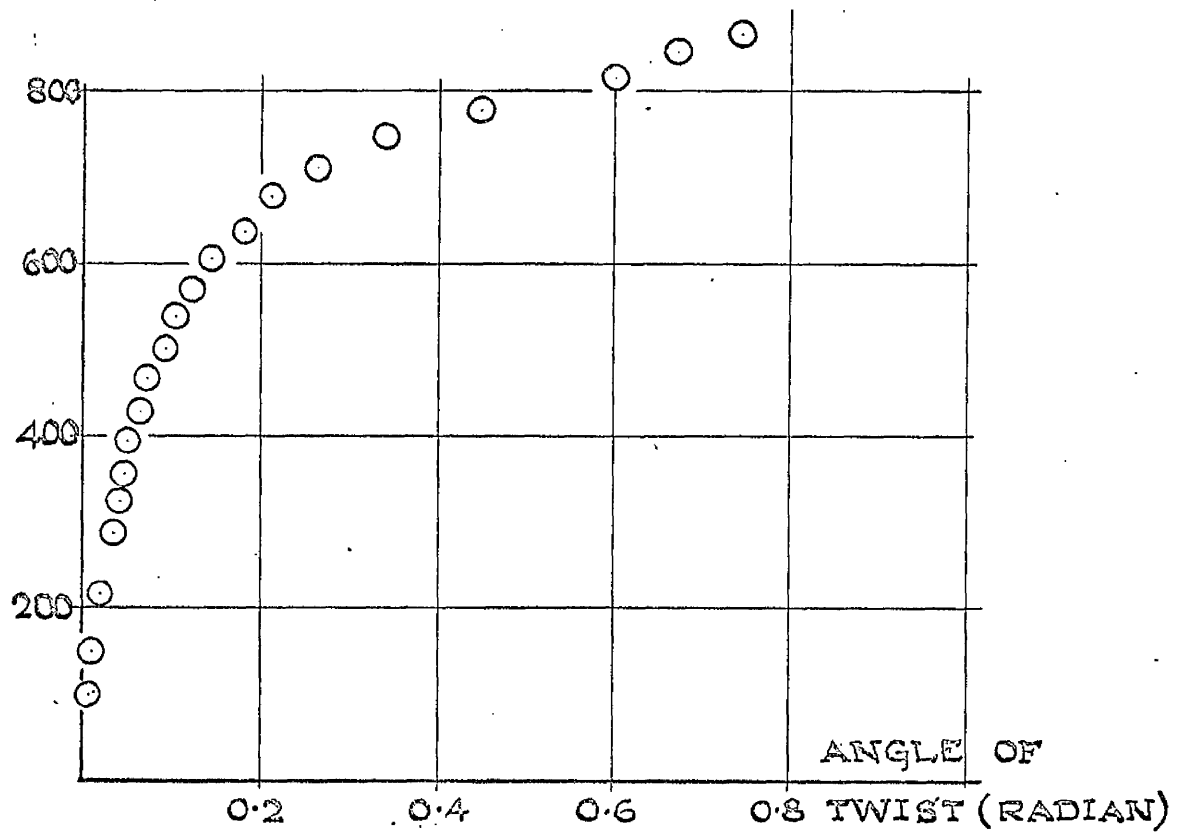
SPECIMEN C1.

PATHS FOLLOWED BY DISC PIN AND
ANGLE APEX AND CENTROID DURING
TEST TO FAILURE.

BENDING MOMENT (in. lbf.)



BENDING MOMENT (in. lbf.)



SPECIMEN A.1.

APPROXIMATE RECTANGULAR HYPERBOLIC
RELATIONSHIPS $M \propto \delta H$ AND $M \propto \delta \beta$.

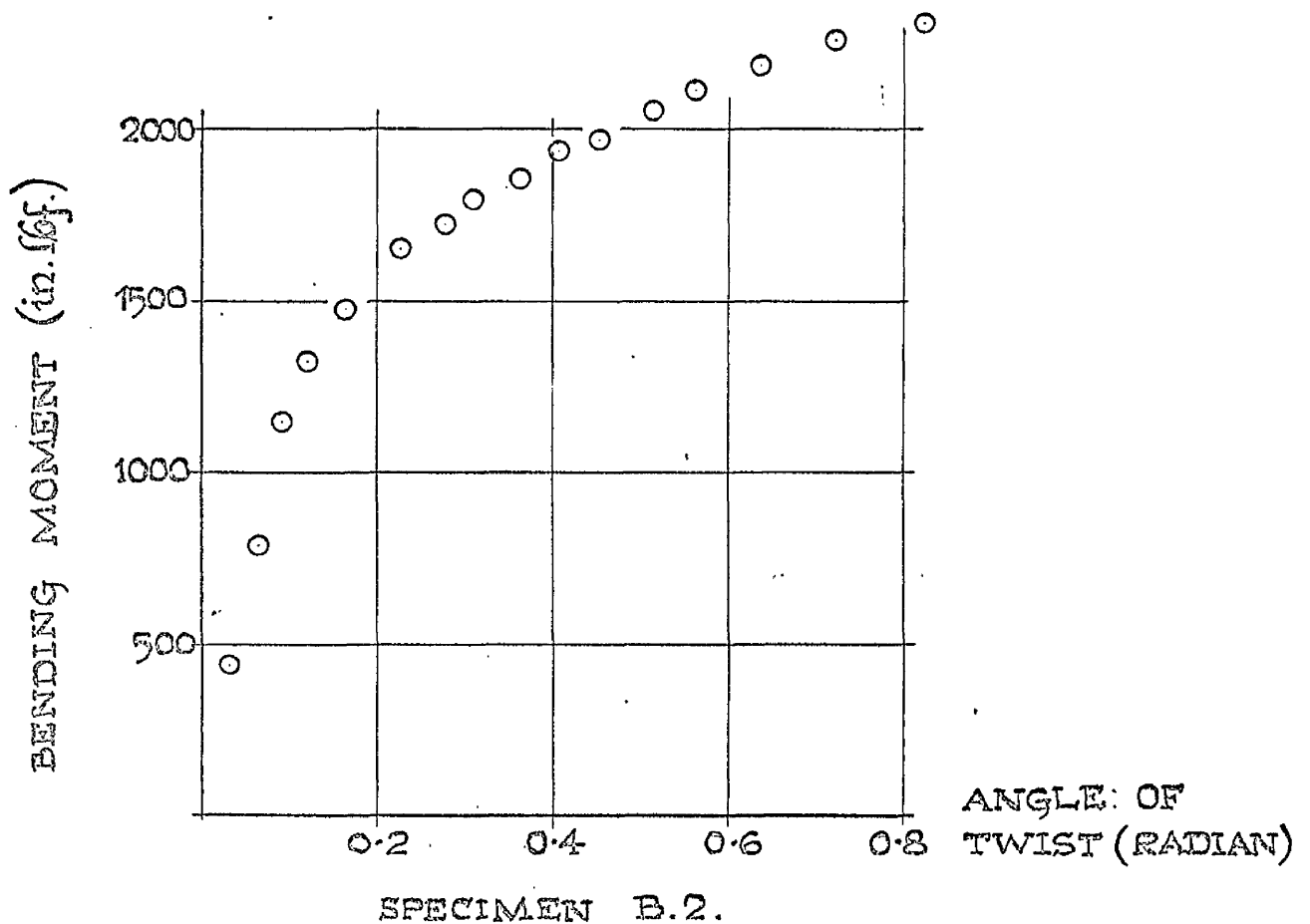
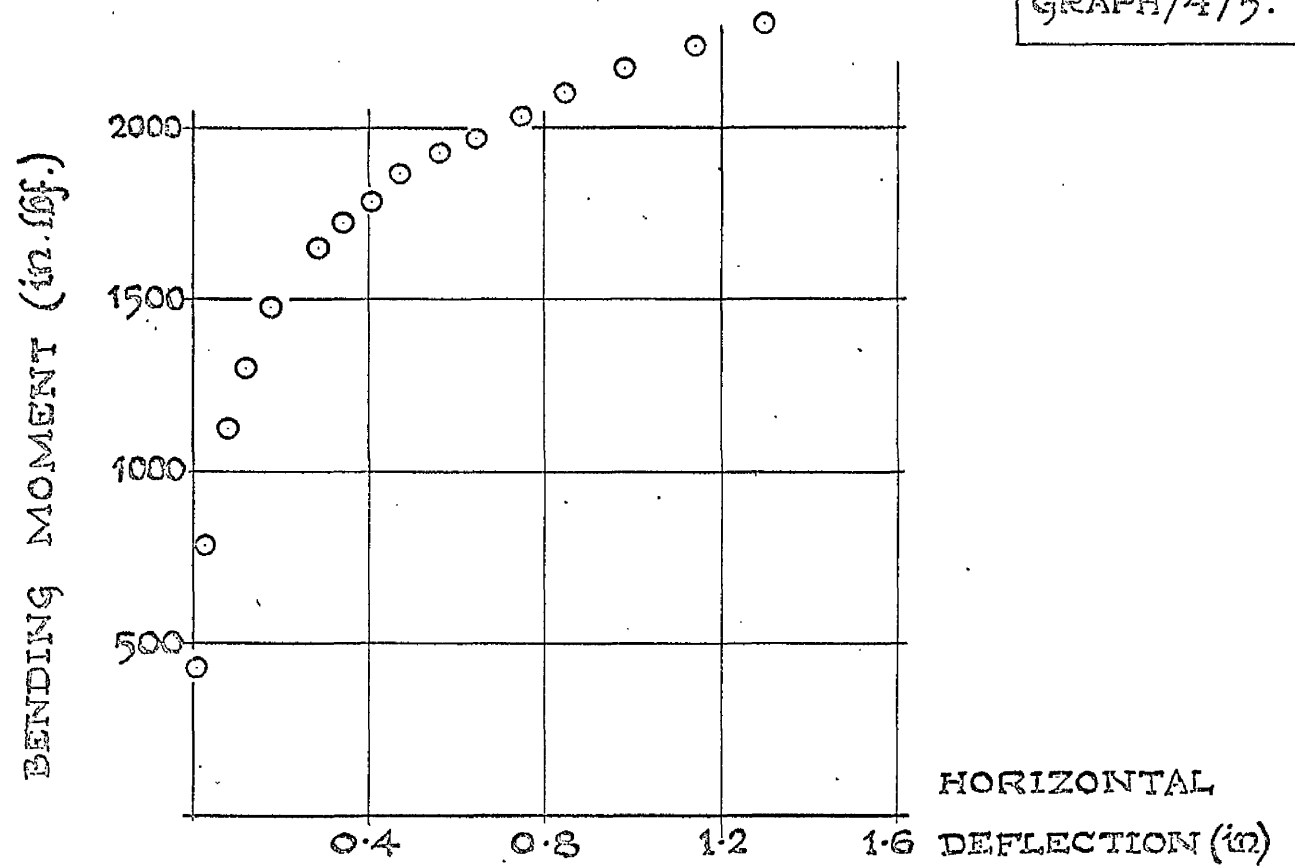
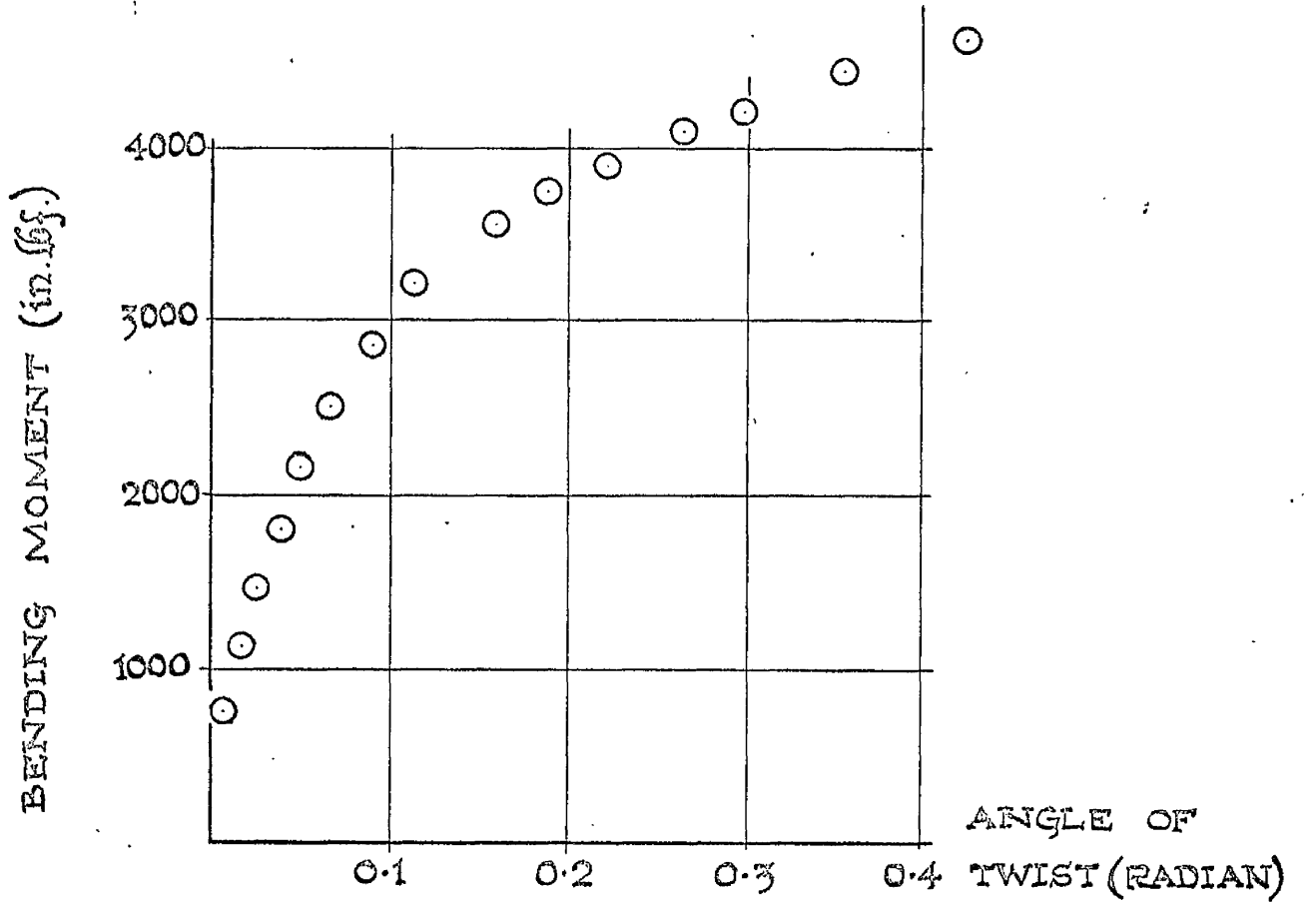
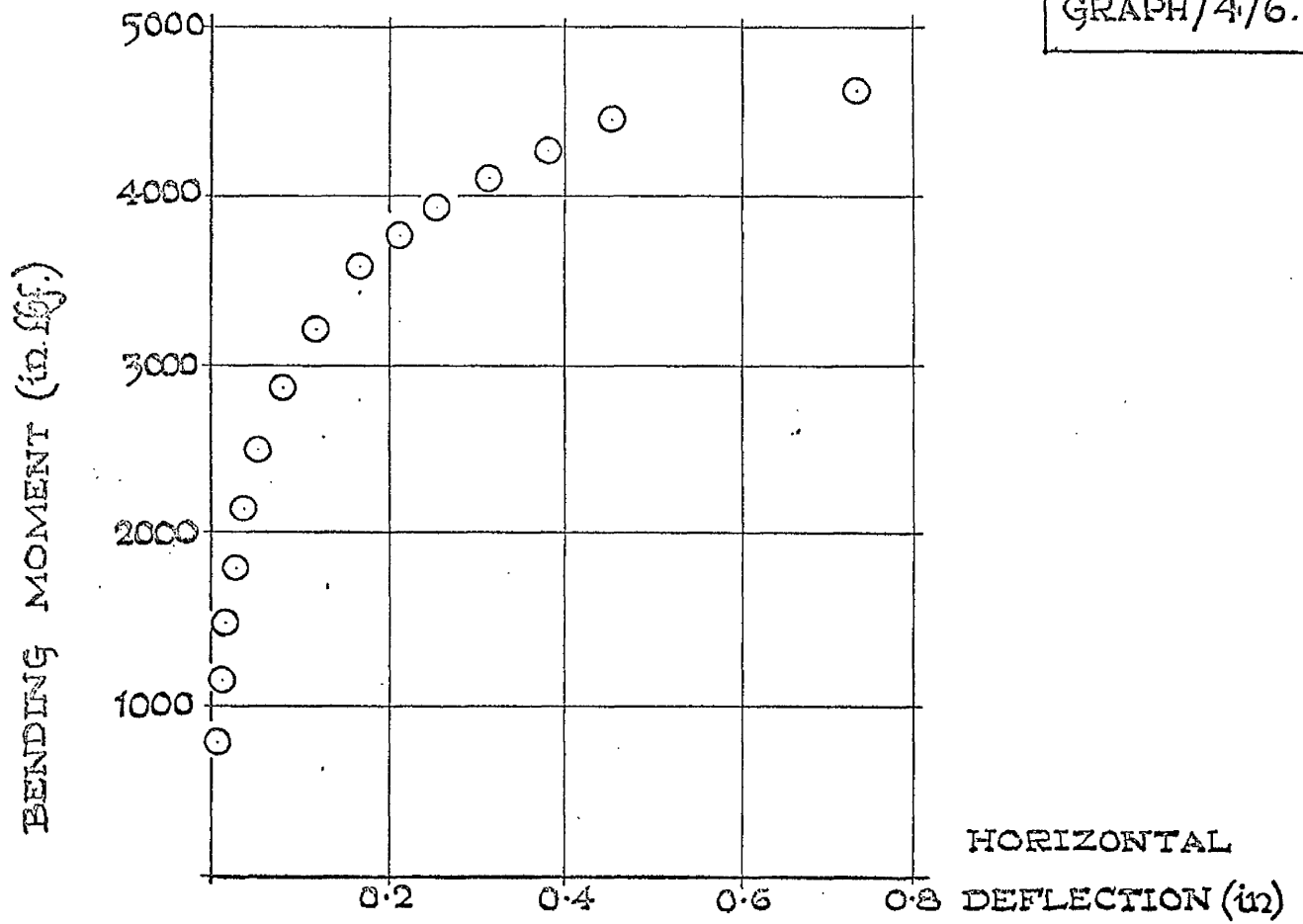
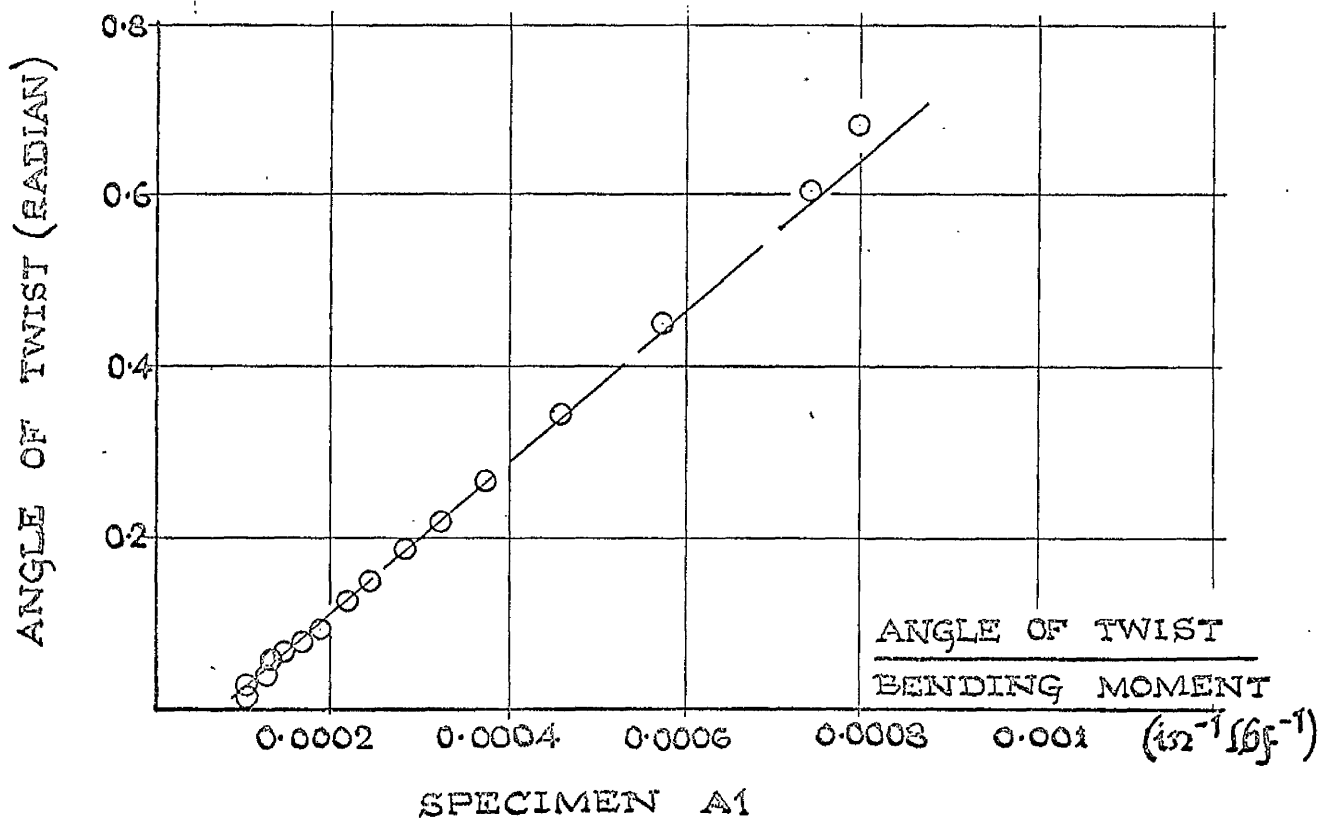
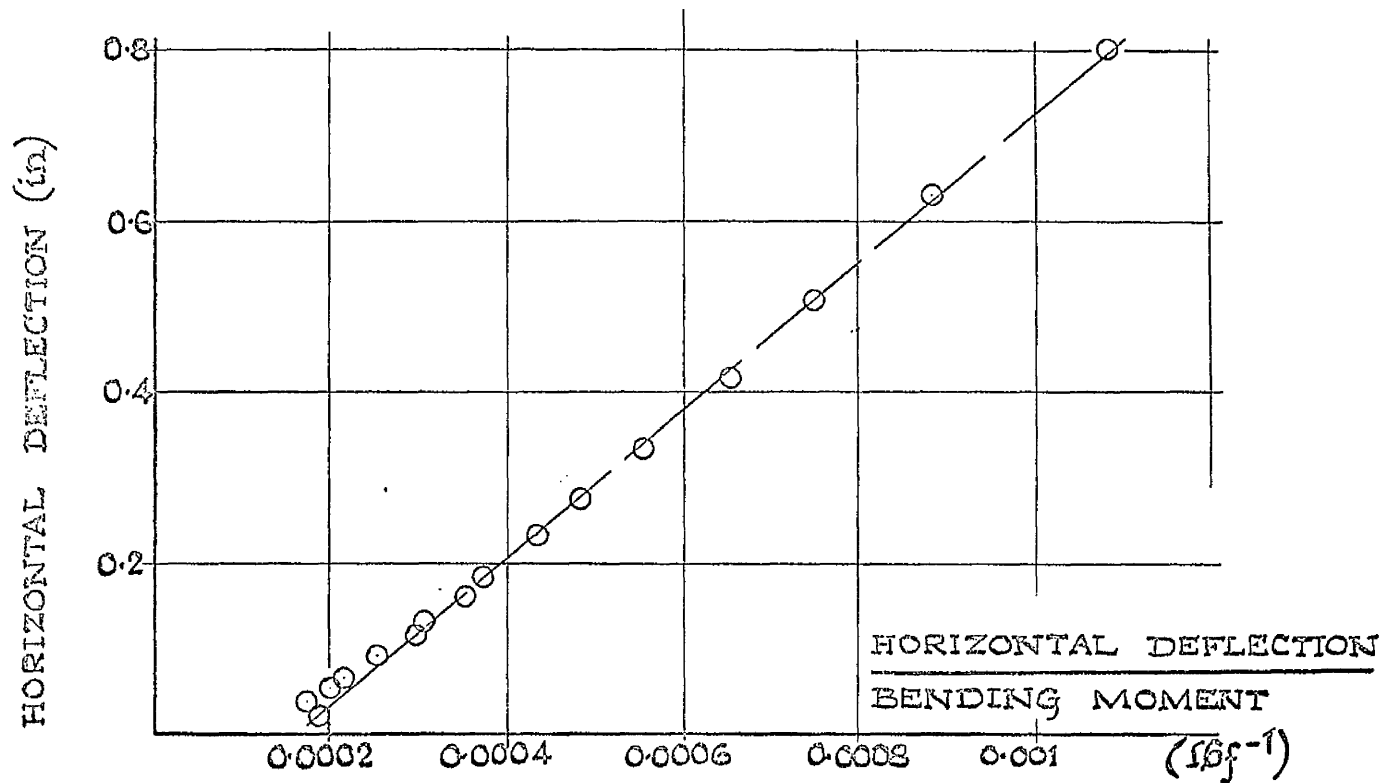


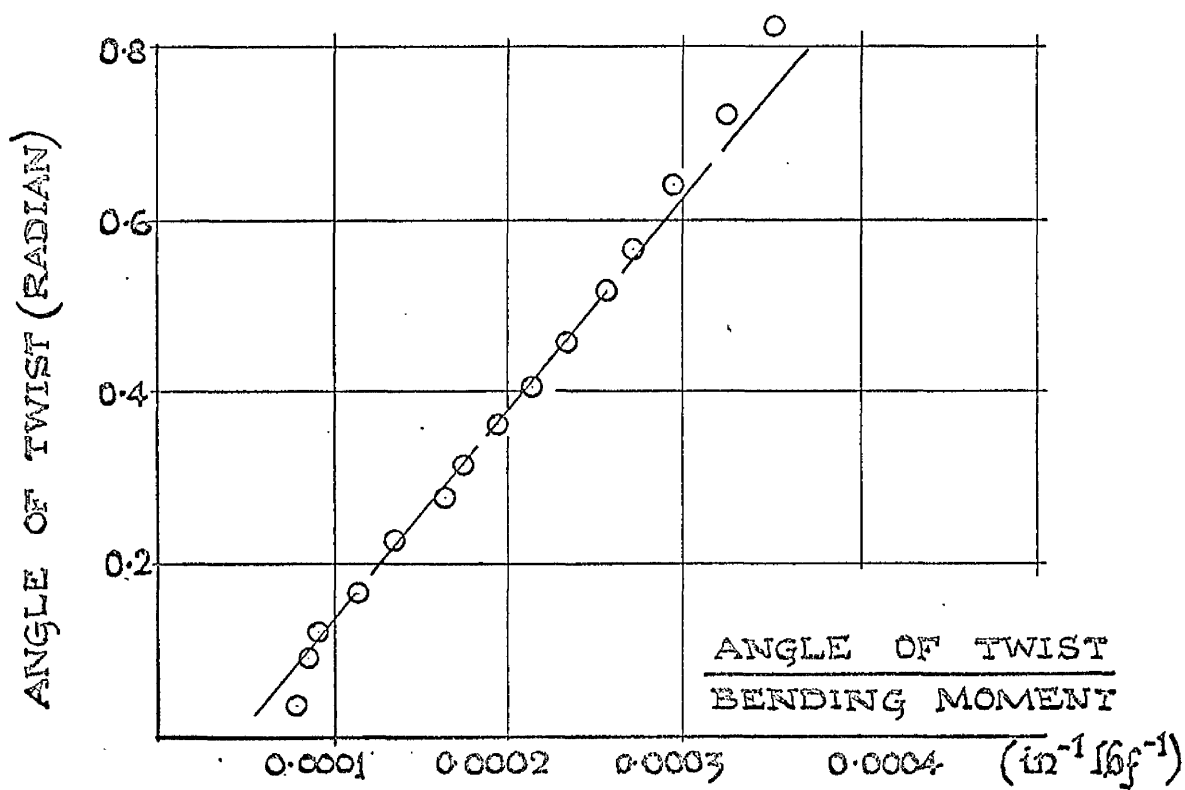
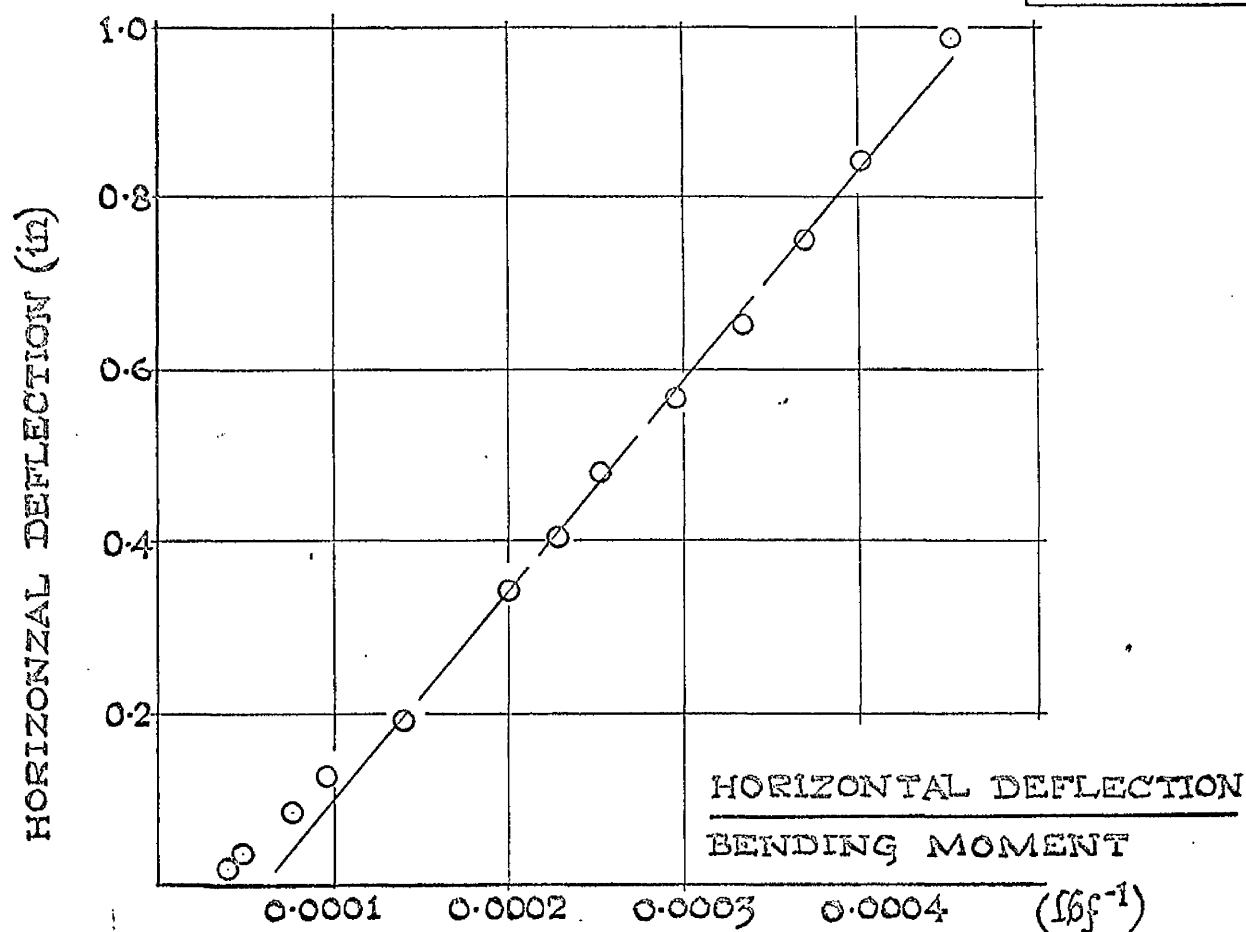
FIG. IV. 19. APPROXIMATE RECTANGULAR HYPERBOLIC RELATIONSHIPS $M \propto \delta H$ AND $M \propto \delta \beta$



SPECIMEN C.1.
APPROXIMATE RECTANGULAR HYPERBOLIC
RELATIONSHIPS $M \propto \delta H$ AND $M \propto \delta \beta$.

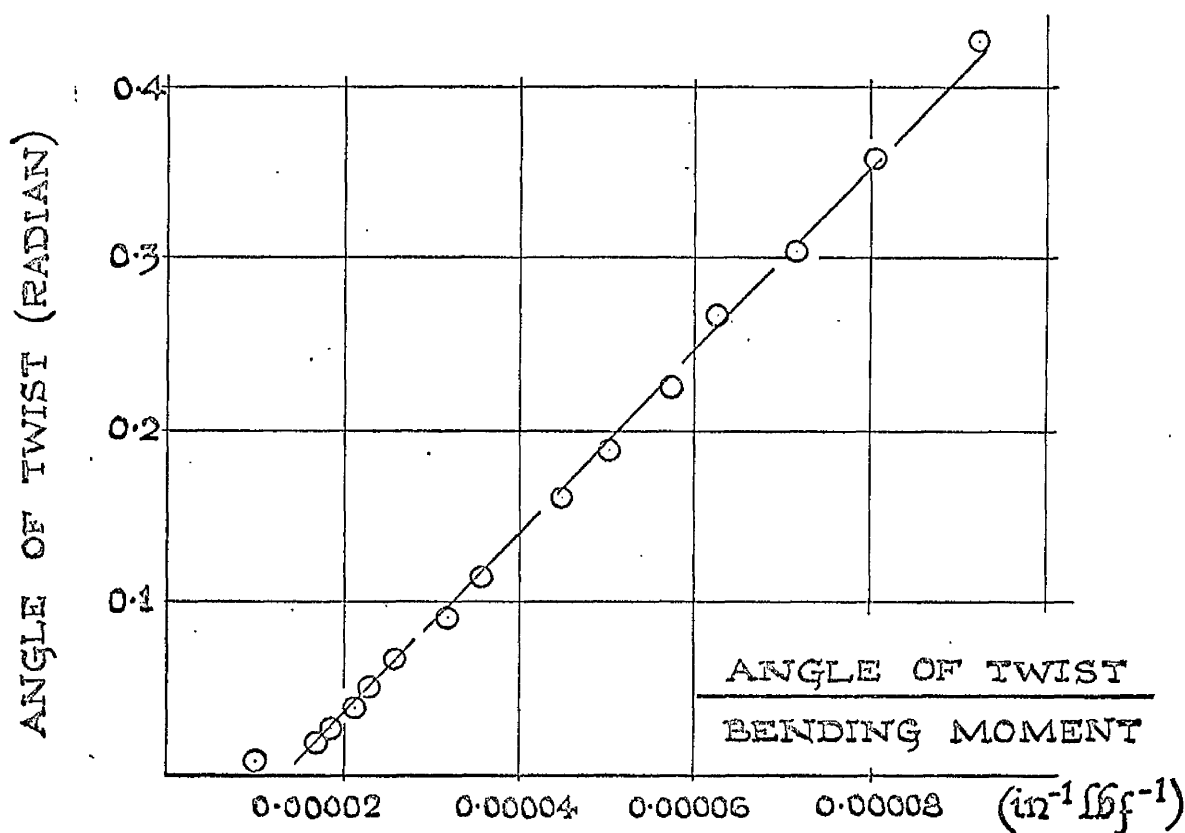
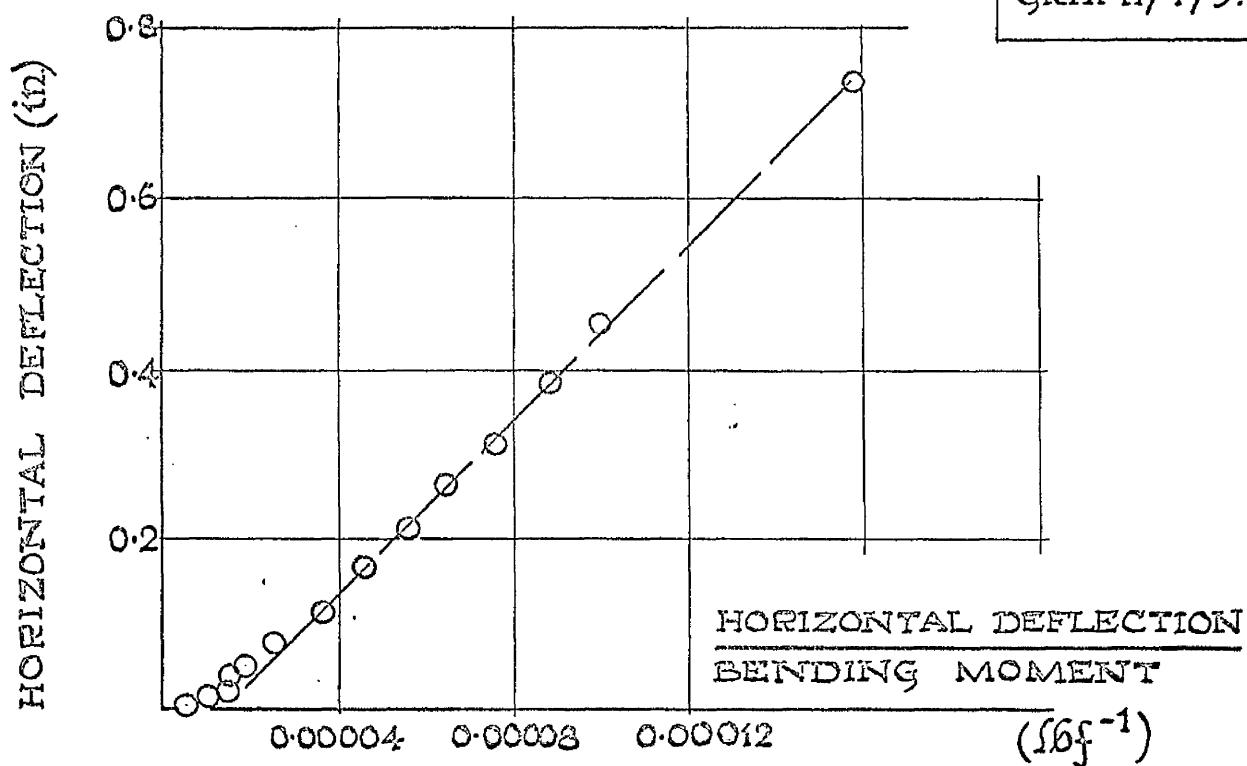


SOUTHWELL INVERSE PLOTS
 $\delta H \propto \delta H/M$ AND $\delta \beta \propto \delta \beta/M$.



SPECIMEN B2.

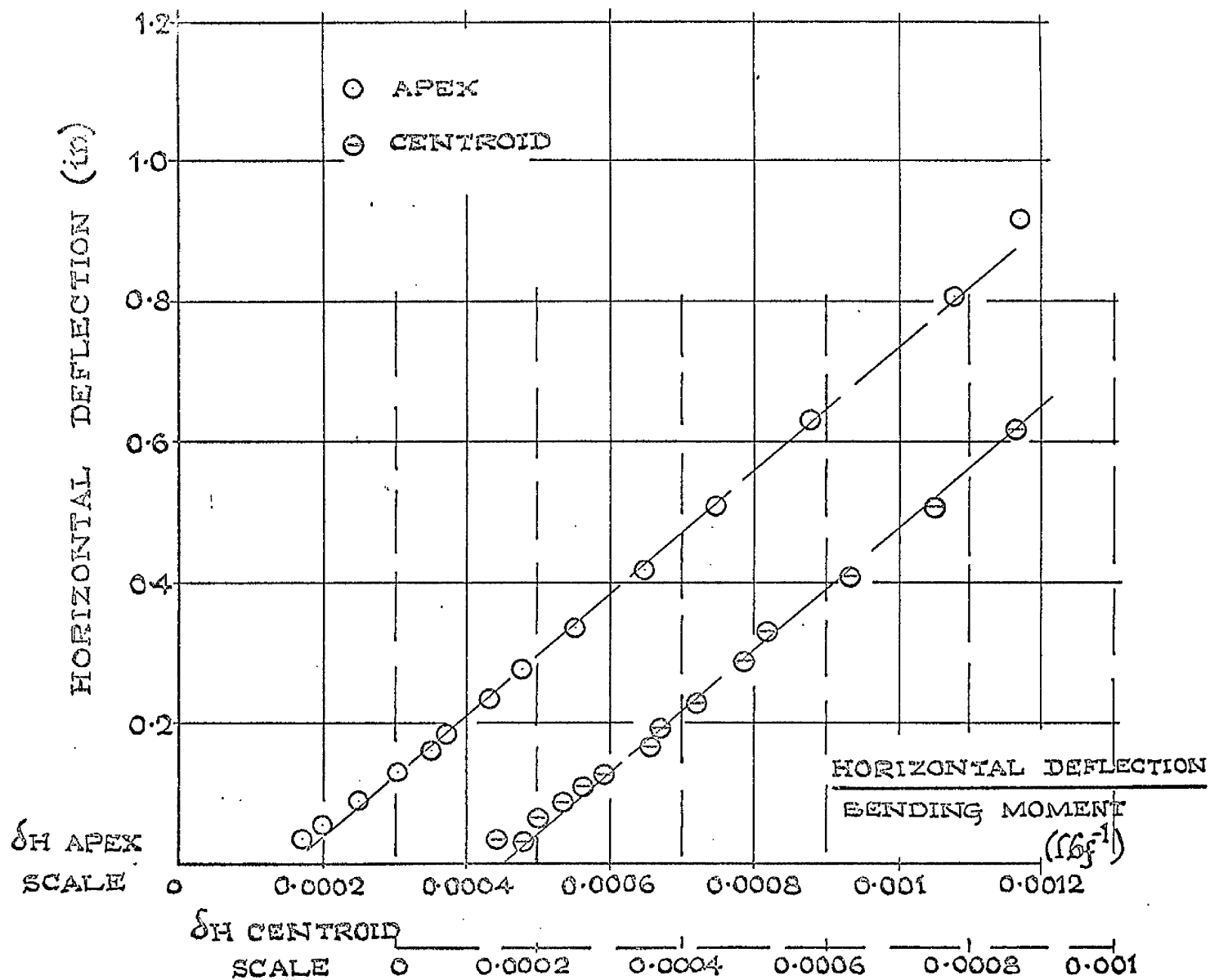
FIG. IV. 20. SOUTHWELL INVERSE PLOTS
 $\delta H \propto \delta H/M$ AND $\delta \beta \propto \delta \beta/M$.



SPECIMEN C.1

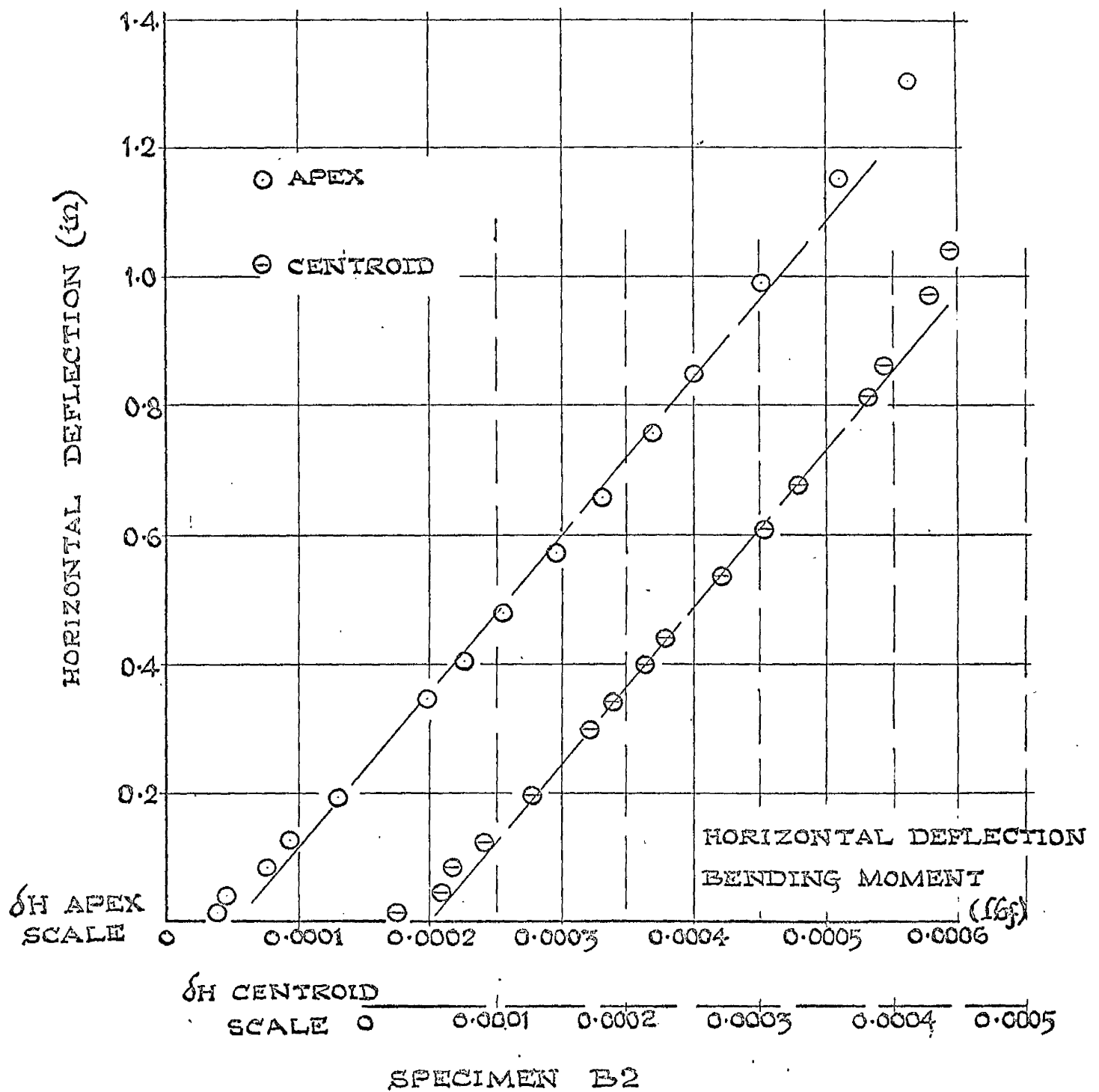
SOUTHWELL INVERSE PLOTS.

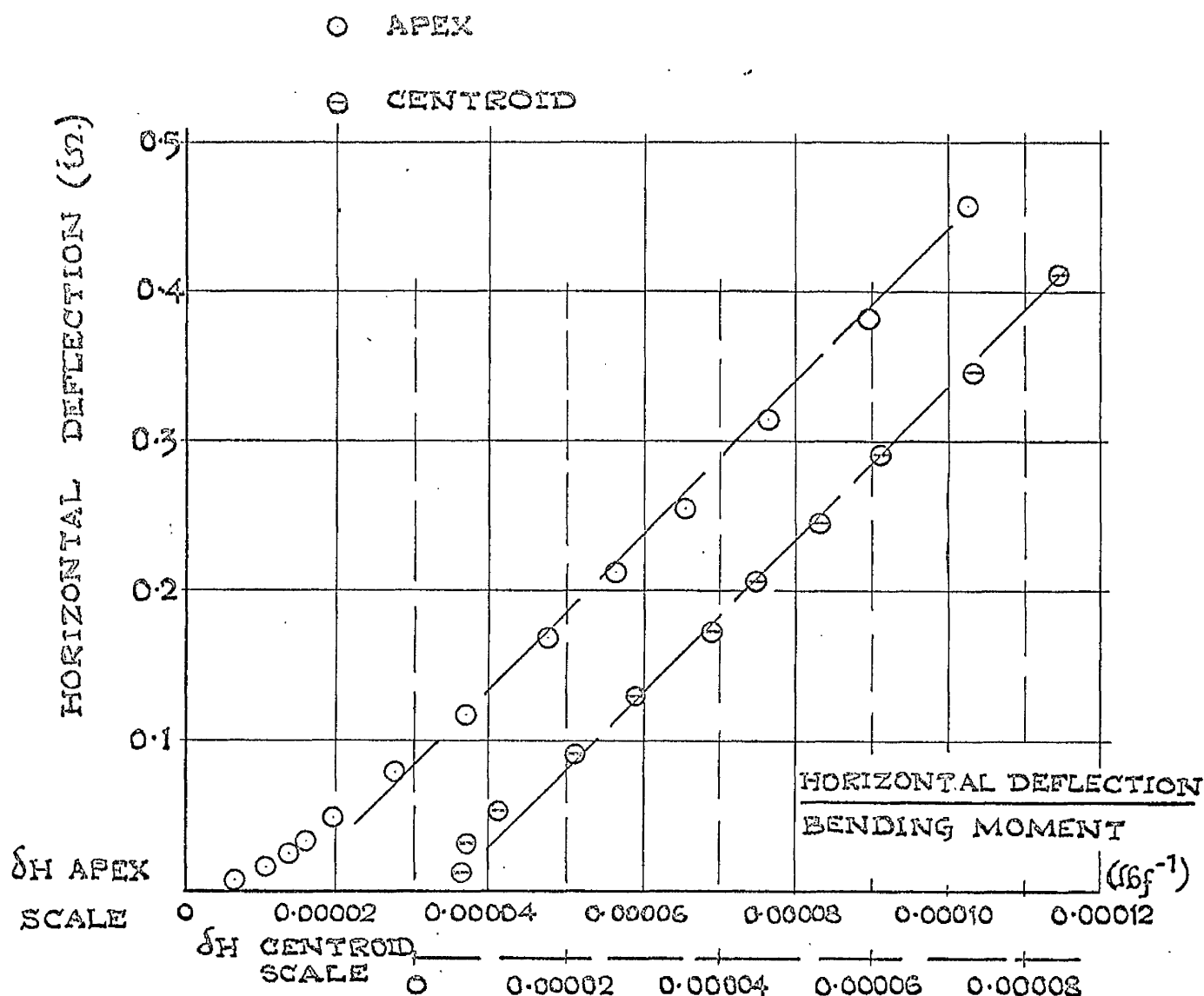
$\delta H \propto \delta H/M$ AND $\delta \beta \propto \delta \beta/M$.



SPECIMEN A1.

SOUTHWELL INVERSE PLOTS FOR δH &
 $\delta H/M$ USING δH -APEX AND δH -CENTROID





SPECIMEN C1.

SOUTHWELL INVERSE PLOTS FOR δH & $\delta H/M$
USING δH - APEX AND δH - CENTROID.

APPENDIX VIII.6Suggested Safe Load Table for Thin Walled Channel Sections

LOADS GIVEN IN lbf/ft

SECTION		SPANS IN FEET							
h in	d in	3	4	5	6	8	10	12	14
10.0 x 2.5									
t =	0.160	2673	1574	1067	793	523	362	273	216
	0.128	2083	1207	802	582	365	267	200	156
	0.104	1665	955	627	448	272	191	147	117
10.0 x 2.0									
t =	0.128	1821	1076	732	546	366	276	208	165
	0.104	1442	838	559	408	259	191	155	122
	0.080	1087	623	409	292	175	124	96	79
9.0 x 2.5									
t =	0.160	2367	1406	963	724	450	315	239	191
	0.128	1836	1070	716	524	335	232	173	137
	0.104	1463	842	555	400	246	175	131	102
8.0 x 2.0									
t =	0.128	1415	853	596	458	290	205	156	125
	0.104	1109	654	444	330	220	153	115	91
	0.080	828	479	318	230	144	105	80	62
7.0 x 2.0									
t =	0.128	1223	750	526	386	243	174	134	107
	0.104	951	567	390	295	183	128	98	78
	0.080	705	411	275	201	129	89	67	53
6.0 x 3.0									
t =	0.160	1489	871	584	427	269	193	149	121
	0.128	1176	679	449	323	198	139	106	85
6.0 x 2.0									
t =	0.128	1041	621	423	314	202	146	113	91
	0.104	789	461	308	224	140	99	75	60
	0.080	587	346	234	172	105	73	55	44

LOADS GIVEN IN lbf/ft

SECTION		SPANS IN FEET							
h in	d in	3	4	5	6	8	10	12	14
6.0 x 1.5									
t =	0.104	714	461	325	243	157	113	87	69
	0.080	506	310	220	171	107	77	59	47
	0.064	387	230	158	119	79	55	42	33
5.0 x 3.0									
t =	0.160	1145	679	462	343	222	162	127	103
	0.128	898	524	350	255	160	115	89	72
5.0 x 2.5									
t =	0.160	1083	654	453	341	225	166	129	104
	0.128	842	498	338	250	160	117	91	74
	0.104	672	392	261	190	119	85	65	53
5.0 x 1.5									
t =	0.104	598	365	255	193	127	92	71	56
	0.080	418	263	179	133	85	62	48	38
	0.064	315	191	134	99	62	44	34	27
5.0 x 1.0									
t =	0.080	391	268	189	143	93	67	50	39
	0.064	273	183	138	104	67	48	37	29
	0.048	184	115	83	67	44	32	24	19
4.0 x 2.5									
t =	0.128	617	373	258	195	129	96	75	61
	0.104	487	289	196	145	94	69	54	44
4.0 x 2.0									
t =	0.128	584	362	257	197	133	98	76	60
	0.104	456	276	191	145	96	71	55	45
	0.080	338	200	135	100	64	46	36	29
4.0 x 1.5									
t =	0.104	435	273	195	150	100	73	55	44
	0.080	316	192	133	101	67	49	38	30
	0.064	244	145	99	73	47	34	27	22
4.0 x 1.0									
t =	0.080	311	198	142	109	71	50	37	29
	0.064	229	145	102	78	51	37	28	22
	0.048	147	96	69	51	33	24	19	15

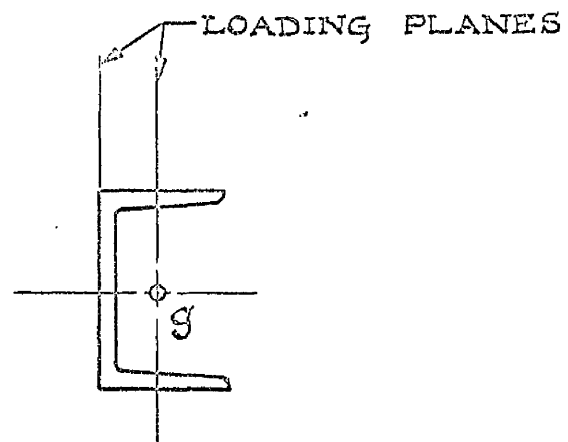
LOADS GIVEN IN lbf/ft

SECTION		SPANS IN FEET							
h in	d in	3	4	5	6	8	10	12	14
3.0 x 2.0									
t = 0.104		313	197	141	109	75	55	43	34
	0.080	227	138	96	73	49	36	29	23
3.0 x 1.5									
t = 0.104		303	198	145	113	76	54	41	32
	0.080	214	134	96	75	51	37	29	23
	0.064	162	99	69	53	35	26	20	16
2.0 x 1.5									
t = 0.080		136	91	68	53	36	26	19	15
	0.064	99	64	47	37	25	19	14	11
2.0 x 1.0									
t = 0.080		139	94	68	52	32	22	16	12
	0.064	99	66	49	38	25	17	12	9
	0.048	64	42	31	24	16	12	9	7
1.5 x 1.0									
t = 0.064		76	52	38	29	18	12	9	7
	0.048	48	33	24	19	13	9	7	5
4.0 x 4.0									
t = 0.160		958	565	383	283	182	133	105	86
	0.128	753	438	291	211	132	94	73	59
3.5 x 3.5									
t = 0.160		762	462	321	243	162	121	96	79
	0.128	592	350	238	177	114	84	66	55
3.0 x 3.0									
t = 0.160		603	380	274	213	147	110	86	69
	0.128	458	280	197	150	102	76	61	49
	0.104	359	215	147	110	73	54	43	35
2.5 x 2.5									
t = 0.160		481	320	238	188	128	93	70	55
	0.128	353	227	166	131	90	67	52	41
	0.104	269	168	120	93	64	48	38	31
	0.080	196	118	82	62	42	31	25	20

LOADS GIVEN IN lbf/ft

SECTION		SPANS IN FEET							
h in	d in	3	4	5	6	8	10	12	14
2.0 x 2.0									
t =	0.160	395	270	200	154	99	68	49	37
	0.128	279	190	142	112	75	53	39	30
	0.104	205	136	102	81	55	40	30	24
	0.080	141	91	66	52	36	27	21	17
	0.064	106	66	47	36	25	19	15	12
1.5 x 1.5									
t =	0.128	231	156	112	83	51	34	24	18
	0.104	162	111	81	62	39	26	19	14
	0.080	107	73	55	43	28	20	15	11
	0.064	75	51	38	30	21	15	11	9
	0.048	49	32	24	19	13	10	8	6
1.0 x 1.0									
t =	0.080	77	49	34	25	14	9	7	5
	0.064	56	37	26	20	12	8	6	4
	0.048	35	24	18	14	9	6	4	3

FIGURES



SECTION A-A.

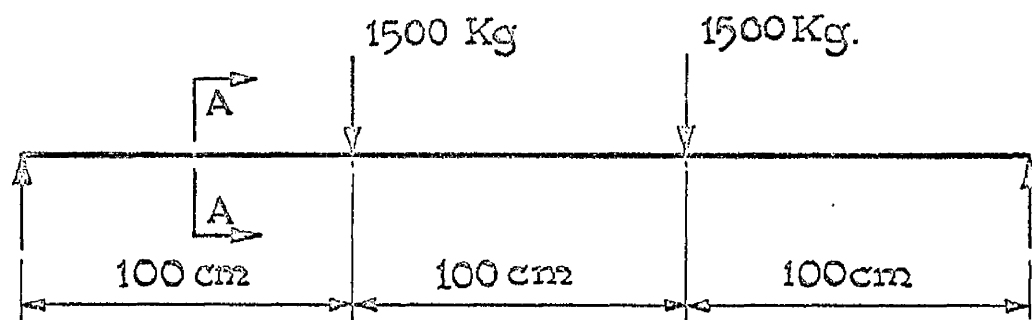


FIG.I.1. BACH'S CHANNEL BEAM TESTS.

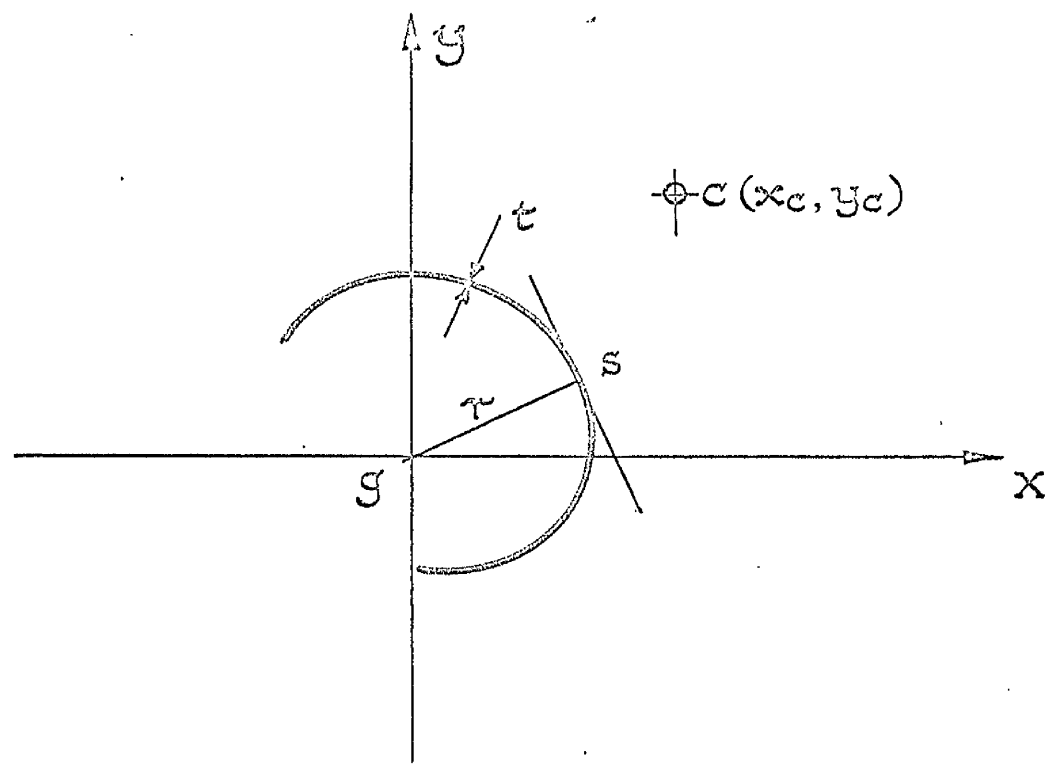


FIG.1.2. SHEAR CENTRE CO-ORDINATES OF A THIN - WALLED OPEN CROSS - SECTION.

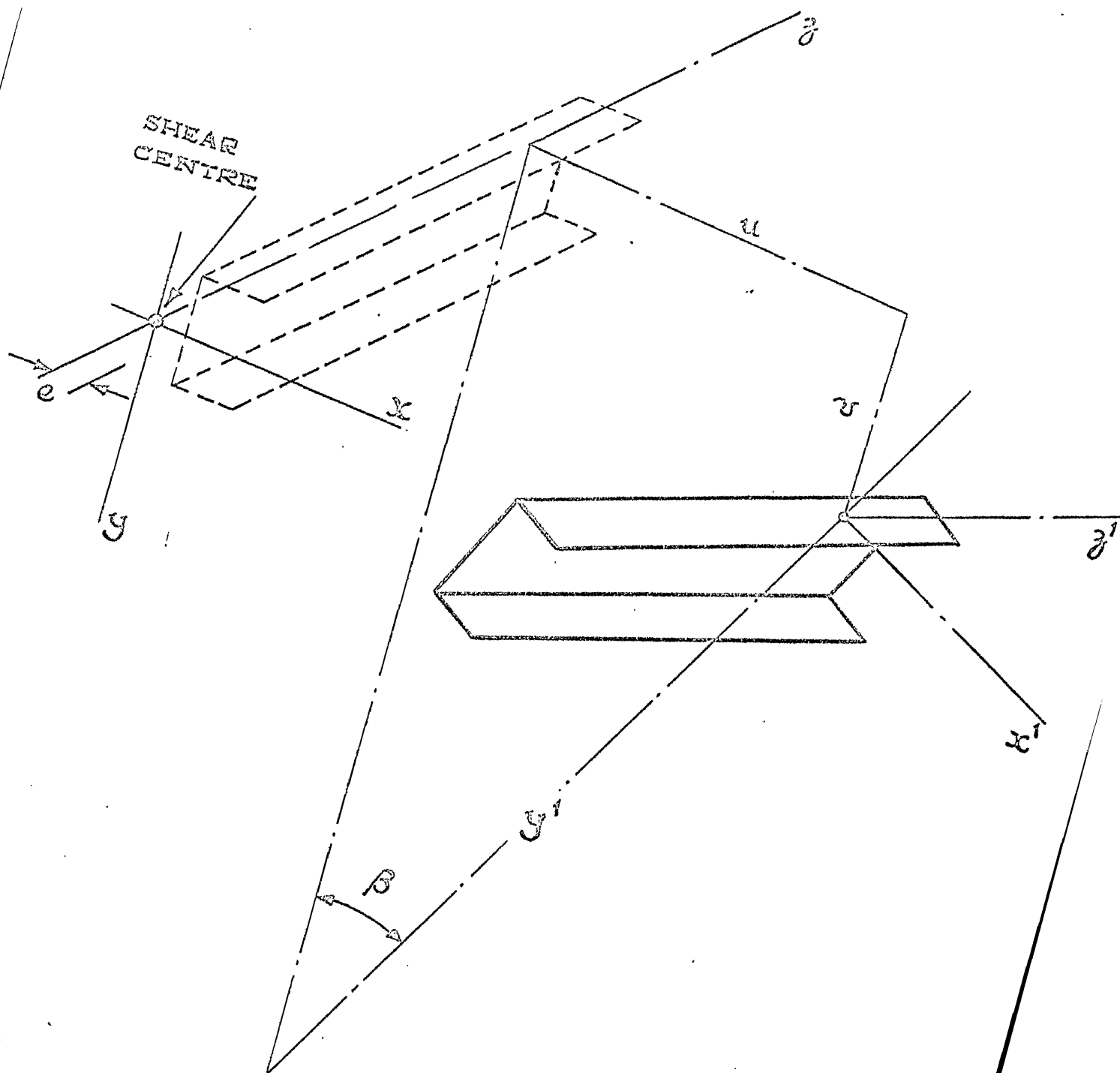


FIG. I.3. ORIGINAL AND DISPLACED CO-ORDINATE AXES. ADOPTED BY WINTER, LANSING AND MCSALLEY.

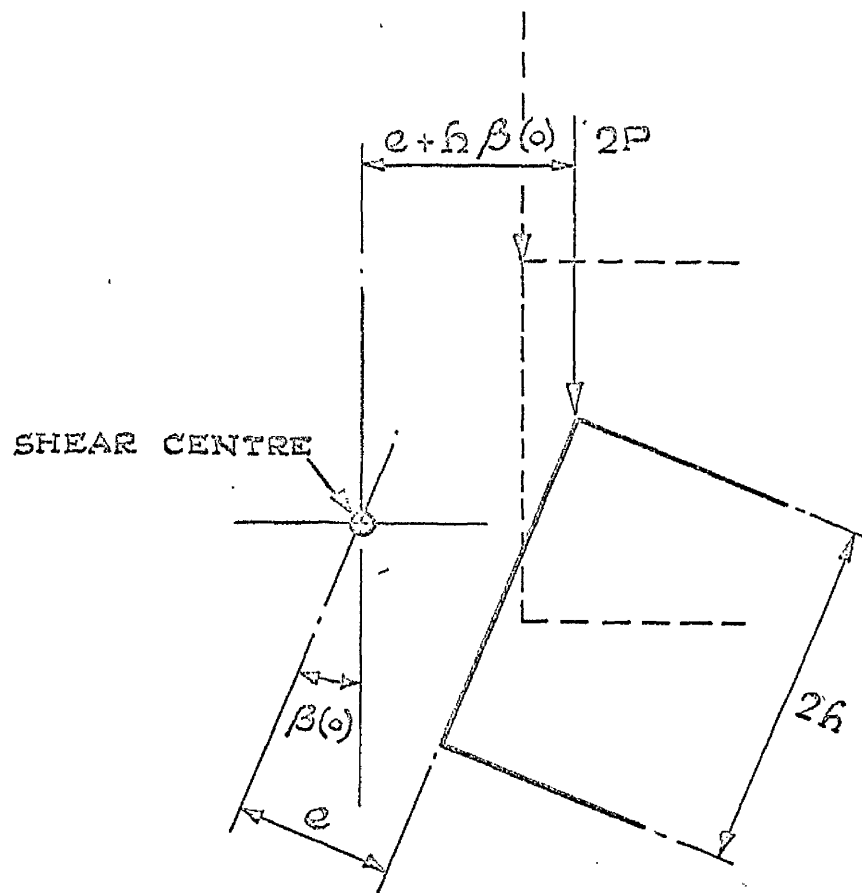


FIG.1.4. DISPLACED MID - SPAN SECTION
OF CHANNEL.

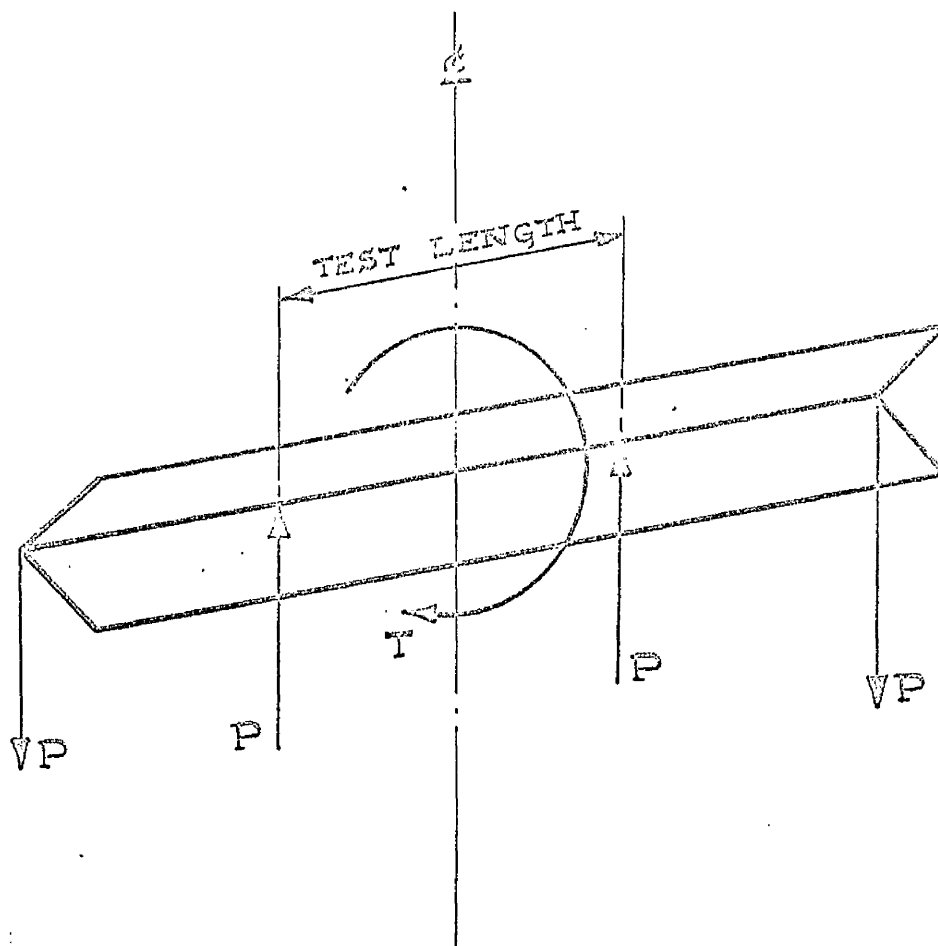


FIG.1.5. BENDING AND TORSION OF ANGLES IN THE TESTS DESCRIBED BY ENGEL AND GOODIER.

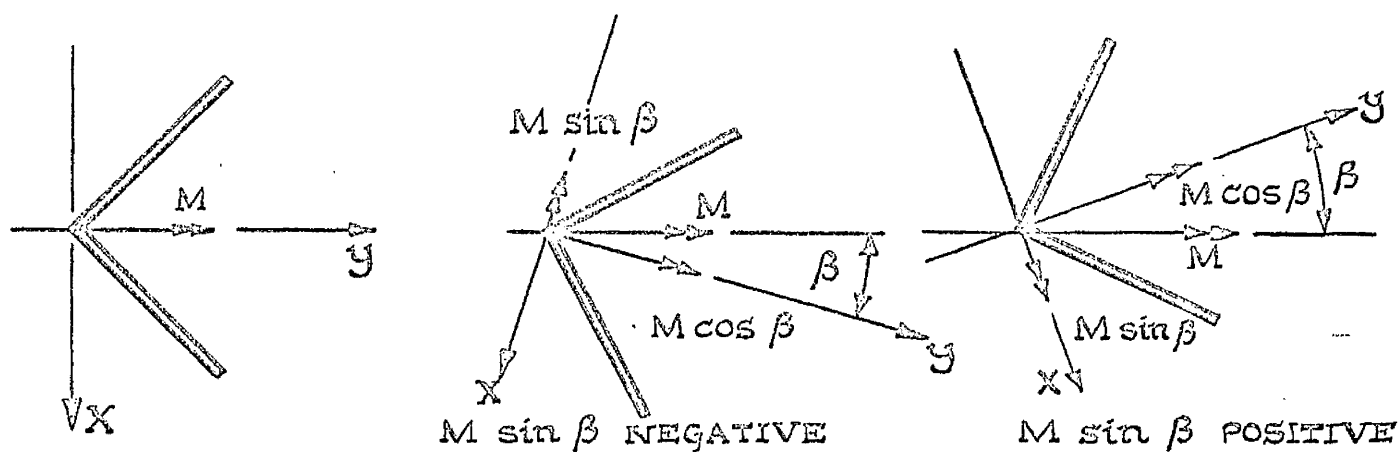


FIG.1.6. EFFECT OF SECTION ROTATION ON BENDING MOMENT COMPONENT CAUSING CHANGES IN TORSIONAL RIGIDITY.

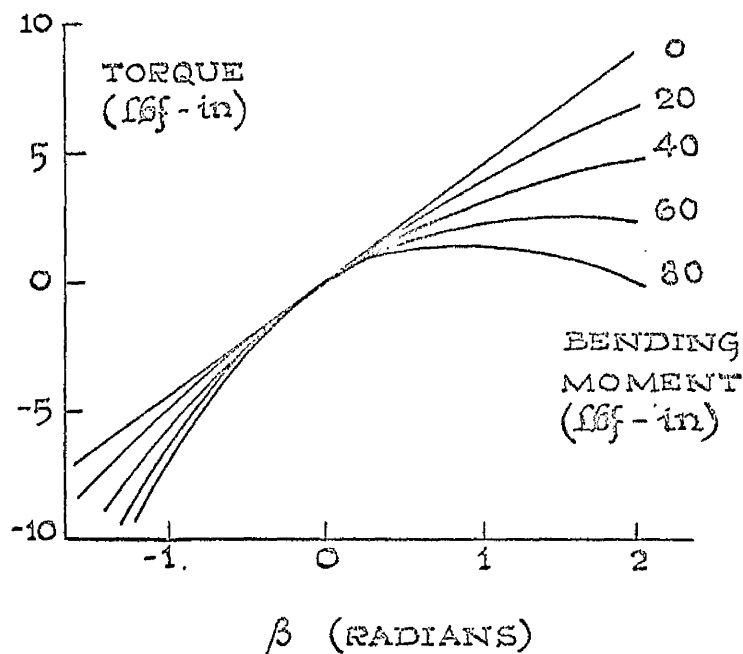


FIG. I.7. THEORETICAL TORQUE/TWIST RELATIONSHIPS FOR VARIOUS BENDING MOMENTS PRESENTED BY ENGEL AND GOODIER.

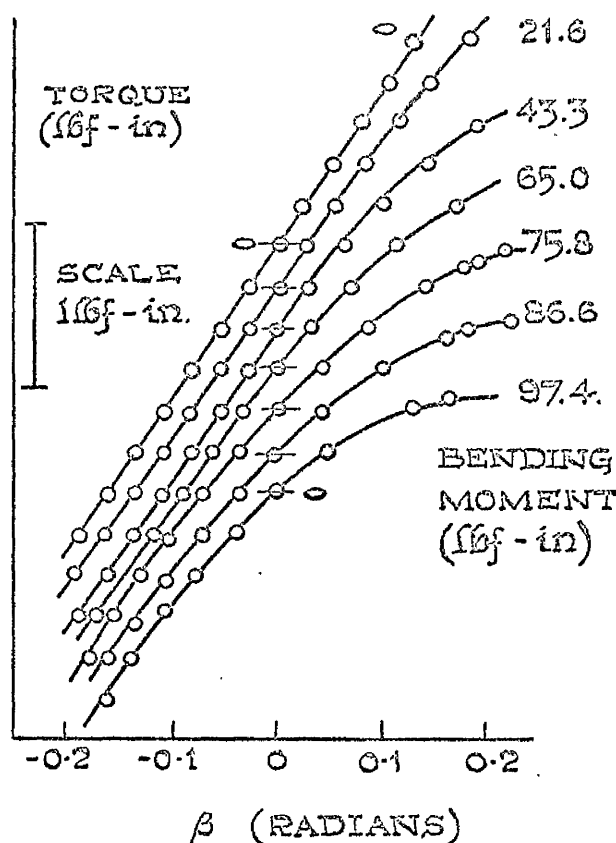


FIG. I.8. EXPERIMENTAL TORQUE/TWIST RELATIONSHIPS FOR VARIOUS BENDING MOMENTS OBTAINED BY ENGEL AND GOODIER.

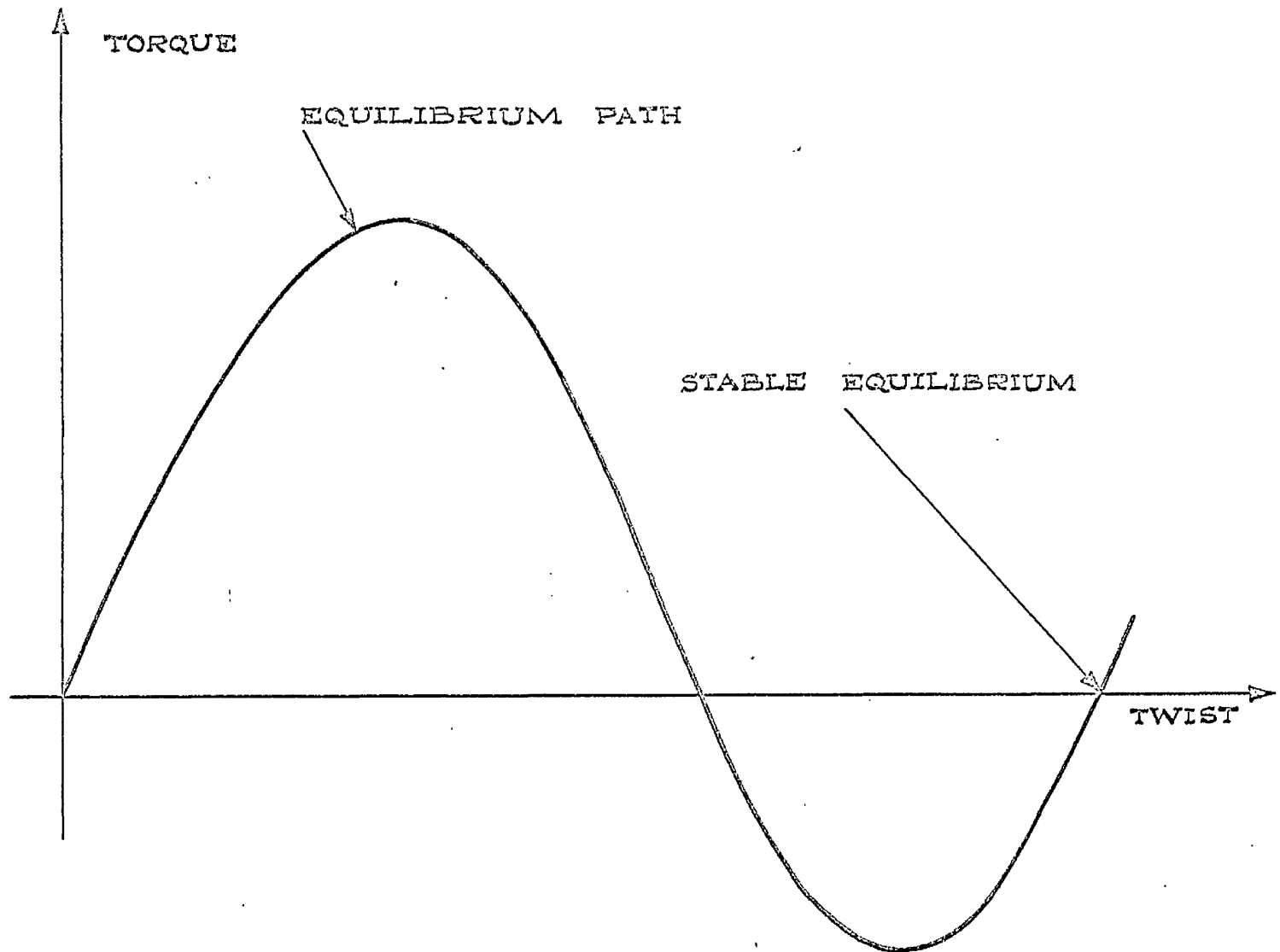


FIG.1.9. STABLE AND UNSTABLE FORM OF TORQUE /TWIST EQUILIBRIUM PATH SUGGESTED BY ENGEL AND GOODIER.

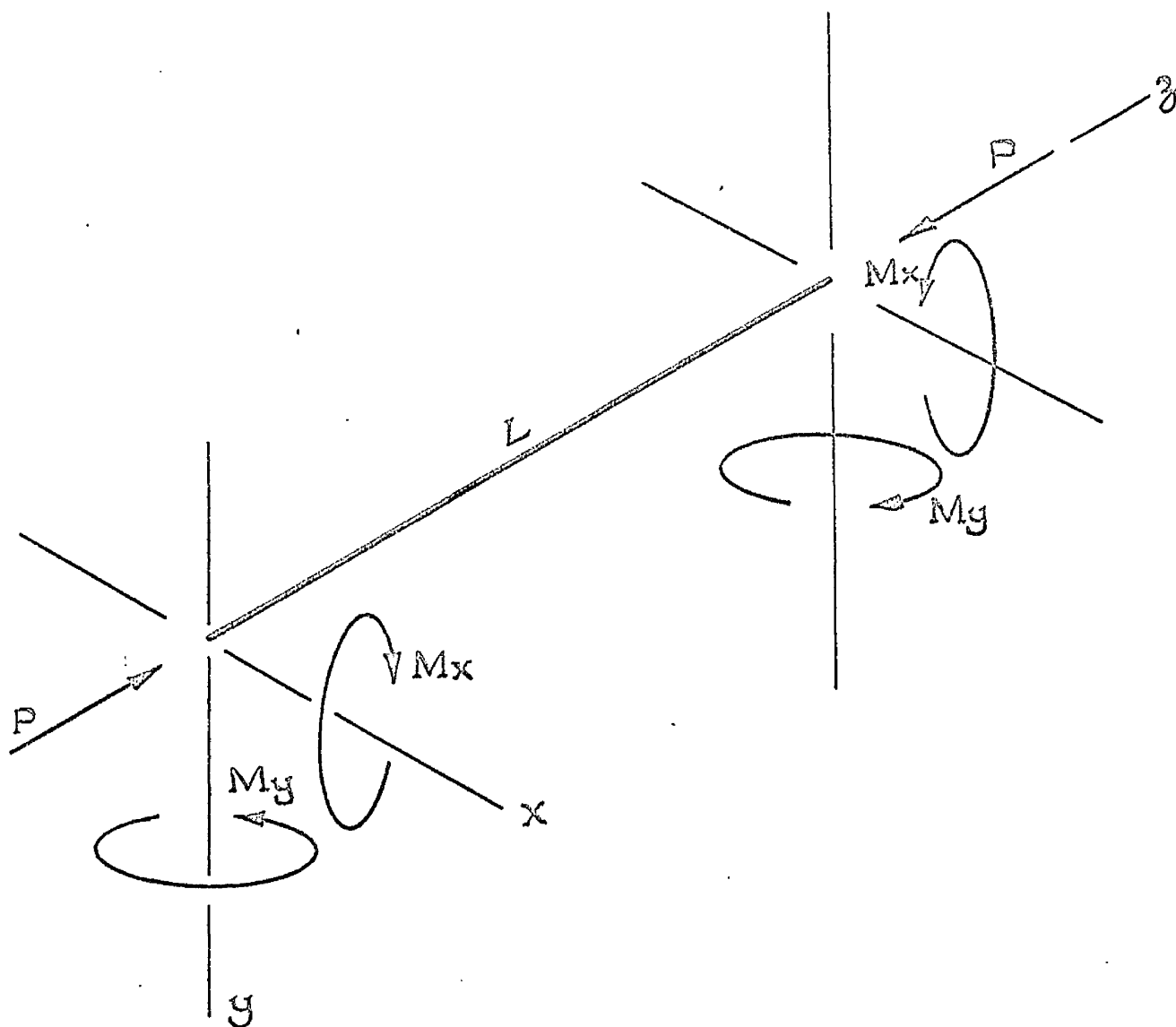


FIG.110. BENDING AND COMPRESSION OF A
THIN-WALLED MEMBER AS CONSIDERED
BY TIMOSHENKO.

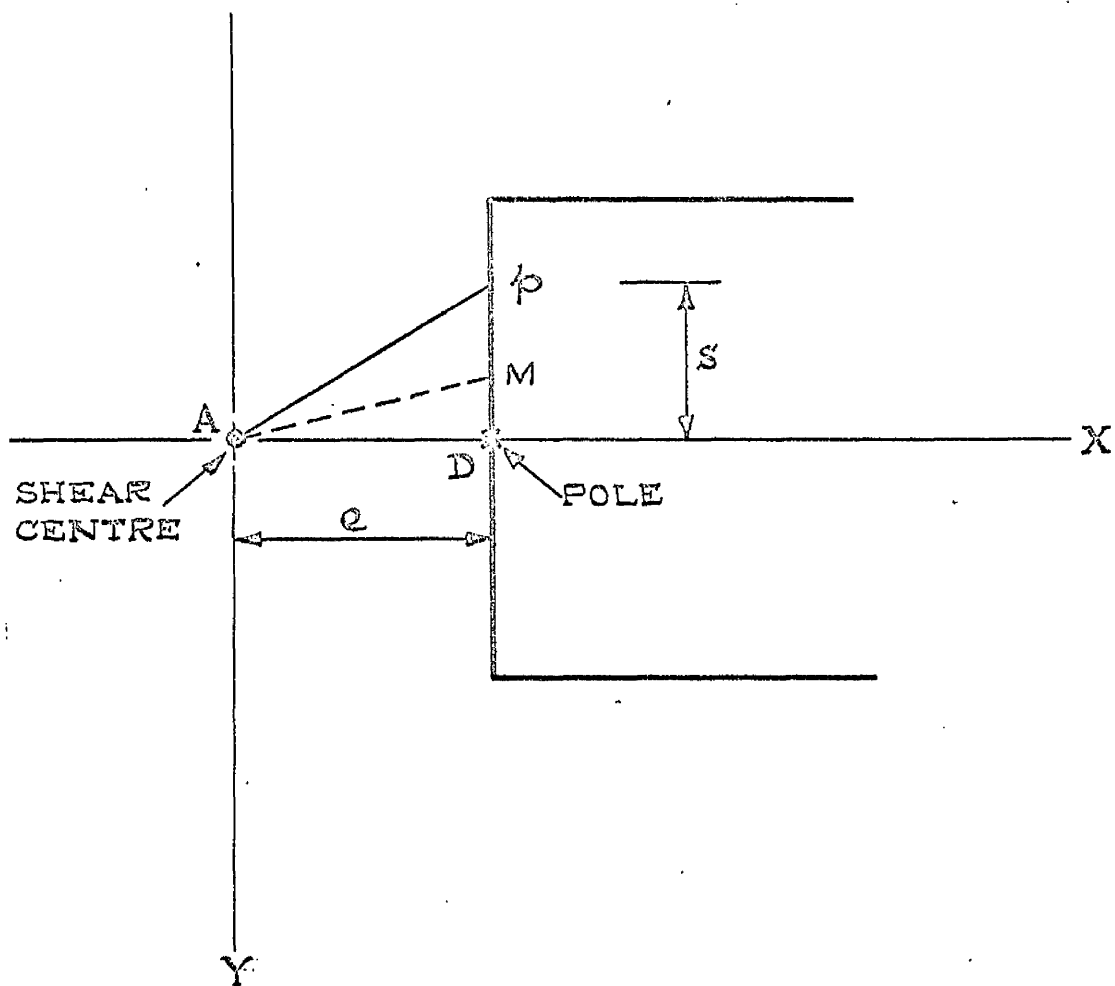


FIG. II.1. EVALUATION OF THE 'SECTORIAL CO-ORDINATE'.

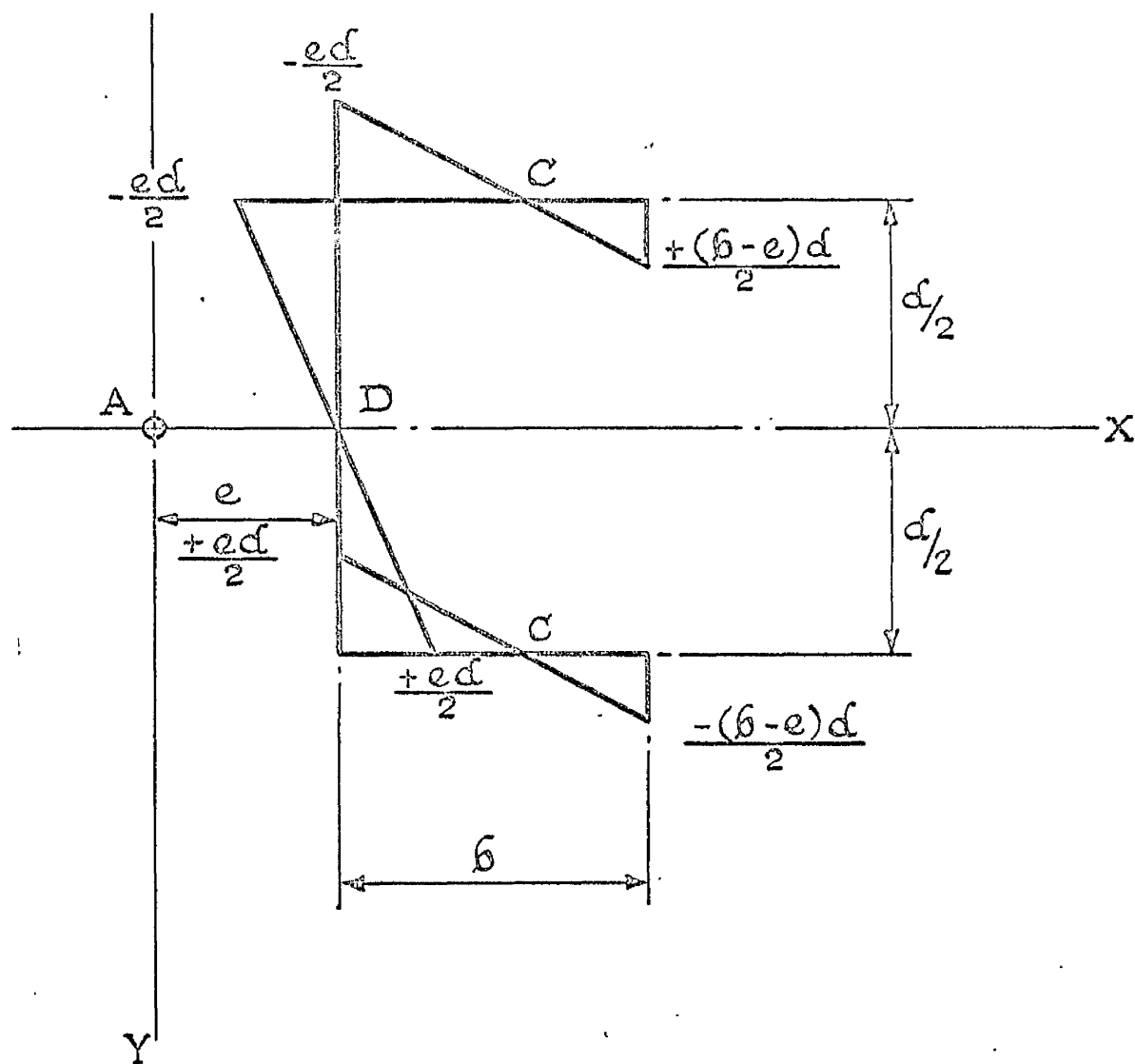


FIG. II.2. SECTORIAL CO-ORDINATE AT ANY POINT IN A CHANNEL SECTION.

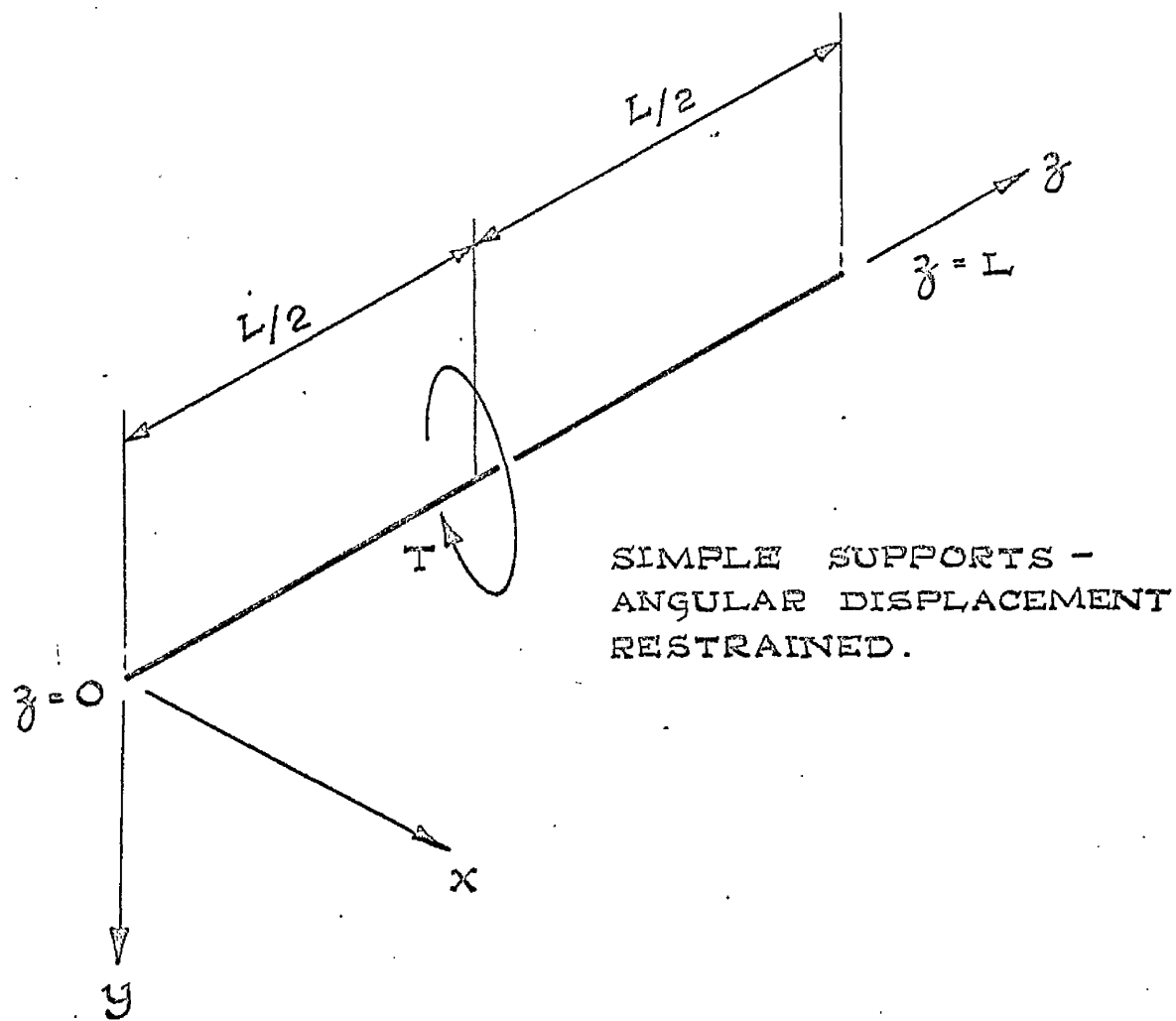


FIG. II.3. BEAM SUBJECTED TO A CONCENTRATED TORQUE AT MID-SPAN.

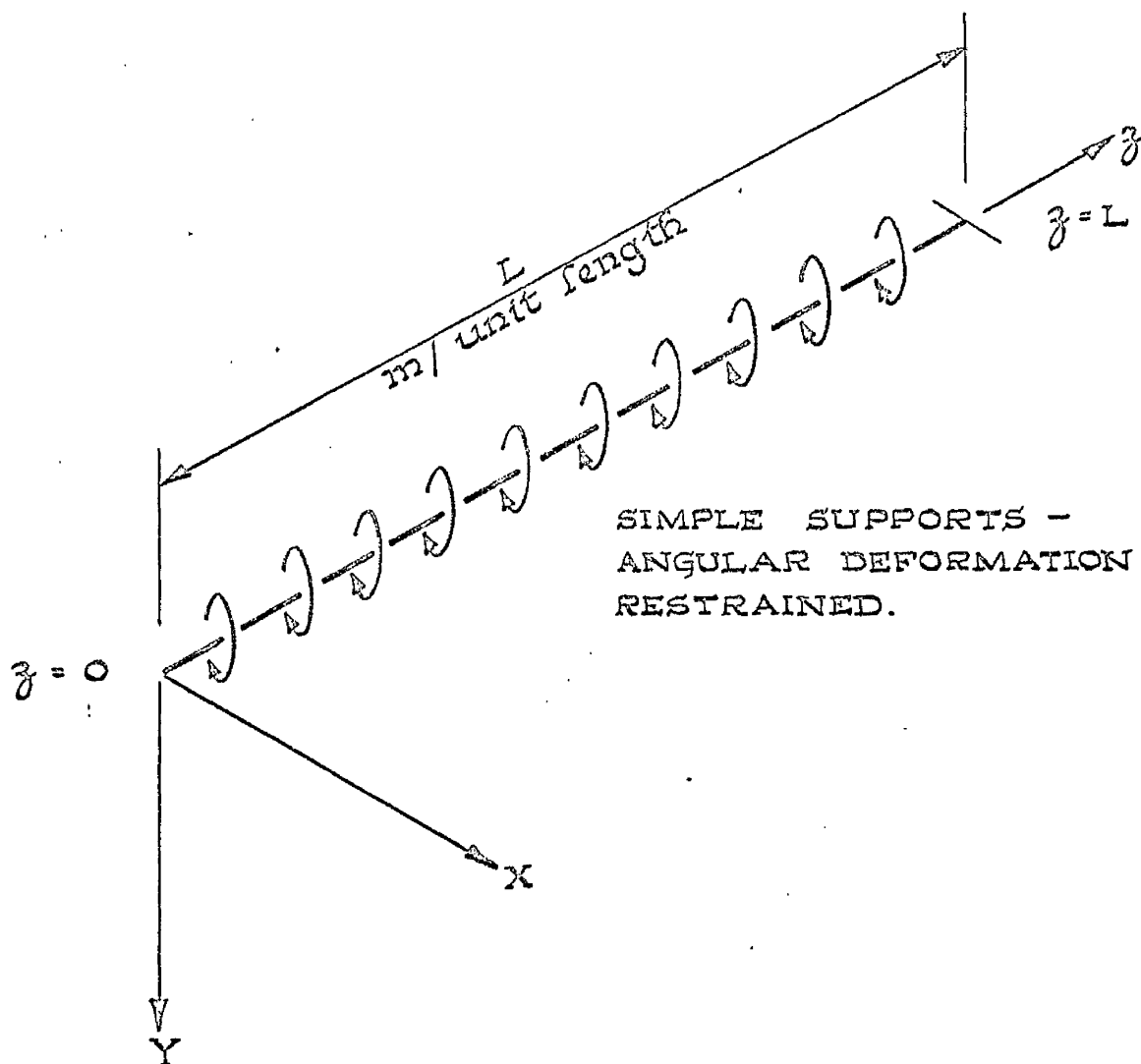


FIG. II.4. BEAM SUBJECTED TO UNIFORMLY
DISTRIBUTED TORQUE OVER
ENTIRE SPAN.

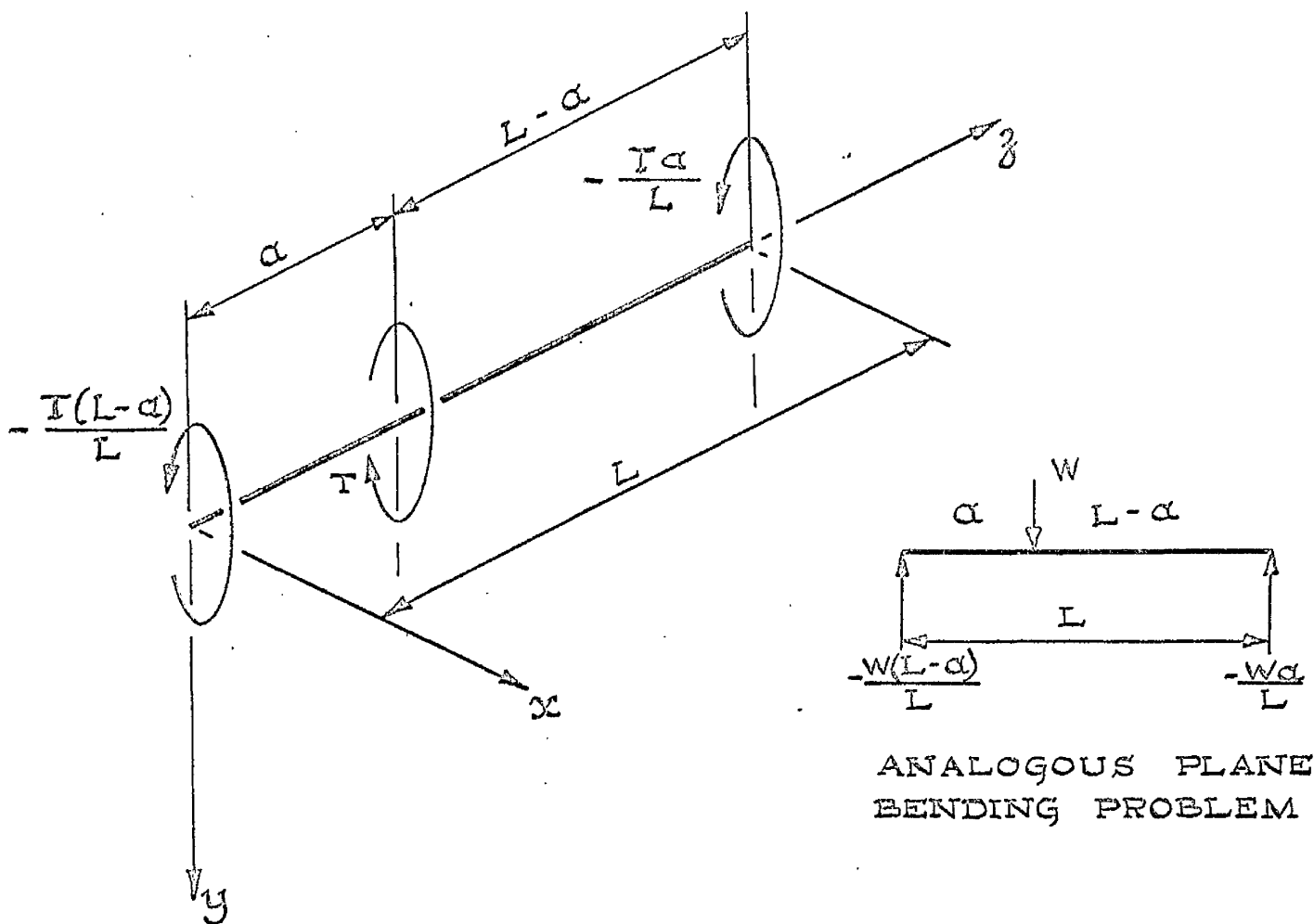
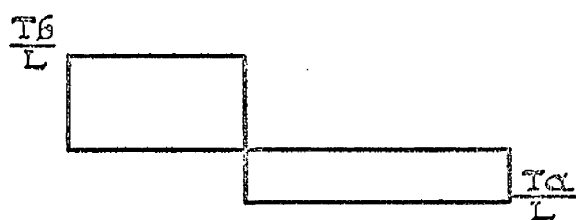
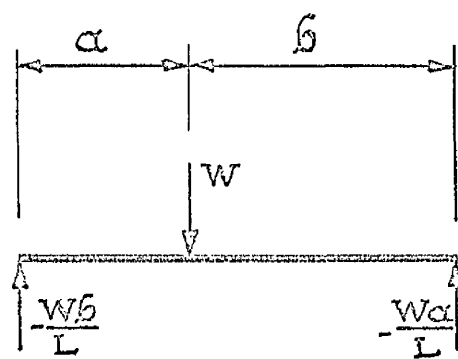
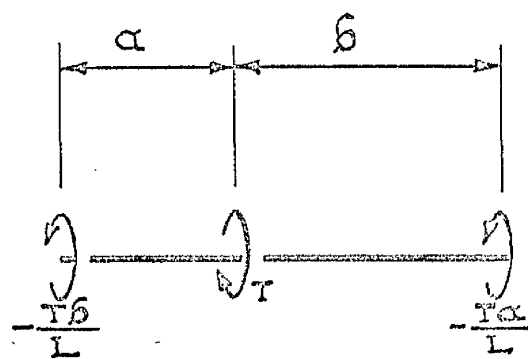
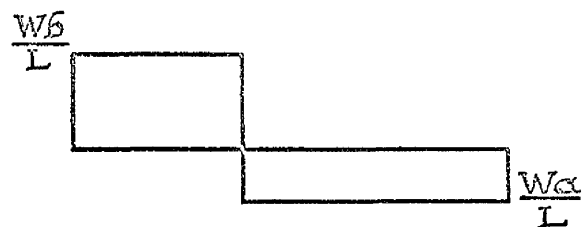


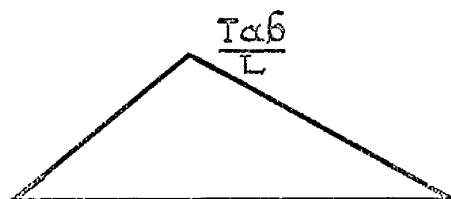
FIG. II.5. BEAM SUBJECTED TO A CONCENTRATED TORQUE AT ANY POINT.



TORQUE

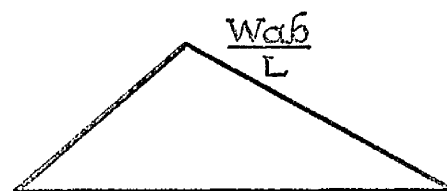


SHEAR FORCE



BI - MOMENT

TORSION



BENDING MOMENT

PLANE BENDING

FIG. II. 6. ANALOGOUS DISTRIBUTIONS OF TORQUE AND SHEAR FORCE AND BI-MOMENT AND BENDING MOMENT.

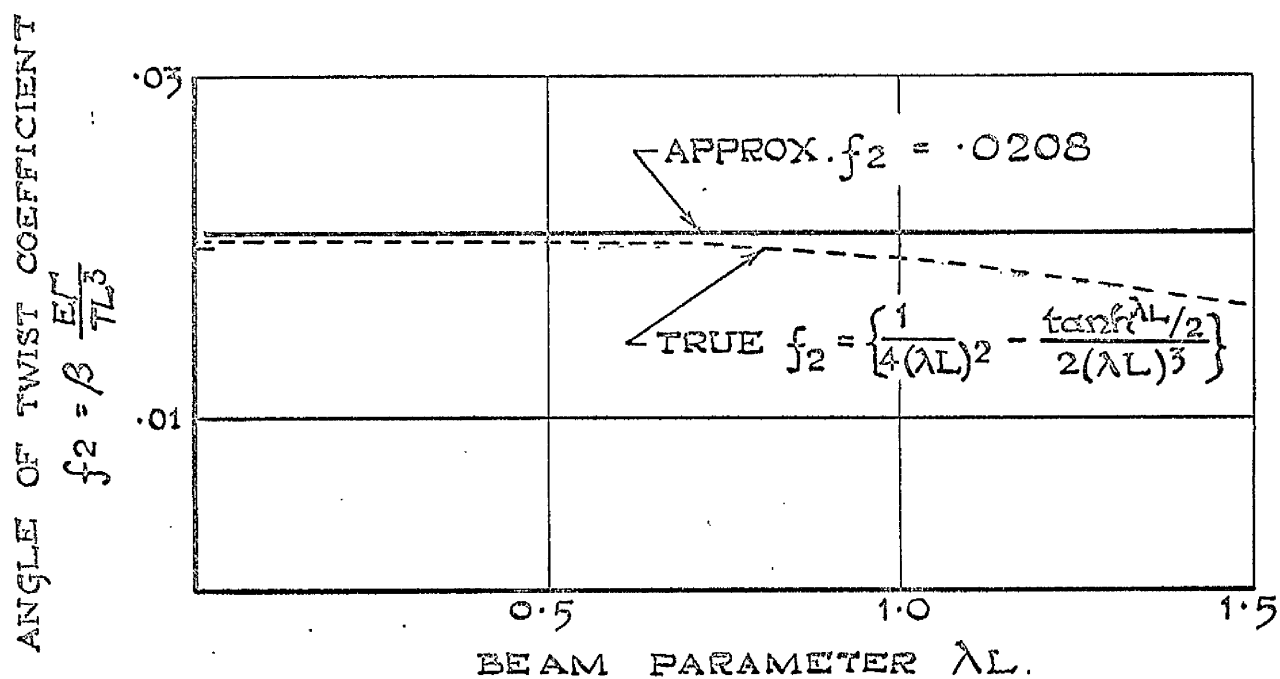
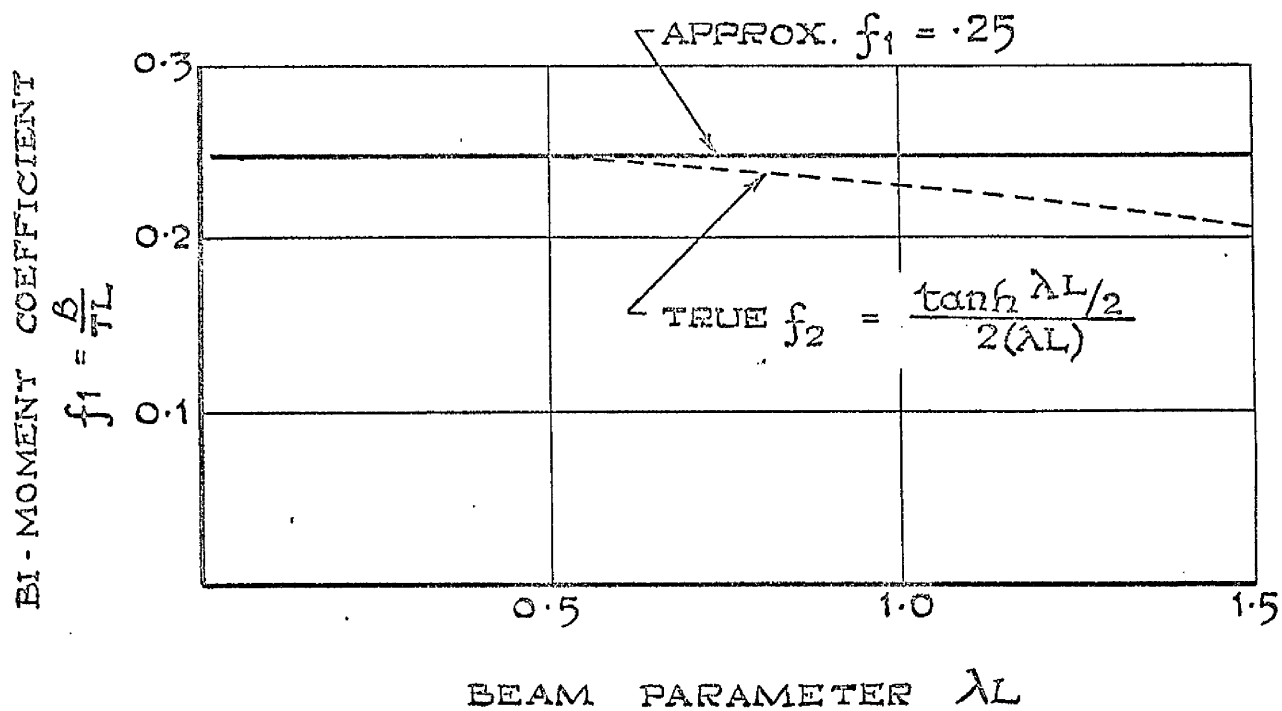
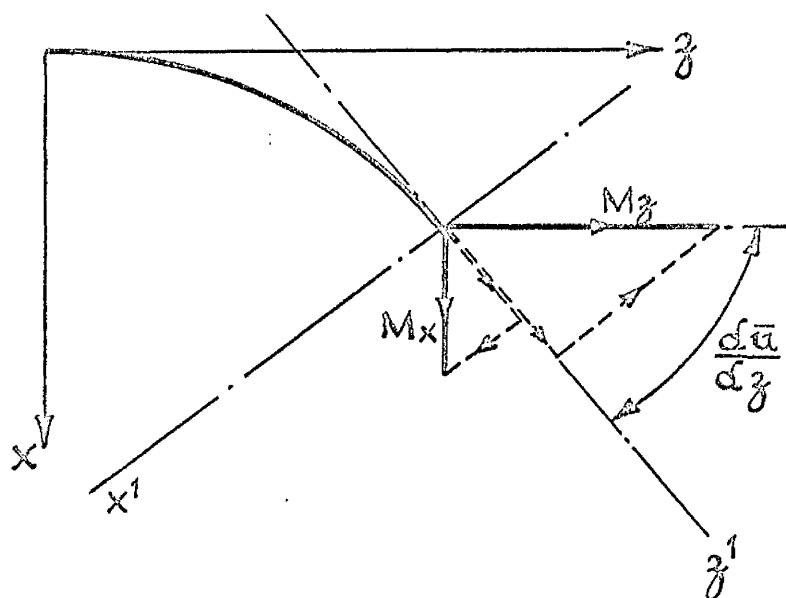
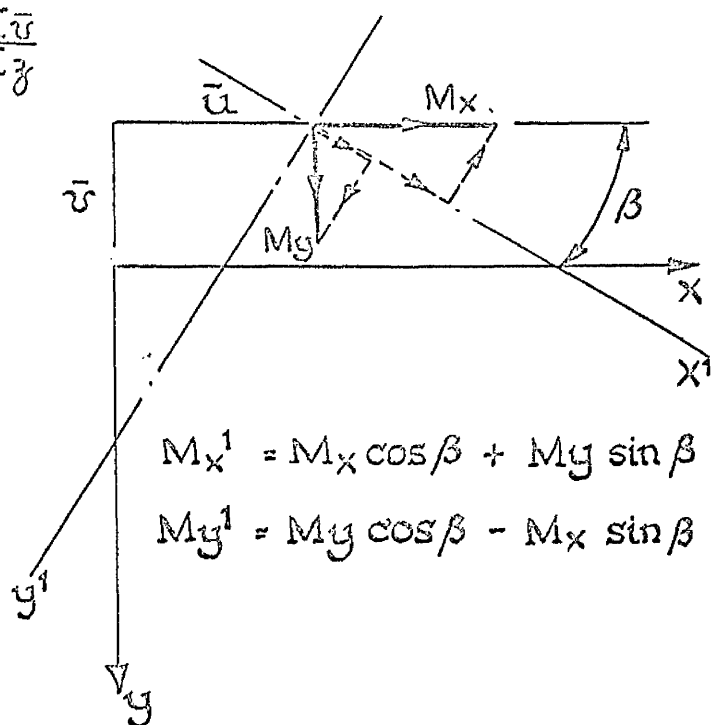
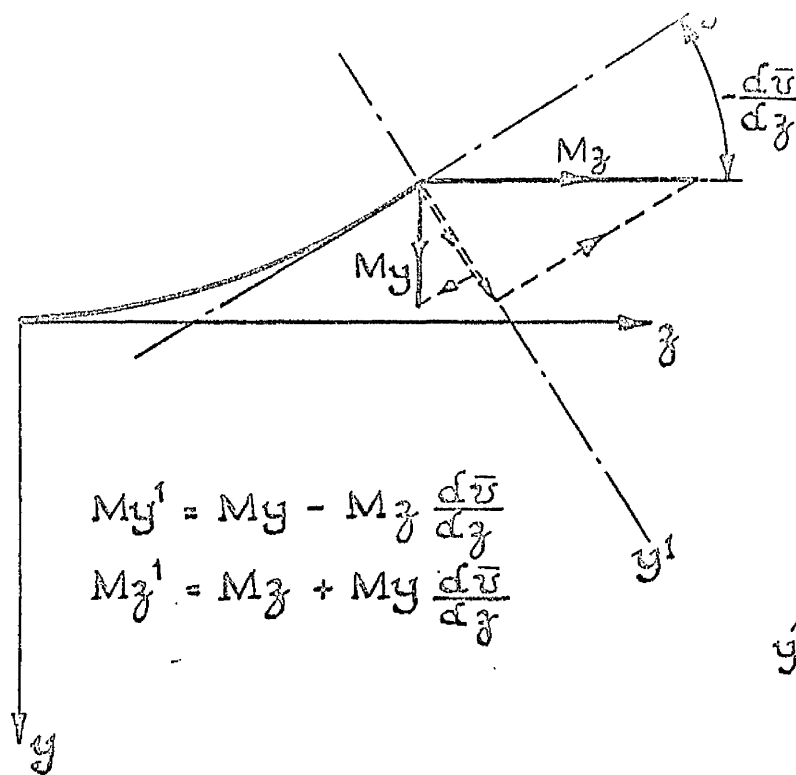
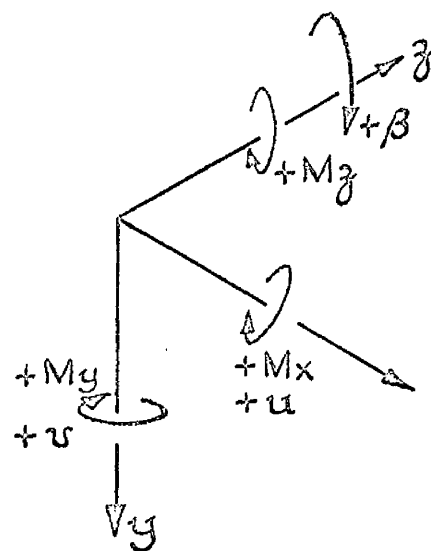


FIG. II. 7. VARIATION OF BI-MOMENT AND ANGLE OF TWIST COEFFICIENTS f_1 AND f_2 WITH BEAM PARAMETER λL



POSITIVE AXES & MOMENTS



RADIUS OF CURVATURE
+ve WHEN SLOPE +ve
AND INCREASING WITH $z + ve$.

FIG. II.8. COMPONENTS OF BENDING MOMENT AND TORQUE ABOUT DISPLACED AXES.

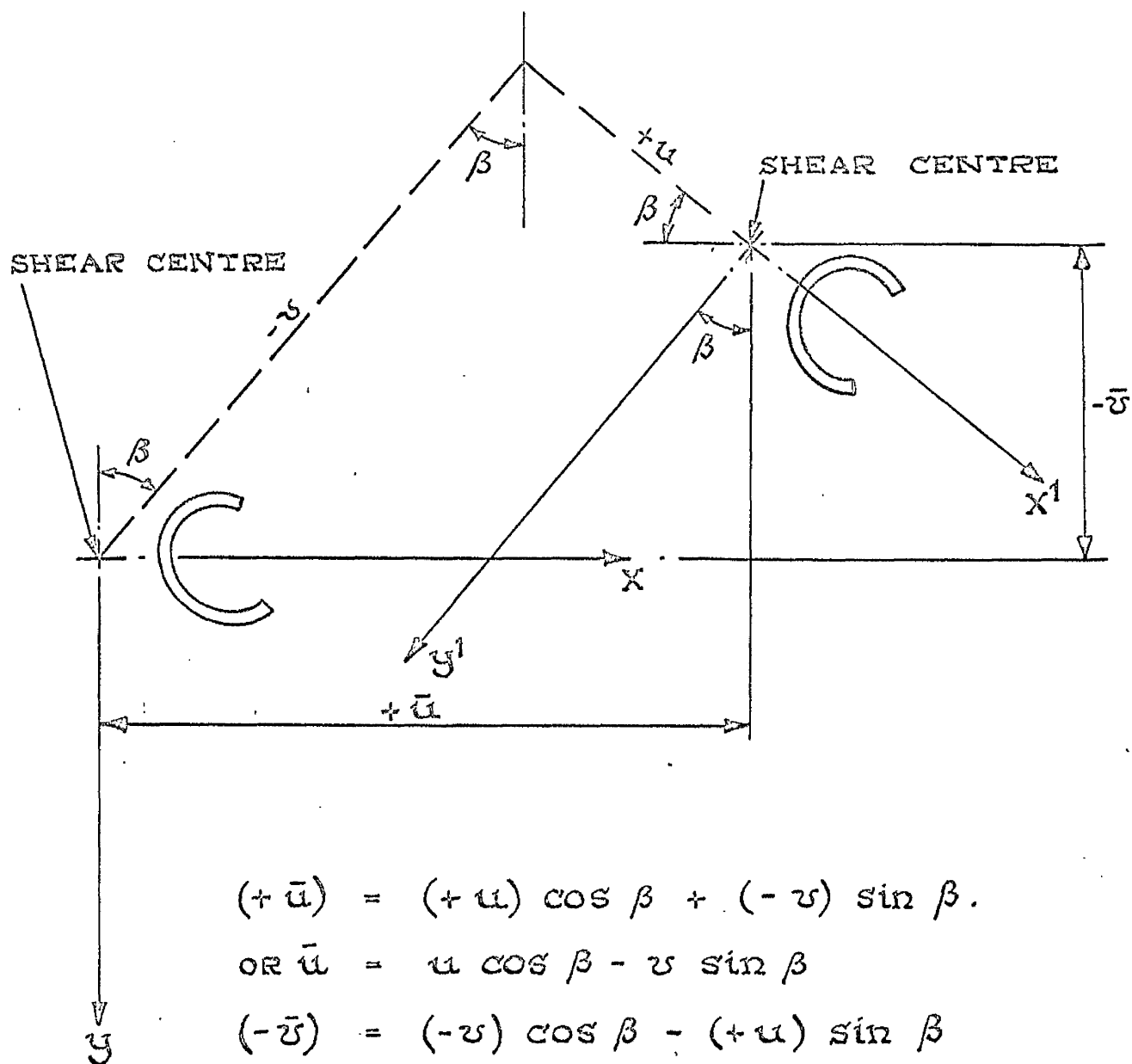


FIG. II. 9. HORIZONTAL AND VERTICAL DEFLECTIONS
RELATIVE TO UNDISPLACED AXES.

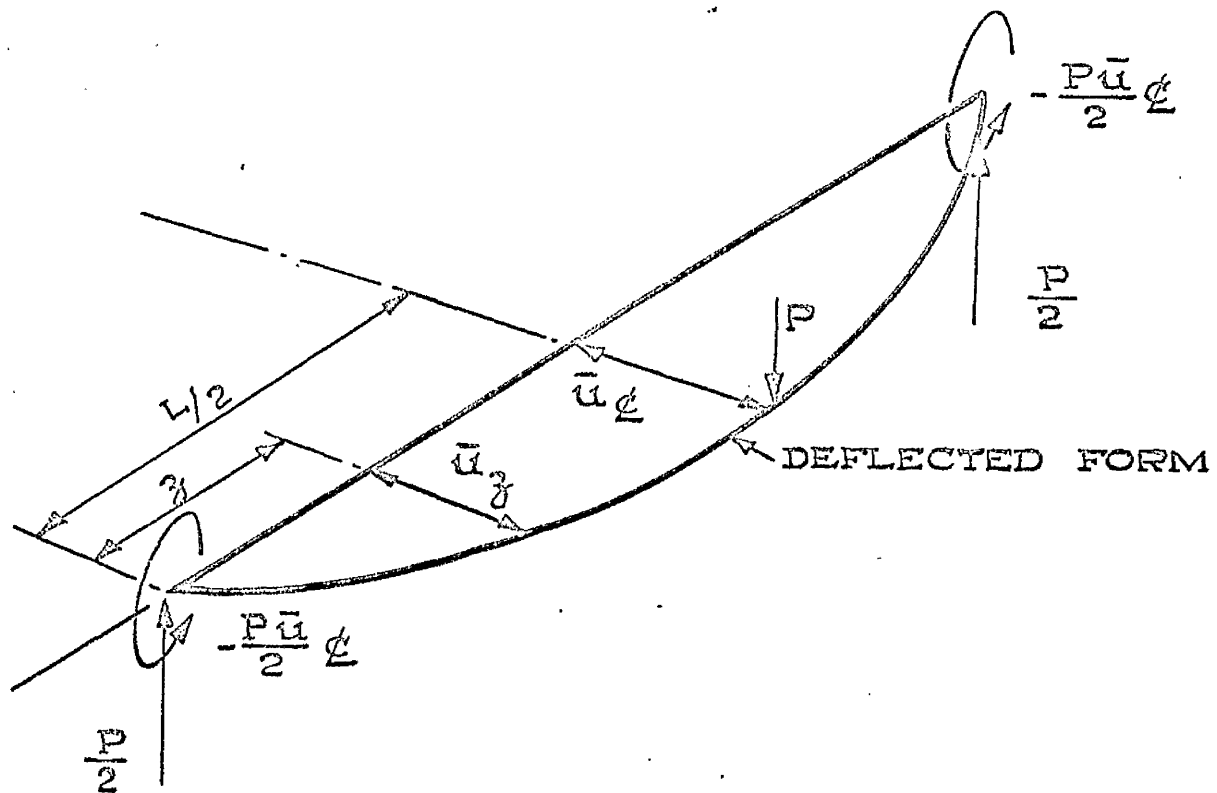


FIG. II.10. ADDITIONAL TORQUE DUE TO DISPLACEMENT OF LOAD POINT.

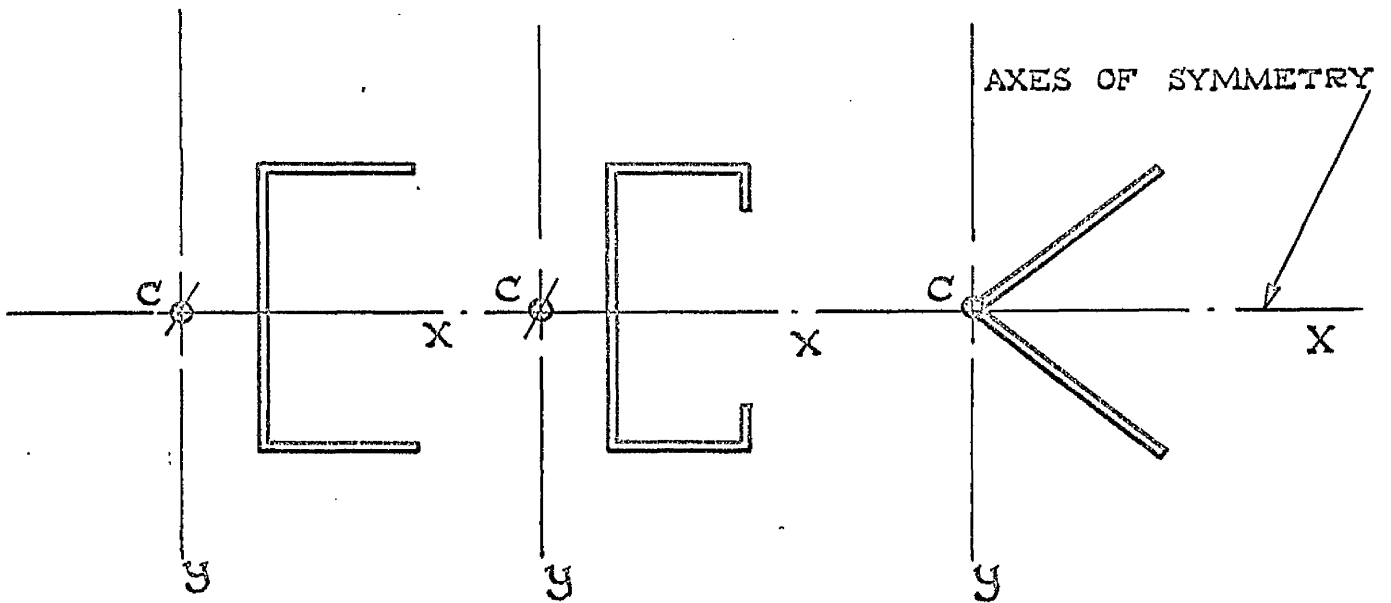


FIG II.11. MONOSYMMETRICAL THIN - WALLED OPEN SECTION BEAMS.

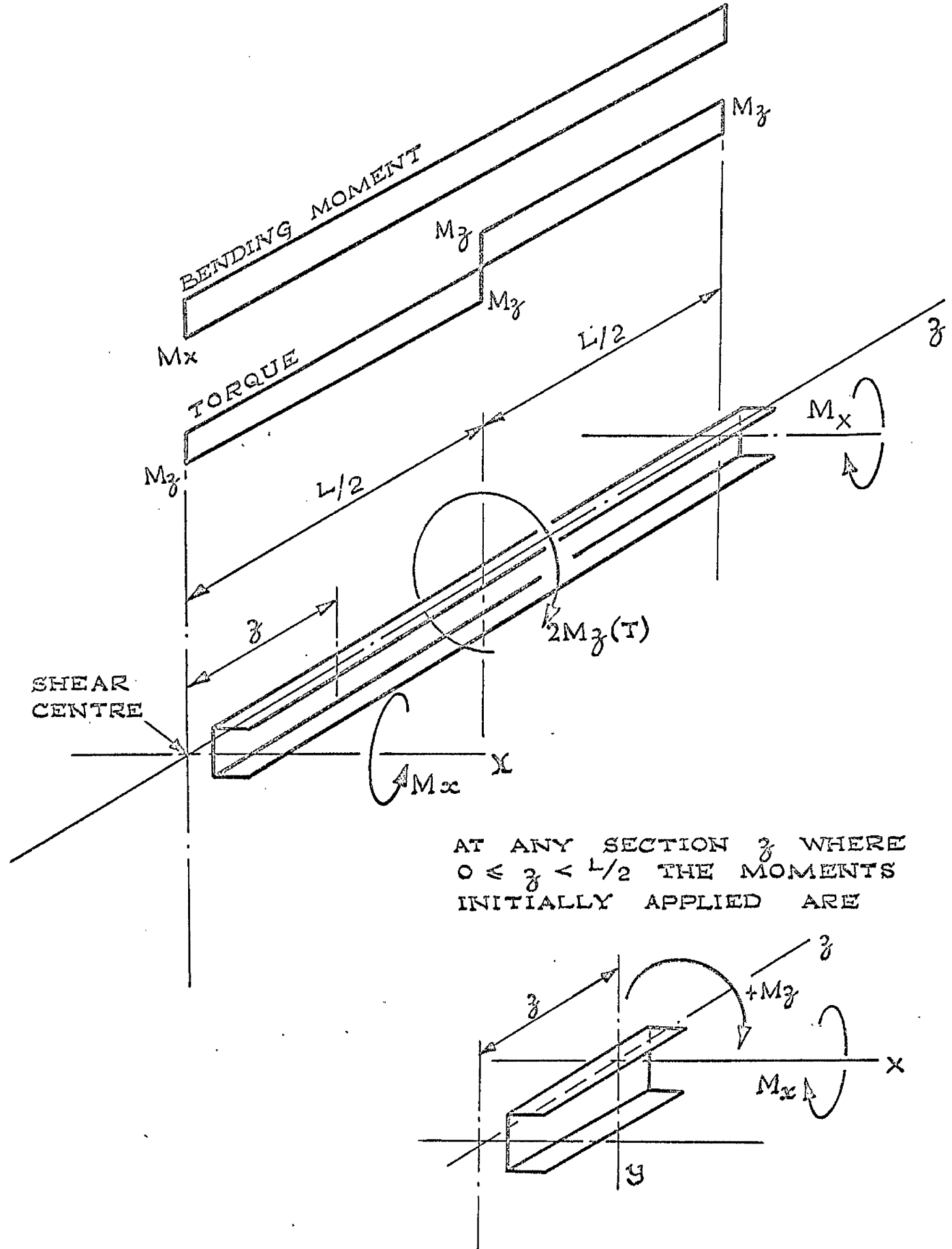


FIG. II.12. APPLIED BENDING MOMENT AND TORQUE CONSIDERED IN THE THEORETICAL ANALYSIS.

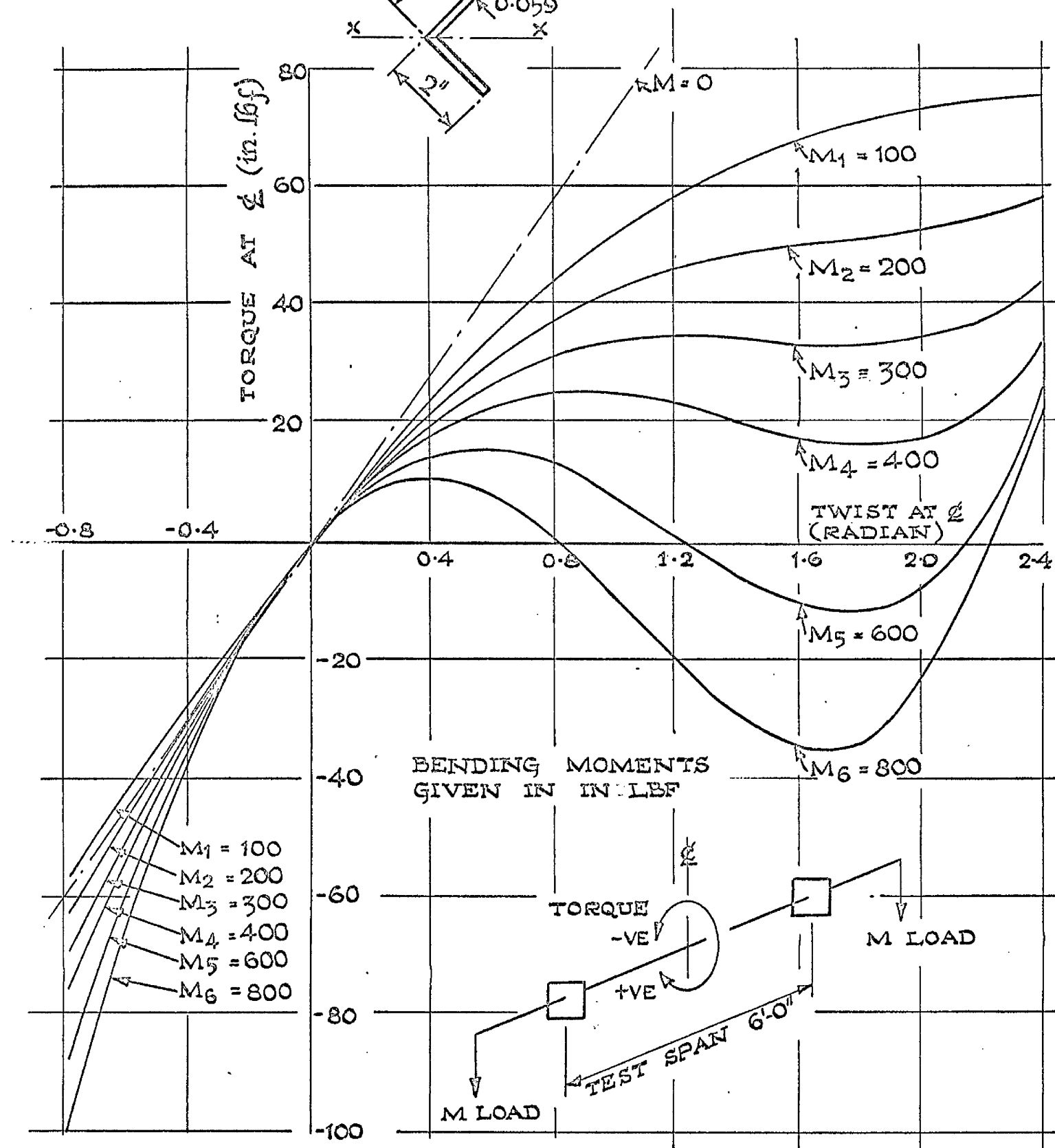
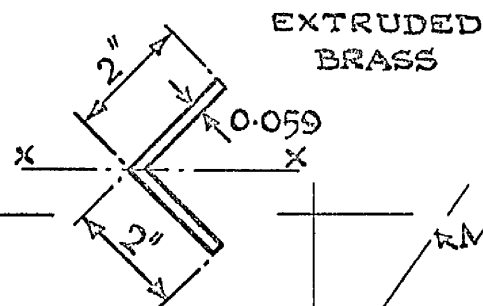


FIG. II.13. THEORETICAL TORQUE / ANGLE OF TWIST EQUILIBRIUM PATHS FOR VARIOUS BENDING MOMENTS.

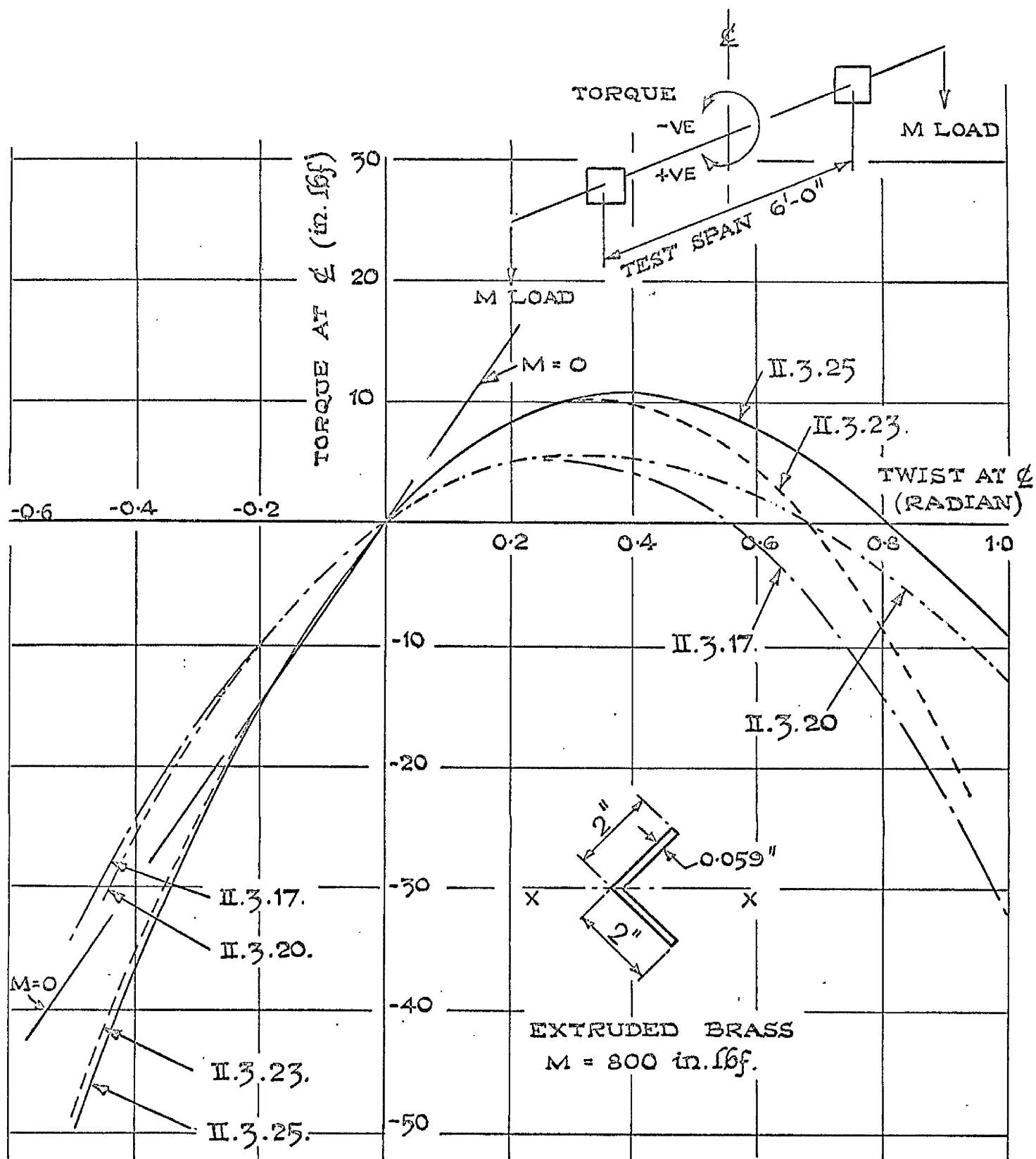


FIG. II. 14. THEORETICAL TORQUE / ANGLE OF TWIST EQUILIBRIUM PATH FOR VARIOUS SOLUTIONS.

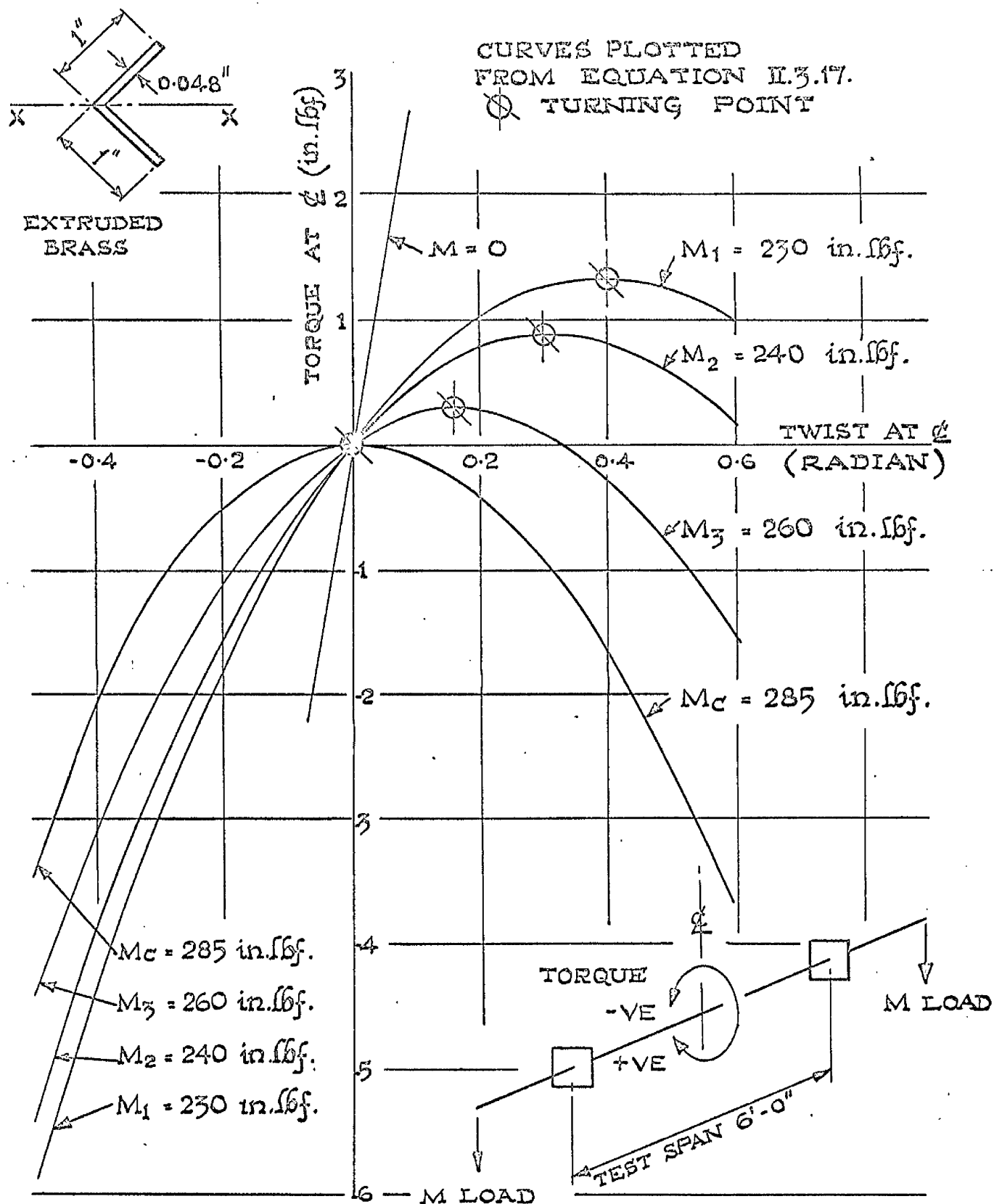


FIG. II.15. THEORETICAL TORQUE / ANGLE OF TWIST EQUILIBRIUM PATHS SHOWING VARYING POSITIONS OF TURNING POINTS.

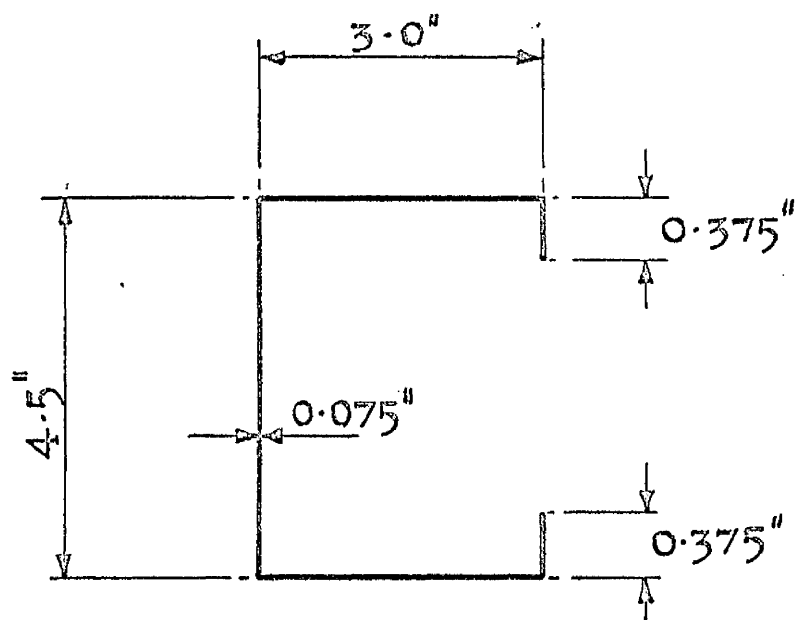


FIG. III.1. DIMENSIONS OF THIN-WALLED LIPPED CHANNEL SECTION TEST BEAM.

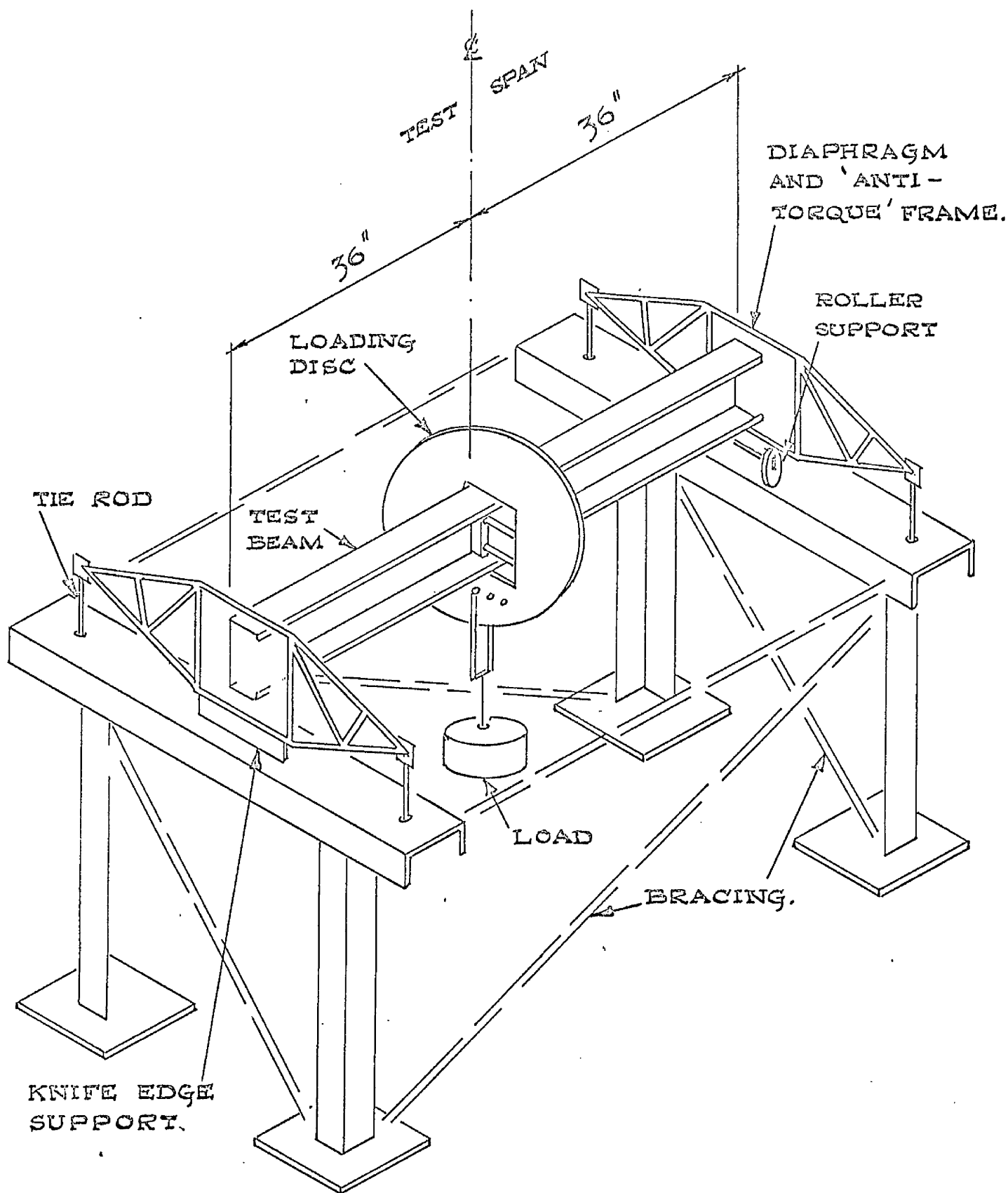


FIG. III.2. DETAILS OF APPARATUS USED FOR COMBINED BENDING AND TORSION TESTS ON THE LIPPED CHANNEL SECTION.

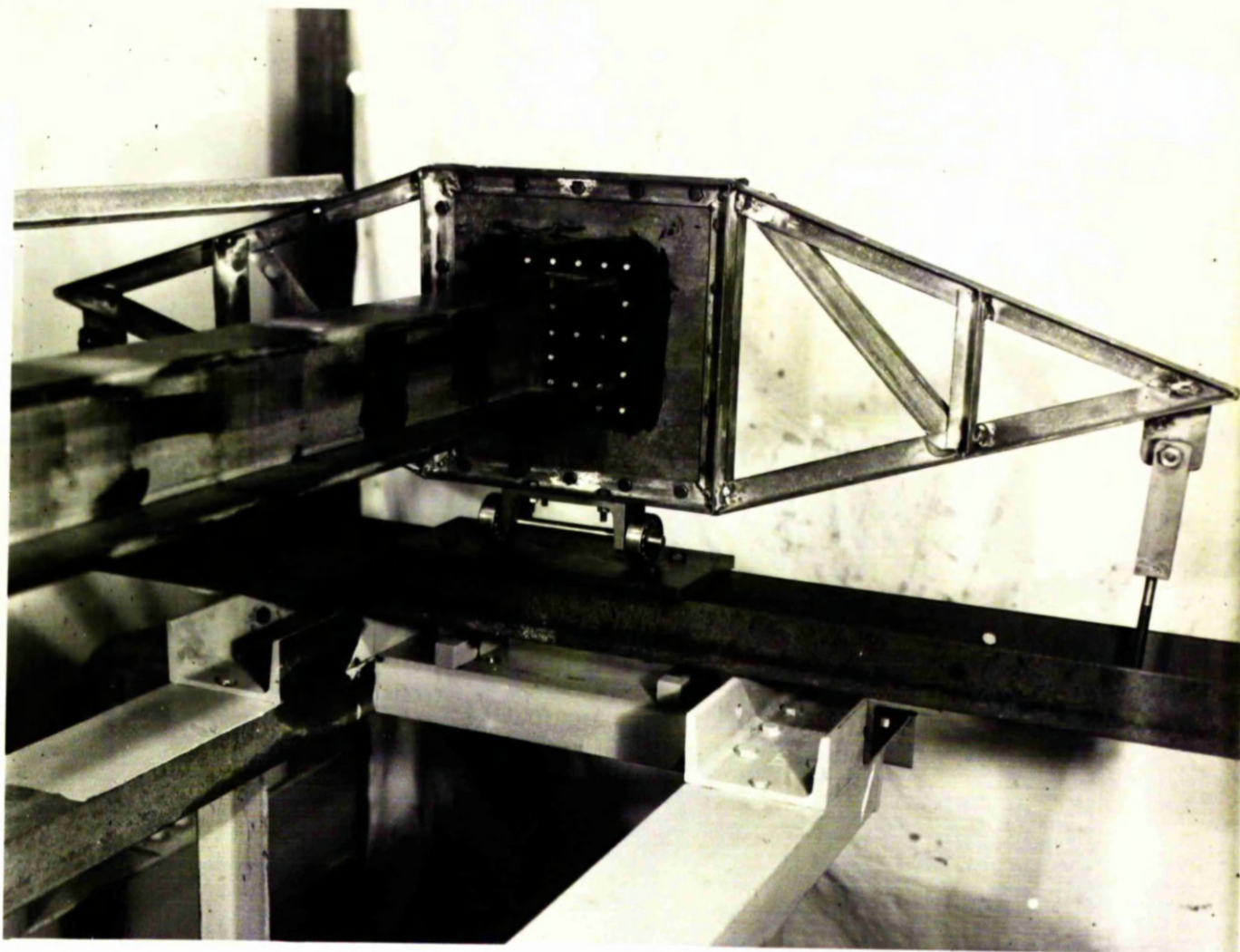


FIG. III.3 DETAIL OF ALUMINIUM ALLOY DIAPHRAGM
SUPPORT USED IN CHANNEL SECTION BEAM TESTS

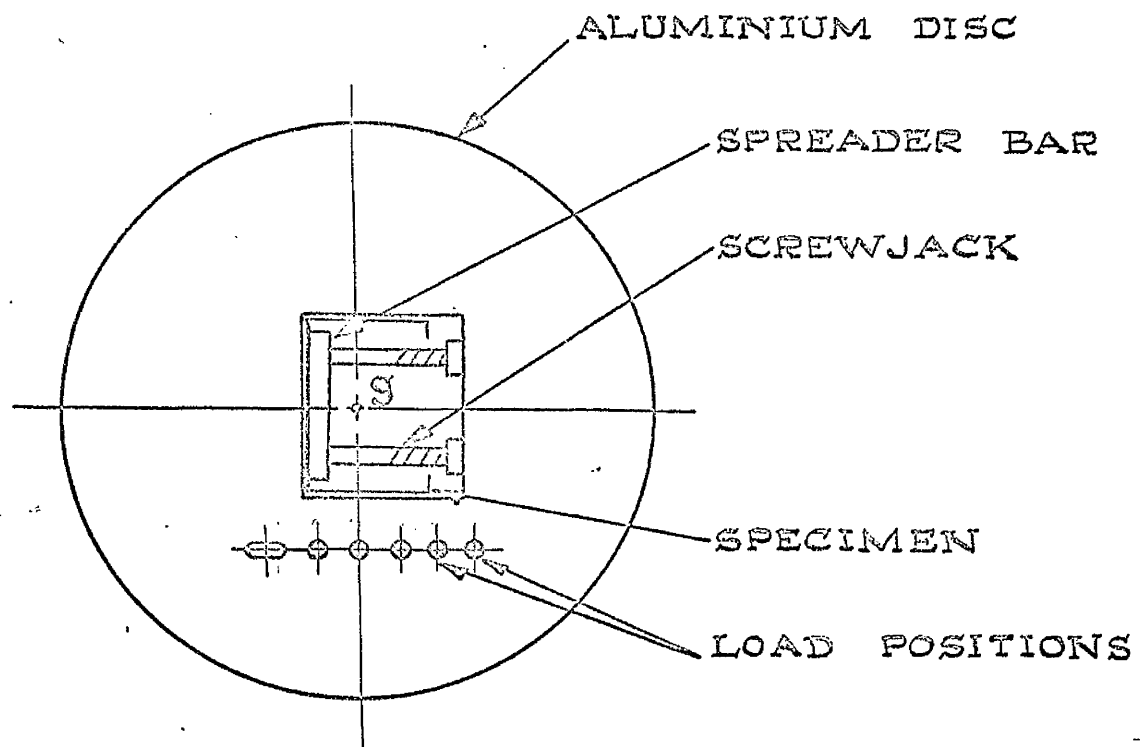


FIG. III. 4. DETAILS OF ALUMINIUM LOAD DISC.

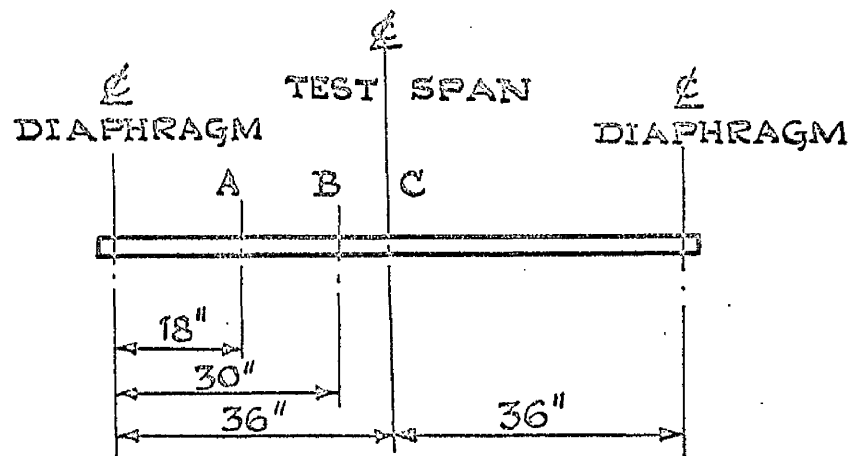
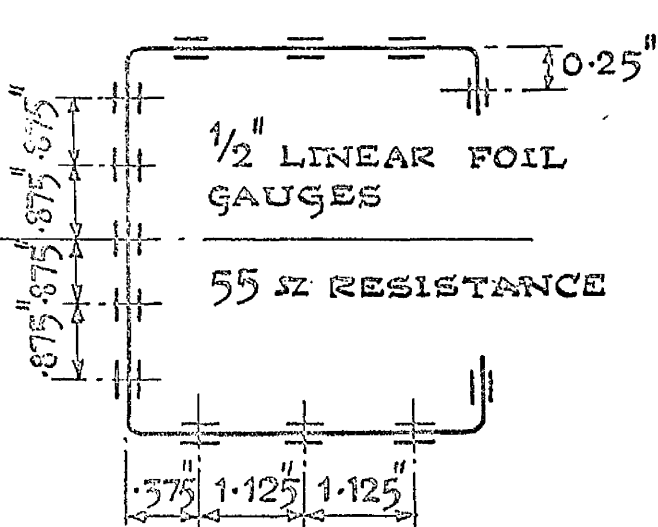


FIG. III. 5.

TEST BEAM CROSS-
SECTION SHOWING
STRAIN GAUGE POSITIONS.

LOCATION OF STRAIN
GAUGED SECTIONS ON
TEST BEAM.

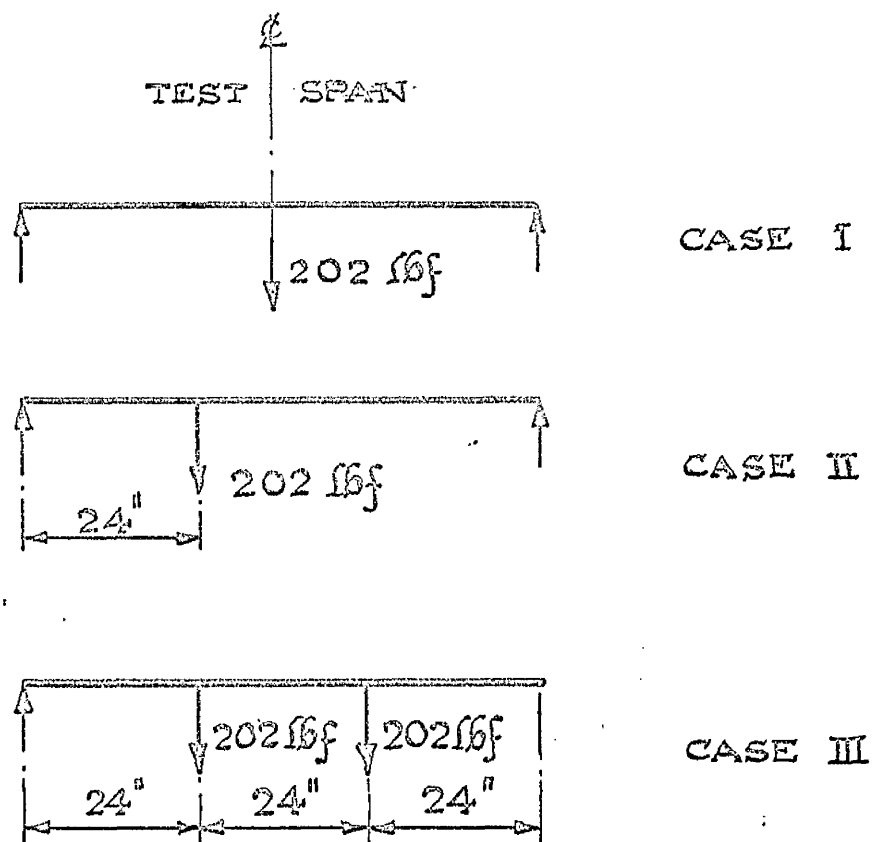


FIG. III.6. LOAD POSITIONS FOR THE THIN - WALLED LIPPED CHANNEL SECTION BEAM TESTS.

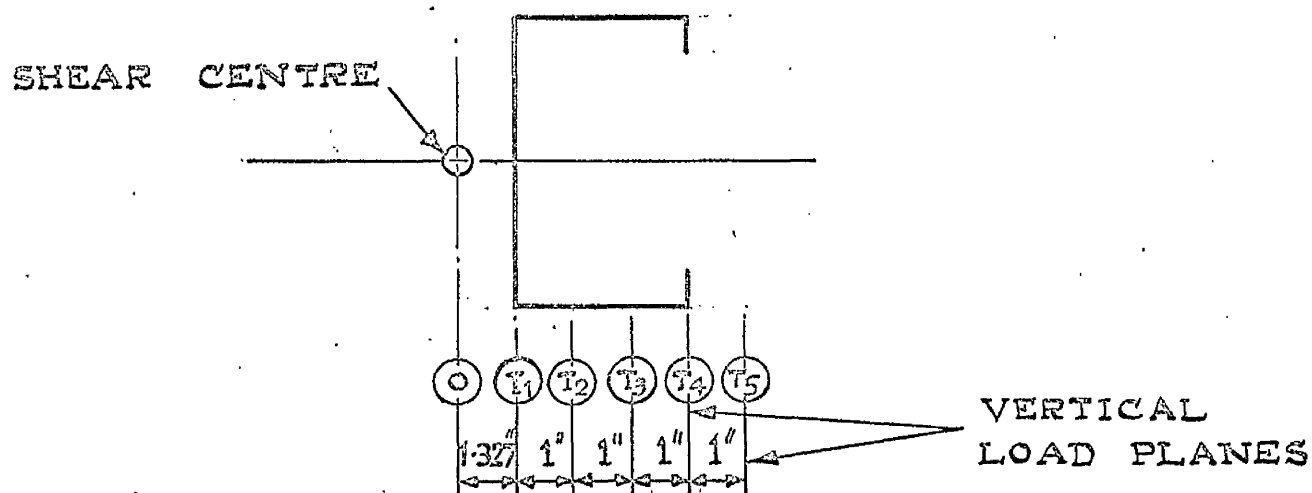


FIG. III.7. LOCATION OF VERTICAL LOAD PLANES FOR THE THIN - WALLED LIPPED CHANNEL SECTION BEAM TESTS.

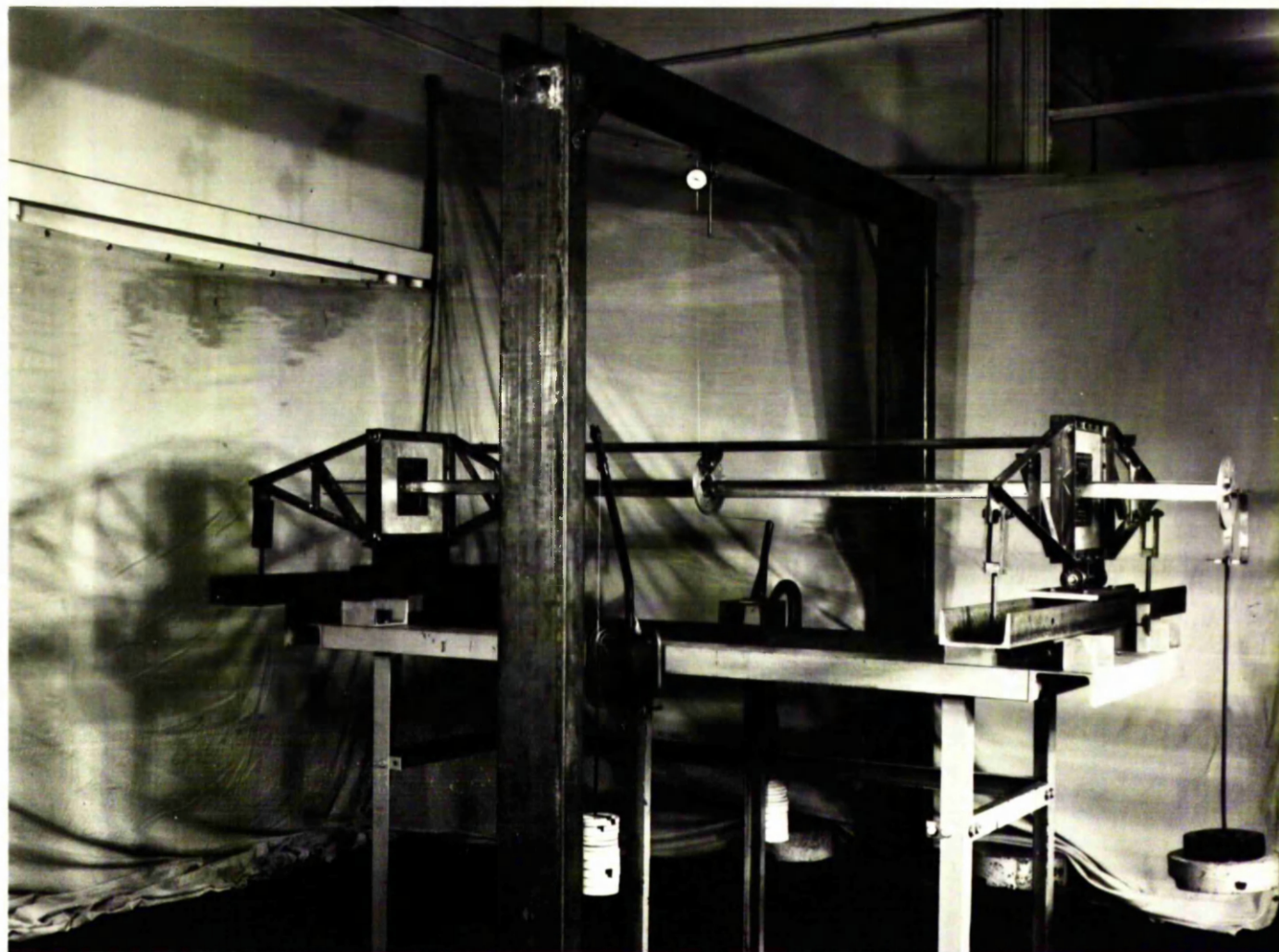


FIG. III.8 EXPERIMENTAL APPARATUS FOR
FLEXURAL-TORSIONAL TESTS ON CHANNEL
SECTION BEAMS

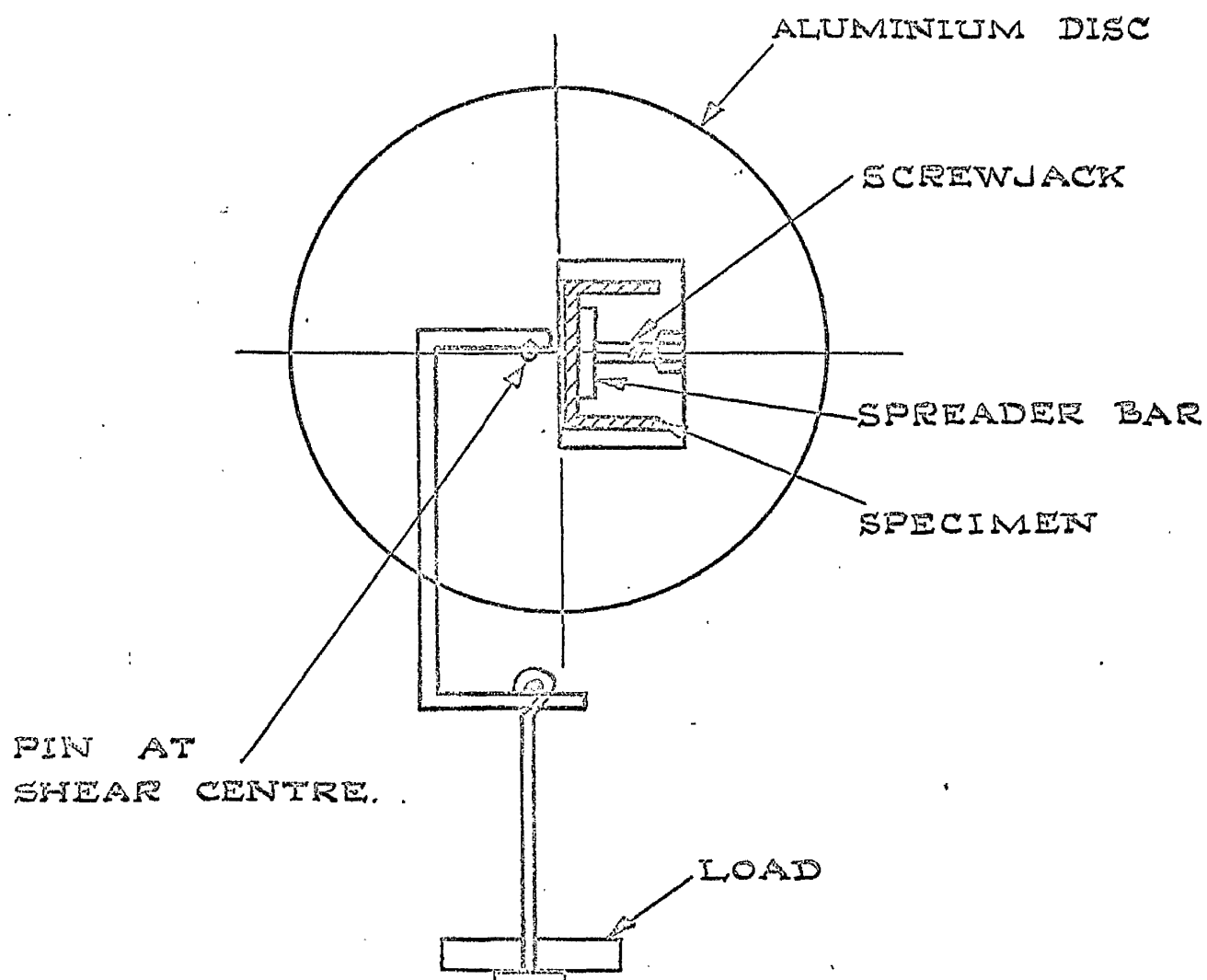


FIG.III.9. LOADING ARRANGEMENT USED TO APPLY VERTICAL LOADS AT THE SHEAR CENTRE IN THE SMALL THIN-WALLED CHANNEL SECTION BEAM TESTS.

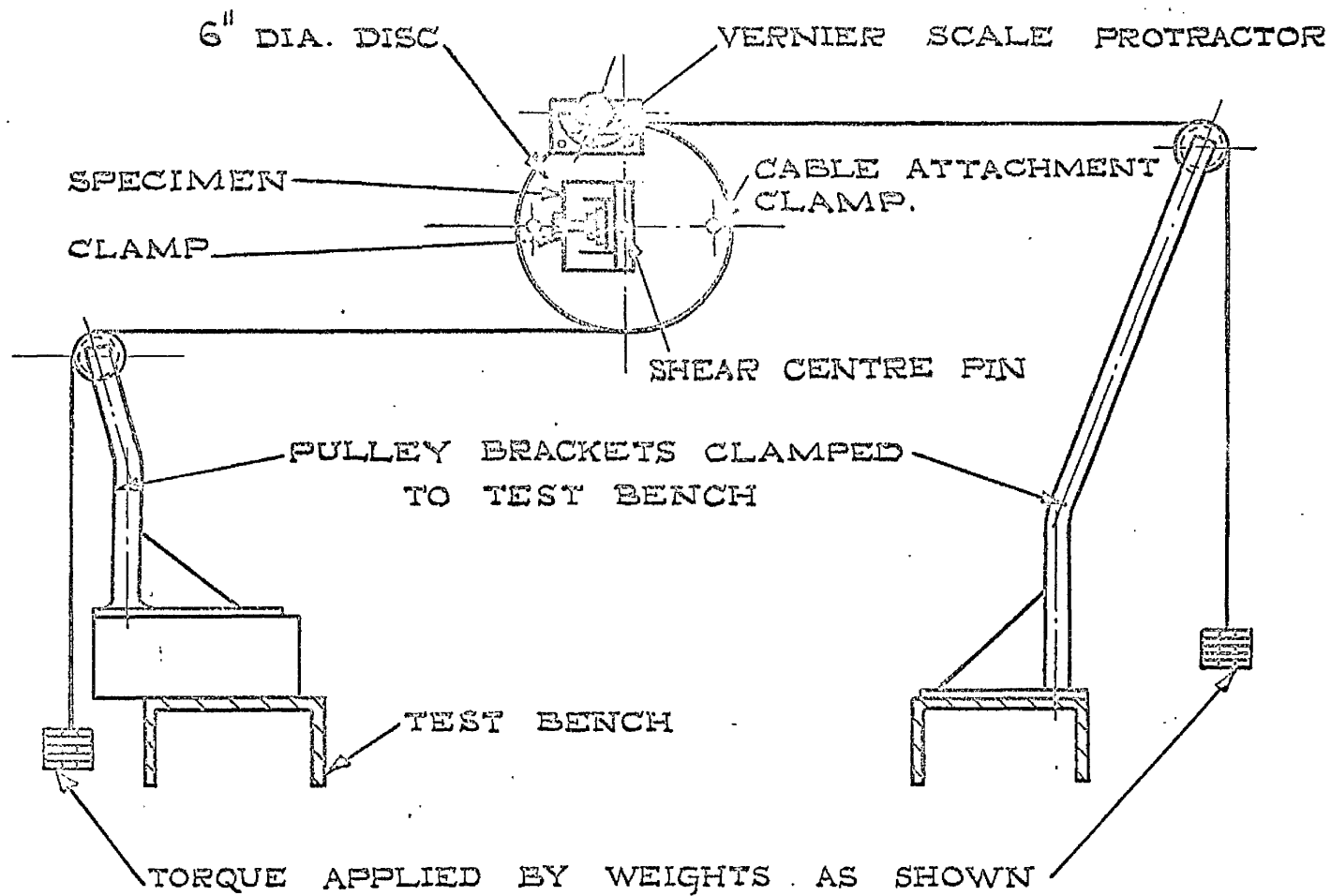


FIG. III.10. PULLEY WHEEL AND CABLE SYSTEM USED TO APPLY TORQUE ABOUT THE SHEAR CENTRE IN THE SMALL THIN - WALLED CHANNEL SECTION BEAM TESTS.

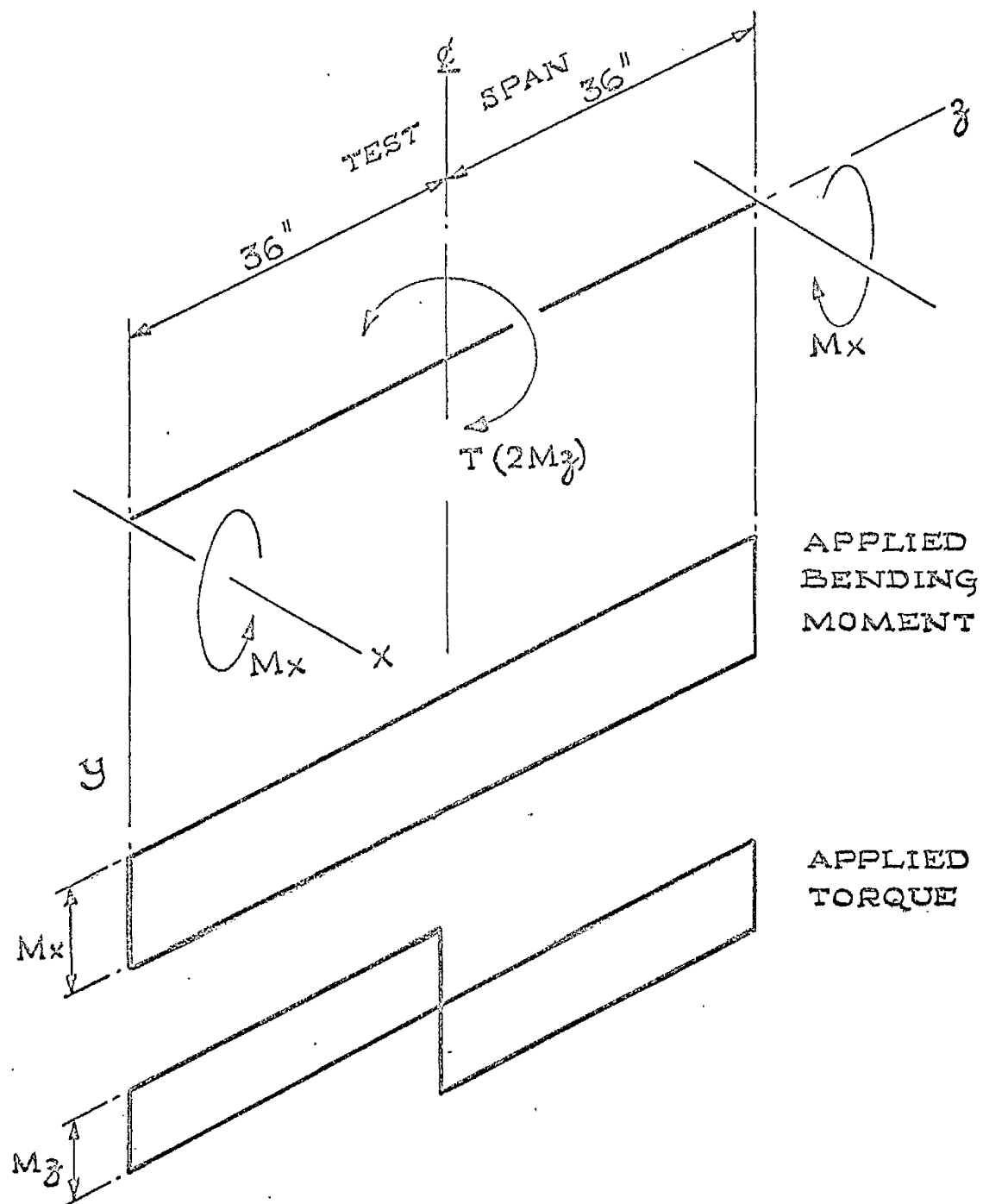


FIG. III. 11 COMBINED BENDING MOMENT AND TORQUE ACTIONS AS APPLIED IN THE SMALL THIN - WALLED CHANNEL SECTION BEAM TESTS.

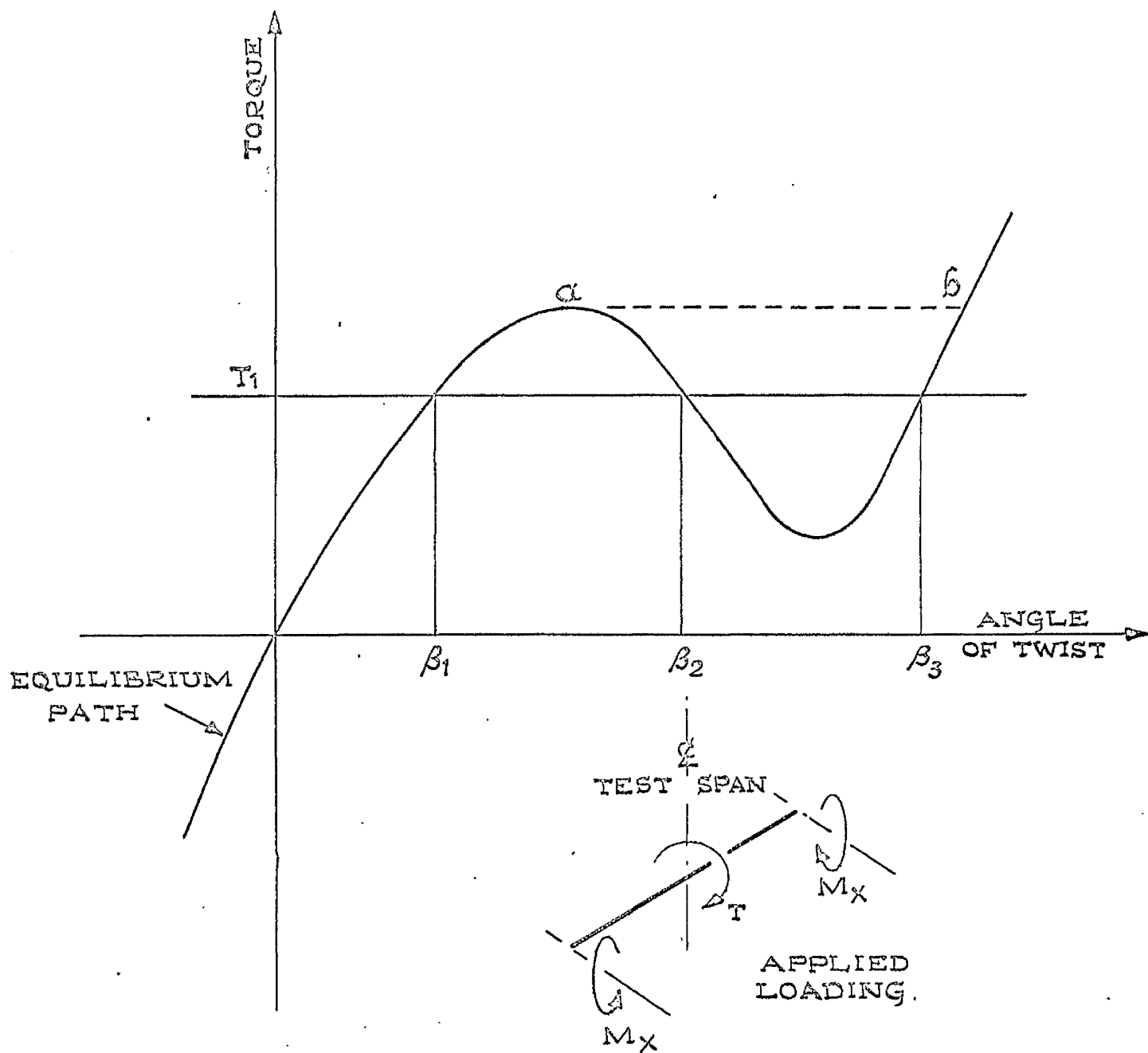


FIG. III. 12. TYPICAL NONLINEAR TORQUE / ANGLE OF TWIST EQUILIBRIUM PATH.

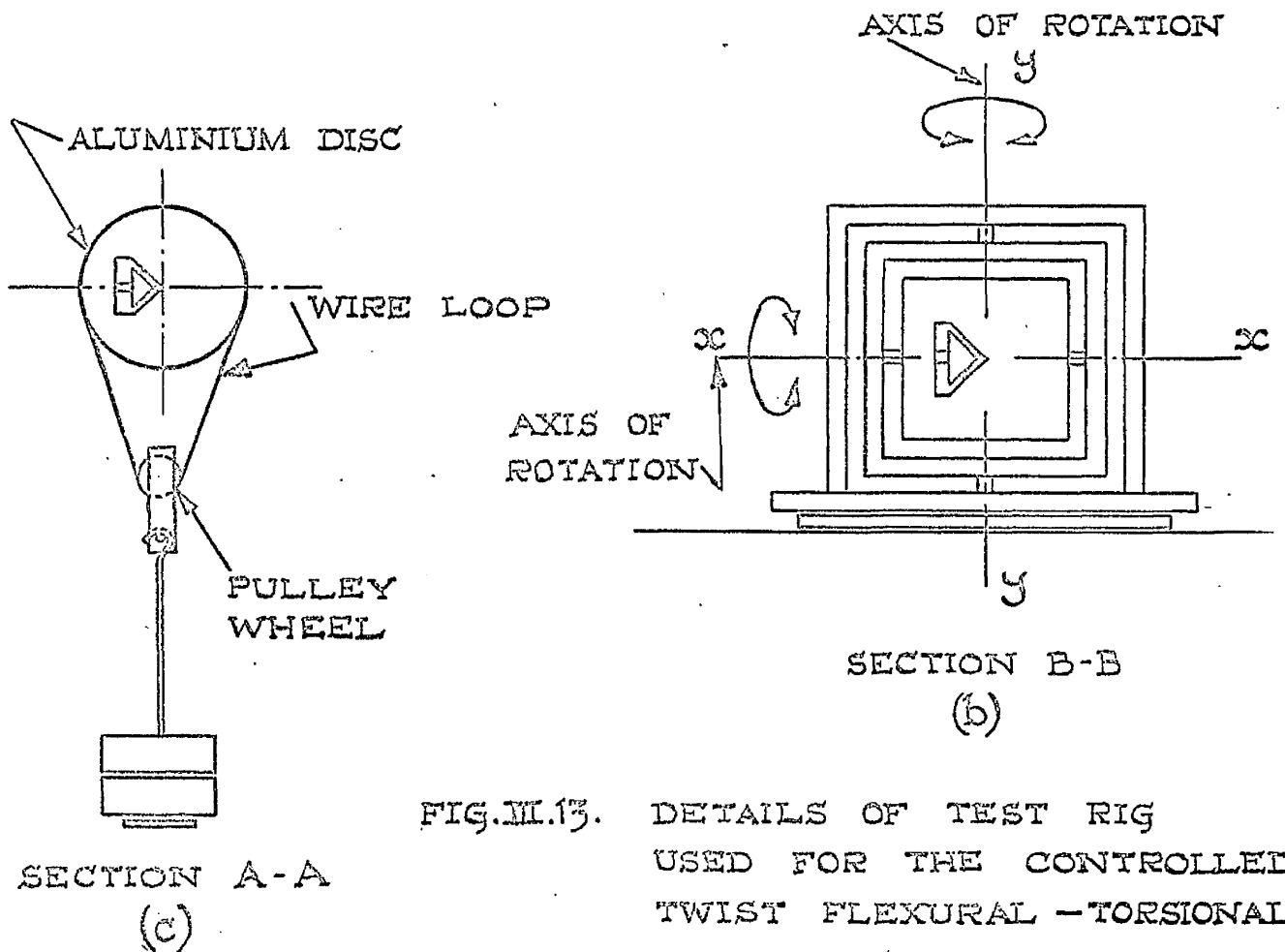
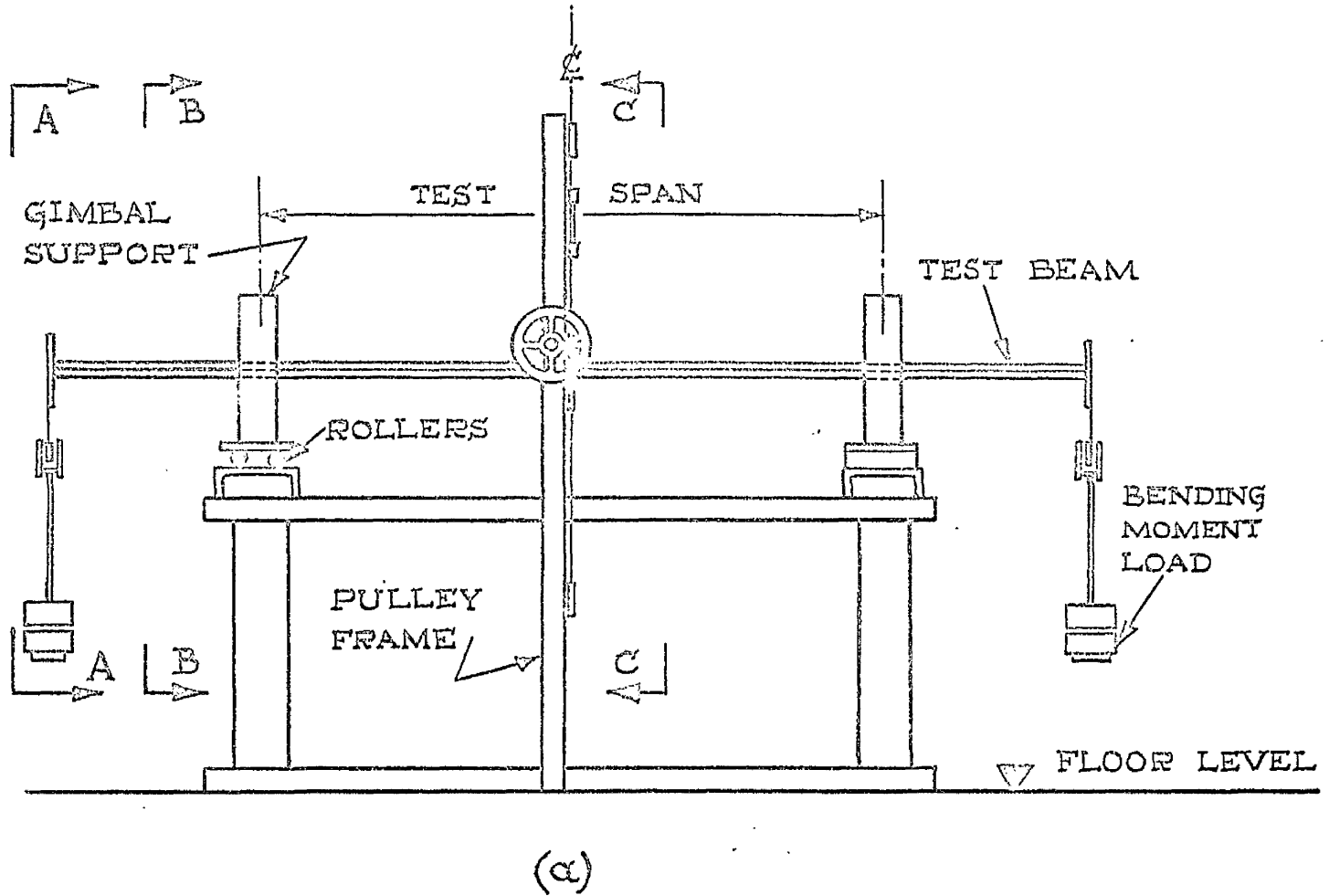
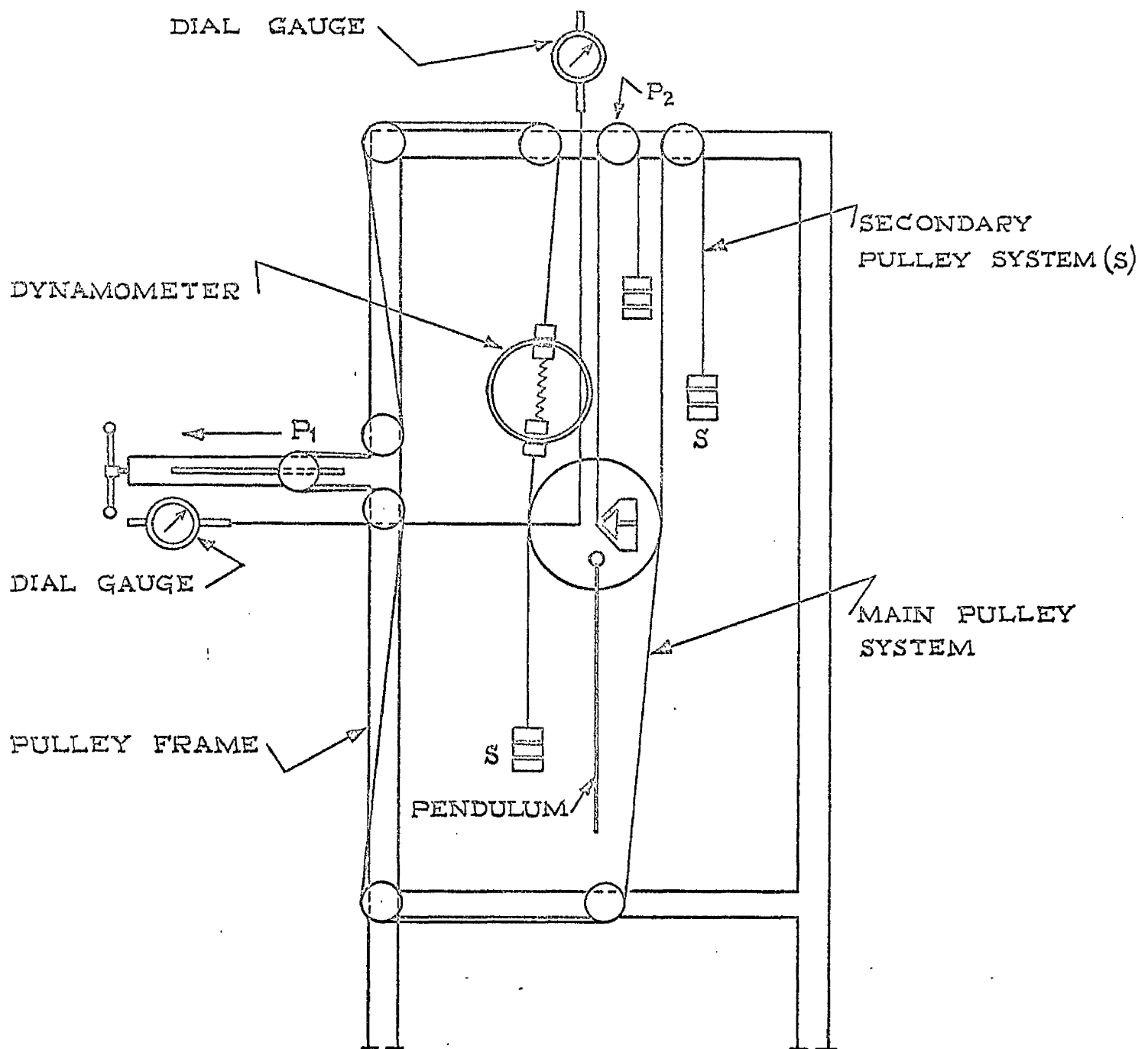


FIG. III.13. DETAILS OF TEST RIG
USED FOR THE CONTROLLED
TWIST FLEXURAL - TORSIONAL
BEAM TESTS.



SECTION C-C

FIG. III. 14. DETAILS OF THE PULLEY SYSTEMS USED IN THE CONTROLLED TWIST LOADING ARRANGEMENT.

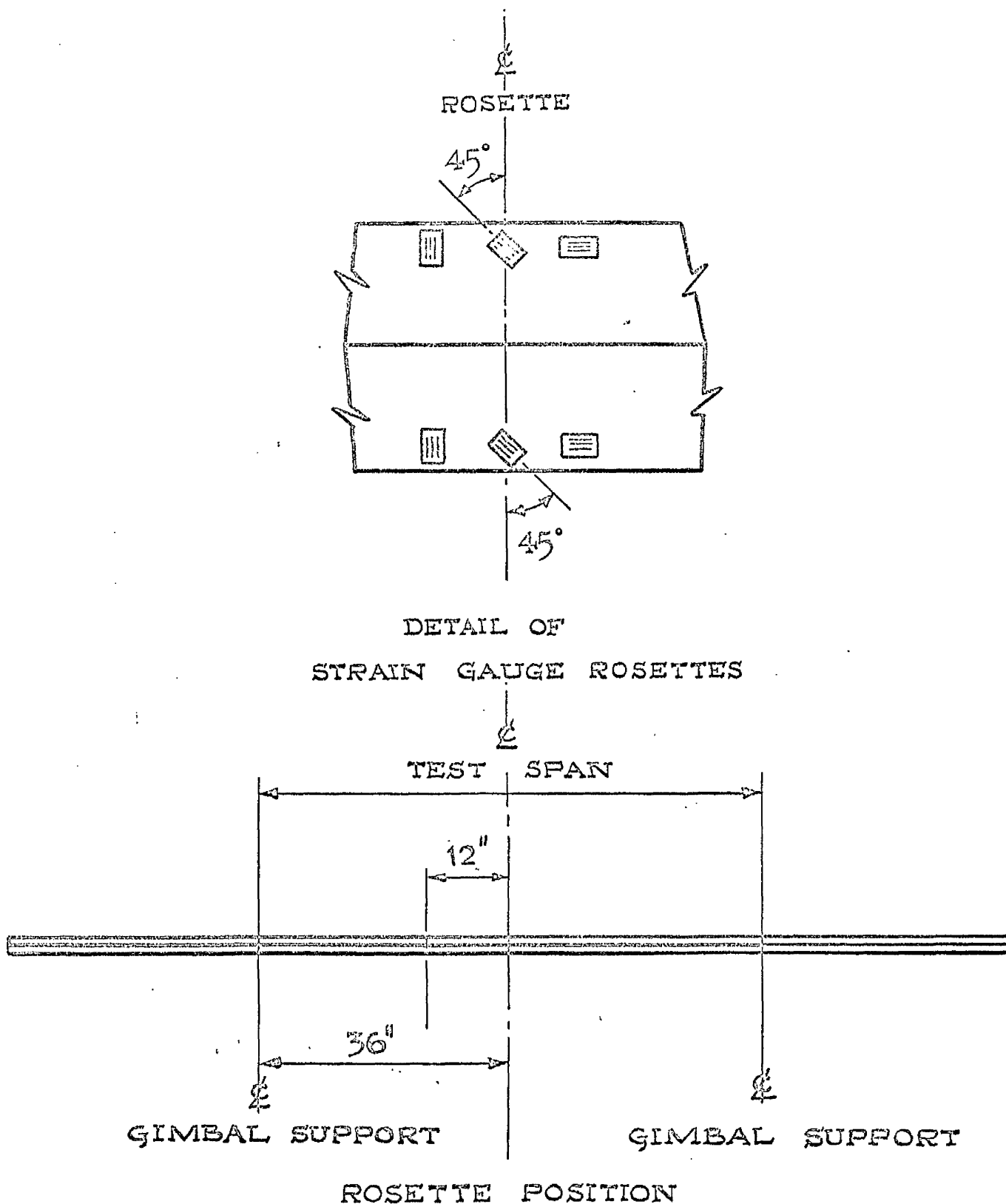


FIG.III.15. DETAILS OF STRAIN GAUGE ROSETTES AND LOCATION OF STRAIN GAUGED SECTIONS IN THE BRASS ANGLE TEST SPECIMENS.

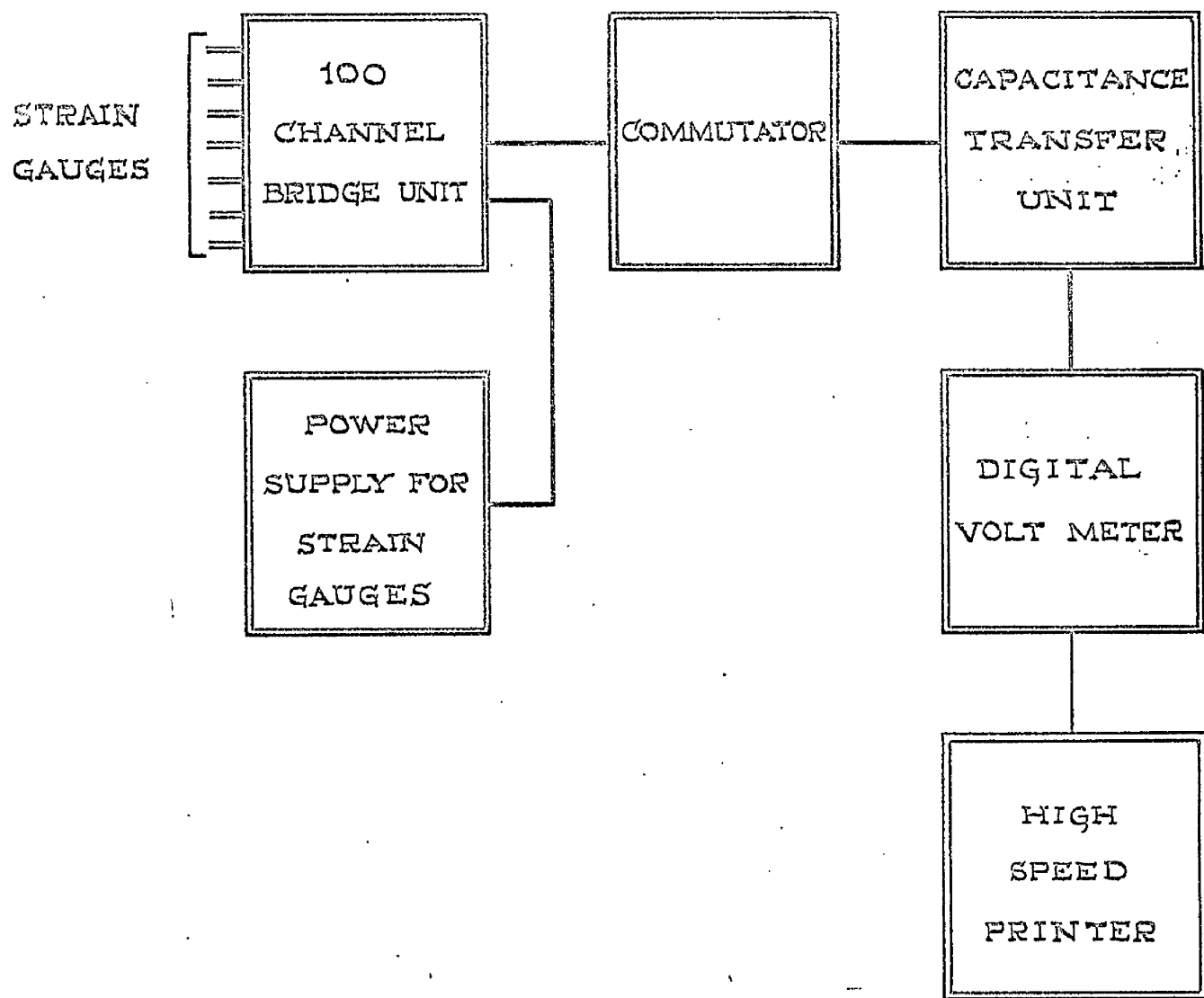


FIG . III. 16. BLOCK LAYOUT OF DATA LOGGING SYSTEM.

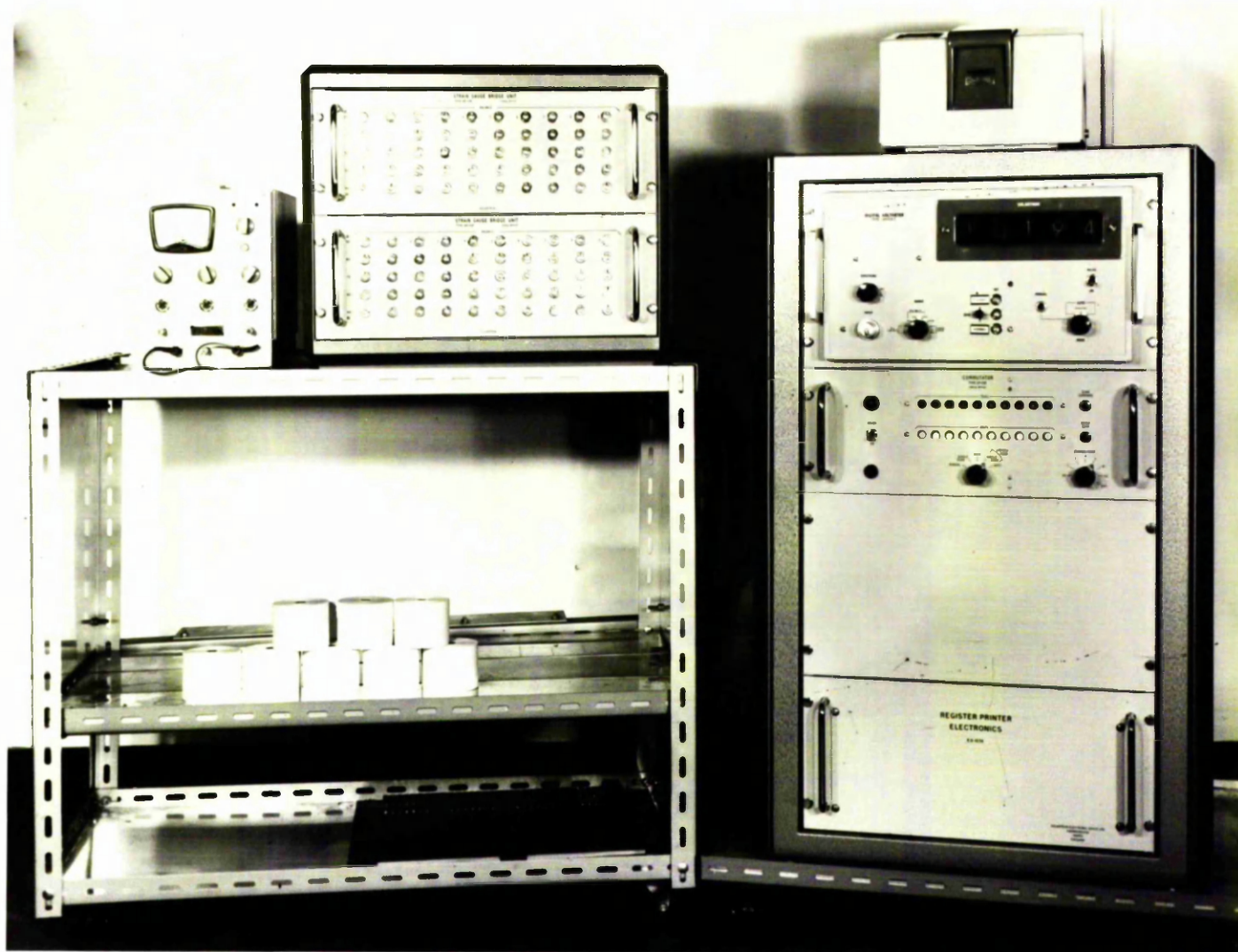


FIG. III.17 SOLARTRON DATA LOGGING EQUIPMENT

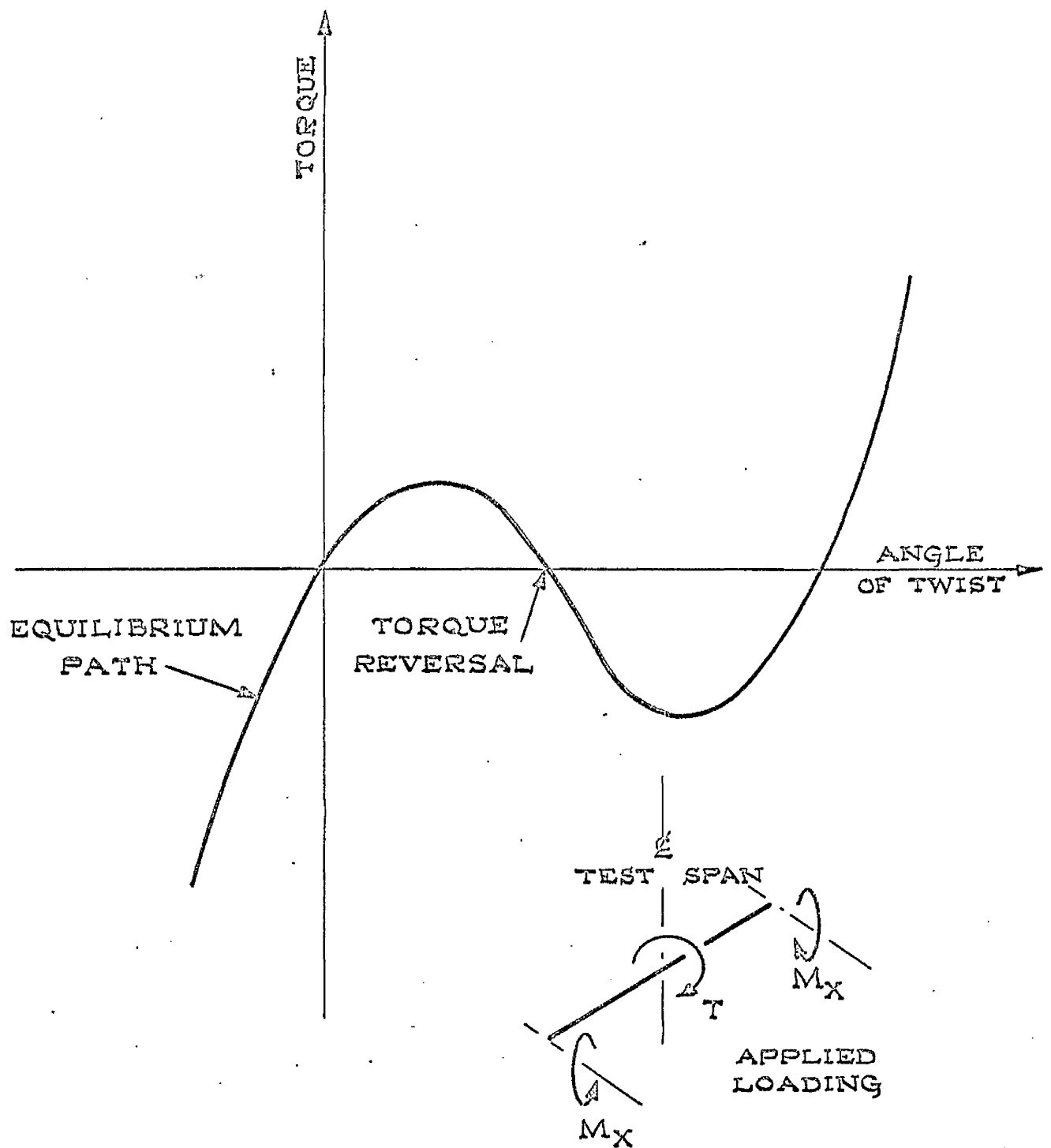


FIG. III. 18. TORQUE / ANGLE OF TWIST EQUILIBRIUM PATH AT LARGE VALUES OF BENDING MOMENT.

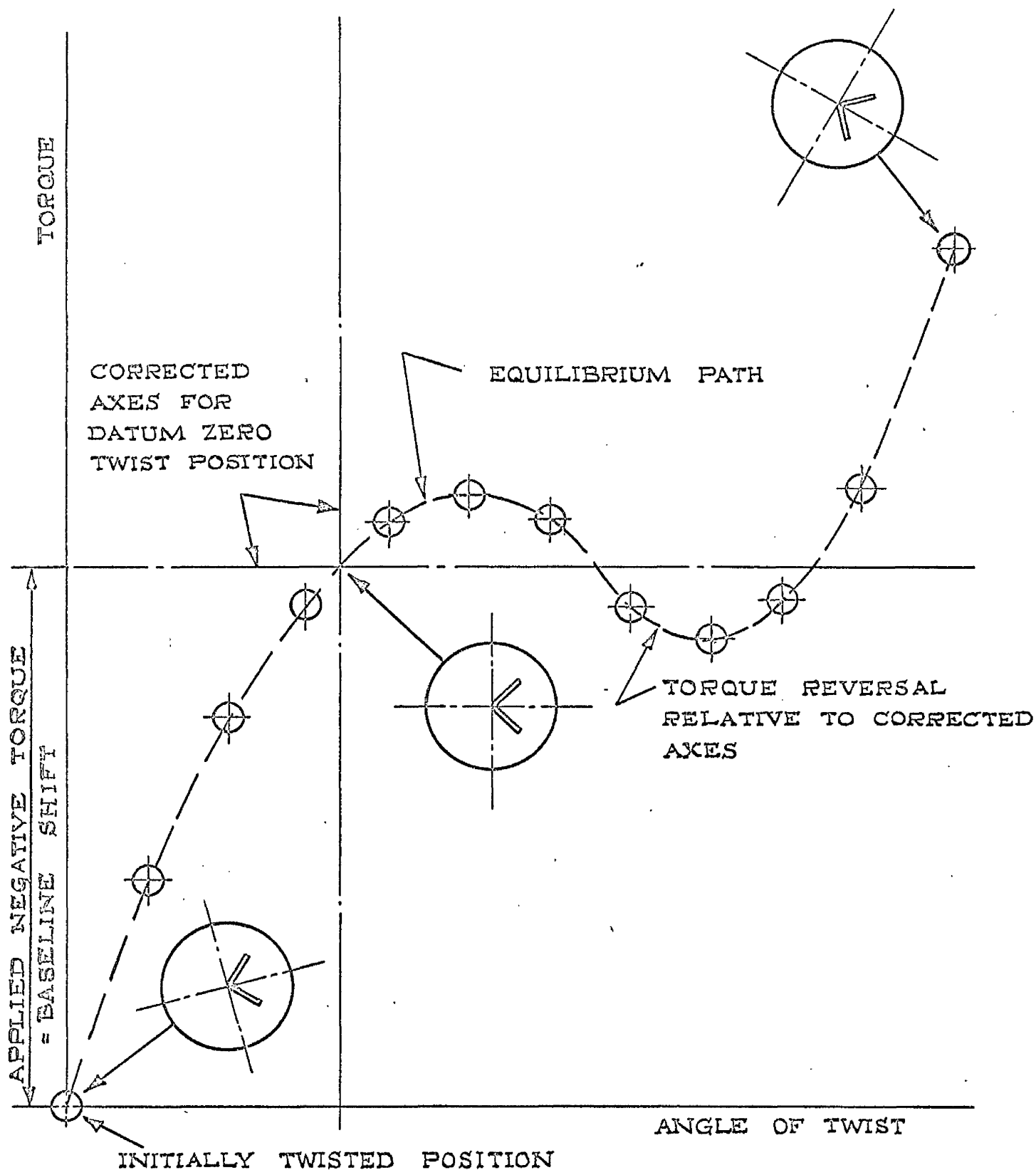


FIG. III. 19. DIAGRAMMATIC REPRESENTATION OF CONTROLLED TWIST TEST PROCEDURE.

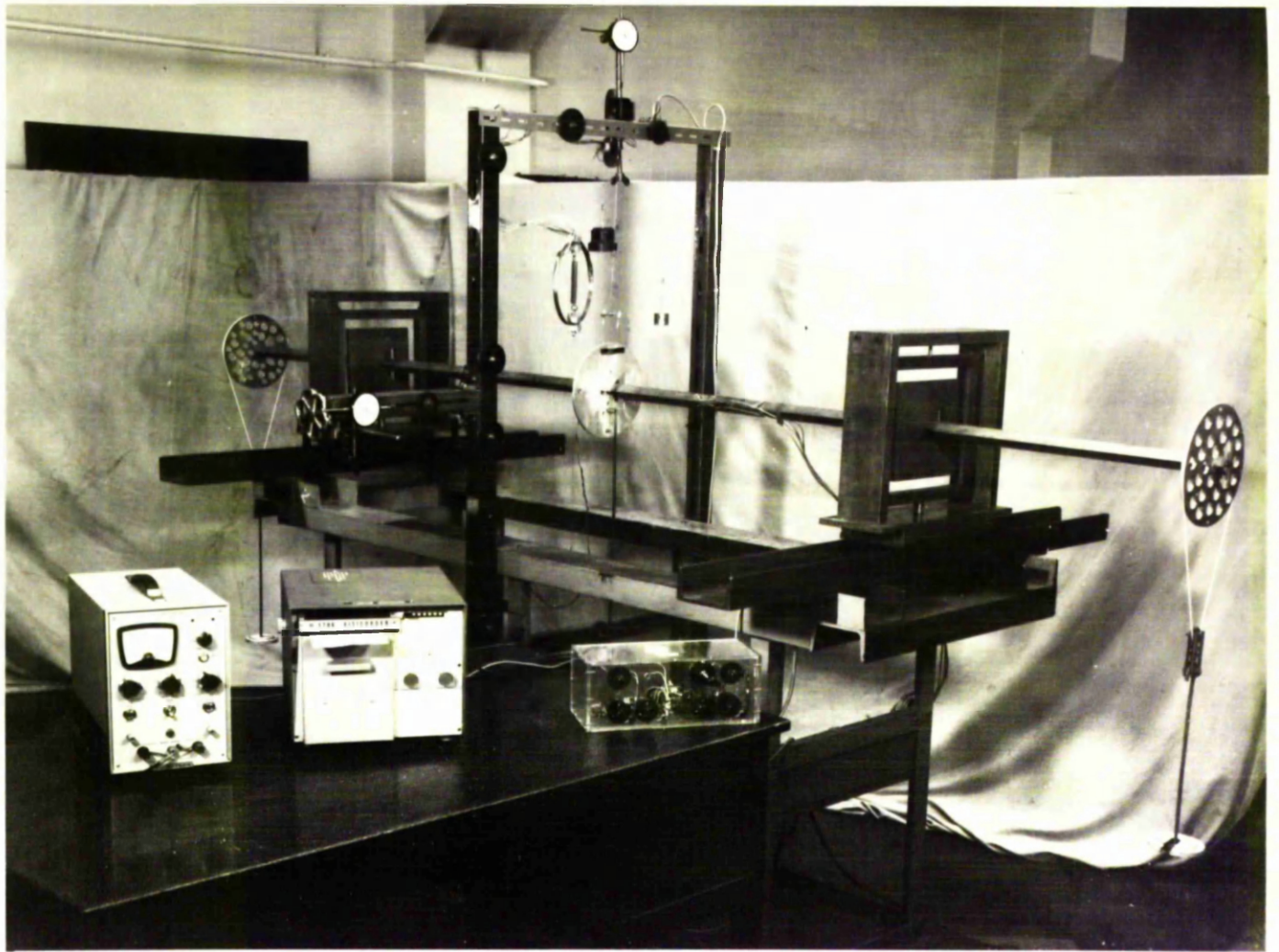


FIG. III.20 EXPERIMENTAL APPARATUS USED FOR
CONTROLLED TWIST TESTING PROCEDURE

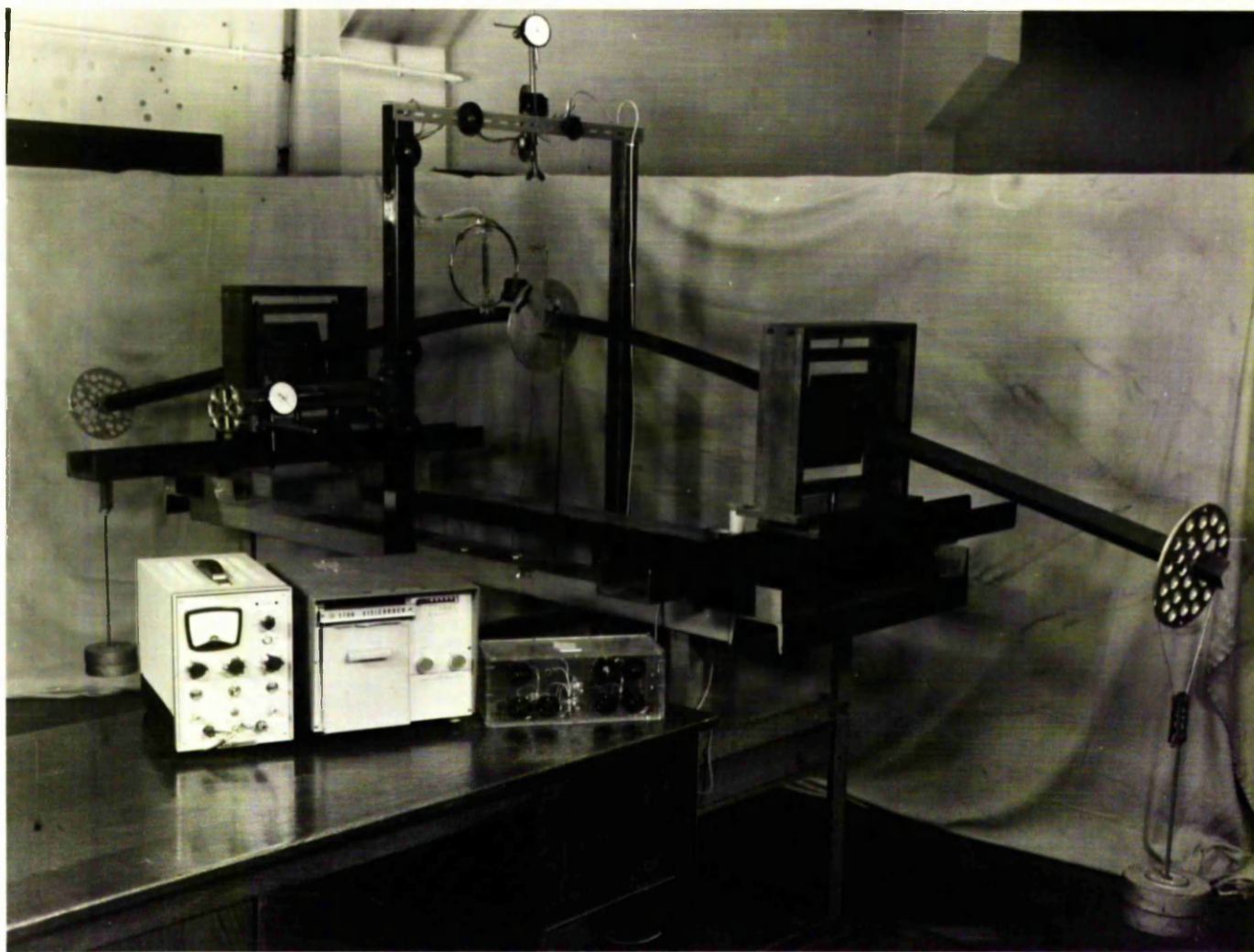


FIG. III.21 ANGLE SECTION BEAM AT FAILURE
DUE TO APPLIED BENDING MOMENT

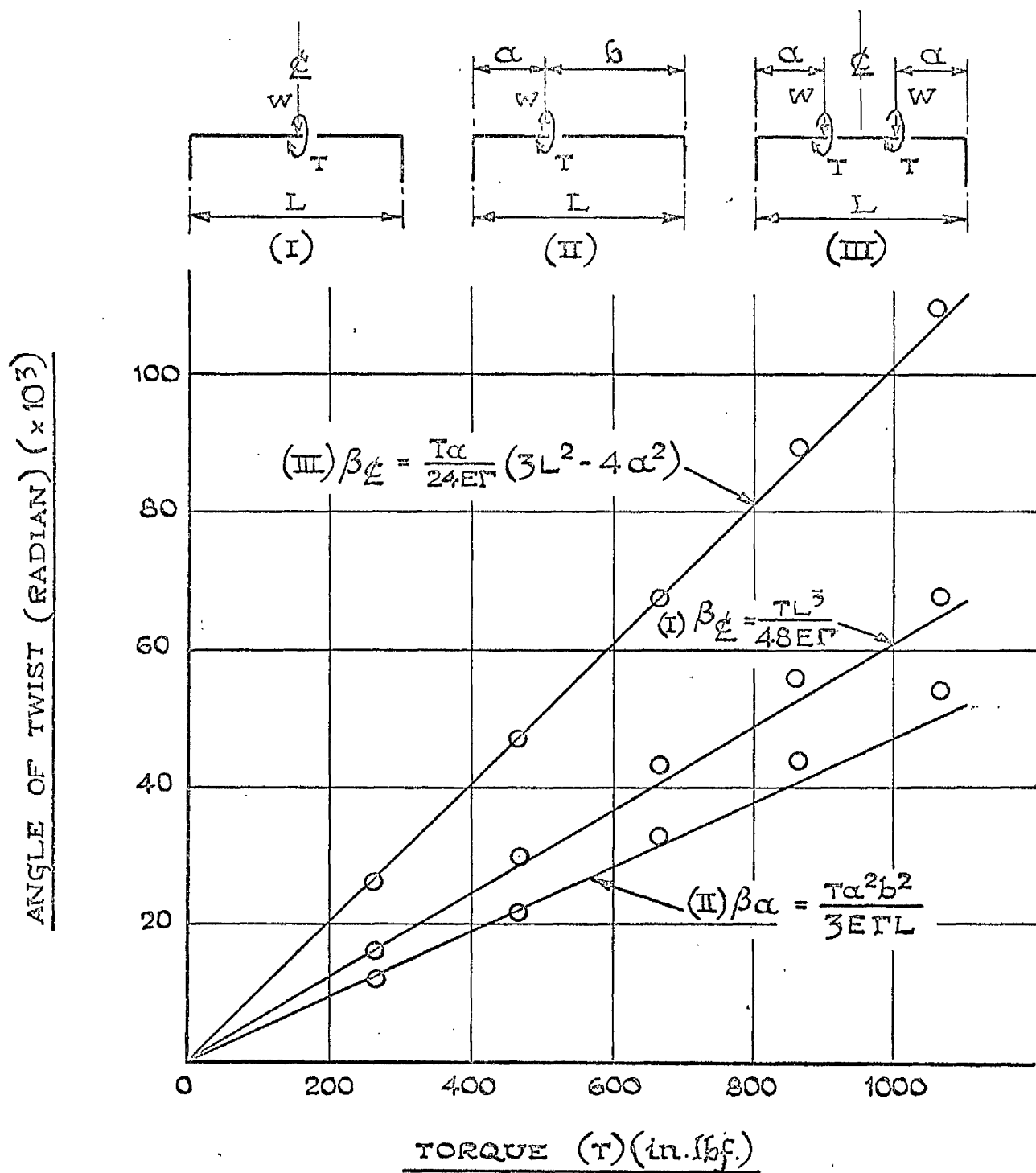
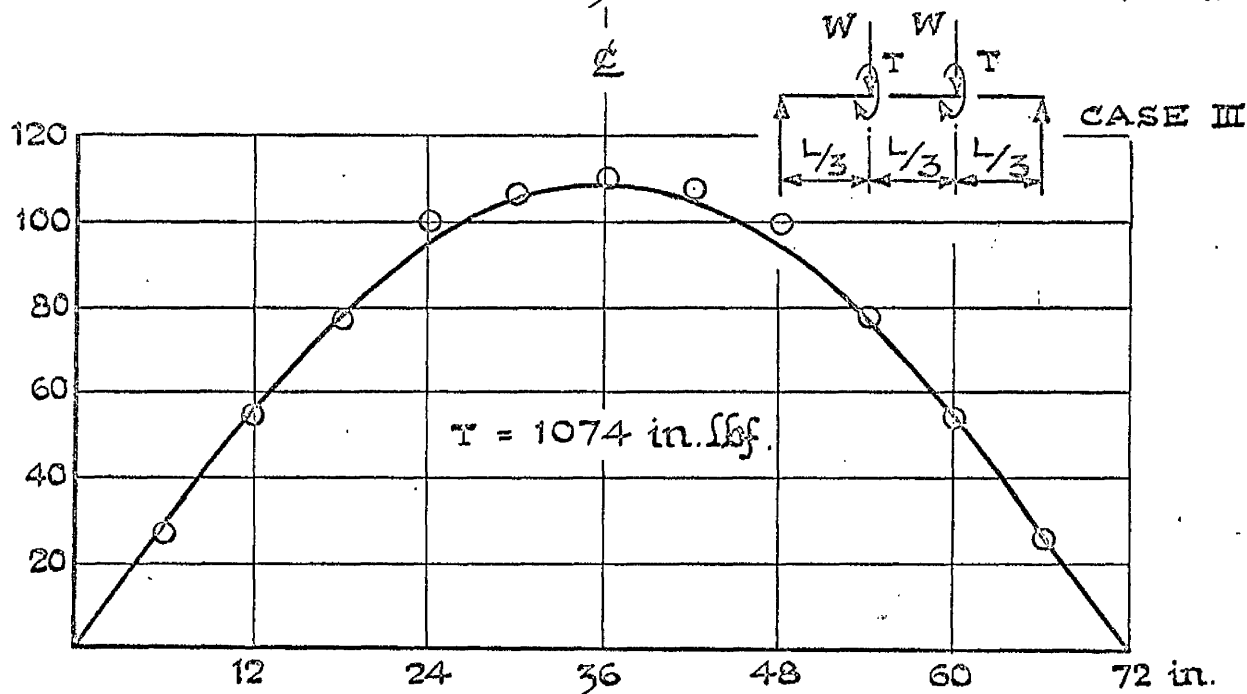
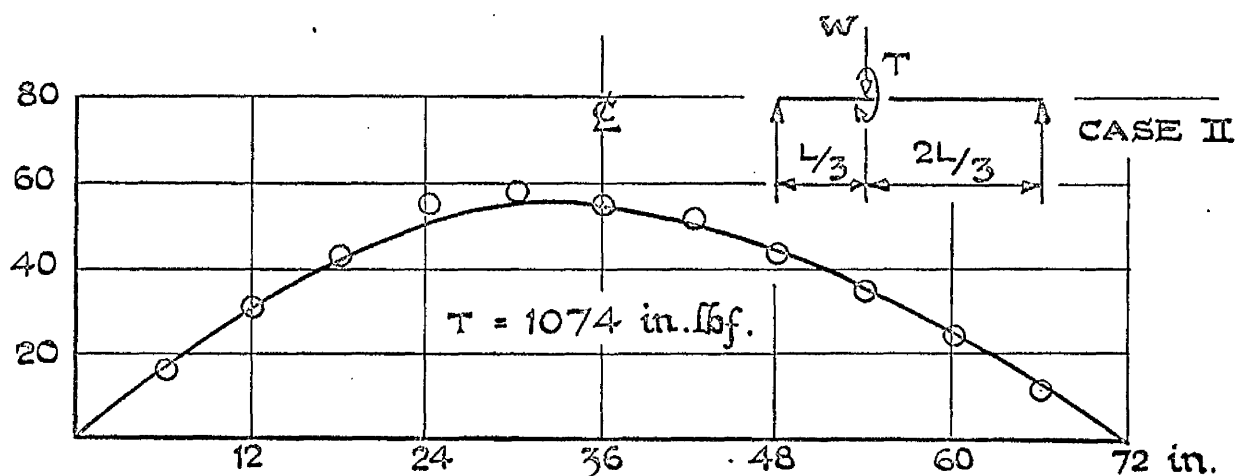
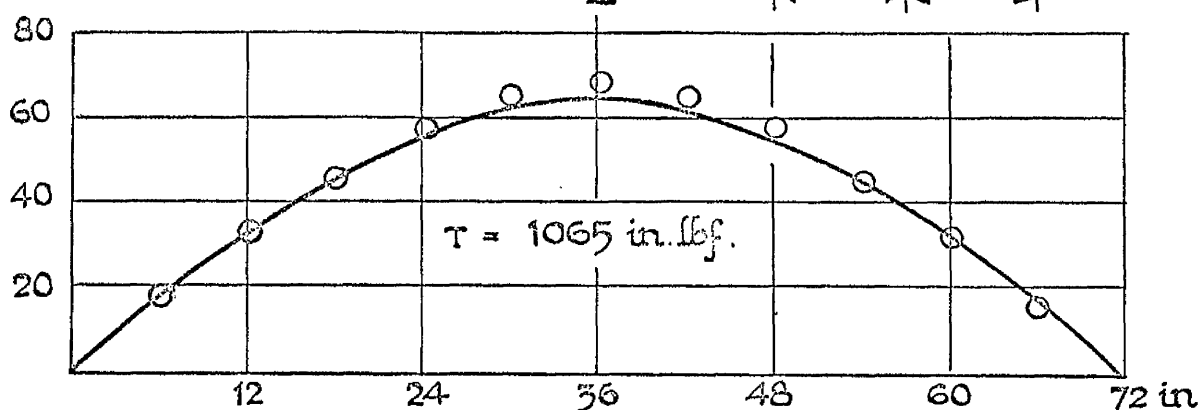


FIG. IV. 1. TYPICAL TORQUE / ANGLE OF TWIST RELATIONSHIPS FOR SMALL DISPLACEMENT BEHAVIOUR.



3' DISTANCE ALONG BEAM.

FIG. IV. 2. TYPICAL DISTRIBUTIONS OF ANGLE OF TWIST OVER TEST SPAN.

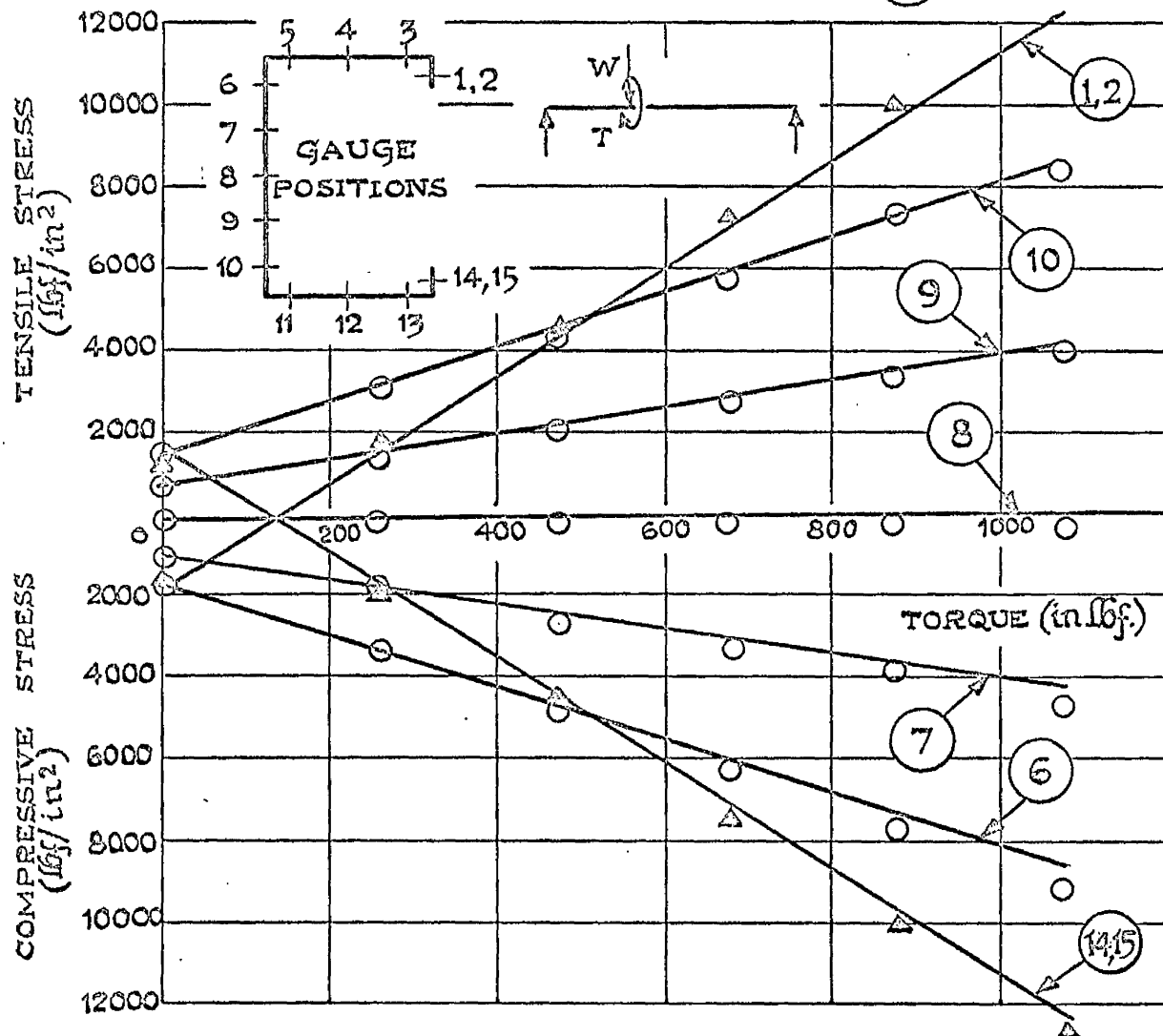
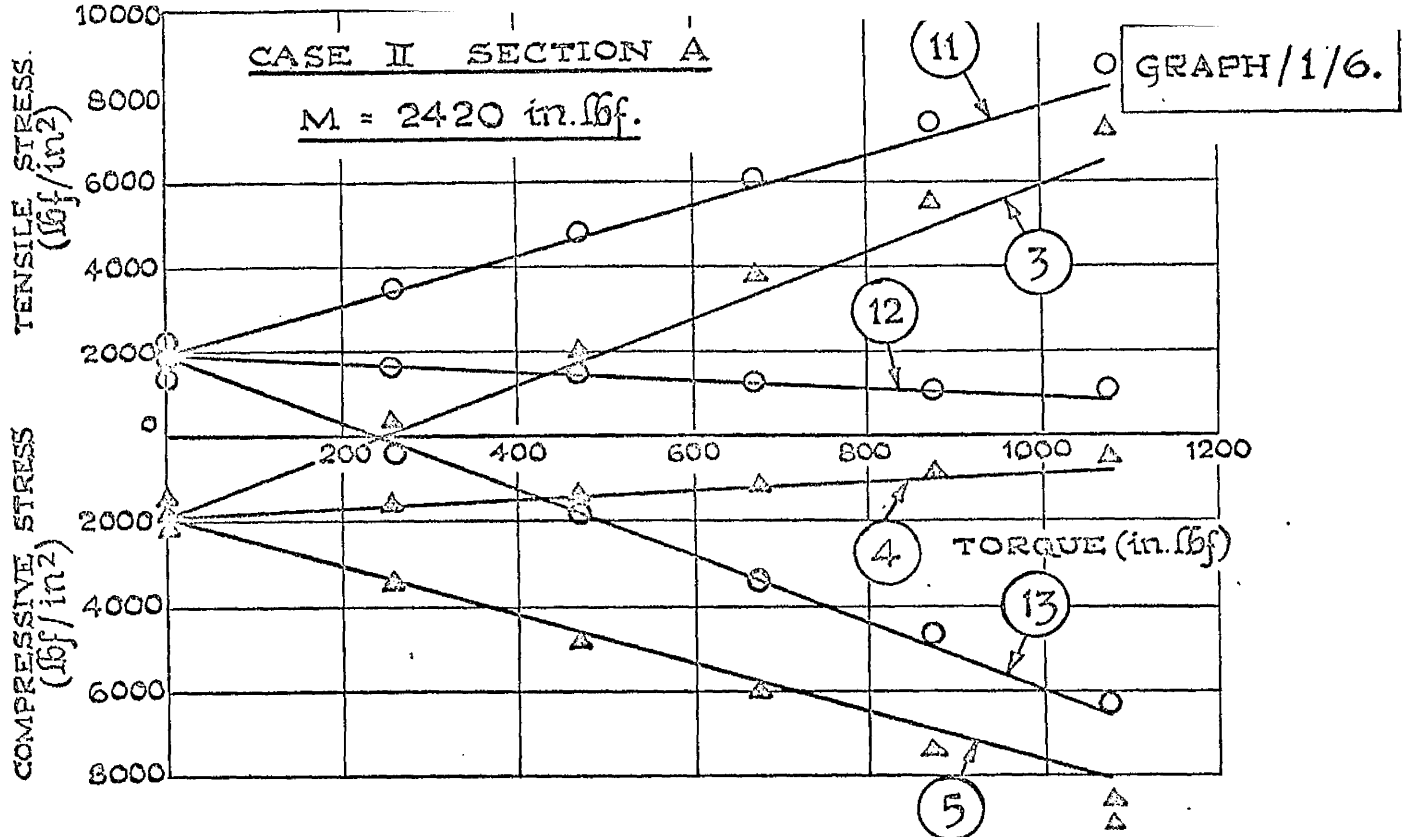


FIG. IV. 3. VARIATION OF LONGITUDINAL STRESS WITH TORQUE.

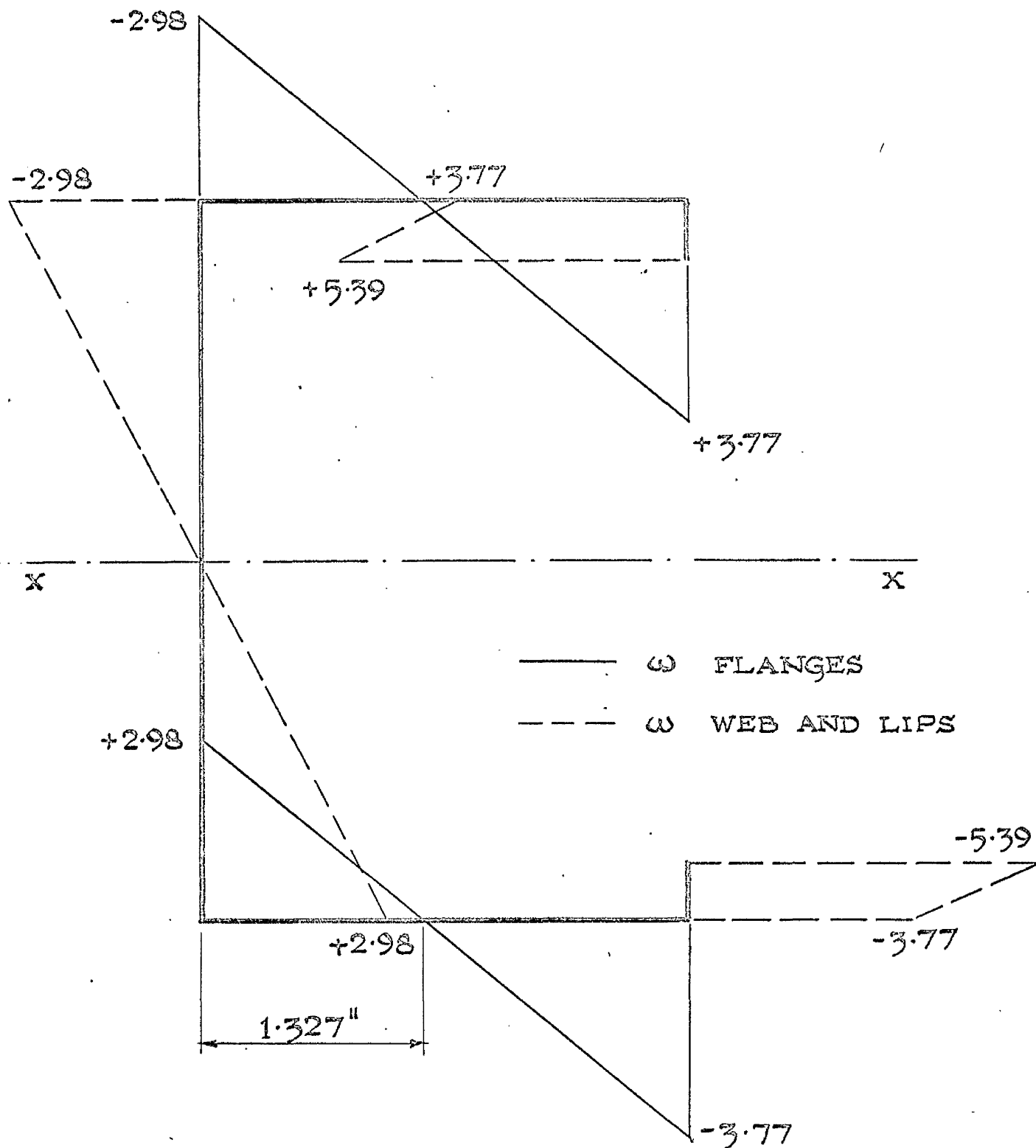


FIG. IV.4. VALUES OF THE SECTORIAL CO-ORDINATE ω FOR THE LIPPED CHANNEL SECTION.

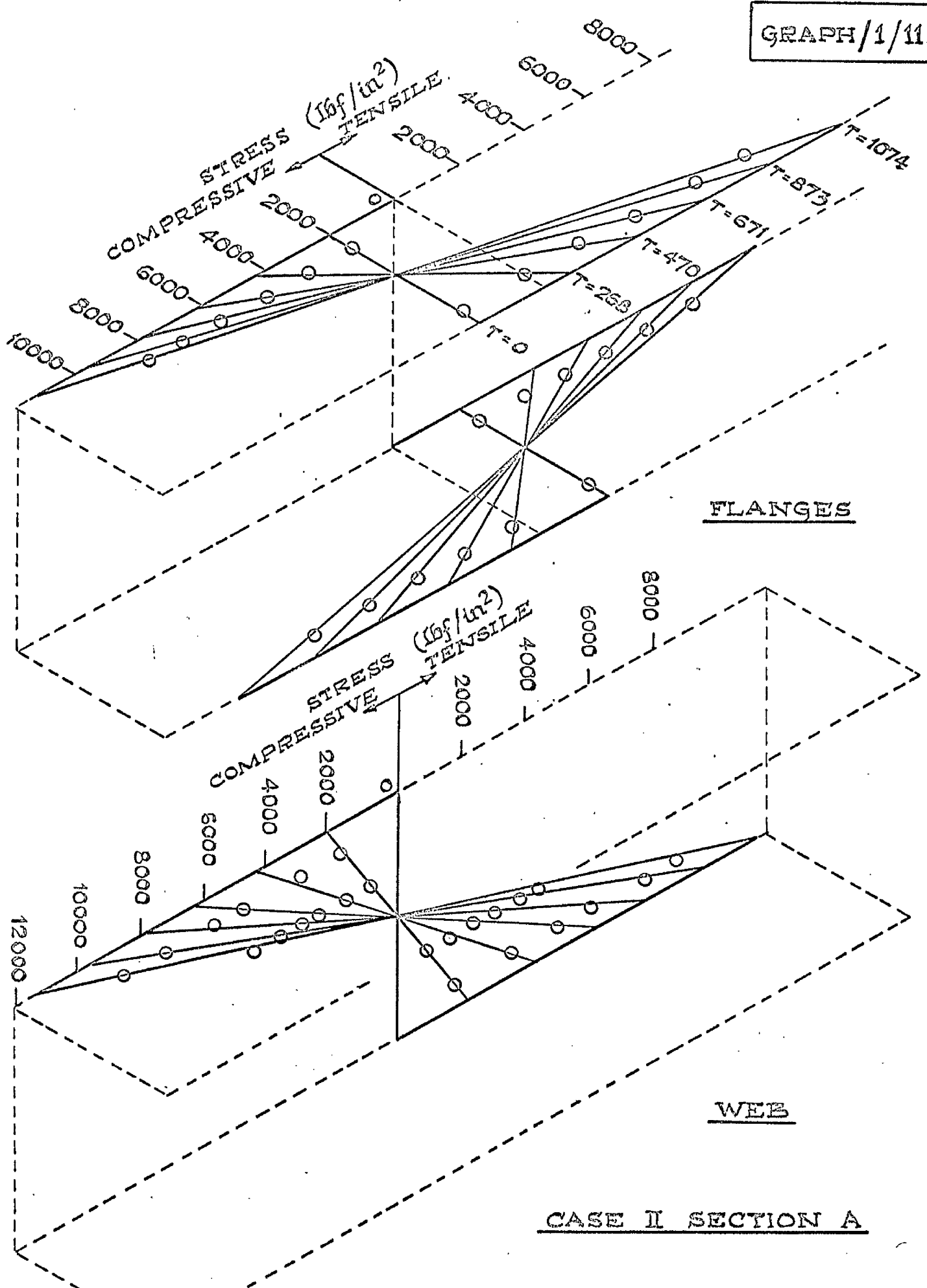
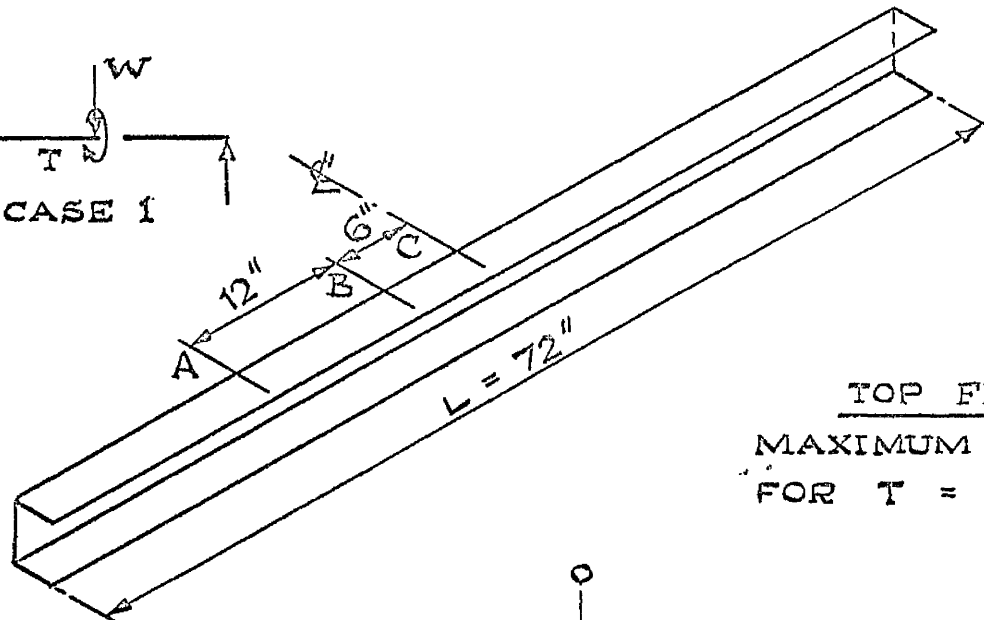
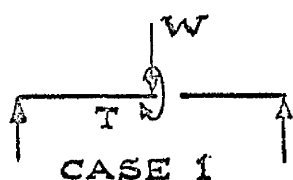


FIG. IV.5. LONGITUDINAL STRESS DISTRIBUTIONS.



TOP FLANGE.
MAXIMUM STRESSES
FOR $T = 1068 \text{ in. lb.}$

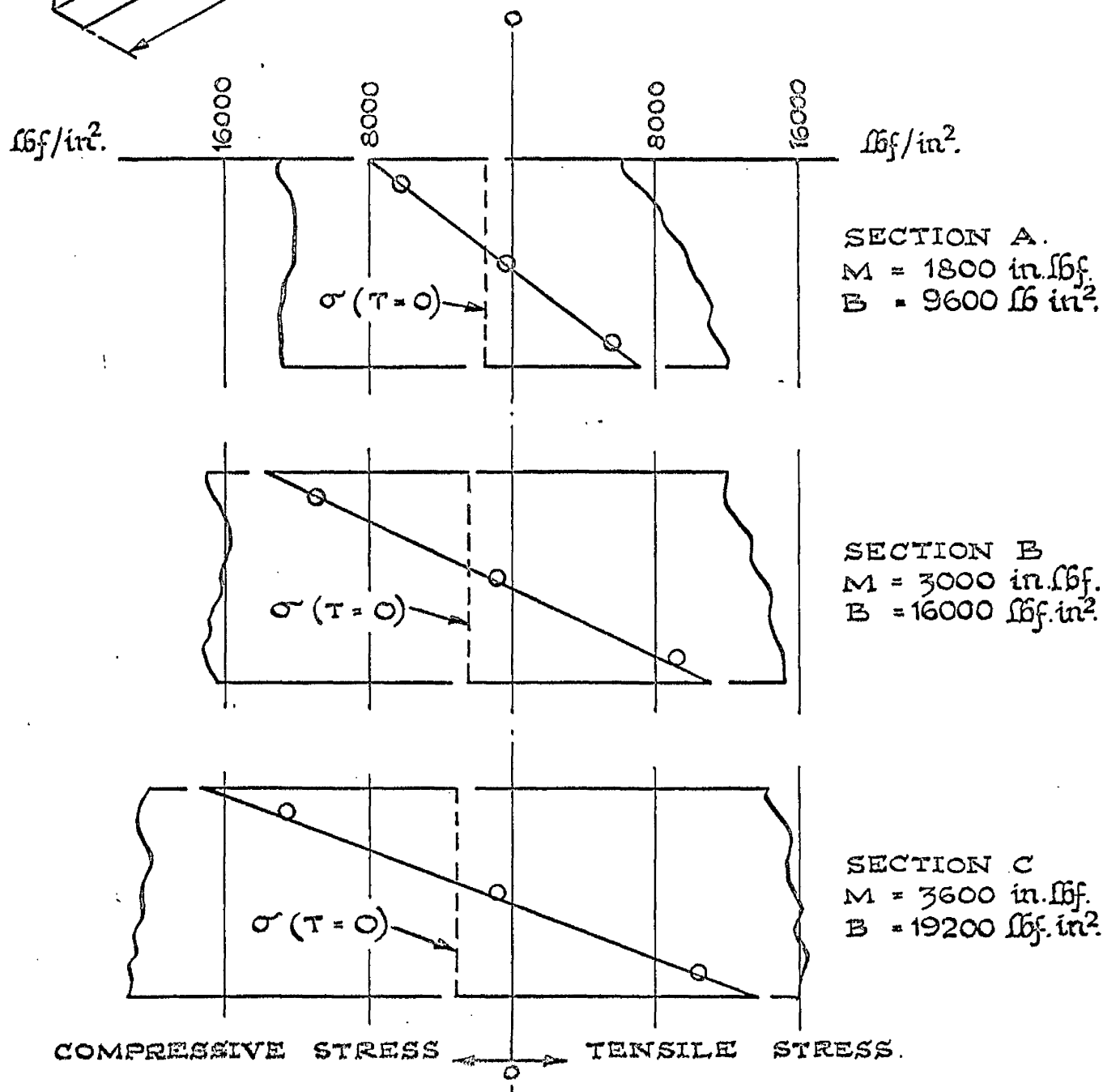


FIG. IV. 6. LONGITUDINAL STRESS DISTRIBUTIONS
AT DIFFERENT CROSS - SECTIONS.

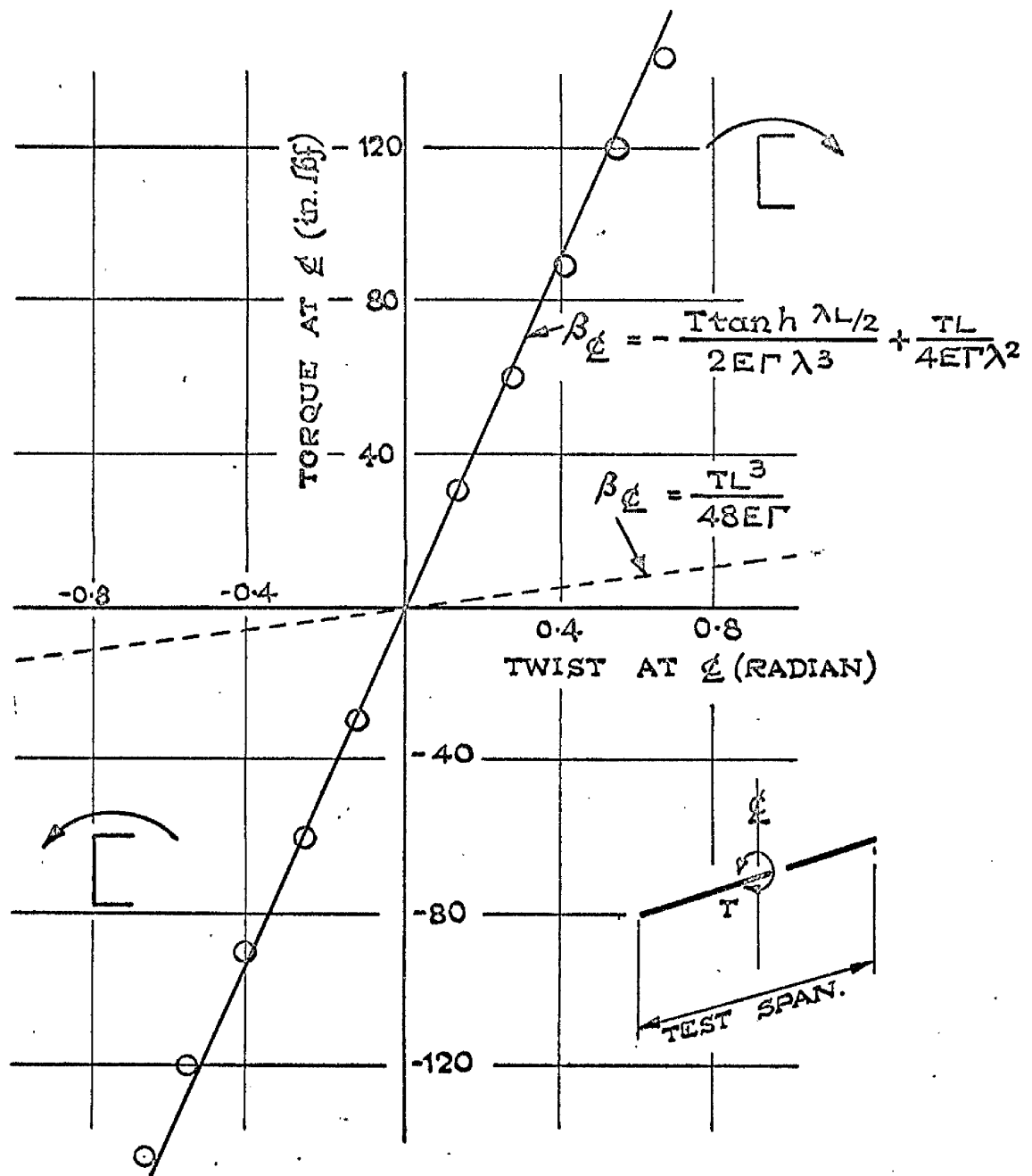


FIG. IV. 7. TORQUE / ANGLE OF TWIST RELATIONSHIP
- LARGE DISPLACEMENT BEHAVIOUR.

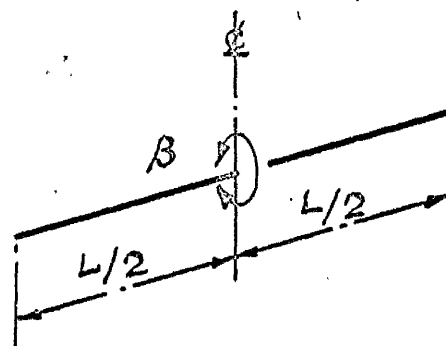
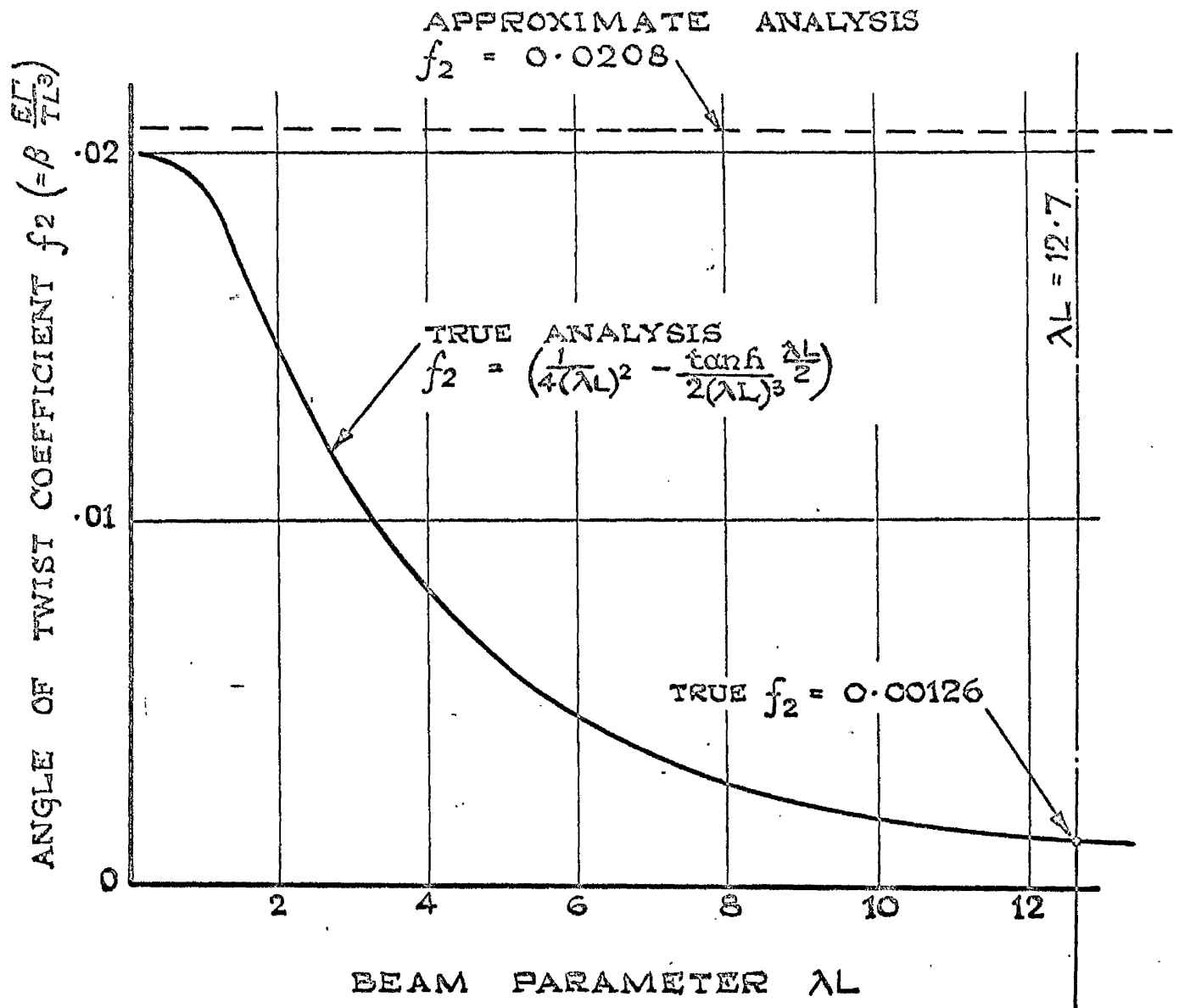


FIG. IV. 8. VARIATION OF ANGLE OF TWIST COEFFICIENT ' f_2 ' WITH BEAM PARAMETER λL .

THEORETICAL SOLUTIONS

(a) EQUATION IV. 2.1.

(b) EQUATION II. 3.20.

(c) EQUATION II. 3.17.

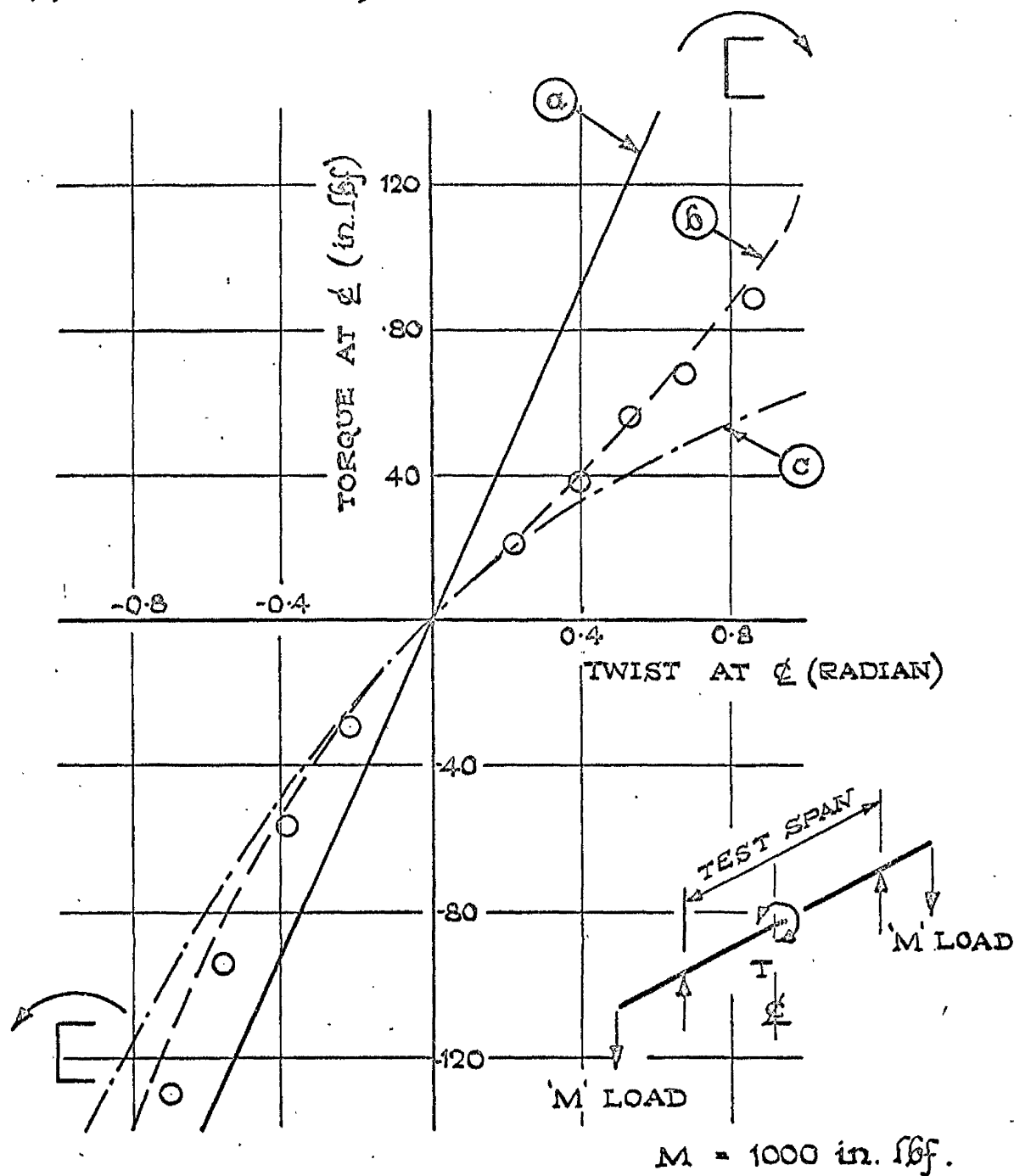


FIG. IV. 9. TORQUE / ANGLE OF TWIST RELATIONSHIP
FOR COMBINED BENDING AND TORSION

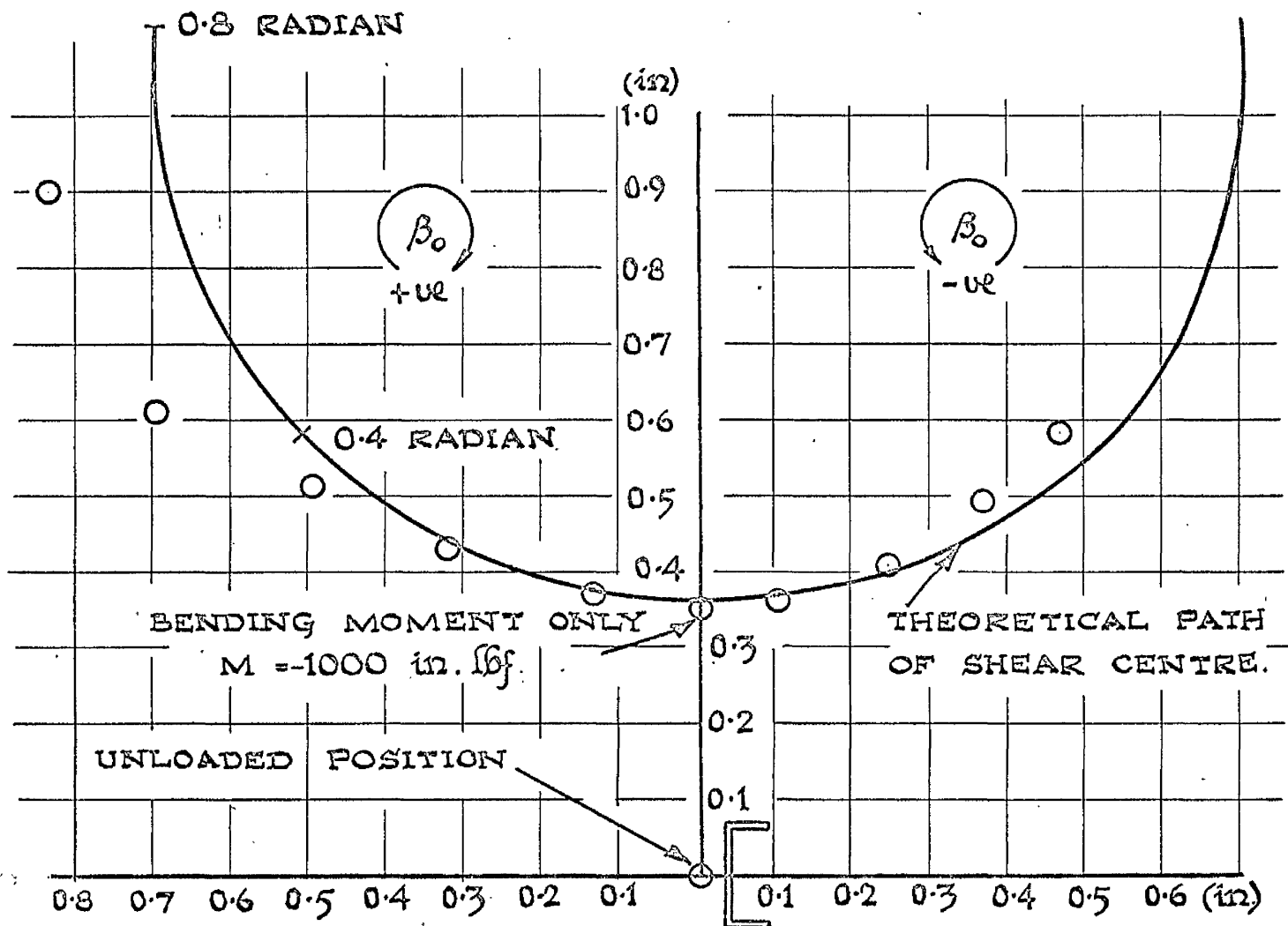
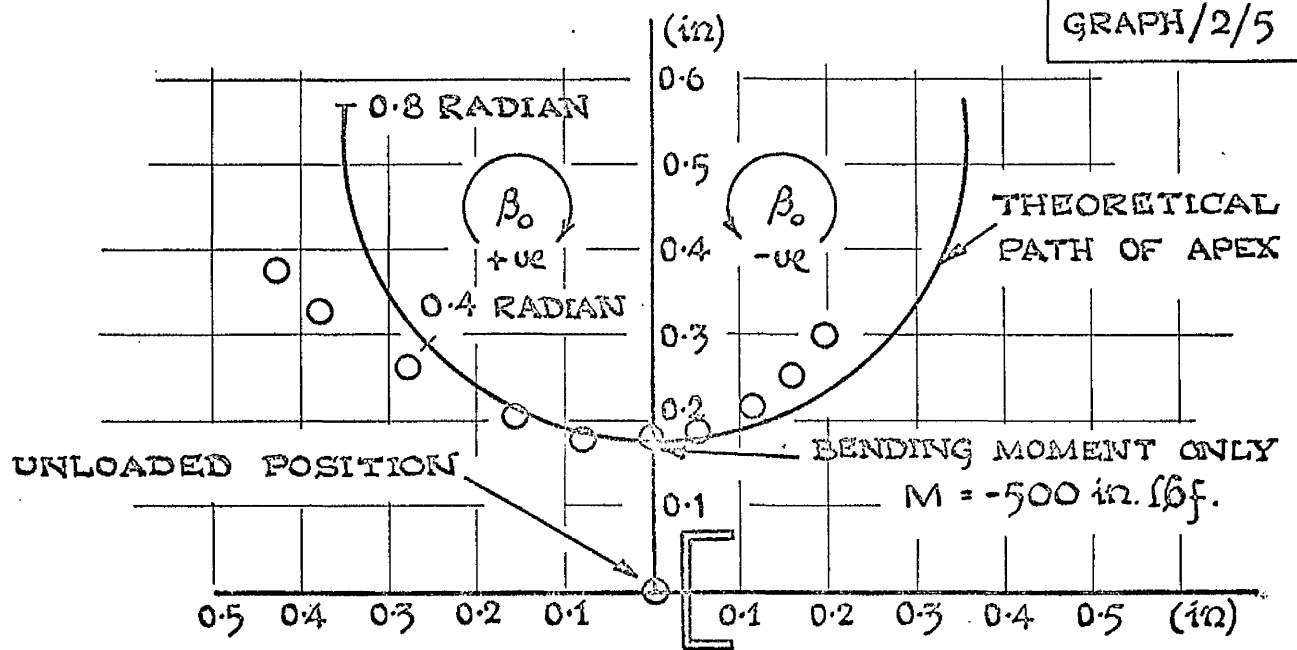


FIG. IV. 10. SHEAR CENTRE DISPLACEMENT PATH AT MID-SPAN. (SMALL CHANNEL BEAM.)

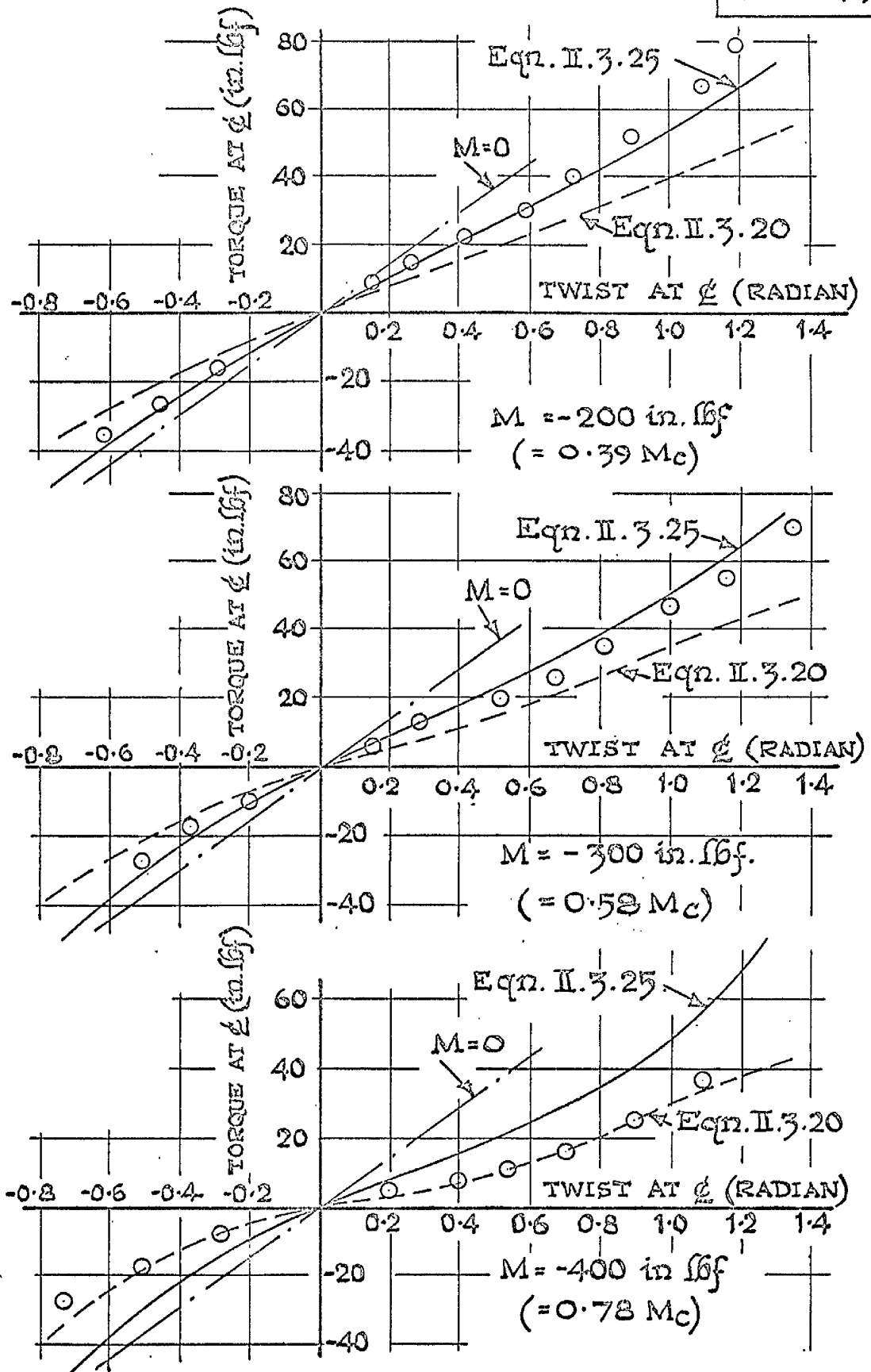


FIG. IV. 11. NONLINEAR TORQUE / ANGLE OF TWIST EQUILIBRIUM PATHS (SPECIMEN A3)

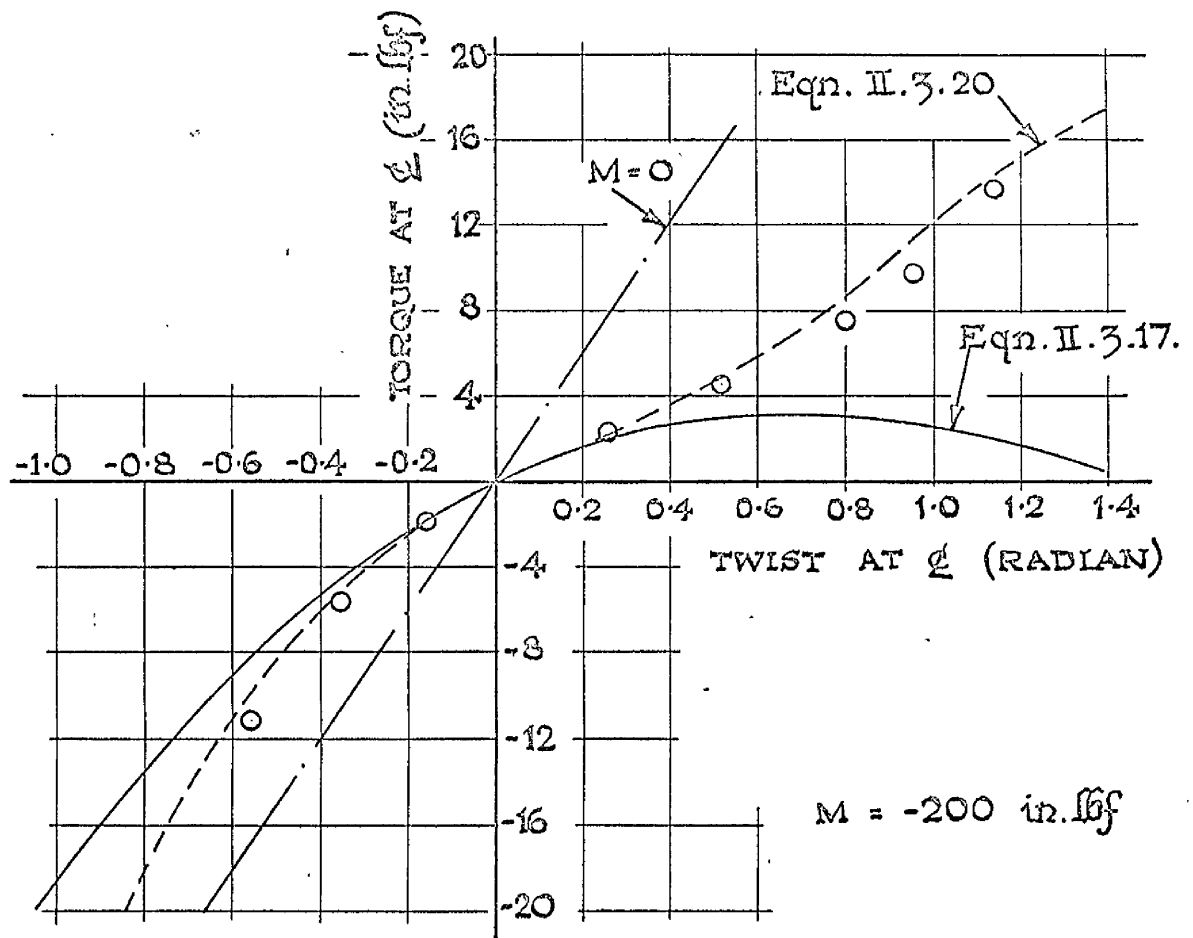


FIG. IV. 12. TORQUE / ANGLE OF TWIST EQUILIBRIUM PATHS - COMPARISON OF SOLUTIONS FOR ONE AND TWO TERMS OF SINE AND COSINE SERIES (SPECIMEN A.1.)

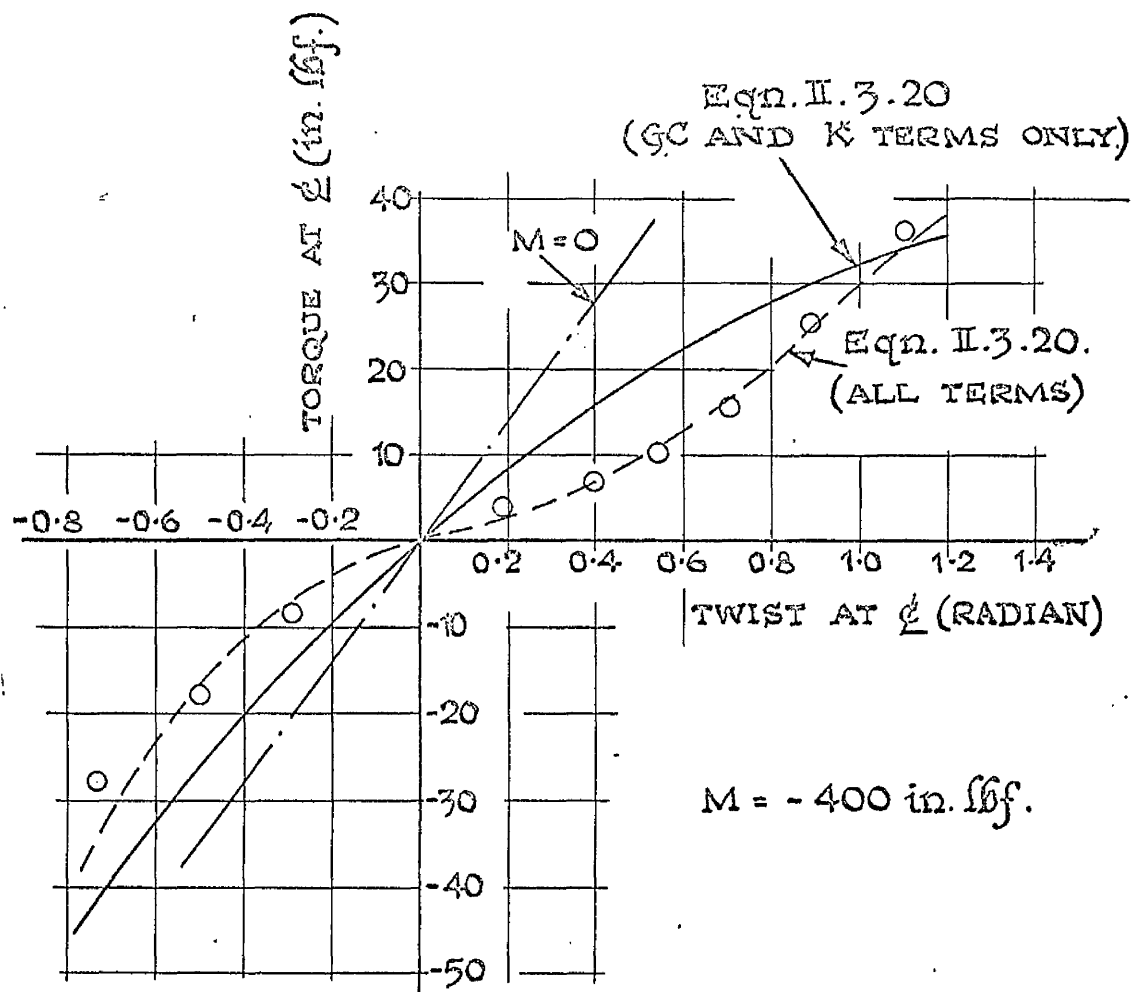


FIG. IV.13. TORQUE / ANGLE OF TWIST EQUILIBRIUM PATHS - COMPARISON OF THEORETICAL SOLUTIONS WITH AND WITHOUT ALL ADDITIONAL EFFECTS. (SPECIMEN A.3)

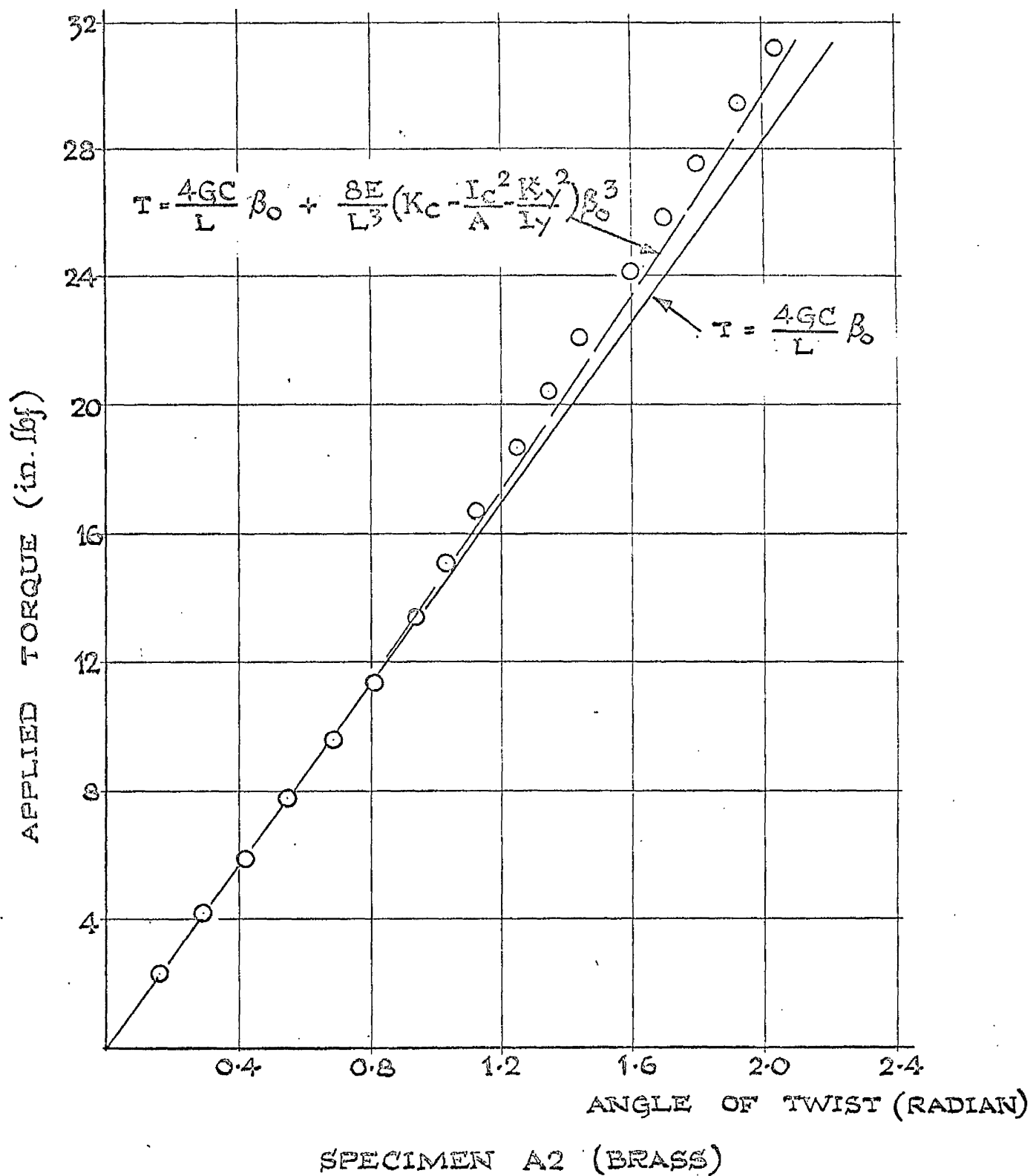


FIG. IV. 14. TORQUE / ANGLE OF TWIST
EQUILIBRIUM PATHS AT MID-SPAN
SECTION FOR APPLIED TORQUE ONLY

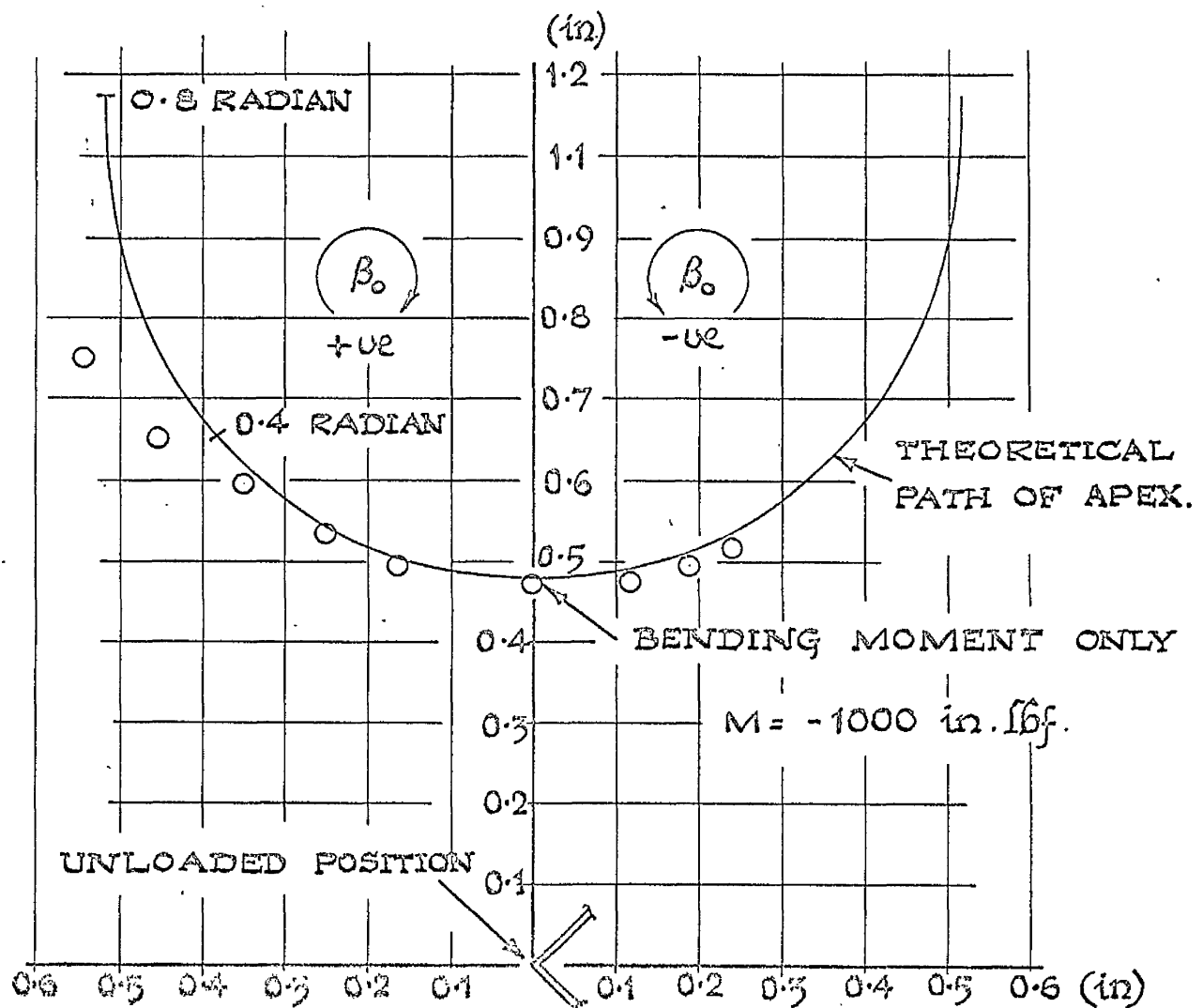
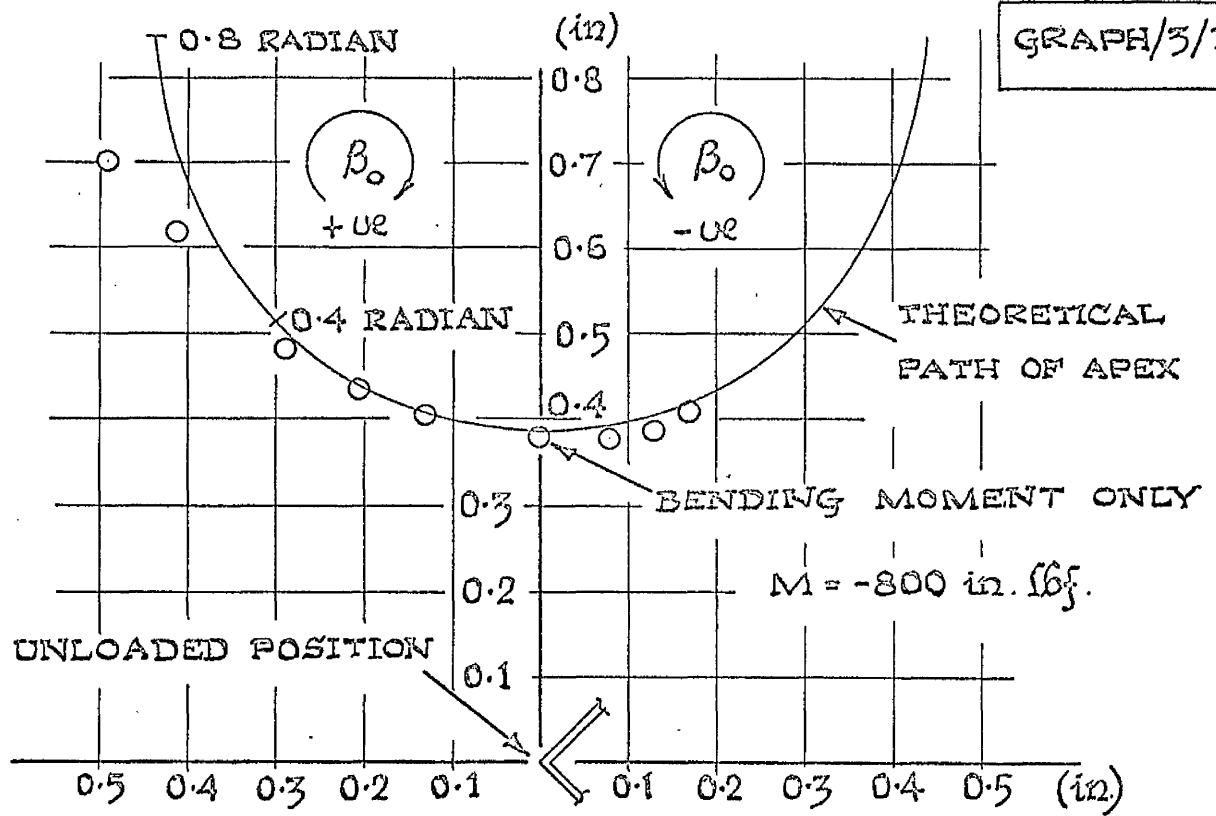
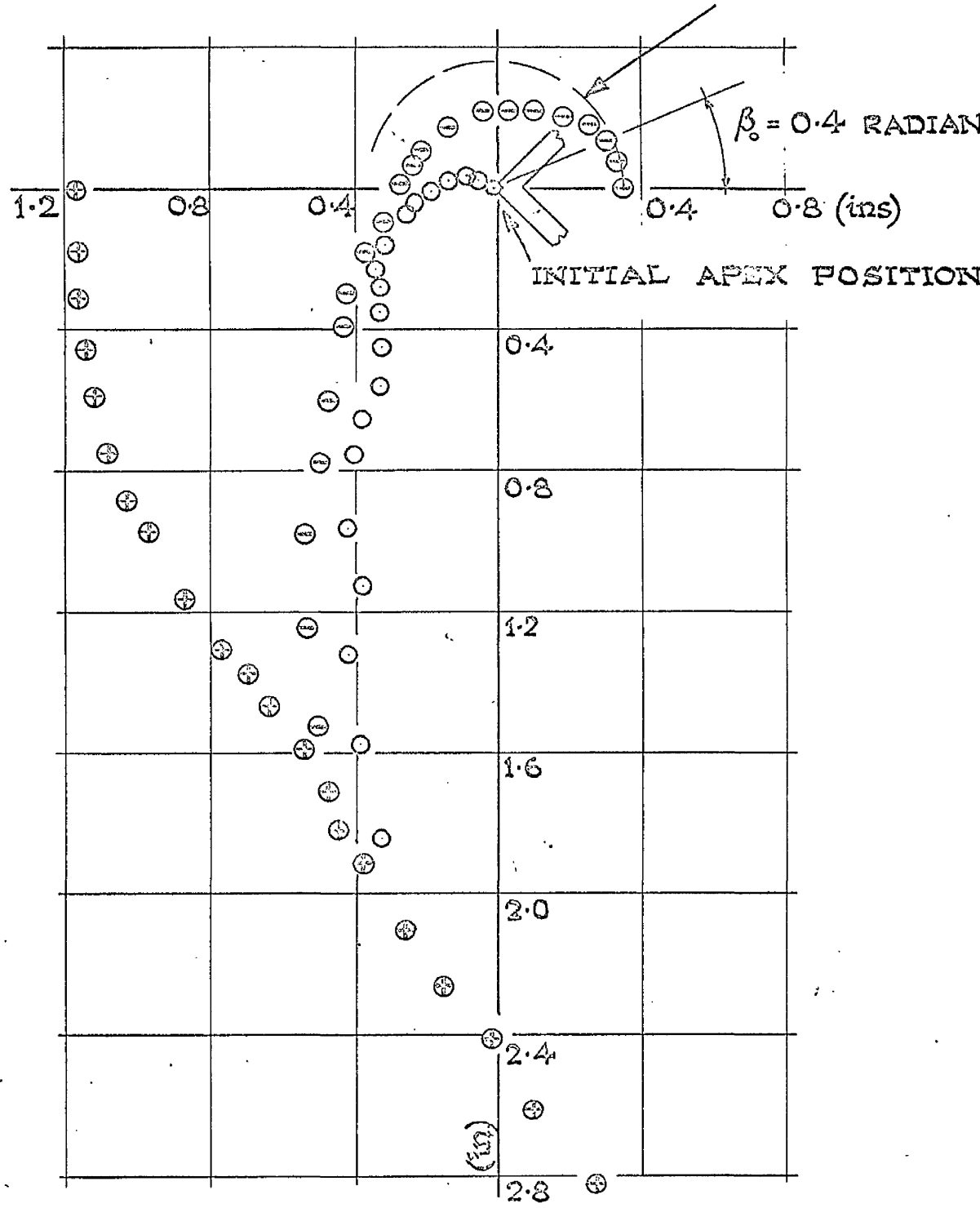


FIG. IX. 15. SHEAR CENTRE (APEX) DISPLACEMENT PATHS AT MID-SPAN (SPECIMEN BI.)

- ⊕ DISC PIN
- APEX
- ⊖ CENTROID

CENTROID PATH FOR
CENTRE OF TWIST AT
INITIAL APEX POSITION



SPECIMEN A2 (BRASS)

FIG. IV. 16. DISC PIN AND ANGLE APEX
AND CENTROID PATH AT MID-
SPAN FOR APPLIED TORQUE ONLY

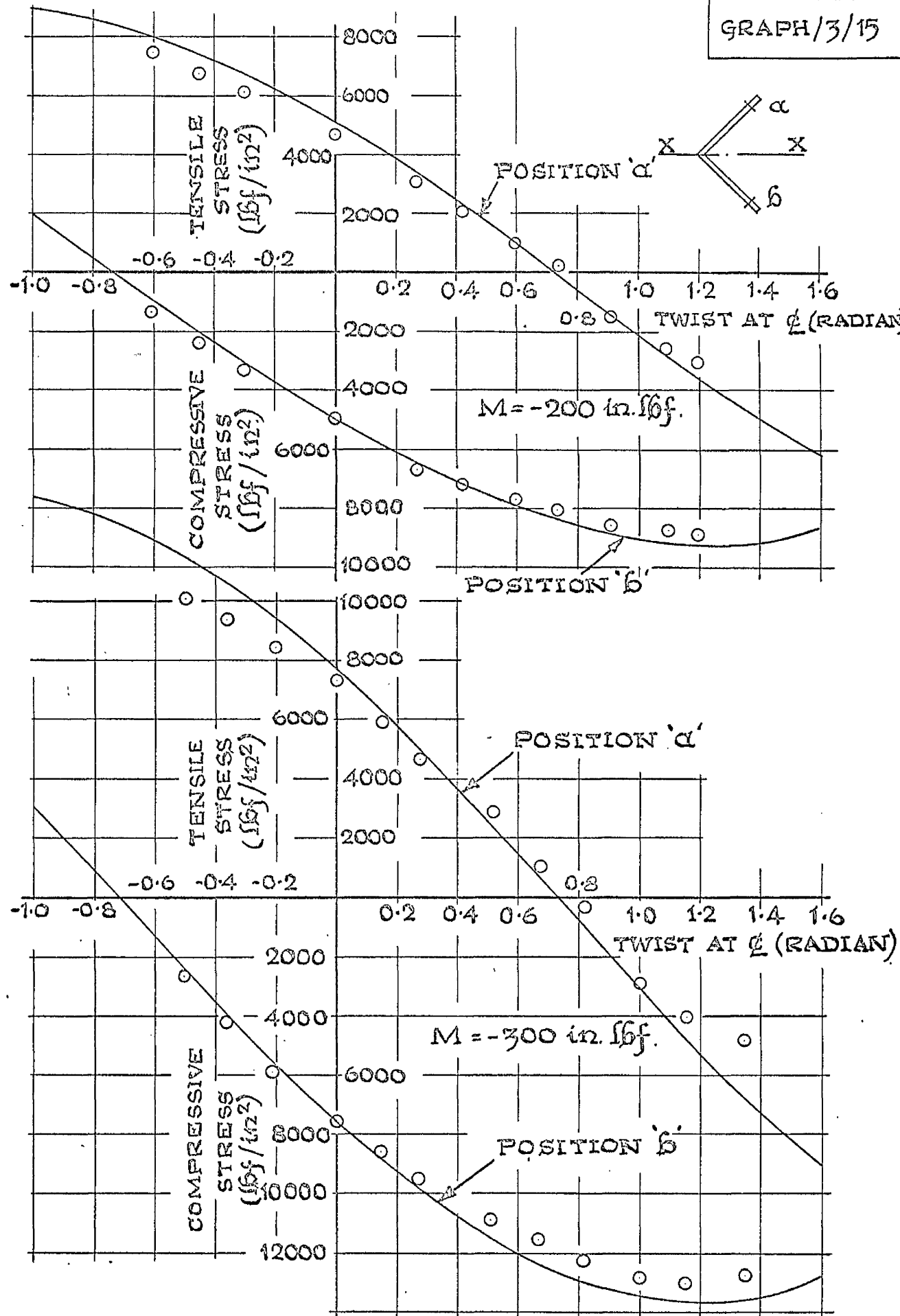


FIG IV.17. VARIATION OF LONGITUDINAL STRESS WITH ANGLE OF TWIST. (SPECIMEN A3).

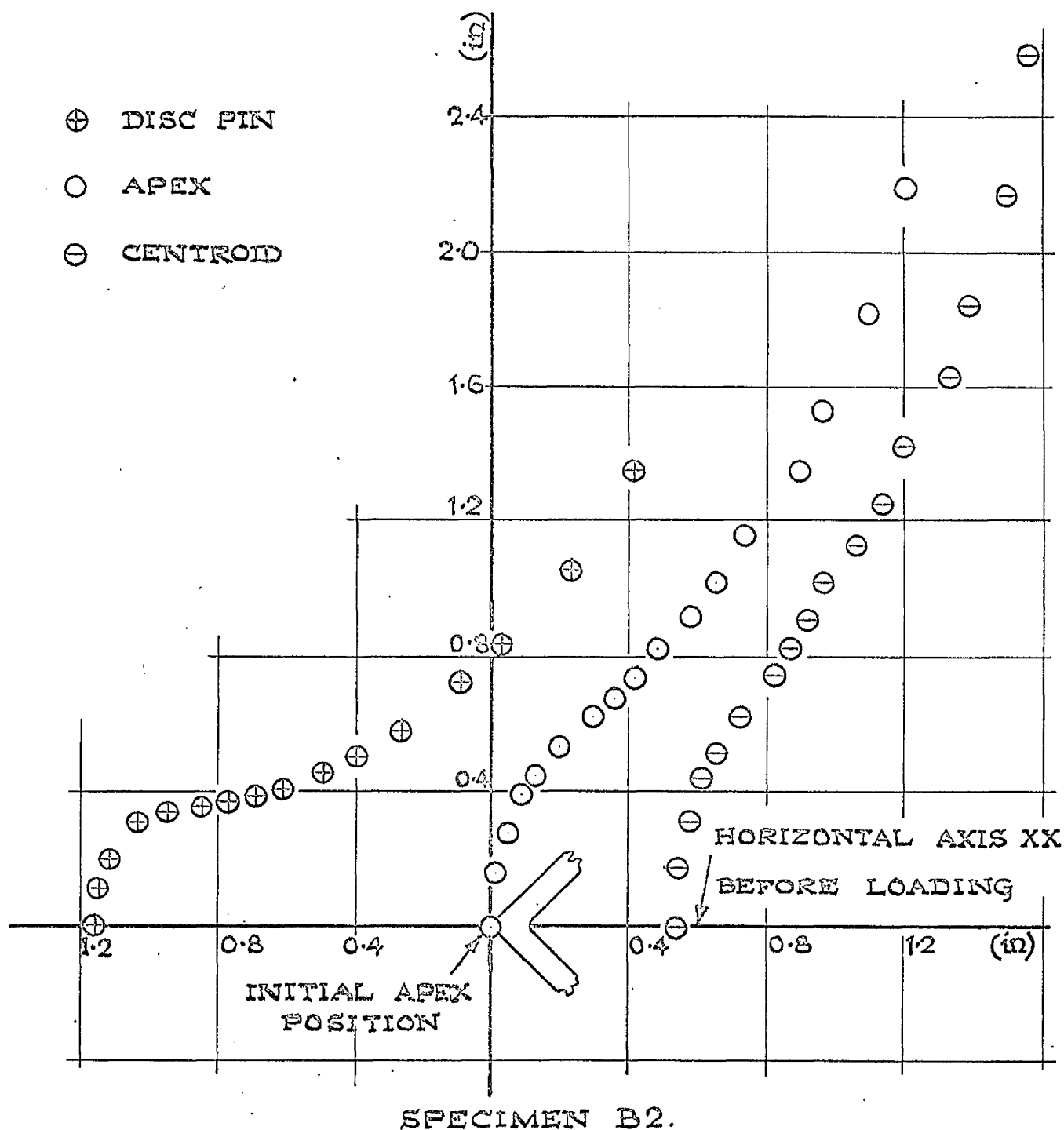
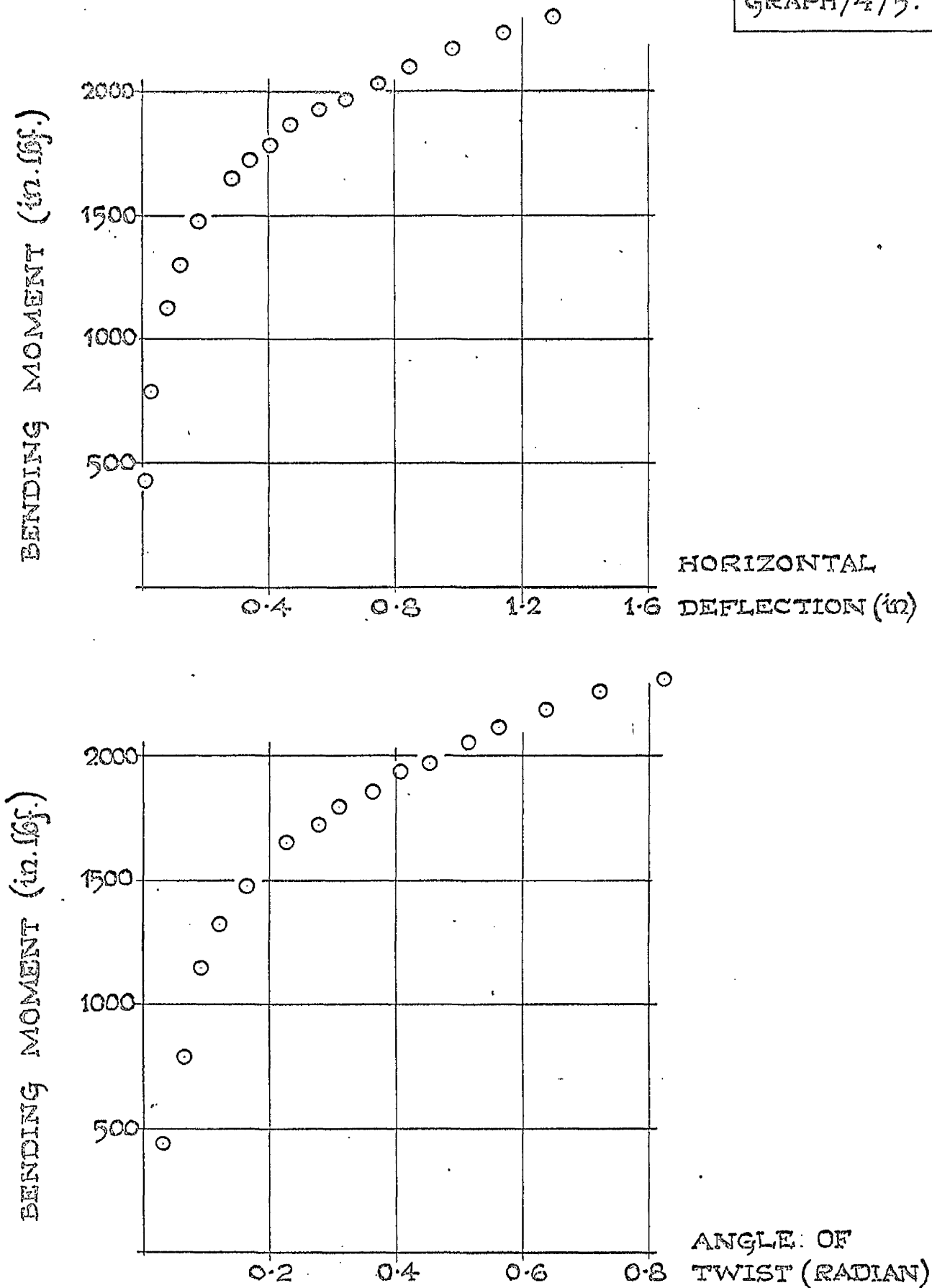
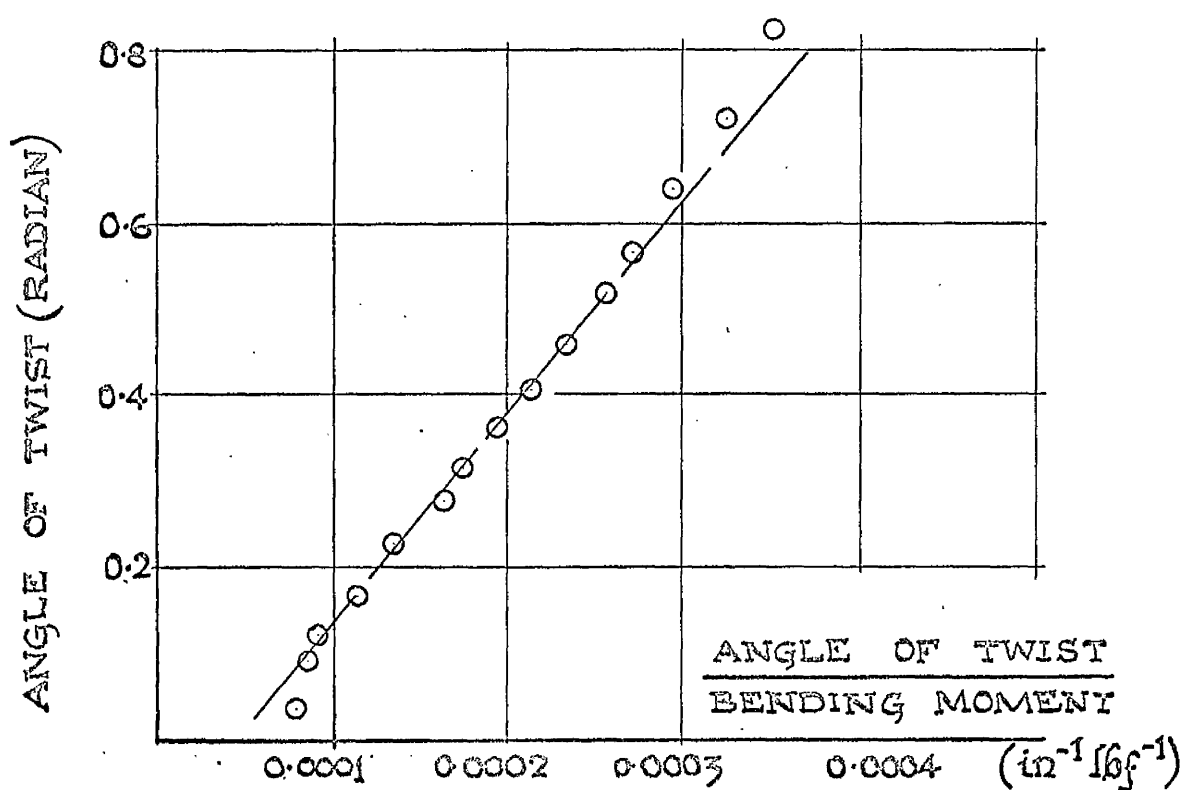
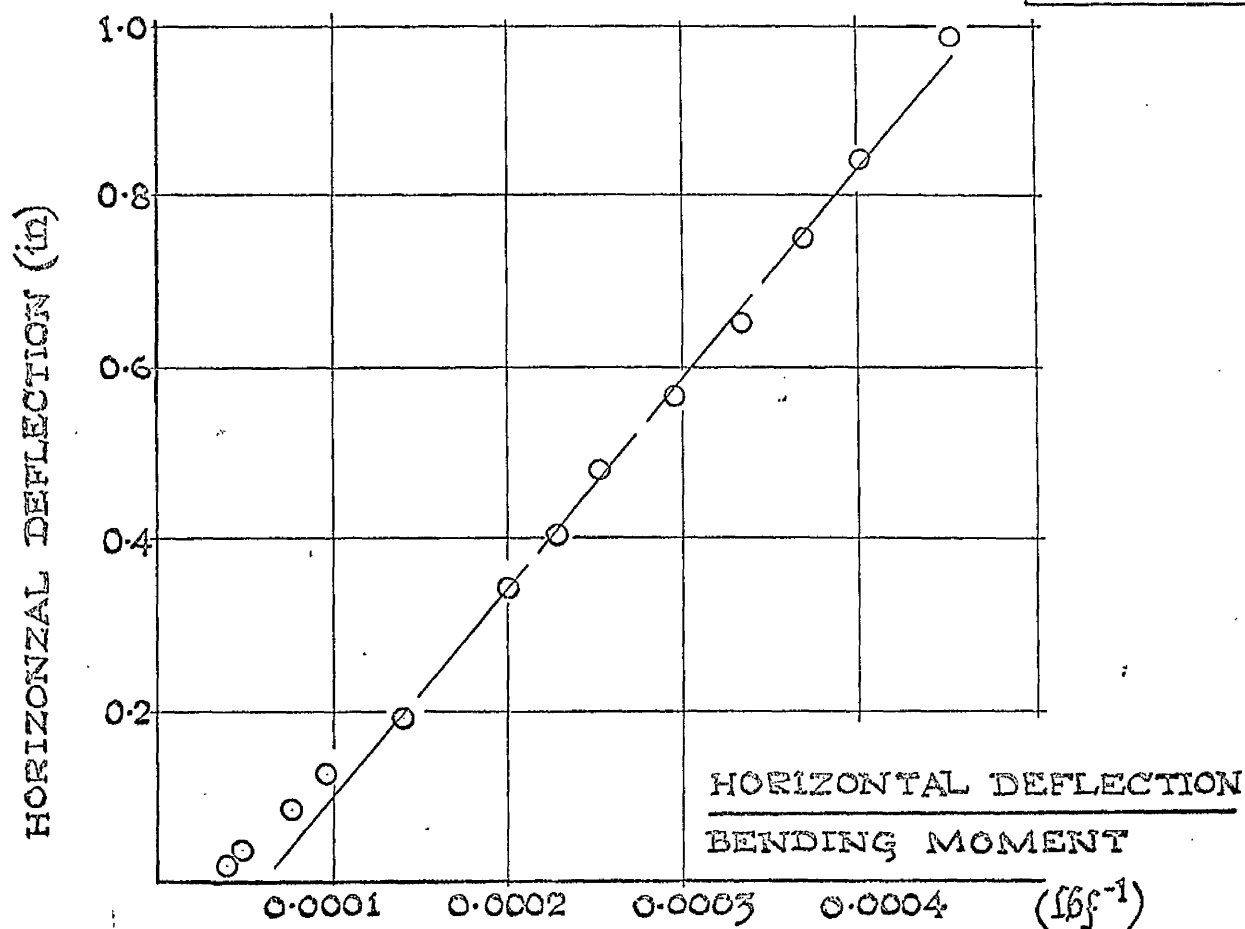


FIG. IV. 18. PATHS FOLLOWED BY DISC PIN AND
ANGLE APEX AND CENTROID DURING
TEST TO FAILURE.



SPECIMEN B.2.

FIG. IV. 19. APPROXIMATE RECTANGULAR HYPERBOLIC RELATIONSHIPS $M \propto \delta_H$ AND $M \propto \delta_\beta$



SPECIMEN B2.

FIG. IV. 20. SOUTHWELL INVERSE PLOTS
 $\delta H \propto \delta H/M$ AND $\delta \beta \propto \delta \beta/M$.

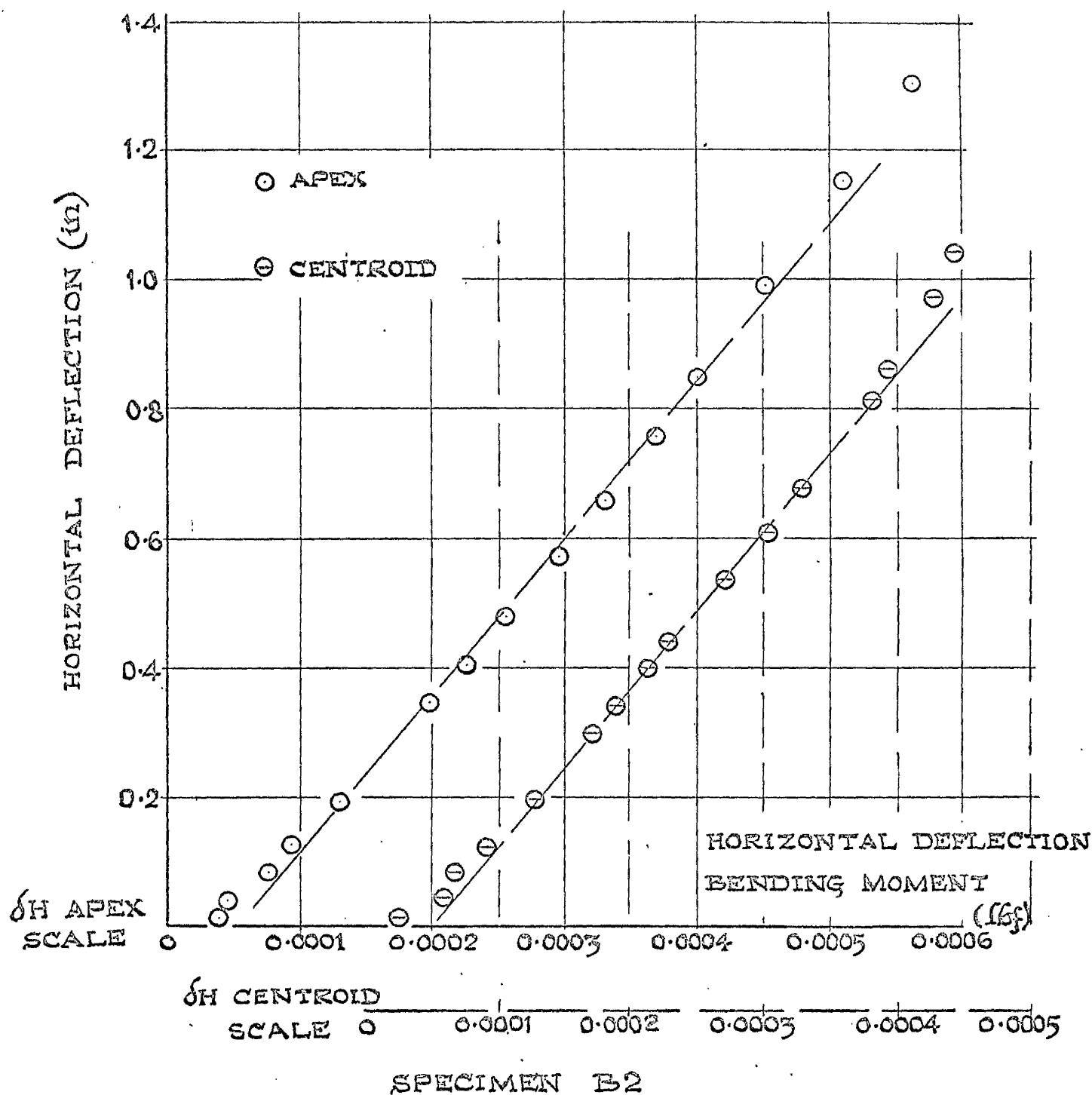


FIG. IV. 21. SOUTHWELL INVERSE PLOTS FOR δH_c $\delta H/M$ USING δH -APEX AND δH -CENTROID.

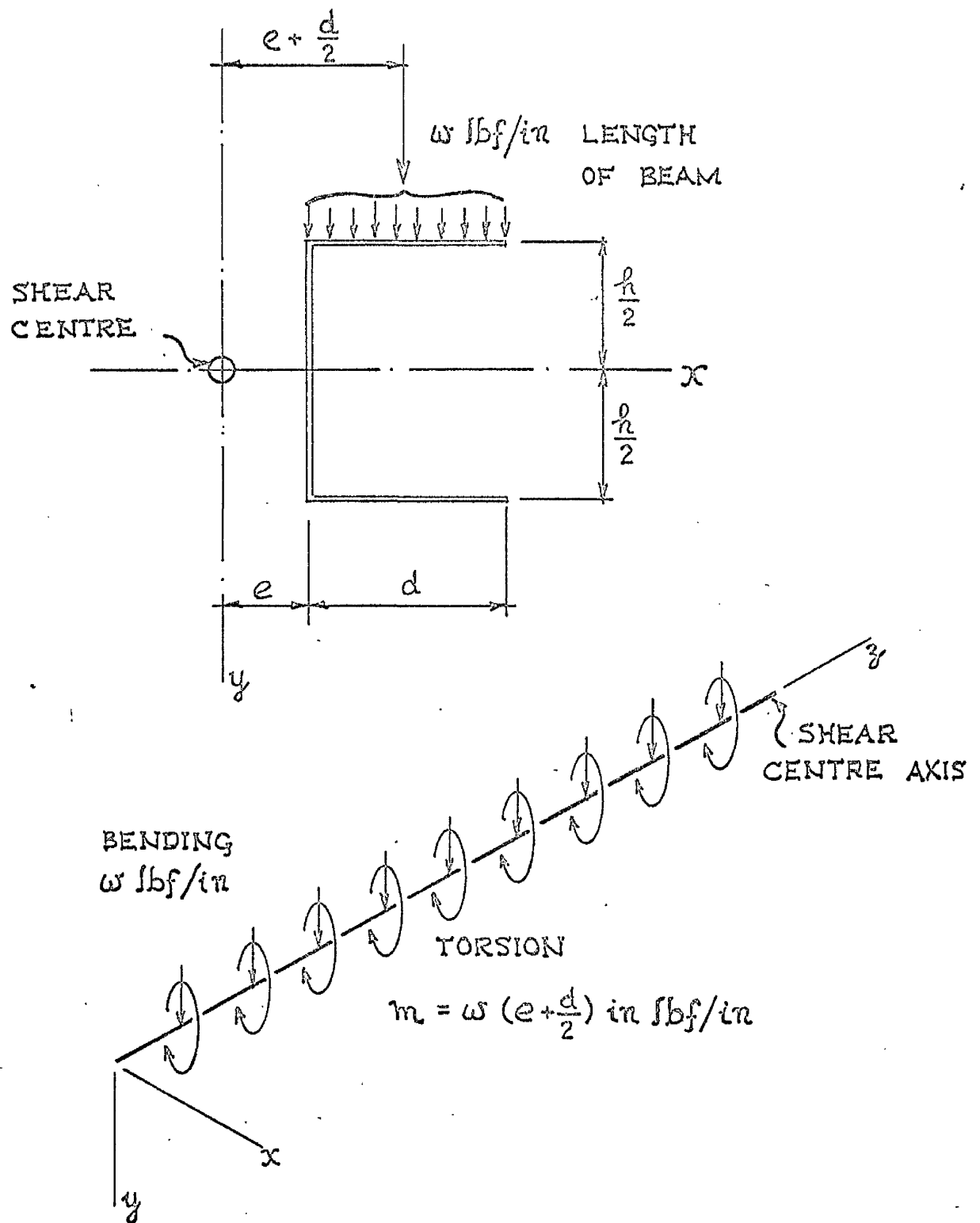
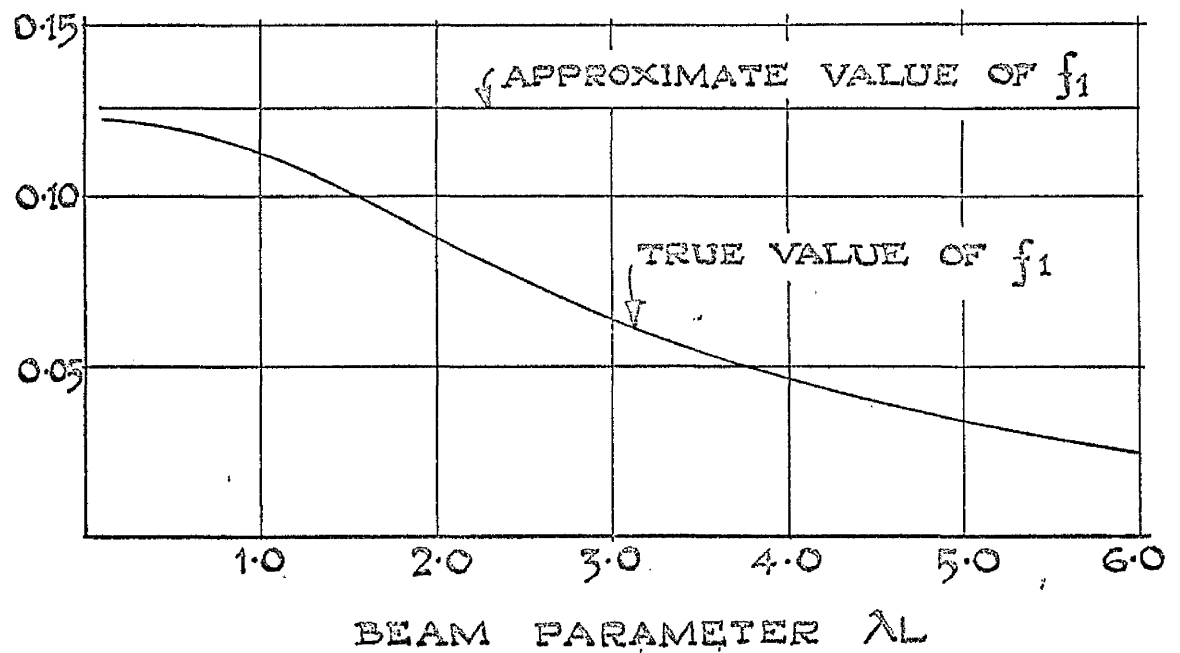


FIG. V. I. DETAILS OF CHANNEL BEAM
AND UNIFORMLY DISTRIBUTED LOADING

BI-MOMENT COEFFICIENT
 $f_1 = B/ML^2$



CORRECTION FACTOR
 $\alpha = B_{TRUE} / B_{APPROX.}$

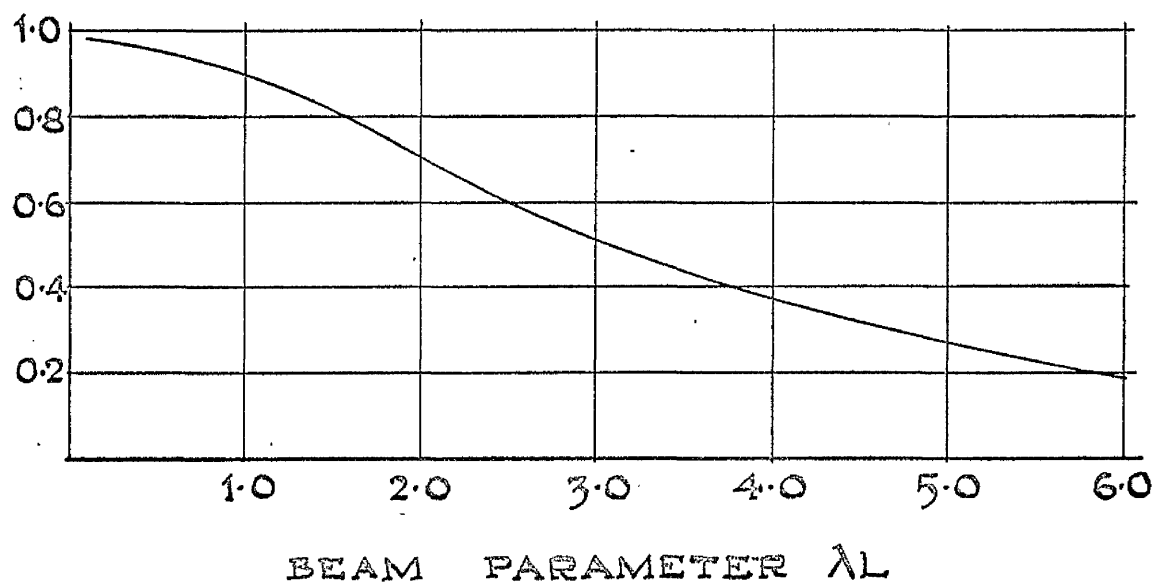
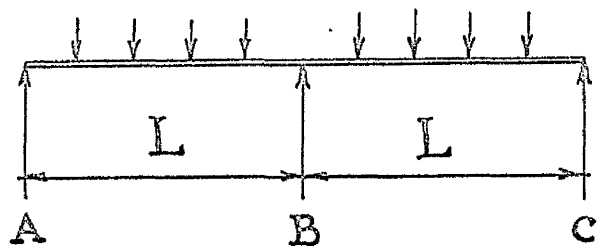


FIG.Y.2. VARIATION OF BI-MOMENT COEFFICIENT (f_1) AND CORRECTION FACTOR (α) WITH BEAM PARAMETER (λL) FOR UNIFORMLY DISTRIBUTED LOADING ON A SIMPLY SUPPORTED SPAN WITH TWIST RESTRAINT AT SUPPORT.

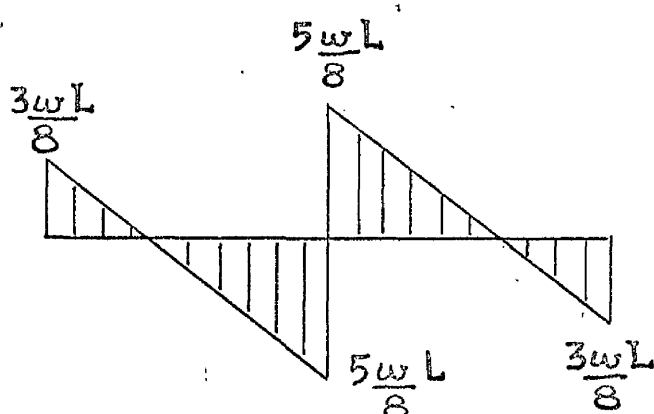
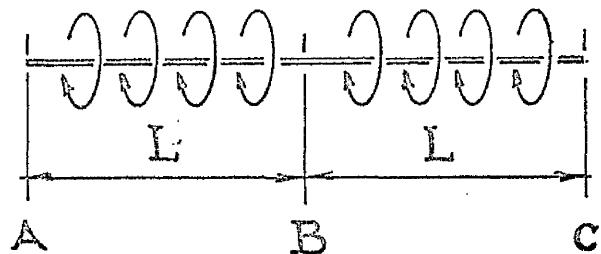
BENDING

w lbf/ft

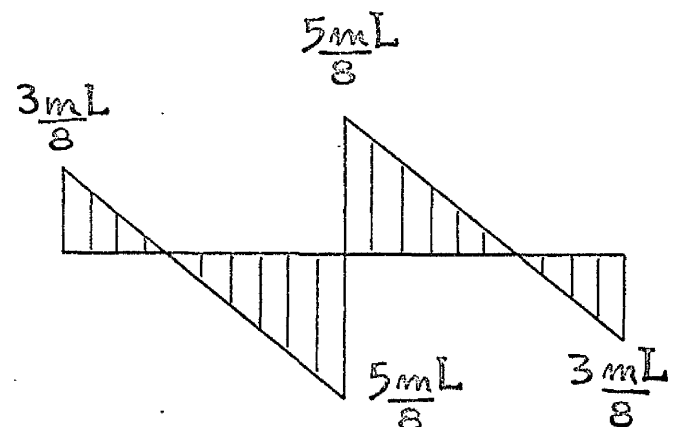


TORSION

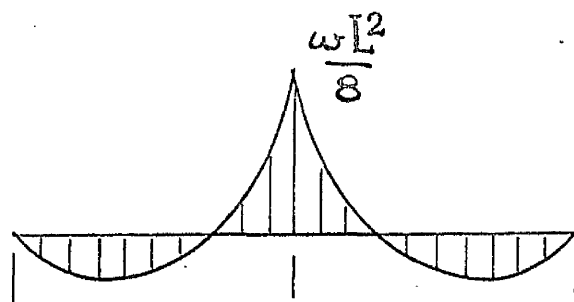
m . in. lbf/ft.



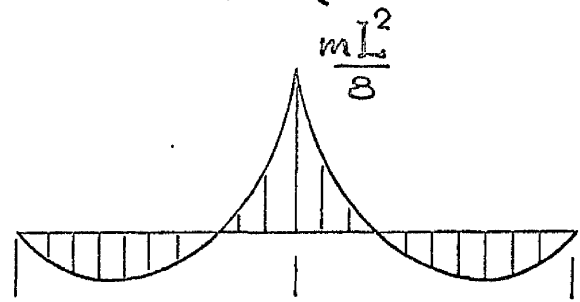
SHEAR FORCE



TORQUE (APPROXIMATE)



BENDING MOMENT



BI-MOMENT (APPROXIMATE)

FIG. V.3. BENDING MOMENT AND
APPROXIMATE BI-MOMENT DIAGRAMS
FOR TWO-SPAN CONTINUOUS BEAM.